

NOTE TO USERS

This reproduction is the best copy available.

UMI[®]

Buckling Analysis of Tapered Composite Plates Using Ritz
Method Based on Classical and Higher-order Theories

Shaikh Mohammad Akhlaque-E-Rasul

A Thesis

In

The Department

Of

Mechanical and Industrial Engineering

Presented in Partial Fulfillment of the Requirements

For the Degree of Master of Applied Science at

Concordia University

Montreal, Quebec, Canada

April 2005

© Shaikh Akhlaque, 2005



Library and
Archives Canada

Bibliothèque et
Archives Canada

Published Heritage
Branch

Direction du
Patrimoine de l'édition

395 Wellington Street
Ottawa ON K1A 0N4
Canada

395, rue Wellington
Ottawa ON K1A 0N4
Canada

Your file *Votre référence*

ISBN: 0-494-10261-6

Our file *Notre référence*

ISBN: 0-494-10261-6

NOTICE:

The author has granted a non-exclusive license allowing Library and Archives Canada to reproduce, publish, archive, preserve, conserve, communicate to the public by telecommunication or on the Internet, loan, distribute and sell theses worldwide, for commercial or non-commercial purposes, in microform, paper, electronic and/or any other formats.

The author retains copyright ownership and moral rights in this thesis. Neither the thesis nor substantial extracts from it may be printed or otherwise reproduced without the author's permission.

AVIS:

L'auteur a accordé une licence non exclusive permettant à la Bibliothèque et Archives Canada de reproduire, publier, archiver, sauvegarder, conserver, transmettre au public par télécommunication ou par l'Internet, prêter, distribuer et vendre des thèses partout dans le monde, à des fins commerciales ou autres, sur support microforme, papier, électronique et/ou autres formats.

L'auteur conserve la propriété du droit d'auteur et des droits moraux qui protègent cette thèse. Ni la thèse ni des extraits substantiels de celle-ci ne doivent être imprimés ou autrement reproduits sans son autorisation.

In compliance with the Canadian Privacy Act some supporting forms may have been removed from this thesis.

Conformément à la loi canadienne sur la protection de la vie privée, quelques formulaires secondaires ont été enlevés de cette thèse.

While these forms may be included in the document page count, their removal does not represent any loss of content from the thesis.

Bien que ces formulaires aient inclus dans la pagination, il n'y aura aucun contenu manquant.


Canada

Abstract

Buckling analysis of tapered composite plates using Ritz method based on classical and higher order theories

Shaikh Mohammad Akhlaque-E-Rasul

Tapered composite plates are being used in various engineering applications such as helicopter yoke, robot arms and turbine blade in which the structure needs to be stiff at one location and flexible at another location. Laminated tapered plates can be manufactured by terminating some plies at discrete locations. Different types of ply drop-off can be achieved depending on the application. Due to the variety of tapered composite plates and complexity of the analysis, no analytical solution is available at present. Therefore in the present work, the Ritz method is used for the calculation of response. Classical (Kirchhoff) plate theory has been widely used to model plate behavior, but is adequate only for thin laminated plates. Since the ratio of the in-plane elastic modulus to the transverse shear modulus is large for composite plates, Kirchhoff theory, which neglects transverse shear deformation, is usually inadequate for the analysis of thick or moderately thick plates. Although the Mindlin-type first-order shear deformation theory is quite accurate for the gross responses, such as buckling of moderately thick laminates, the accuracy of solutions will be strongly dependent on predicting better estimates for the shear correction factors. High-order shear deformation theories can overcome the

limitations of the first-order theory by introducing additional degrees of freedom (DOF). In the present thesis, the buckling of different types of tapered composite plates are analyzed based on classical laminated plate theory, first-order shear deformation theory and third-order shear deformation theory. The developed formulation is applied to the analysis of various types of tapered composite plates. The efficiency and accuracy of the developed formulation are established in comparison with available solutions, where applicable. A detailed parametric study has been conducted on various types of tapered composite plates, all made of NCT / 301 graphite-epoxy, in order to investigate the effects of boundary conditions, laminate configuration, taper angle and the thickness ratio.

Acknowledgments

I would like to express my gratitude to all those who gave me the possibility to complete this thesis. First and foremost, I want to express my most sincere gratitude to my supervisor Dr. Rajamohan Ganesan, not only for his guidance in writing this thesis, but also for his advice, concern, patience, and encouragement during my study and research in Concordia University.

I would like to acknowledge the financial support provided to this work by the supervisor from his NSERC research grant.

I would like to acknowledge Abolghassem Zabihollah, Lin Chen and Mohammad Ibrahim for their friendship and valuable technical discussions.

Finally, I would also like to express my heartfelt appreciation to my wife Shameema Chowdhury. Without her support and encouragement, this work would not have been possible.

CONTENTS

List of Figures	xii
List of Tables	xiv
Nomenclature	xvii
List of Abbreviations	xx
Chapter 1 Introduction, Literature Survey and Scope of the Thesis	1
1.1 Analysis and design	1
1.1.1 Buckling analysis in mechanical design	1
1.1.2 Composite material and structure	2
1.1.3 Energy method, variational method and Ritz method	3
1.2 Literature Survey	6
1.2.1 Buckling analysis of tapered laminates based on classical laminated plate theory (CLPT)	7
1.2.2 Buckling analysis of tapered laminates based on First-order Shear Deformation Theory (FSDT)	9
1.2.3 Buckling analysis of tapered laminates based on Third-order Shear Deformation Theory (TSDT)	9
1.3 Objectives of the present work	10
1.4 Layout of this thesis	11

Chapter 2 Buckling Analysis Based On Classical Laminated Plate Theory (CLPT)

	12
2.1 Introduction	12
2.2 The [A], [B] and [D] matrices of tapered laminate	13
2.2.1 Steps to calculate the [A], [B] and [D] matrices of tapered laminate	13
2.2.2 Step-1: Stiffness matrix of ply	15
2.2.3 Step-2: Stress and strain transformation matrices	16
2.2.3.1 <i>Axis Transformation For Rotation About z'' Axis (clock- wise rotation)</i>	16
2.2.3.2 <i>Rotation of laminate about y' axis (clock- wise rotation)</i>	18
2.2.4 Step-3: Stiffness matrix of each ply in the tapered laminate	20
2.2.4.1 <i>Accounting for the taper and fiber angles</i>	20
2.2.4.2 <i>Tapered laminate stiffness calculation</i>	22
2.2.5 Step-4: Elasticity equations for plane stress state	23
2.2.6 Step-5: Geometric analysis of tapered part of the laminate	25
2.2.6.1 <i>Tapered laminate</i>	25
2.2.6.2 <i>Resin pocket</i>	26
2.2.7 Step-6: [A], [B] and [D] matrices of tapered laminate	27
2.3 Analysis of transformed reduced stiffness (TRS), Q_{ij}	28
2.3.1 Plots of Q_{ij}	28
2.3.2 Observations from Q_{ij} plots	32
2.4 Buckling analysis of tapered plate using Ritz method	33
2.4.1 General expressions for buckling analysis	33
2.4.2 Buckling analysis of thick part	35

2.4.3	Buckling analysis of tapered part	36
2.4.3.1	<i>Laminate</i>	36
2.4.3.2	<i>Resin</i>	36
2.4.4	Buckling analysis of thin part	38
2.4.5	Final form of the equation for critical buckling load	39
2.5	Analysis of taper models with different boundary conditions	40
2.5.1	Simply supported laminated plate	41
2.5.2	Laminated plate clamped at two adjacent ends and with other two ends free (CFCF)	42
2.5.3	Laminated plate clamped at four ends (CCCC)	43
2.5.4	Laminated plate simply supported at two opposite ends and with other two ends free (SSFF)	45
2.6	Exact solutions for uniform laminated beam and plate	46
2.6.1	Uniform laminated beam	46
2.6.2	Uniform laminated plate	47
2.7	Numerical examples	48
2.7.1	Examples of uniform laminate	48
2.7.1.1	<i>Discussion of results for uniform laminates</i>	49
2.7.2	Examples of tapered laminated beam and plate	49
2.7.2.1	<i>Discussion of results for tapered laminates</i>	50
2.7.3	Example of tapered plate analyzed using Ritz method	51
2.7.3.1	<i>Discussion on model A</i>	52
2.7.3.2	<i>Discussion of models A, B, C and D</i>	54

2.8	Discussions and conclusions	55
CHAPTER 3 Buckling Analysis Based On First-order Shear Deformation		
	Theory(FSDT)	56
3.1	Introduction	56
3.2	Fundamental equations for buckling	57
3.2.1	Displacement field	57
3.2.2	Strain field with transverse shear	58
3.2.3	Stress field	58
3.2.4	Constitutive equation	60
3.3	Energy formulation	61
3.3.1	Energy equations for tapered laminate and resin pocket	61
3.3.2	General expressions for buckling analysis	65
3.3.3	The system equations of tapered laminate for special cases	67
3.3.4	The system equations of resin pocket for special cases	71
3.3.5	Tapered laminated plate simply supported at four ends	71
3.3.6	Tapered laminated plate clamped at four ends (CCCC)	72
3.4	Example of tapered plate analyzed using Ritz method based on FSDT	73
3.4.1	Example	73
3.4.2	Discussion on model A	75
3.4.3	Discussion of models A, B, C and D	79
3.5	Discussions and conclusions	80

Chapter 4 Buckling Analysis Based on Third-order Shear Deformation Theory (TSDT)	81
4.1 Introduction	81
4.2 Fundamental equations for buckling	82
4.2.1 Displacement field	82
4.2.2 Strain field with transverse shear	84
4.2.3 Stress field	86
4.2.4 Constitutive equation	87
4.3 Energy formulation	89
4.3.1 Energy equations for tapered laminate and resin pocket	89
4.3.1.1 <i>Strain energy</i>	89
4.3.1.2 <i>Potential energy</i>	96
4.3.2 General expressions	96
4.3.3 The system equations	98
4.3.4 Tapered laminated plate simply supported at four ends	99
4.3.5 Numerical results and discussion	100
4.3.5.1 <i>Example</i>	100
4.3.5.2 <i>Discussion of models A, B, C and D</i>	105
4.4 Discussions and conclusions	106
Chapter 5 Parametric Study on Tapered Copposite Plates Models	107
5.1 Introduction	107
5.2 Comparison of critical buckling co-efficients	108
5.2.1 Example	108

5.3	Comparison of buckling load of tapered plate with that of equivalent uniform plate	109
5.3.1	Example	109
5.4	Critical buckling loads calculated using different plate theories	112
5.4.1	Example	112
5.5	Effect of laminate configuration	114
5.5.1	Example	114
5.6	Discussion and conclusion	115
Chapter 6	Conclusions and Future Work	116
	References	120
Appendix A	System Equations Based on TSDT	126
Appendix B	MATLAB ® programs	149

List of Figures

Figure 2.1 Orientation of fibers and laminate	14
Figure 2.2 Laminate and ply material co-ordinates	21
Figure 2.3 Final orientation of ply after rotation	22
Figure 2.4 Detailed Drawing of a Ply in the Tapered Part Of The Laminate	25
Figure 2.5 Detailed Drawing of Resin Pocket	27
Figure 2.6 Plot Of Q_{ij} For Constant Taper Angle (0°) And Varying Fiber Orientation Angle	28
Figure 2.7 Plot Of Q_{ij} For Constant Taper Angle (8°) And Varying Fiber Orientation Angle	29
Figure 2.8 Plot Of Q_{ij} For Constant Taper Angle (15°) And Varying Fiber Orientation Angle	29
Figure 2.9 Plot Of Q_{ij} For Constant Fiber Orientation Angle (0°) And Varying Taper Angle	30
Figure 2.10 Plot Of Q_{ij} For Constant Fiber Orientation Angle (30°) And Varying Taper Angle	30
Figure 2.11 Plot Of Q_{ij} For Constant Fiber Orientation Angle (60°) And Varying Taper Angle	31
Figure 2.12 Plot Of Q_{ij} When Both Fiber Orientation Angle And Taper Angle Vary	31
Figure 3.1 Explanation of rotations considered in FSDT	57
Figure 3.2 Effect of transverse shear on buckling co-efficient for simply supported tapered laminate model A	74

Figure 3.3 Variation of buckling co-efficient due to thickness variation for simply supported tapered laminate model A	75
Figure 3.4 Effect of transverse shear on buckling co-efficient for simply supported tapered laminate model B	76
Figure 3.5 Effect of transverse shear on buckling co-efficient for simply supported tapered laminate model C	77
Figure 3.6 Effect of transverse shear on buckling co-efficient for simply supported tapered laminate model D	78
Figure 3.7 Effect of transverse shear on buckling co-efficient for simply supported tapered laminate models A, B, C and D	79
Figure 4.1 Explanation of displacement terms for TSDT	83
Figure 4.2 Effect of transverse shear on buckling co-efficient for simply supported tapered laminate model A	101
Figure 4.3 Effect of transverse shear on buckling co-efficient for simply supported tapered laminate model B	102
Figure 4.4 Effect of transverse shear on buckling co-efficient for simply supported tapered laminate model C	103
Figure 4.5 Effect of transverse shear on buckling co-efficient for simply supported tapered laminate model D	104
Figure 4.6 Effect of transverse shear on buckling co-efficient for simply supported tapered laminate models A, B, C and D	105
Figure 5.1 Tapered laminate models AA, BB, CC and DD for buckling analysis.	109

List of Tables

Table 2.1 Direction cosines for rotating x'' and y'' axes about z'' axis	16
Table 2.2 Direction cosines for rotation of laminate about y' axis.	18
Table 2.3 Co-efficients of the clamped-free beam functions.	43
Table 2.4 Co-efficients of the clamped-clamped beam functions.	45
Table 2.5 Values of co-efficients of the free-free beam function.	46
Table 2.6 Comparison of critical buckling Load ($\times 10^4\text{N}$) for uniform laminates.	48
Table 2.7 Comparison of critical buckling Load ($\times 10^4\text{N}$) of taper model-C with the result of corresponding tapered beam.	50
Table 2.8 Comparison of critical buckling Load ($\times 10^4\text{N}$) of taper model-D with the result of corresponding tapered beam.	50
Table 2.9 Critical buckling load ($\times 10^4\text{N}$) of tapered part of model A	51
Table 2.10 Critical buckling load ($\times 10^4\text{N}$) of tapered part of model B	52
Table 2.11 Critical buckling load ($\times 10^4\text{N}$) of tapered part of model C	53
Table 2.12 Critical buckling load ($\times 10^4\text{N}$) of tapered part of model D	53
Table 3.1 Critical buckling load ($\times 10^4\text{N}$) for different support conditions for tapered laminate model A	74
Table 3.2 Critical buckling load ($\times 10^4\text{N}$) for different support conditions for tapered laminate model B	76
Table 3.3 Critical buckling load ($\times 10^4\text{N}$) for different support conditions for tapered laminate model C	77

Table 3.4 Critical buckling load ($\times 10^4\text{N}$) for different support conditions for tapered laminate model D	78
Table 4.1 Comparison of critical buckling loads ($\times 10^4\text{N}$) for simply supported tapered laminate model A	101
Table 4.2 Comparison of critical buckling loads ($\times 10^4\text{N}$) for simply supported tapered laminate model B	102
Table 4.3 Comparison of critical buckling loads ($\times 10^4\text{N}$) for simply supported tapered laminate model C	103
Table 4.4 Comparison of critical buckling loads ($\times 10^4\text{N}$) for simply supported tapered laminate model D	104
Table 5.1 Comparison of buckling co-efficient with previously published results.	108
Table 5.2 Comparison of critical buckling load ($\times 10^4\text{N}$) for tapered laminate model AA with that of equivalent uniform plate for simply supported boundary conditions.	110
Table 5.3 Comparison of critical buckling load ($\times 10^4\text{N}$) for tapered laminate model BB with that of equivalent uniform plate for simply supported boundary conditions.	110
Table 5.4 Comparison of critical buckling load ($\times 10^4\text{N}$) for tapered laminate model CC with that of equivalent uniform plate for simply supported boundary conditions.	111
Table 5.5 Comparison of critical buckling load ($\times 10^4\text{N}$) for tapered laminate model DD with that of equivalent uniform plate for simply supported boundary conditions.	111
Table 5.6 List of different tapered laminate configurations.	113
Table 5.7 Influence of different theories on critical buckling load ($\times 10^4\text{N}$) for the laminate configuration LC(1) with simply supported ends.	113

Table 5.8 Effect of laminate configuration on critical buckling load ($\times 10^4\text{N}$) for simply supported ends.	114
Table 6.1 Physical explanation for variation of geometric properties of laminates	118

Nomenclature

φ	Taper angle
θ	Orientation of ply
x, y, z	Reference coordinate
x'', y'', z''	Ply coordinate
ε_{ij}	Strain corresponding to coordinate system x, y, z
ε'_{ij}	Strain corresponding to coordinate system $x' y' z'$
ε''_{ij}	Strain corresponding to coordinate system x'', y'', z''
σ_{ij}	Stress corresponding to coordinate system x, y, z
σ'_{ij}	Stress corresponding to coordinate system $x' y' z'$
σ''_{ij}	Stress corresponding to coordinate system x'', y'', z''
C_{ij}	Co-efficient of stiffness matrix to coordinate system x, y, z
C''_{ij}	Co-efficient of stiffness matrix to coordinate system x'', y'', z''
$\{\varepsilon\}_{xyz}$	Strain vector corresponding to coordinate system x, y, z
$\{\sigma\}_{xyz}$	Stress vector corresponding to coordinate system x, y, z
$[T_{\sigma\theta}]$	Stress transformation matrix of ply due to angle θ
$[T_{\varepsilon\theta}]$	Strain transformation matrix of ply due to angle θ
$[T_{\sigma\varphi}]$	Stress transformation matrix of ply due to angle φ
$[T_{\varepsilon\varphi}]$	Strain transformation matrix of ply due to angle φ
$[]'$	Transpose of the matrix

Q_{ij}	Co-efficient of the reduced ply stiffness matrix
L	Total length of the plate
b	Width of the plate
h	Height of the plate
E_1	Modulus of elasticity in fiber direction
E_2	Modulus of elasticity in transverse direction
ν_{ij}	Poisson ratio of ply
G_{23}	Out-of-plane shear modulus
G_{13}	In-plane shear modulus
E	Modulus of elasticity of resin
ν	Poisson ratio of resin
G	Shear modulus of resin
u	Displacement in x -direction
v	Displacement in y -direction
w	Displacement in thickness direction
u_o	Mid-plane displacement in x -direction
v_o	Mid-plane displacement in y -direction
w_o	Mid-plane displacement in z -direction
κ_x^o	Curvature of the mid-plane
ϕ_x	Rotation of transverse normal on plan $z = 0$ about x axis
ϕ_y	Rotation of transverse normal on plan $z = 0$ about y axis
ϕ_z	Extension of transverse normal
φ_z	Interpreted as a higher-order rotation of transverse normal

N_x	Axial force per unit width
A_{ij}	Co-efficients of stretching stiffness matrix of composite plate
B_{ij}	Co-efficients of bending-stretching coupling matrix of composite plate
D_{ij}	Co-efficients of bending stiffness matrix of composite plate
z_k	Coordinate of the center of the k^{th} layer of composite plate
e_k	Thickness of the k^{th} layer of composite plate
U	Strain energy
w	Potential energy
$[K]$	Stiffness matrix of plate
N_{cr}	Critical buckling load
N_{ij}	In plan resultant force
M_{ij}	Resultant moments (bending and twisting)
P_{ij}	Higher-order moments
S_{ij}	Higher-order moments

List of Abbreviations

CLPT	Classical Laminated Plate Theory
FSDT	First-order Shear Deformation Theory
TSDT	Third-order Shear Deformation Theory
TRS	Transformed Reduced Stiffness
DOF	Degree of Freedom
ESL	Equivalent Single Layer
LC	Laminate Configuration
AIAA	American Institute of Aeronautics and Astronautics

The following abbreviations have been used to represent the boundary conditions for the plates:

CFCF	Clamped Boundary condition for two adjacent edges and free boundary condition for the other two edges
CCCC	Clamped boundary condition for all the four edges
SSFF	Simply supported boundary condition for two opposite edges and free boundary condition for the other two edges

The Chapter 1

Introduction, Literature Survey and Scope of the Thesis

1.1 Analysis and design

1.1.1 Buckling analysis in mechanical design

Change in the geometry of a structure or a mechanical component under compression results in the loss of its ability to resist loading. Stability of structures under compression can be grouped into two categories: (1) instability associated with a bifurcation of equilibrium; (2) instability that is associated with a limit of maximum load. The first category is characterized by the fact that as the compressive load increases, the member or system that originally deflects in the direction of applied force, suddenly deflects in a different direction. This phenomenon is called buckling. The point of transition from the usual deflection mode under load to an alternative deflection mode is referred to as the point of bifurcation of equilibrium. The lowest load at the point of bifurcation is called critical buckling load.

Buckling analysis is basically a sub-topic of non-linear rather than linear mechanics. In linear mechanics of deformable bodies, displacements are proportional to the loads. In buckling, disproportional increase in displacement occurs due to a small increase in the load. The instability due to buckling can lead to a catastrophic failure of a structure and it must be taken into account when one designs a structure.

1.1.2 Composite material and structure

A composite material consists of two or more materials of different nature but with complementing mechanical properties and allows us to obtain a material the performance characteristics of which are greater than that of the components taken separately [1]. The major reason for the success of composite materials is that no homogeneous structural material can fulfill all the requirements for a given application. Originally, structural composites were developed for the aerospace industry as they offered attractive properties of stiffness and strength, compared to their weight. Thus, they replaced previously used aluminum alloys, which also combined quite good mechanical properties with low specific weight. The latter nevertheless suffered major drawbacks, such as their fatigue behavior. On the other hand, in addition to the well-known high strength and stiffness to density ratios, fiber composites exhibit high tensile fatigue resistance, notch insensitivity, ease of fabrication and lower scrap rate. Furthermore, fiber composites provide the unique opportunity to simultaneously optimize structure configuration, material make-up, fabrication process and structural integrity.

Today, composites have found their way into a much more wide range of applications than simply the aerospace sector. Fiber reinforced composite materials are the engineering materials which are most commonly used in modern industries and composite plate is one of the most widely used structural elements. They are made by stacking together many plies of fiber-reinforced layers in different orientations to achieve the desired properties. Then these stacked layers are permanently bonded together under heat and pressure using a hot press or autoclave. In some specific applications, composite

plates need to be stiff at one end and flexible at the other end. Such plates can be made by dropping off some plies at discrete locations to reduce the stiffness of the plates. This results in a tapered shape, which is considered in the present thesis.

1.1.3 Energy method, variational method and Ritz method

For simple mechanical systems, the vector methods provide an easy and direct way of deriving the equations. However, for complicated systems, the procedure becomes more cumbersome and intractable. In such cases, variational statements can be used to obtain governing equations, associated boundary conditions, and, in certain simple cases, solutions for displacements and forces at selective points of a structure.

Variational statement of a physical body can be used in two analysis methods: “energy method” and “variational method”. The ‘energy methods’ refer to the methods that make use of the energy of a system to obtain values of the unknown at a specific point. These include Castigliano’s theorems, unit-dummy-load and displacement methods, and Betti and Maxwell’s theorems. These methods are limited to the (exact or approximate) determination of generalized displacements or generalized forces at fixed points in the structure, and they can not be used to determine the solution (i.e., displacements and/or forces) as a function of position in the structure. The phrase ‘variational methods’ refer to the methods that make use of the variational principles, such as the principle of virtual displacements, to determine approximate displacements as continuous functions of position in a body. In the classical sense, variational principle has to do with the minimization of a functional, which includes all the intrinsic features of the

problem, such as the governing equations, boundary and/or initial conditions, and constraint conditions.

The approximate methods may be employed as the variational statements (i.e., either variational principles or weak formulations) to determine continuous solutions of problems in mechanics. To obtain the governing differential equations and boundary conditions of various problems we need to apply the virtual-work principles or their derivatives. These principles involve setting the first variation of an appropriate functional with respect to the dependent variables to zero. The procedure of the calculus of variations can then be applied to obtain the governing (Euler-Lagrange) equations of the problem. In contrast, the method applied in this thesis seeks a solution in terms of adjustable parameters that are determined by substituting the assumed solutions into the functional and finding its stationary value with respect to the parameters. Such solution methods are called direct methods, because the approximate solutions are obtained directly by applying the same variational principle that was used to derive the governing equation. The assumed solutions in the variational methods are in the form of a finite linear combination of undetermined parameters with appropriately chosen functions. This amounts to representing a continuous function by a finite linear combination of functions. Since the solution of a continuum problem in general can not be completely represented by a finite set of functions, error is introduced into the solution. Therefore, the solution obtained is an approximation of the true solution for the equations describing a physical problem. As a number of linearly independent terms in the assumed solution is increased, the error in the approximation will be reduced and the assumed solution converges to the desired solution of Euler's equations.

The equations governing a physical problem themselves are approximate. The approximations are introduced via several sources, including the geometry, the representation of specified loads and displacements, and the material constitution. In the present study, our primary concern is to determine accurate approximate solutions to appropriate analytical descriptions of physical problems.

The variational methods of approximation include those of Rayleigh and Ritz, Galerkin, Petrov-Galerkin (weighted-residuals), Kantorovitch, Treffiz, and the finite element method, which is a "piecewise" application of the Ritz-Galerkin method.

In the principle of virtual displacements, the Euler equations are the equilibrium equations, whereas in the principle of virtual forces, they are the compatibility equations. These Euler equations are in the form of differential equations that are not always tractable by exact methods of solution. A number of approximate methods exist for solving differential equations [e.g., finite-difference methods, perturbation methods, etc.]. The most direct methods bypass the derivation of the Euler equations and go directly from a variational statement of the problem to the solution of the Euler equations. One such direct method was proposed by Lord Rayleigh (whose actual name was John William Strutt, 1842~1919). A generalization of the method was proposed independently by Ritz (1878-1909).

The basic idea of the Ritz method is described here using the principle of virtual displacements. In this method, we approximate each of the displacements u_1 , u_2 and u_3 as a linear combination of the form:

$$u_1 \approx U_1 = \sum_{i=1}^N \sum_{j=1}^M c_{ij}^1 \phi_i^1 \phi_j^1 \quad (1.1a)$$

$$u_2 \approx U_2 = \sum_{i=1}^N \sum_{j=1}^M c_{ij}^2 \phi_i^2 \phi_j^2 \quad (1.1b)$$

$$u_3 \approx U_3 = \sum_{i=1}^N \sum_{j=1}^M c_{ij}^3 \phi_i^3 \phi_j^3 \quad (1.1c)$$

Then we determine the parameters c_{ij}^1 , c_{ij}^2 , and c_{ij}^3 by requiring that the principle of virtual displacements hold for arbitrary variations of the parameters. In equations (1.1a – 1.1c) c_{ij}^1 , c_{ij}^2 , and c_{ij}^3 denote undetermined parameters, $\phi_i^\alpha, \phi_j^\alpha$ ($\alpha = 1, 2, 3$) denote appropriate functions of position (x, y, z).

1.2 Literature Survey

In this section, a comprehensive literature survey is presented on the buckling of tapered composite laminates and on the application of the Ritz method to tapered composite plates. Important works done on the buckling analysis of uniform and thickness-tapered composite plates using Ritz method have been chronicled. The majority of works done on the buckling analysis of plates are limited to homogeneous material and based on the Classical Laminated Plate Theory (CLPT). The works on the buckling analysis of tapered composite plates based on CLPT, First-order Shear Deformation Theory (FSDT) and Third-order Shear Deformation Theory (TSDT) are presented at the end, though the quantity of such works is of course very limited.

1.2.1 Buckling analysis of tapered laminates based on classical laminated plate theory (CLPT)

Most of the works on composite plates have concentrated on delamination and failure analysis of composite plates. Few works deal with buckling analysis of laminated plates.

Whitney [2] investigated the effect of boundary conditions on the bending, vibrations and buckling of uniform unsymmetrically laminated rectangular plates. Ashton [3] discussed the requirements on the boundary conditions of the assumed series in a Ritz solution for anisotropic uniform plates for classical and elastically restrained boundary conditions. Baharlu and Leissa [4] developed a method for the analysis of free vibration and buckling of generally laminated composite uniform plates having arbitrary edge conditions using Ritz method. Venini and Meriani [5] dealt with free vibrations of uncertain composite plates via stochastic Rayleigh Ritz approach. Chao and Kim [6] used a stress function-based variational method to determine the thermal stresses near the dropped plies.

Cheung and Zhou [7] obtained the eigenfrequency equation by the use of Ritz method to develop a new set of admissible functions which are the static solutions of the tapered beam (or a strip taken from a rectangular plate), under an arbitrary static load expanded into a Taylor series. Curry, Johnson and Starnes [8] studied the reduction in the tensile and compressive strengths of graphite-epoxy laminates with thickness discontinuities due to dropped plies by experiment and analysis. Mukharjee and Varughese [9] designed a drop-off to reduce the stress concentration by studying the

effect of important parameters that determine the strength of laminate. Varughese and Mukharjee [10] developed a novel ply drop-off element for the analysis of tapered laminated composites. Thomas and Webber [11] applied a fracture mechanics based analysis to predict the tensile delamination load of tapered laminated plates. Mukherjee and Varughese [12] presented a global-local approach for the analysis of tapered laminated composites. Wang and Lu [13] investigated the buckling behavior of local delamination near the surface of fiber reinforced laminated plates under mechanical and thermal loads. Gaudenzi [14] studied the effect of the presence of a delamination on the buckling load of composite laminates under compression loads. Fish and Lee [15] investigated the delamination of tapered composite laminates with multiple internal ply drop steps. They conducted both experimental testing of glass-epoxy coupon specimens and finite element modeling of the tapered region. Zabihollah [16] presented the vibration and buckling analysis of uniform and tapered composite beams using conventional and advanced finite element methods based on the classical laminate theory and the first-order shear deformation theory. DiNardo and Lagace [17] conducted an experiment and analytical investigation using Ritz method on the buckling and post buckling behavior of laminated graphite-epoxy plates with ply drop off under uniaxial compression.

1.2.2 Buckling analysis of tapered laminates based on First-order Shear Deformation Theory (FSDT)

Few works are available on buckling analysis of tapered laminated plates using Ritz method based on FSDT.

Whitney [18] developed a procedure for accurately calculating the mechanical behavior of a thick composite laminate or sandwich plate of arbitrary stacking sequence. Kabir [19] presented an analytical boundary-continuous solution of moderately thick plates with arbitrary lamination for simply supported boundary condition. Jensen and Lagace [20] performed an experimental and analytical investigation on the buckling and post buckling behavior of generally anisotropic laminated thick plate. The Rayleigh-Ritz and finite element methods were used to predict the buckling loads; different anisotropic couplings inherent in unbalanced and unsymmetric laminates were isolated and their effects were studied.

1.2.3 Buckling analysis of tapered laminates based on Third-order Shear Deformation Theory (TSDT)

The works on the buckling analysis of tapered laminated plate using Ritz method based on TSDT are very rare.

Wu and Chen [21] used a local higher-order deformation theory to determine the natural frequencies and buckling loads of laminated composite plates. Matsunaga [22] analyzed natural frequencies and buckling stresses of cross-ply laminated composite

plates by taking into account the effects of shear deformation, thickness change and rotary inertia. Wang, Tseng and Lin [23] developed a higher-order shear deformable plate finite strip element and employed it for the calculation of critical buckling loads of laminated composite plates. Kulkarni and Bajoria [24] presented the finite element formulation of a degenerate shell element, using higher-order shear deformation theory taking the piezoelectric effect into account. Chattopadhyay and Radu [25] used a higher-order shear deformation theory to investigate the instability associated with composite plates subjected to dynamic loads. Matsunaga [26] analyzed interlaminar stresses and displacements in cross-ply laminated composite and sandwich plates subjected to lateral pressures by a global higher-order plate theory. Matsunaga [27] analyzed natural frequencies and buckling stresses of laminated composite beams by taking into account the complete effects of transverse shear and normal stresses and rotary inertia. Rao and Ganesan [28] investigated harmonic response of width-tapered composite beams by using a finite element model based on a higher-order shear deformation theory.

1.3 Objectives of the present work

The objectives of the present thesis are: (1) to determine the mechanical behavior of tapered laminates considering the effect on the stiffness of plies caused by the taper angle; (2) to analyze the thickness-tapered composite plates for buckling using Ritz method based on Classical Laminated Plate Theory (CLPT), the First-order Shear Deformation Theory (FSDT) and Third-order Shear Deformation Theory (TSDT), and (3) to conduct a detailed parametric study on the buckling of tapered composite plates.

The formulations using Ritz method are developed. The formulations are analyzed for their accuracy and performance in the buckling analysis of uniform and thickness-tapered composite plates based on the classical laminated plate theory, the first-order shear deformation theory and the third-order shear deformation theory. These formulations are then used to analyze the buckling of tapered composite plates with different types of tapers and subjected to compressive axial forces.

1.4 Layout of this thesis

The present chapter provided introduction to the thesis work and literature survey on the Ritz method and other related methods used in laminate analysis and the buckling analysis of uniform and tapered composite plates.

In chapter 2 different types of taper models are analyzed applying Classical Laminated Plate Theory (CLPT) and then results are evaluated by comparing with exact solutions and beam theory.

In chapter 3 the taper models are analyzed applying First-order Shear Deformation Theory (FSDT) and results are compared with that obtained based on CLPT.

In chapter 4 taper models are analyzed applying Third-order Shear Deformation Theory (TSDT) and results are compared with that obtained based on CLPT and FSDT.

Chapter 5 is devoted to the parametric study, which includes the effects of the boundary conditions, laminate configurations, taper angle, taper model and axial forces on the buckling of the tapered plates.

Chapter 6 brings the thesis to its end by providing an overall conclusion of the present work and some recommendations for future work.

Chapter 2

Buckling Analysis Based On Classical Laminated Plate Theory (CLPT)

2.4 Introduction

The mechanical behavior of laminated composite plates is strongly dependent on the degree of orthotropy of individual layers, the ratio of transverse shear modulus to the in-plane elastic modulus and the stacking sequence of laminates. Buckling problems which have attracted the attention of many researchers up to the present are among the most important problems for laminated composite plates.

The application of tapered laminate is common in wing and fin skin structures, helicopter rotor blades, yokes, etc. The rotor blades of helicopters or wings of an aircraft have thick section of laminate at roots and thin sections at their tip obtained through termination of plies at different locations. On the other hand, the termination of internal plies is an effective method for stiffness tailoring which is not possible with constant thickness laminates.

The classical laminated plate theory (CLPT) based on ‘Kirchhoff Hypothesis’ is considered in the present chapter. Within the limitation of CLPT, the Ritz method is used

with trigonometric or plate functions as displacement functions. These functions are modified such that the geometric boundary conditions are satisfied.

The [A], [B] and [D] matrices of tapered laminate are calculated considering fiber orientation and taper angle. Applying Ritz method the system of equations for buckling is developed. Critical buckling loads of tapered laminated plates are compared with that of tapered laminated beams, analyzed using finite element method. Finally, different taper models are analyzed for different boundary conditions.

2.4 The [A], [B] and [D] matrices of tapered laminate

2.4.1 Steps to calculate the [A], [B] and [D] matrices of tapered laminate

We shall consider as in the Figure 2.1 a layer of unidirectional material in a tapered laminate with principal directions (x'' , y'' , z''), the plane (x'' , y'') being identified with the plane of the layer and the direction x'' with the direction of the fibers- the warp direction. Tapered laminates make an angle φ with reference axis x and fibers make an angle θ with the direction x' . The angle φ is obtained by rotating laminate about y axis and the angle θ corresponds to the rotation of fibers about z' axis as shown in the Figure 2.1. Further details are shown in Figures 2.2 and 2.3. Throughout this chapter clockwise direction is considered negative and anti-clockwise positive.

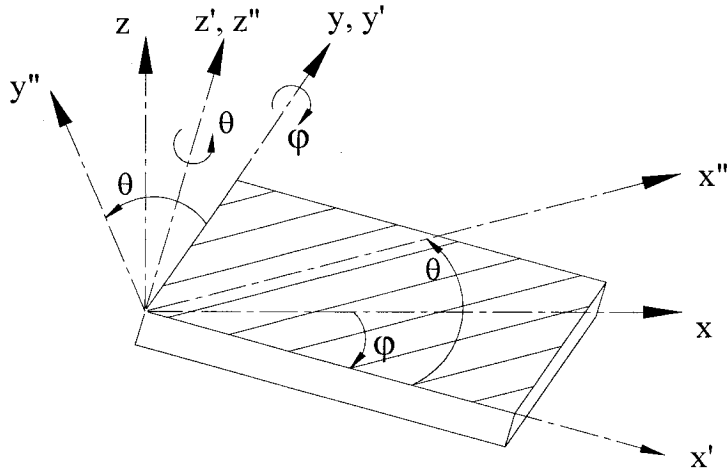


Figure 2.1 Orientation of fibers and laminate

The [A], [B] and [D] matrices are calculated applying the following steps:

Step-1: Calculation of stiffness matrix for transversely isotropic ply.

Step-2: Calculation of stress and strain transformation matrices.

Step-3: Development of stiffness matrix for each ply in the tapered laminate.

Step-4: Calculation of elasticity equations for tapered laminate considering plane stress state.

Step-5: Geometric analysis of tapered laminate and resin pocket.

Step-6: Calculation of [A], [B] and [D] matrices.

2.4.2 Step-1: Stiffness matrix of ply

Hooke's law for orthotropic materials in principal directions can be written as [29]:

$$\begin{Bmatrix} \sigma_{x''x''} \\ \sigma_{y''y''} \\ \sigma_{z''z''} \\ \tau_{y''z''} \\ \tau_{x''z''} \\ \tau_{x''y''} \end{Bmatrix} = \begin{bmatrix} C''_{11} & C''_{12} & C''_{13} & 0 & 0 & 0 \\ C''_{12} & C''_{22} & C''_{23} & 0 & 0 & 0 \\ C''_{13} & C''_{23} & C''_{33} & 0 & 0 & 0 \\ 0 & 0 & 0 & C''_{44} & 0 & 0 \\ 0 & 0 & 0 & 0 & C''_{55} & 0 \\ 0 & 0 & 0 & 0 & 0 & C''_{66} \end{bmatrix} \begin{Bmatrix} \varepsilon_{x''x''} \\ \varepsilon_{y''y''} \\ \varepsilon_{z''z''} \\ \gamma_{y''z''} \\ \gamma_{x''z''} \\ \gamma_{x''y''} \end{Bmatrix} \quad (2.1)$$

where σ''_{ij} and τ''_{ij} are the normal stress and shear stress respectively and, ε''_{ij} and γ''_{ij} are the normal strain and shear strain respectively with $i, j = x'', y'', z''$ in coordinate system $x'' y'' z''$. $C''_{11}, C''_{12}, \dots$ etc are the corresponding stiffness co-efficients.

Equation (2.1) can be expressed as:

$$\{\sigma''\} = [C'']\{\varepsilon''\} \quad (2.2)$$

The stiffness co-efficients are:

$$C''_{11} = (1 - \nu_{23}\nu_{32}) / (E_2 E_3 \Delta) \quad (2.3)$$

$$C''_{12} = (\nu_{12} + \nu_{32}\nu_{13}) / (E_1 E_3 \Delta) \quad (2.4)$$

$$C''_{13} = (\nu_{13} + \nu_{12}\nu_{23}) / (E_1 E_2 \Delta) \quad (2.5)$$

$$C''_{22} = (1 - \nu_{13}\nu_{31}) / (E_1 E_3 \Delta) \quad (2.6)$$

$$C''_{23} = (\nu_{23} + \nu_{21}\nu_{13}) / (E_1 E_2 \Delta) \quad (2.7)$$

$$C''_{33} = (1 - \nu_{12}\nu_{21}) / (E_1 E_2 \Delta) \quad (2.8)$$

$$C''_{44} = G_{23} \quad (2.9)$$

$$C''_{55} = G_{13} \quad (2.10)$$

$$C''_{66} = G_{12} \quad (2.11)$$

$$\Delta = (1 - \nu_{12}\nu_{21} - \nu_{23}\nu_{32} - \nu_{31}\nu_{13} - 2\nu_{21}\nu_{32}\nu_{13}) / (E_1 E_2 E_3) \quad (2.12)$$

where, ν_{ij} , E_{ij} and G_{ij} with $i, j = 1, 2, 3$, are the Poisson's ratios, elastic moduli and shear moduli respectively.

In the case of transversely isotropic ply:

$$\nu_{13} = \nu_{12} \quad (2.13)$$

$$\nu_{32} = \nu_{23} \quad (2.14)$$

$$\nu_{31} = \nu_{13} E_3 / E_1 \quad (2.15)$$

$$\nu_{21} = \nu_{12} E_2 / E_1 \quad (2.16)$$

$$E_3 = E_2 \quad (2.17)$$

$$G_{12} = G_{13} \quad (2.18)$$

2.4.3 Step-2: Stress and strain transformation matrices

2.2.3.1 Axis Transformation For Rotation About z'' Axis (clock-wise rotation)

Direction cosines are tabulated in the following table [30].

	x''	y''	z''
x'	$L_1 = \cos(\theta)$	$L_2 = -\sin(\theta)$	$L_3 = 0$
y'	$M_1 = \sin(\theta)$	$M_2 = \cos(\theta)$	$M_3 = 0$
z'	$N_1 = 0$	$N_2 = 0$	$N_3 = 1$

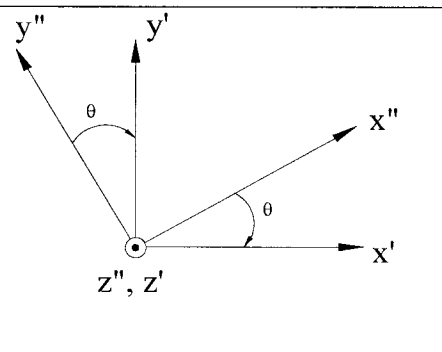


Table 2.1 Direction cosines for rotating x'' and y'' axes about z'' axis

Stress transformation can be expressed applying direction cosines mentioned in the Table 2.1 [31]:

$$\begin{Bmatrix} \sigma_{x'x'} \\ \sigma_{y'y'} \\ \sigma_{z'z'} \\ \tau_{y'z'} \\ \tau_{x'z'} \\ \tau_{x'y'} \end{Bmatrix} = \begin{bmatrix} L_1^2 & L_2^2 & L_3^2 & 2L_2L_3 & 2L_1L_3 & 2L_1L_2 \\ M_1^2 & M_2^2 & M_3^2 & 2M_2M_3 & 2M_1M_3 & 2M_1M_2 \\ N_1^2 & N_2^2 & N_3^2 & 2N_2N_3 & 2N_1N_3 & 2N_1N_2 \\ N_1M_1 & M_2N_2 & M_3N_3 & M_3N_2 + M_2N_3 & M_3N_1 + M_1N_3 & M_2N_1 + M_1N_2 \\ N_1L_1 & L_2N_2 & L_3N_3 & L_3N_2 + L_2N_3 & L_3N_1 + L_1N_3 & L_2N_1 + L_1N_2 \\ L_1M_1 & M_2L_2 & M_3L_3 & L_3M_2 + L_2M_3 & L_3M_1 + L_1M_3 & L_2M_1 + L_1M_2 \end{bmatrix} \begin{Bmatrix} \sigma_{x'x'} \\ \sigma_{y'y'} \\ \sigma_{z'z'} \\ \tau_{y'z'} \\ \tau_{x'z'} \\ \tau_{x'y'} \end{Bmatrix} \quad (2.19)$$

Equation (2.19) can be expressed as:

$$\{\sigma'\} = [T_{\sigma\theta}] \{\sigma''\} \quad (2.20)$$

where $\{\sigma'\}$ and $\{\sigma''\}$ are the stress vectors in coordinate systems $x'y'z'$ and $x''y''z''$ respectively. $[T_{\sigma\theta}]$ is the stress transformation matrix due to fiber orientation angle θ .

Substituting the values of L_i and M_i , $i = 1, 2, 3$, from Table 2.1, transformation matrix $[T_{\sigma\theta}]$ takes the form:

$$[T_{\sigma\theta}] = \begin{bmatrix} \cos^2 \theta & \sin^2 \theta & 0 & 0 & 0 & -2 \cos \theta \sin \theta \\ \sin^2 \theta & \cos^2 \theta & 0 & 0 & 0 & 2 \cos \theta \sin \theta \\ 0 & 0 & 1 & 0 & 0 & 0 \\ 0 & 0 & 0 & \cos \theta & \sin \theta & 0 \\ 0 & 0 & 0 & -\sin \theta & \cos \theta & 0 \\ \cos \theta \sin \theta & -\cos \theta \sin \theta & 0 & 0 & 0 & \cos^2 \theta - \sin^2 \theta \end{bmatrix} \quad (2.21)$$

Similarly, strain transformation can be expressed applying direction cosines mentioned in the Table 2.1 [31]:

$$\begin{Bmatrix} \epsilon_{xx''} \\ \epsilon_{yy''} \\ \epsilon_{zz''} \\ \gamma_{y'z''} \\ \gamma_{x'z''} \\ \gamma_{x'y''} \end{Bmatrix} = \begin{bmatrix} L_1^2 & L_2^2 & L_3^2 & L_2L_3 & L_1L_3 & L_1L_2 \\ M_1^2 & M_2^2 & M_3^2 & M_2M_3 & M_1M_3 & M_1M_2 \\ N_1^2 & N_2^2 & N_3^2 & N_2N_3 & N_1N_3 & N_1N_2 \\ 2N_1M_1 & 2M_2N_2 & 2M_3N_3 & M_3N_2 + M_2N_3 & M_3N_1 + M_1N_3 & M_2N_1 + M_1N_2 \\ 2N_1L_1 & 2L_2N_2 & 2L_3N_3 & L_3N_2 + L_2N_3 & L_3N_1 + L_1N_3 & L_2N_1 + L_1N_2 \\ 2L_1M_1 & 2M_2L_2 & 2M_3L_3 & L_3M_2 + L_2M_3 & L_3M_1 + L_1M_3 & L_2M_1 + L_1M_2 \end{bmatrix} \begin{Bmatrix} \epsilon_{xx''} \\ \epsilon_{yy''} \\ \epsilon_{zz''} \\ \gamma_{y'z''} \\ \gamma_{x'z''} \\ \gamma_{x'y''} \end{Bmatrix} \quad (2.22)$$

It can be written as:

$$\{\varepsilon'\} = [T_{\varepsilon\theta}]\{\varepsilon''\} \quad (2.23)$$

where $\{\varepsilon'\}$ and $\{\varepsilon''\}$ are the strain vectors in coordinate systems $x'y'z'$ and $x''y''z''$ respectively. In terms of fiber orientation angle θ the strain transformation matrix, $[T_{\varepsilon\theta}]$, can be defined as:

$$[T_{\varepsilon\theta}] = \begin{bmatrix} \cos^2 \theta & \sin^2 \theta & 0 & 0 & 0 & -\cos\theta \sin\theta \\ \sin^2 \theta & \cos^2 \theta & 0 & 0 & 0 & \cos\theta \sin\theta \\ 0 & 0 & 1 & 0 & 0 & 0 \\ 0 & 0 & 0 & \cos\theta & \sin\theta & 0 \\ 0 & 0 & 0 & -\sin\theta & \cos\theta & 0 \\ 2\cos\theta \sin\theta & -2\cos\theta \sin\theta & 0 & 0 & 0 & \cos^2 \theta - \sin^2 \theta \end{bmatrix} \quad (2.24)$$

From equations (2.21) and (2.24) we can relate the stress and strain transformation matrices as:

$$[T_{\varepsilon\theta}]^{-1} = [T_{\sigma\theta}]^t \quad (2.25)$$

$$[T_{\sigma\theta}]^{-1} = [T_{\varepsilon\theta}]^t \quad (2.26)$$

where, superscript 't' denotes the transpose.

2.2.3.2 Rotation of laminate about y' axis (clock-wise rotation)

Direction cosines are tabulated in the following table [30].

	x'	y'	z'	
x	$L_1 = \cos(\varphi)$	$L_2 = 0$	$L_3 = \sin(\varphi)$	
y	$M_1 = 0$	$M_2 = 1$	$M_3 = 0$	
z	$N_1 = -\sin(\varphi)$	$N_2 = 0$	$N_3 = \cos(\varphi)$	

Table 2.2 Direction cosines for rotation of laminate about y' axis.

Stress transformation can be expressed applying direction cosines mentioned in the Table 2.2 [31]:

$$\begin{Bmatrix} \sigma_{xx} \\ \sigma_{yy} \\ \sigma_{zz} \\ \tau_{yz} \\ \tau_{xz} \\ \tau_{xy} \end{Bmatrix} = \begin{bmatrix} L_1^2 & L_2^2 & L_3^2 & 2L_2L_3 & 2L_1L_3 & 2L_1L_2 \\ M_1^2 & M_2^2 & M_3^2 & 2M_2M_3 & 2M_1M_3 & 2M_1M_2 \\ N_1^2 & N_2^2 & N_3^2 & 2N_2N_3 & 2N_1N_3 & 2N_1N_2 \\ N_1M_1 & M_2N_2 & M_3N_3 & M_3N_2 + M_2N_3 & M_3N_1 + M_1N_3 & M_2N_1 + M_1N_2 \\ N_1L_1 & L_2N_2 & L_3N_3 & L_3N_2 + L_2N_3 & L_3N_1 + L_1N_3 & L_2N_1 + L_1N_2 \\ L_1M_1 & M_2L_2 & M_3L_3 & L_3M_2 + L_2M_3 & L_3M_1 + L_1M_3 & L_2M_1 + L_1M_2 \end{bmatrix} \begin{Bmatrix} \sigma_{x'x'} \\ \sigma_{y'y'} \\ \sigma_{z'z'} \\ \tau_{y'z'} \\ \tau_{x'z'} \\ \tau_{x'y'} \end{Bmatrix} \quad (2.27)$$

Equation (2.27) can be expressed as:

$$\{\sigma\} = [T_{\sigma\varphi}] \{\sigma'\} \quad (2.28)$$

where $\{\sigma\}$ and $\{\sigma'\}$ are the stress vectors in coordinate systems xyz and $x'y'z'$ respectively. $[T_{\sigma\varphi}]$ is the stress transformation matrix due to taper angle φ .

Substituting the values of L_i and M_i , $i = 1, 2, 3$, from Table 2.2 the transformation matrix, $[T_{\sigma\varphi}]$, can be defined as:

$$[T_{\sigma\varphi}] = \begin{bmatrix} \cos^2 \varphi & 0 & \sin^2 \varphi & 0 & 2 \cos \varphi \sin \varphi & 0 \\ 0 & 1 & 0 & 0 & 0 & 0 \\ \sin^2 \varphi & 0 & \cos^2 \varphi & 0 & -2 \cos \varphi \sin \varphi & 0 \\ 0 & 0 & 0 & \cos(\varphi) & 0 & -\sin \varphi \\ -\cos \varphi \sin \varphi & 0 & \cos \varphi \sin \varphi & 0 & \cos^2 \varphi - \sin^2 \varphi & 0 \\ 0 & 0 & 0 & \sin \varphi & 0 & \cos \varphi \end{bmatrix} \quad (2.29)$$

Similarly, strain transformation can be expressed applying direction cosines mentioned in the Table 2.2 [31]:

$$\begin{Bmatrix} \varepsilon_{xx} \\ \varepsilon_{yy} \\ \varepsilon_{zz} \\ \gamma_{yz} \\ \gamma_{xz} \\ \gamma_{xy} \end{Bmatrix} = \begin{bmatrix} L_1^2 & L_2^2 & L_3^2 & L_2L_3 & L_1L_3 & L_1L_2 \\ M_1^2 & M_2^2 & M_3^2 & M_2M_3 & M_1M_3 & M_1M_2 \\ N_1^2 & N_2^2 & N_3^2 & N_2N_3 & N_1N_3 & N_1N_2 \\ 2N_1M_1 & 2M_2N_2 & 2M_3N_3 & M_3N_2 + M_2N_3 & M_3N_1 + M_1N_3 & M_2N_1 + M_1N_2 \\ 2N_1L_1 & 2L_2N_2 & 2L_3N_3 & L_3N_2 + L_2N_3 & L_3N_1 + L_1N_3 & L_2N_1 + L_1N_2 \\ 2L_1M_1 & 2M_2L_2 & 2M_3L_3 & L_3M_2 + L_2M_3 & L_3M_1 + L_1M_3 & L_2M_1 + L_1M_2 \end{bmatrix} \begin{Bmatrix} \varepsilon_{x'x'} \\ \varepsilon_{y'y'} \\ \varepsilon_{z'z'} \\ \gamma_{y'z'} \\ \gamma_{x'z'} \\ \gamma_{x'y'} \end{Bmatrix} \quad (2.30)$$

Equation (2.30) can be written as:

$$\{\varepsilon\} = [T_{\varepsilon\varphi}] \{\varepsilon'\} \quad (2.31)$$

where $\{\varepsilon\}$ and $\{\varepsilon'\}$ are the strain vectors in coordinate systems xyz and $x'y'z'$ respectively. In terms of taper angle φ the strain transformation matrix, $[T_{\varepsilon\varphi}]$, can be defined as:

$$[T_{\varepsilon\varphi}] = \begin{bmatrix} \cos^2 \varphi & 0 & \sin^2 \varphi & 0 & \cos \varphi \sin \varphi & 0 \\ 0 & 1 & 0 & 0 & 0 & 0 \\ \sin^2 \varphi & 0 & \cos^2 \varphi & 0 & -\cos \varphi \sin \varphi & 0 \\ 0 & 0 & 0 & \cos \varphi & 0 & -\sin \varphi \\ -2 \cos \varphi \sin \varphi & 0 & 2 \cos \varphi \sin \varphi & 0 & \cos^2 \varphi - \sin^2 \varphi & 0 \\ 0 & 0 & 0 & \sin \varphi & 0 & \cos \varphi \end{bmatrix} \quad (2.32)$$

From equations (2.29) and (2.32) the stress and strain transformation matrices can be related as:

$$[T_{\varepsilon\varphi}]^{-1} = [T_{\sigma\varphi}]^t \quad (2.33)$$

$$[T_{\sigma\varphi}]^{-1} = [T_{\varepsilon\varphi}]^t \quad (2.34)$$

2.2.4 Step-3: Stiffness matrix of each ply in the tapered laminate

2.2.4.1 Accounting for the taper and fiber angles

To account for the taper and fiber angles in the stiffness equation with respect to the reference co-ordinates we need to know the relative orientation of reference co-ordinates with respect to ply material co-ordinates. To do so, we first rotate laminate about y axis, then fiber orientation is obtained by rotating about z' axis ($xyz \rightarrow x'y'z' \rightarrow x''y''z''$). Due to anti-clockwise rotation the taper angle (φ) and fiber orientation angle (θ) of Figure 2.3 are positive.

The procedure is shown in the following Figures:

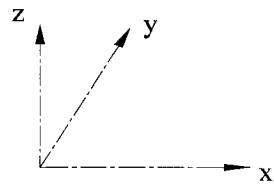


Fig.-2.2.a

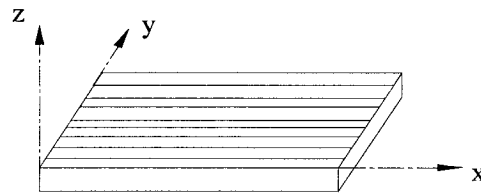


Fig.-2.2.b

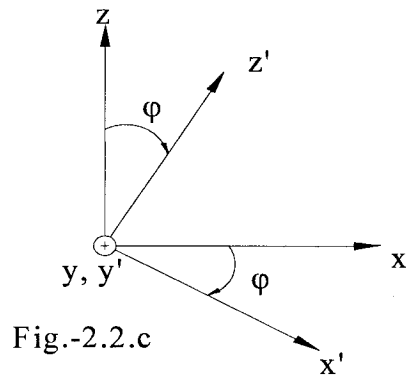


Fig.-2.2.c

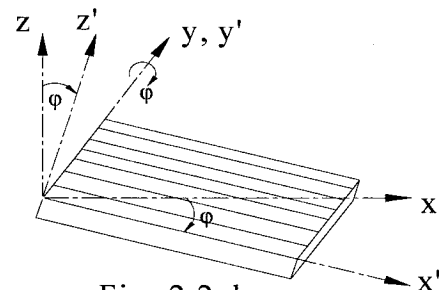


Fig.-2.2.d

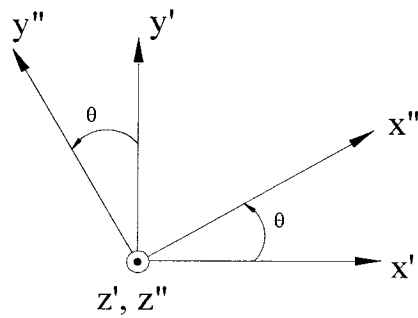


Fig.-2.2.e

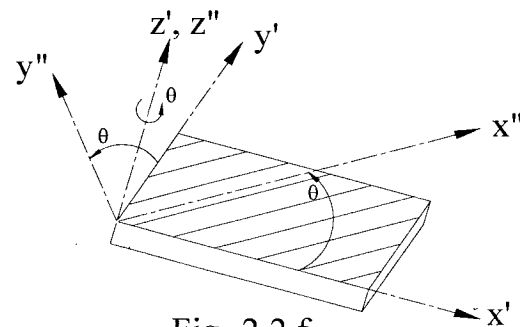


Fig.-2.2.f

Figure 2.2 Laminate and ply material co-ordinates

The tapered laminate is shown below:

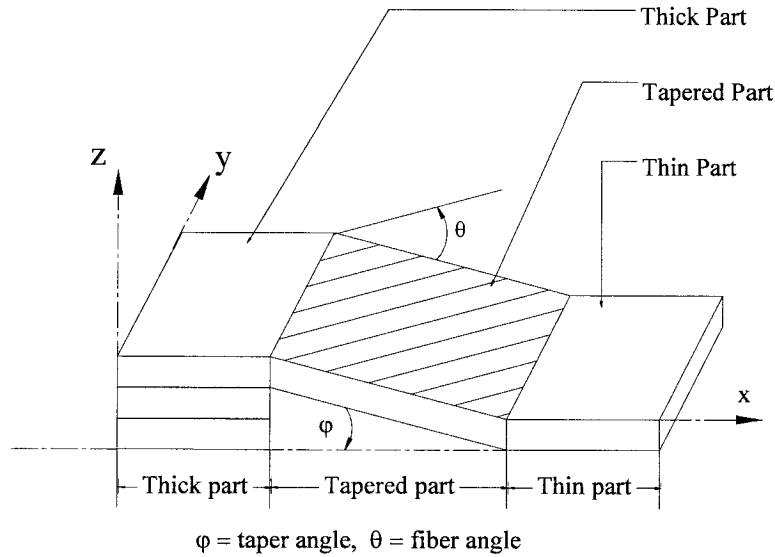


Figure 2.3 Final orientation of ply after rotation

2.2.4.2 Tapered laminate stiffness calculation

The elastic properties of a layer are given in its principal directions by the equation (2.1) but the final form of the equations are in reference co-ordinates, so layer properties should be transformed to reference directions from its principal directions through the following rotations.

--First, rotation of x'' and y'' about z'' axis (see Figure inside Table 2.1)

--Second, rotation of x' and z' about y' axis (see Figure inside Table 2.2)

Combining equations (2.20) and (2.28) we get,

$$\{\sigma\} = [T_{\sigma\phi}] [T_{\sigma\theta}] \{\sigma''\} \quad (2.35)$$

From equations (2.23) and (2.31) we get

$$\{\varepsilon\} = [T_{\varepsilon\phi}] [T_{\varepsilon\theta}] \{\varepsilon''\} \quad (2.36)$$

Solving for $\{\sigma''\}$ and $\{\varepsilon''\}$ from equations (2.35) and (2.36) and using those values into equation (2.2) and combining the equations (2.25) and (2.33) we get:

$$\{\sigma\} = [T_{\sigma\phi}] [T_{\sigma\theta}] [C''] [T_{\sigma\theta}]^t [T_{\sigma\phi}]^t \{\varepsilon\} \quad (2.37)$$

The above equation can be expressed in a short form:

$$[\sigma] = [C] \{\varepsilon\} \quad (2.38)$$

Thus, the stiffness matrix $[C]$ in the reference coordinate system xyz can be expressed by the stiffness matrix $[C'']$ in the principal coordinate system $x''y''z''$ and the transformation matrices as:

$$[C] = [T_{\sigma\phi}] [T_{\sigma\theta}] [C''] [T_{\sigma\theta}]^t [T_{\sigma\phi}]^t \quad (2.39)$$

The values of $[C'']$, $[T_{\sigma\theta}]$ and $[T_{\sigma\phi}]$ are given in the equations (2.1), (2.21) and (2.29) respectively.

2.2.5 Step-4: Elasticity equations for plane stress state

In case of plane stress state,

$$\sigma_i \neq 0 \quad \text{if } i = 1, 2, 6 \quad (2.40)$$

$$\varepsilon_i \neq 0 \quad \text{if } i = 1, 2, 3, 6 \quad (2.41)$$

$$\sigma_i = 0 \quad \text{if } i = 3, 4, 5 \quad (2.42)$$

$$\varepsilon_i = 0 \quad \text{if } i = 4, 5 \quad (2.43)$$

where, σ_i and ε_i are the stress and strain respectively in the reference co-ordinate system xyz.

Applying equations (2.40 - 2.43) in equation (2.38):

$$\begin{Bmatrix} \sigma_1 \\ \sigma_2 \\ \sigma_3 = 0 \\ \sigma_4 = 0 \\ \sigma_5 = 0 \\ \sigma_6 \end{Bmatrix}_{xyz} = \begin{bmatrix} C_{11} & C_{12} & C_{13} & C_{14} & C_{15} & C_{16} \\ C_{12} & C_{22} & C_{23} & C_{24} & C_{25} & C_{26} \\ C_{13} & C_{23} & C_{33} & C_{34} & C_{35} & C_{36} \\ C_{14} & C_{24} & C_{34} & C_{44} & C_{45} & C_{46} \\ C_{15} & C_{25} & C_{35} & C_{45} & C_{55} & C_{56} \\ C_{16} & C_{26} & C_{36} & C_{46} & C_{56} & C_{66} \end{bmatrix} \begin{Bmatrix} \varepsilon_1 \\ \varepsilon_2 \\ \varepsilon_3 \\ \varepsilon_4 = 0 \\ \varepsilon_5 = 0 \\ \varepsilon_6 \end{Bmatrix}_{xyz} \quad (2.44)$$

And also:

$$\sigma_1 = C_{11}\varepsilon_1 + C_{12}\varepsilon_2 + C_{13}\varepsilon_3 + C_{16}\varepsilon_6 \quad (2.45)$$

$$\sigma_2 = C_{12}\varepsilon_1 + C_{22}\varepsilon_2 + C_{23}\varepsilon_3 + C_{26}\varepsilon_6 \quad (2.46)$$

$$0 = C_{13}\varepsilon_1 + C_{23}\varepsilon_2 + C_{33}\varepsilon_3 + C_{36}\varepsilon_6 \quad (2.47)$$

$$\sigma_6 = C_{16}\varepsilon_1 + C_{26}\varepsilon_2 + C_{36}\varepsilon_3 + C_{66}\varepsilon_6 \quad (2.48)$$

Solving equations (2.45 - 2.48) :

$$\varepsilon_3 = -(1/C_{33})(C_{13}\varepsilon_1 + C_{23}\varepsilon_2 + C_{36}\varepsilon_6) \quad (2.49)$$

$$\sigma_1 = (C_{11} - C_{13}^2/C_{33})\varepsilon_1 + (C_{12} - C_{13}C_{23}/C_{33})\varepsilon_2 + (C_{16} - C_{13}C_{36}/C_{33})\varepsilon_6 \quad (2.50)$$

Equations for σ_2 and σ_6 are analogous to that for σ_1 .

Therefore, the reduced stiffness matrix is in the form:

$$\begin{Bmatrix} \sigma_1 \\ \sigma_2 \\ \sigma_6 \end{Bmatrix}_{xyz} = \begin{bmatrix} Q_{11} & Q_{12} & Q_{16} \\ Q_{12} & Q_{22} & Q_{26} \\ Q_{16} & Q_{26} & Q_{66} \end{bmatrix} \begin{Bmatrix} \varepsilon_1 \\ \varepsilon_2 \\ \varepsilon_6 \end{Bmatrix}_{xyz} \quad (2.51)$$

where,

$$Q_{11} = C_{11} - C_{13}^2/C_{33} \quad (2.52)$$

Considering slope φ , the following two trigonometric relations can be written:

$$(h_k)_y = -\tan(\varphi) * x + (h_o)_k \quad (2.60)$$

$$(h_{k-1})_y = -\tan(\varphi) * x + (h_o)_{k-1} \quad (2.61)$$

Therefore, from the equations (2.58), (2.60) and (2.61) we get:

$$(Z_k)_y = -\tan(\varphi) * x + h_i \quad (2.62)$$

$$\text{where, } h_i = ((h_o)_k + (h_o)_{k-1})/2 \quad \text{and } i = 1, 2, \dots, n \quad (2.63)$$

2.2.6.2 Resin pocket

Resin pocket is represented as a combination of inclined imaginary isotropic plies [16]. Resin pocket is divided as needed. In the Figure 2.5 resin pocket is divided into two parts by the line 'de'. Area 'A-d-e-C' = area 'A-d-h-i' as $\Delta ehy = \Delta yiC$. Similarly area 'd-B-e' = area 'd-B-f-g' as $\Delta Bfx = \Delta xge$; where Δ represents the area of specified triangle.

Stiffness of each ply is calculated separately and cumulative stiffness is the total stiffness of resin pocket.

The parameter (e_k) and the distance from the ply centre to mid-plane (z_k) of resin plies are calculated using the equations (2.59) and (2.62) respectively. Variable length, L_i , is calculated as follows:

$$L_i = \cot(\varphi) [(T_t/N_r) * i - (T_t / (2 * N_r))] \quad (2.64)$$

where,

T_t = Thickness of composite lamina,

N_r = No. of divisions of each lamina,

2.3 Analysis of Transformed Reduced Stiffness (TRS), Q_{ij}

A computer program is written in MATLAB[®] to compute and plot the values of transformed reduced stiffness, Q_{ij} , $i, j = 1, 2, 6$ as a function of φ and θ ; where the range of angles in plot are: $-20^\circ \leq \varphi \leq 20^\circ$ and $-90^\circ \leq \theta \leq 90^\circ$ for two dimensional plot, and $-90^\circ \leq \varphi \leq 90^\circ$ and $-90^\circ \leq \theta \leq 90^\circ$ for three dimensional plot. In practice, taper angle φ varies from 2° to 15° .

2.3.1 Plots of Q_{ij}

Figures 2.6 to 2.8 show the plots of Q_{ij} with constant taper angle (φ) and varying ply orientation angle (θ). On the other hand Figures 2.9 to 2.11 show the plots of Q_{ij} with constant θ and varying φ . And the Figure 2.12 is the plot of Q_{ij} where both φ and θ vary.

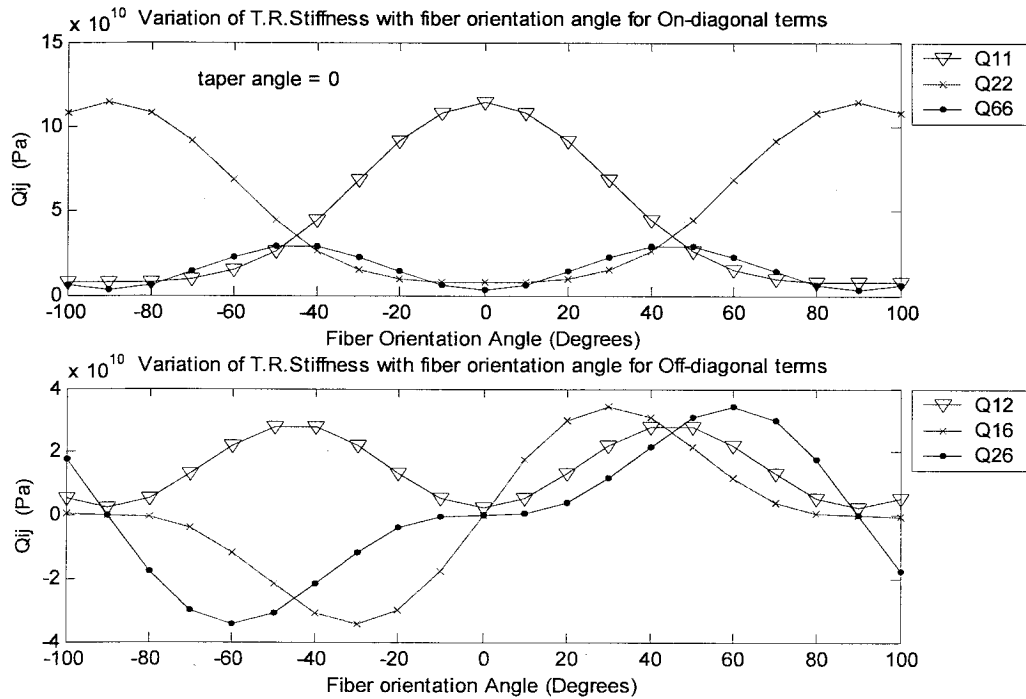


Figure 2.6 Plot Of Q_{ij} For Constant Taper Angle (0°) And Varying Fiber Orientation Angle

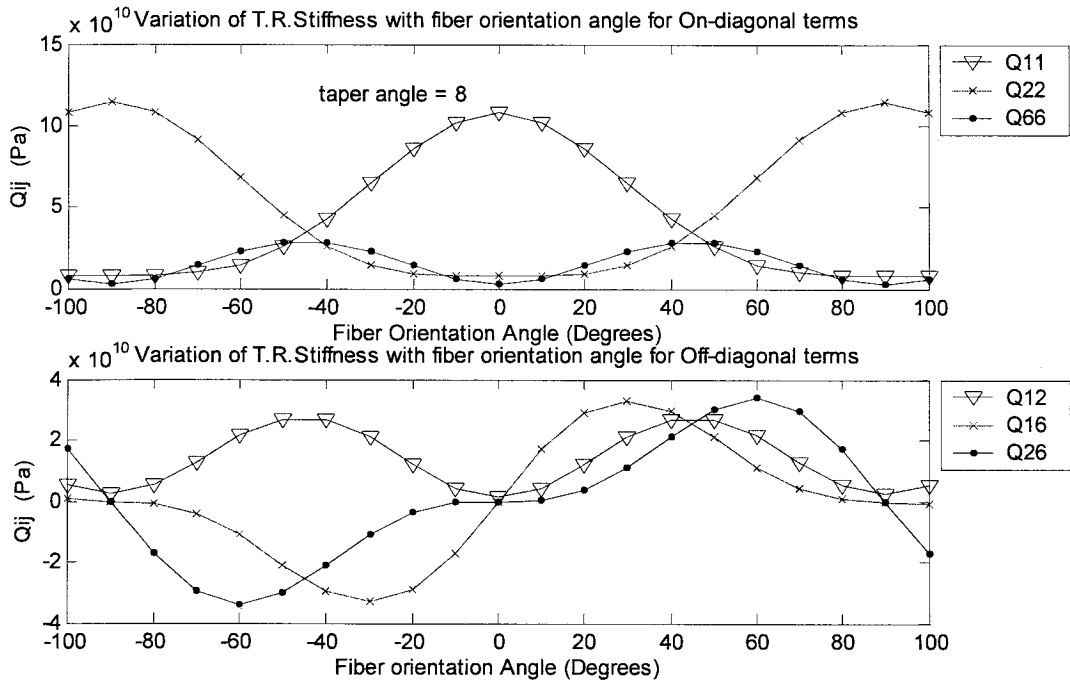


Figure 2.7 Plot Of Q_{ij} For Constant Taper Angle (8°) And Varying Fiber Orientation Angle

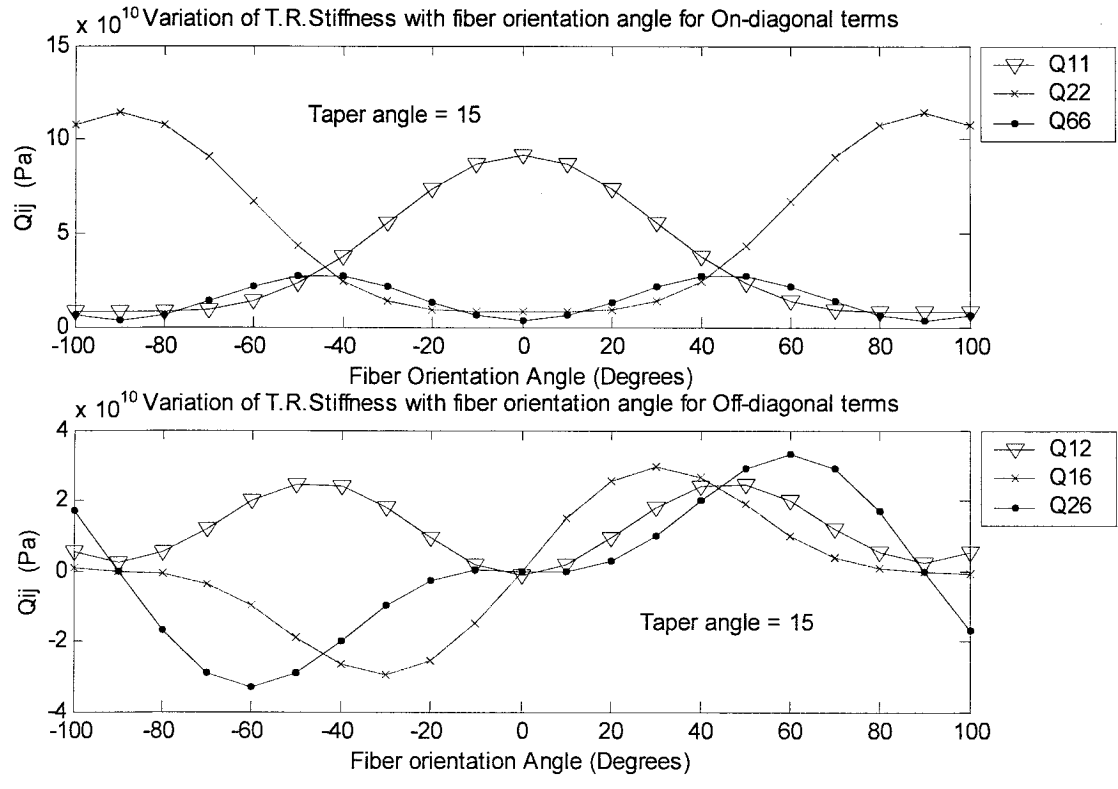


Figure 2.8 Plot Of Q_{ij} For Constant Taper Angle (15°) And Varying Fiber Orientation Angle

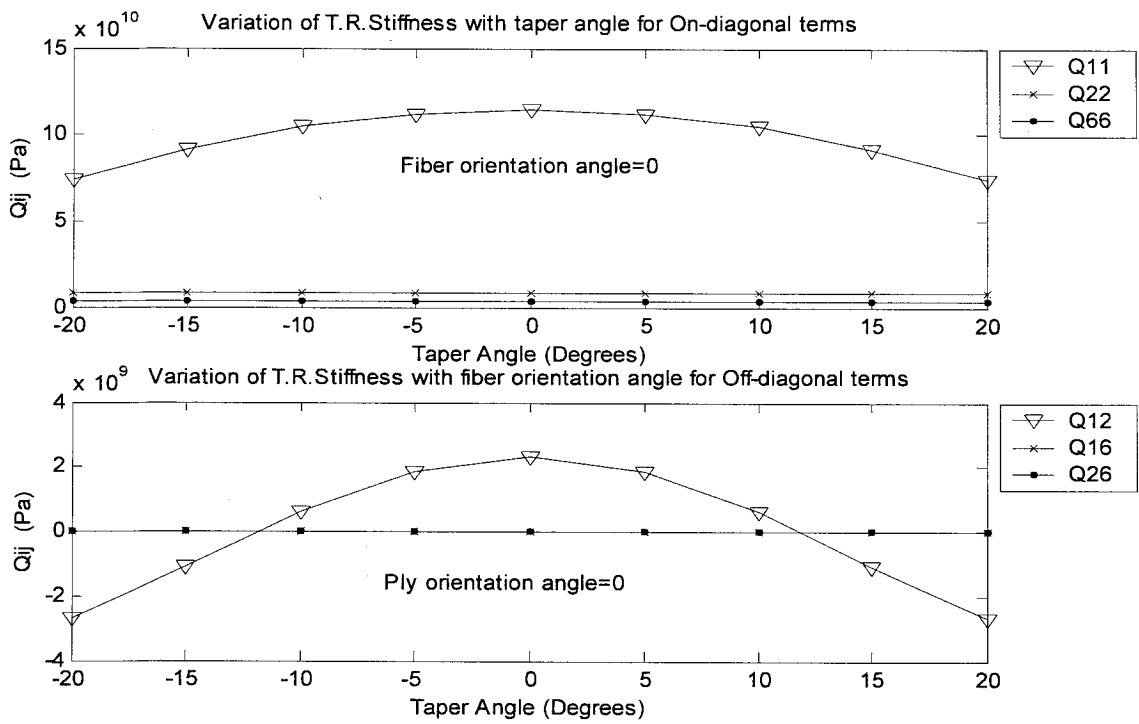


Figure 2.9 Plot Of Q_{ij} For Constant Fiber Orientation Angle (0°) And Varying Taper Angle

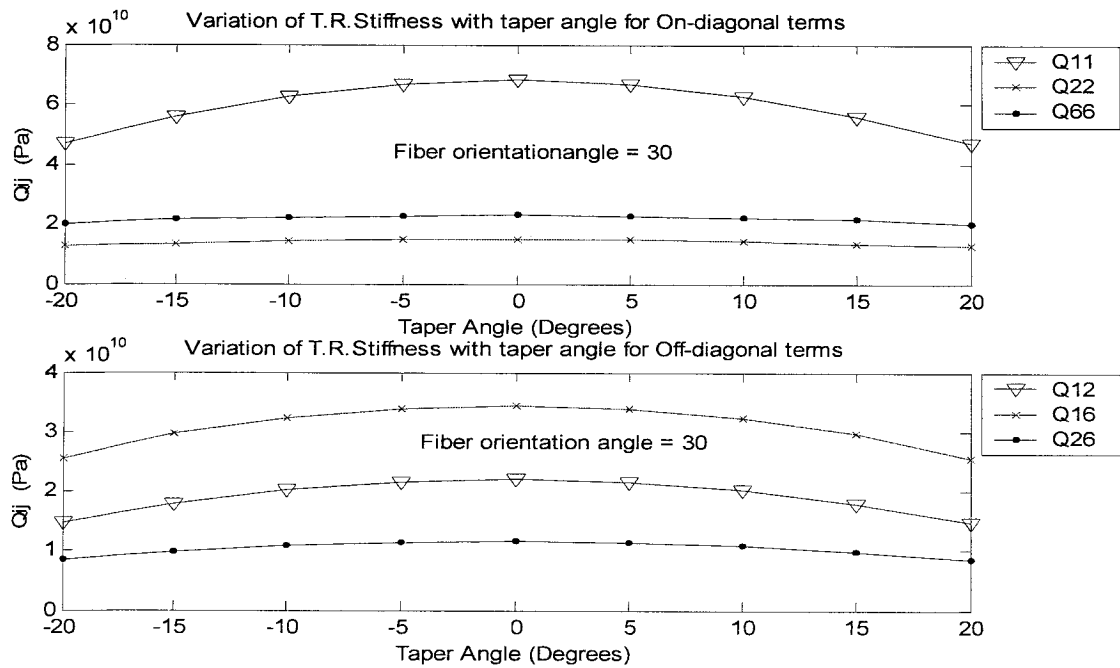


Figure 2.10 Plot Of Q_{ij} For Constant Fiber Orientation Angle (30°) And Varying Taper Angle

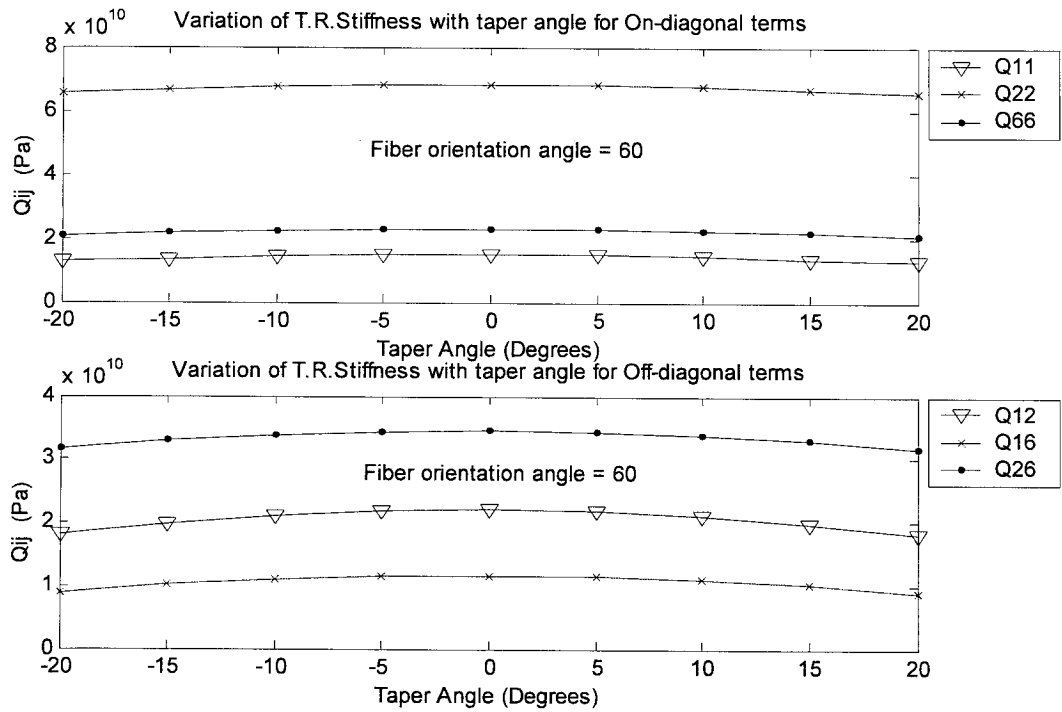


Figure 2.11 Plot Of Q_{ij} For Constant Fiber Orientation Angle (60°) And Varying Taper Angle

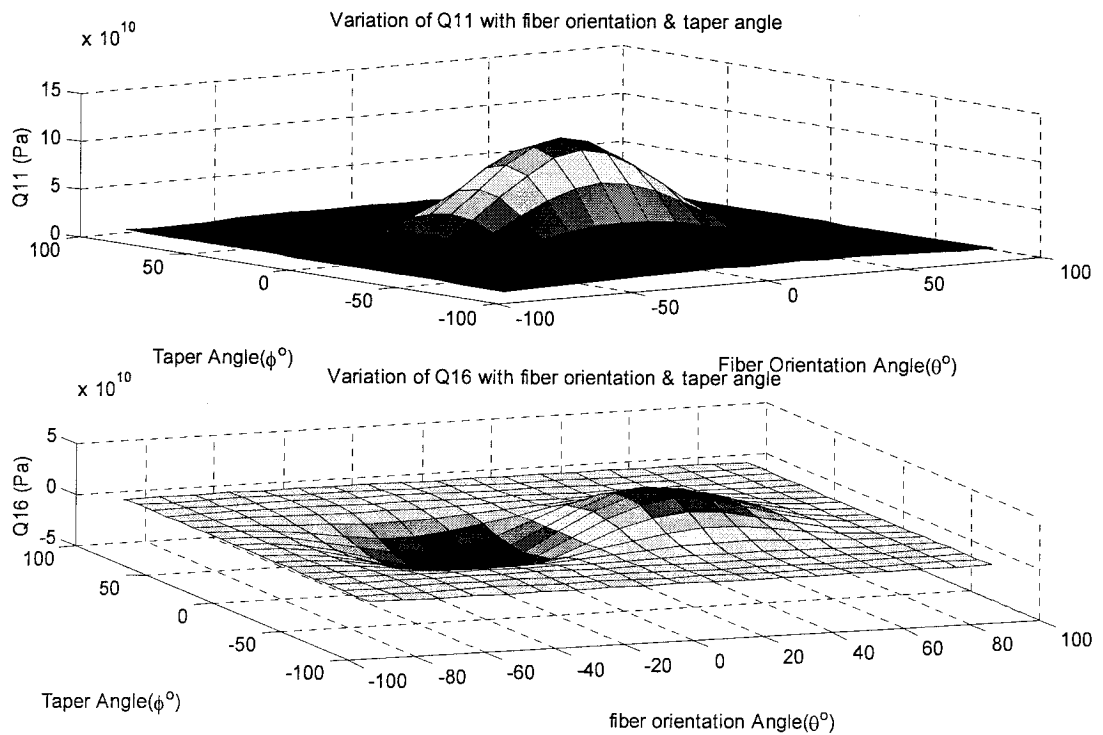


Figure 2.12 Plot Of Q_{ij} When Both Fiber Orientation Angle And Taper Angle Vary

2.3.2 Observations from Q_{ij} plots

- In the Figures 2.6, 2.7 and 2.8 the values of Q_{ij} change rapidly with the increase of fiber orientation angle, θ .
- On the other hand, in the Figures 2.9, 2.10 and 2.11 the values of Q_{ij} change at a rate slower than that in previous Figures with the increase of taper angle, φ .
- The co-efficients Q_{22} , Q_{16} and Q_{26} are sensitive to fiber orientation angle (θ) for a given taper angle (φ).
- On the other hand, Q_{11} and Q_{12} are sensitive to both taper angle (φ) and fiber orientation angle (θ).
- In the Figure 2.12 only one on-diagonal stiffness, Q_{11} and one off-diagonal stiffness, Q_{16} are plotted. The fiber orientation angles have more influence on Q_{ij} than the taper angles.

2.4 Buckling analysis of tapered plate using Ritz method

In the case of a tapered plate with various boundary conditions on the edges the exact solutions to the buckling problem are not available as the terms D_{16} and D_{26} introduce odd derivatives of w_0 . Therefore, approximate methods such as the Ritz method have to be used.

2.4.1 General expressions for buckling analysis

Strain energy of a laminate based on classical laminated plate theory, for which $\sigma_{zz} = 0$, $\gamma_{xz} = \gamma_{yz} = 0$, can be written as [17]:

$$U = 1/2 \iint_A \left[\{\varepsilon^o\} [A] \{\varepsilon^o\} + 2 \{\varepsilon^o\} [B] \{\kappa\} + \{\kappa\} [D] \{\kappa\} \right] dx dy \quad (2.68)$$

where, $\{\varepsilon^o\}$ and $\{\kappa\}$ are the mid-plane strain matrix and curvature matrix respectively that are expressed as:

$$\{\varepsilon^o\} = \begin{Bmatrix} \varepsilon_x^o \\ \varepsilon_y^o \\ \gamma_{xy}^o \end{Bmatrix} = \begin{Bmatrix} \frac{\partial u_o}{\partial x} \\ \frac{\partial v_o}{\partial y} \\ \frac{\partial u_o}{\partial y} + \frac{\partial v_o}{\partial x} \end{Bmatrix} \quad (2.69)$$

$$\{\kappa\} = \begin{Bmatrix} \kappa_x^o \\ \kappa_y^o \\ \kappa_{xy}^o \end{Bmatrix} = \begin{Bmatrix} -\frac{\partial^2 w_o}{\partial x^2} \\ -\frac{\partial^2 w_o}{\partial y^2} \\ -2 \frac{\partial^2 w_o}{\partial x \partial y} \end{Bmatrix} \quad (2.70)$$

where, u_o , v_o and w_o are the mid-plane displacements in x, y and z directions.

The matrices [A], [B] and [D] are given by the equations (2.65), (2.66) and (2.67) respectively.

Following assumptions are considered [29]:

- Initial curvature (pre-buckling) is neglected, $w_o^i = 0$;
- Laminate is symmetric, $B_{ij} = 0$;
- Pure bending, $u_o = v_o = 0$.

Considering these assumptions the equation (2.68) becomes:

$$U = 1/2 \iint_A \{\kappa\}^T [D] \{\kappa\} dx dy \quad (2.71)$$

$$U = 1/2 \int_{y=0}^b \int_{x=0}^L \left[D_{11} \left(\frac{\partial^2 w_o}{\partial x^2} \right)^2 + 2D_{12} \left(\frac{\partial^2 w_o}{\partial x^2} \cdot \frac{\partial^2 w_o}{\partial y^2} \right) + D_{22} \left(\frac{\partial^2 w_o}{\partial y^2} \right)^2 + 4 \left(D_{16} \frac{\partial^2 w_o}{\partial x^2} + D_{26} \frac{\partial^2 w_o}{\partial y^2} \right) \frac{\partial^2 w_o}{\partial x \partial y} + 4D_{66} \left(\frac{\partial^2 w_o}{\partial x \partial y} \right)^2 \right] dx dy + C \quad (2.72)$$

The potential energy owed to the uniaxial load N_x is:

$$W = -(1/2) \iint_A N_x \left(\frac{\partial w_o}{\partial x} \right)^2 dx dy \quad (2.73)$$

The approximate solution is expressed as a double series:

$$w_o(x, y) = \sum_{m=1}^M \sum_{n=1}^N A_{mn} X_m(x) Y_n(y) \quad (2.74)$$

The functions $X_m(x)$ and $Y_n(y)$ are chosen so as to satisfy the boundary conditions and the co-efficients A_{mn} are determined by the stationarity condition:

$$\frac{\partial U}{\partial A_{mn}} = \frac{\partial W}{\partial A_{mn}} \quad (2.75)$$

where U and W are given by the equations (2.72) and (2.73) respectively.

Now applying the approximate solution of w_o , equation (2.74), into equations

(2.72) and (2.73) and differentiating with respect to A_{mn} , we get [29]:

$$\begin{aligned}
\frac{\partial U}{\partial A_{mn}} = & \sum_{i=1}^M \sum_{j=1}^N \left\{ \int_0^L D_{11} \frac{d^2 X_m}{dx^2} \frac{d^2 X_i}{dx^2} dx \int_0^b Y_n Y_j dy \right. \\
& + \left[\int_0^L D_{12} X_m \frac{d^2 X_i}{dx^2} dx \int_0^b \frac{d^2 Y_n}{dy^2} Y_j dy + \int_0^L D_{12} \frac{d^2 X_m}{dx^2} X_i dx \int_0^b Y_n \frac{d^2 Y_j}{dy^2} dy \right] \\
& + \int_0^L D_{22} X_m X_i dx \int_0^b \frac{d^2 Y_n}{dy^2} \frac{d^2 Y_j}{dy^2} dy + 4 \int_0^L D_{66} \frac{dX_m}{dx} \frac{dX_i}{dx} dx \int_0^b \frac{dY_n}{dy} \frac{dY_j}{dy} dy \\
& + 2 \left[\int_0^L D_{16} \frac{dX_m}{dx} \frac{d^2 X_i}{dx^2} dx \int_0^b \frac{dY_n}{dy} Y_j dy + \int_0^L D_{16} \frac{d^2 X_m}{dx^2} \frac{dX_i}{dx} dx \int_0^b Y_n \frac{dY_j}{dy} dy \right] \\
& \left. + 2 \left[\int_0^L D_{26} X_m \frac{dX_i}{dx} dx \int_0^b \frac{d^2 Y_n}{dy^2} \frac{dY_j}{dy} dy + \int_0^L D_{26} \frac{dX_m}{dx} X_i dx \int_0^b \frac{dY_n}{dy} \frac{d^2 Y_j}{dy^2} dy \right] \right\} A_{ij}
\end{aligned} \tag{2.76}$$

$$\frac{\partial w}{\partial A_{mn}} = \sum_{i=1}^M \sum_{j=1}^N \left\{ N_o \int_0^L \frac{dX_m}{dx} \frac{dX_i}{dx} dx \int_0^b Y_n Y_j dy \right\} A_{ij} \tag{2.77}$$

where $N_o = -N_x$; L and b are the total length and width respectively of the laminated plate.

2.4.2 Buckling analysis of thick part

For thick part $(D_{ij})_a$ is calculated from equation (2.67) by setting the taper angle to zero ($\varphi = 0$) and differentiating potential and strain energy equations with respect to A_{mn} :

$$\frac{\partial W_a}{\partial A_{mn}} = \sum_{i=1}^M \sum_{j=1}^N \left\{ N_o \int_0^{L_a} \frac{dX_m}{dx} \frac{dX_i}{dx} dx \int_0^b Y_n Y_j dy \right\} \tag{2.78}$$

where, L_a is the length of thick part of the laminated plate and subscript 'a' stands for thick part.

$$\begin{aligned}
\frac{\partial U_a}{\partial A_{mn}} = & \sum_{i=1}^M \sum_{j=1}^N \left\{ \int_0^{La} (D_{11})_a \frac{d^2 X_m}{dx^2} \frac{d^2 X_i}{dx^2} dx \int_0^b Y_n Y_j dy \right. \\
& + \left[\int_0^{La} (D_{12})_a X_m \frac{d^2 X_i}{dx^2} dx \int_0^b \frac{d^2 Y_n}{dy^2} Y_j dy + \int_0^{La} (D_{12})_a \frac{d^2 X_m}{dx^2} X_i dx \int_0^b Y_n \frac{d^2 Y_j}{dy^2} dy \right] \\
& + \int_0^{La} (D_{22})_a X_m X_i dx \int_0^b \frac{d^2 Y_n}{dy^2} \frac{d^2 Y_j}{dy^2} dy + 4 \int_0^{La} (D_{66})_a \frac{dX_m}{dx} \frac{dX_i}{dx} dx \int_0^b \frac{dY_n}{dy} \frac{dY_j}{dy} dy \\
& + 2 \left[\int_0^{La} (D_{16})_a \frac{dX_m}{dx} \frac{d^2 X_i}{dx^2} dx \int_0^b \frac{dY_n}{dy} Y_j dy + \int_0^{La} (D_{16})_a \frac{d^2 X_m}{dx^2} \frac{dX_i}{dx} dx \int_0^b Y_n \frac{dY_j}{dy} dy \right] \\
& \left. + 2 \left[\int_0^{La} (D_{26})_a X_m \frac{dX_i}{dx} dx \int_0^b \frac{d^2 Y_n}{dy^2} \frac{dY_j}{dy} dy + \int_0^{La} (D_{26})_a \frac{dX_m}{dx} X_i dx \int_0^b \frac{dY_n}{dy} \frac{d^2 Y_j}{dy^2} dy \right] \right\} A_{mn}
\end{aligned} \tag{2.79}$$

2.4.3 Buckling analysis of tapered part

Tapered part of laminated plate is divided into two parts: transversely isotropic tapered laminate and isotropic resin pocket.

2.4.3.1 Laminate

$(D_{ij})_b$ is calculated from the equation (2.67) using the values of Q_{ij} from equations (2.52 - 2.57) and differentiating potential and strain energy equations with respect to A_{mn} :

$$\frac{\partial W_b}{\partial A_{mn}} = \sum_{i=1}^M \sum_{j=1}^N \left\{ N_o \int_0^{Lb} \frac{dX_m}{dx} \frac{dX_i}{dx} dx \int_0^b Y_n Y_j dy \right\} \tag{2.80}$$

$$\begin{aligned}
\frac{\partial U_b}{\partial A_{mn}} = & \sum_{i=1}^M \sum_{j=1}^N \left\{ \int_0^{L_b} (D_{11})_b \frac{d^2 X_m}{dx^2} \frac{d^2 X_i}{dx^2} dx \int_0^b Y_n Y_j dy \right. \\
& + \left[\int_0^{L_b} (D_{12})_b X_m \frac{d^2 X_i}{dx^2} dx \int_0^b \frac{d^2 Y_n}{dy^2} Y_j dy + \int_0^{L_b} (D_{12})_b \frac{d^2 X_m}{dx^2} X_i dx \int_0^b Y_n \frac{d^2 Y_j}{dy^2} dy \right] \\
& + \int_0^{L_b} (D_{22})_b X_m X_i dx \int_0^b \frac{d^2 Y_n}{dy^2} \frac{d^2 Y_j}{dy^2} dy + 4 \int_0^{L_b} (D_{66})_b \frac{dX_m}{dx} \frac{dX_i}{dx} dx \int_0^b \frac{dY_n}{dy} \frac{dY_j}{dy} dy \\
& + 2 \left[\int_0^{L_b} (D_{16})_b \frac{dX_m}{dx} \frac{d^2 X_i}{dx^2} dx \int_0^b \frac{dY_n}{dy} Y_j dy + \int_0^{L_b} (D_{16})_b \frac{d^2 X_m}{dx^2} \frac{dX_i}{dx} dx \int_0^b Y_n \frac{dY_j}{dy} dy \right] \\
& \left. + 2 \left[\int_0^{L_b} (D_{26})_b X_m \frac{dX_i}{dx} dx \int_0^b \frac{d^2 Y_n}{dy^2} \frac{dY_j}{dy} dy + \int_0^{L_b} (D_{26})_b \frac{dX_m}{dx} X_i dx \int_0^b \frac{dY_n}{dy} \frac{d^2 Y_j}{dy^2} dy \right] \right\} A_{mn}
\end{aligned} \tag{2.81}$$

where, L_b is the length of tapered part of the laminated plate and subscript 'b' stands for tapered part.

2.4.3.2 Resin pocket

Reduced stiffness matrix, $[Q_{ij}]_r$, of isotropic material is in the form of :

$$[Q_{ij}]_r = \begin{bmatrix} \frac{E}{1-\nu^2} & \frac{\nu E}{1-\nu^2} & 0 \\ \frac{\nu E}{1-\nu^2} & \frac{E}{1-\nu^2} & 0 \\ 0 & 0 & \frac{E}{2(1+\nu)} \end{bmatrix} \tag{2.82}$$

where, E is the Young's Modulus and ν is the Poisson's Ratio.

For resin pocket:

- ply angle is zero ($\theta = 0$);
- $D_{16} = D_{26} = 0$;
- $(D_{ij})_r$ is calculated from equation (2.67) by using the values of $(Q_{ij})_r$ from equation (2.82);

- Length is variable (L_i'); $i= 1, 2 \dots n$
- Stiffness and Potential Energy (P.E.) are calculated separately for each imaginary ply;
- Cumulative stiffness and P.E. are the total stiffness and total P.E. of resin pocket.

For each resin layer:

$$\begin{aligned}
\frac{\partial U_r}{\partial A_{mn}} = & \sum_{i=1}^M \sum_{j=1}^N \left\{ (D_{11})_r \int_0^{L_i'} \frac{d^2 X_m}{dx^2} \frac{d^2 X_i}{dx^2} dx \int_0^b Y_n Y_j dy \right. \\
& + (D_{12})_r \left[\int_0^{L_i'} X_m \frac{d^2 X_i}{dx^2} dx \int_0^b \frac{d^2 Y_n}{dy^2} Y_j dy + \int_0^{L_i'} \frac{d^2 X_m}{dx^2} X_i dx \int_0^b Y_n \frac{d^2 Y_j}{dy^2} dy \right] \\
& \left. + (D_{22})_r \int_0^{L_i'} X_m X_i dx \int_0^b \frac{d^2 Y_n}{dy^2} \frac{d^2 Y_j}{dy^2} dy + 4(D_{33})_r \int_0^{L_i'} \frac{dX_m}{dx} \frac{dX_i}{dx} dx \int_0^b \frac{dY_n}{dy} \frac{dY_j}{dy} dy \right\} A_{mn}
\end{aligned} \tag{2.83}$$

$$\frac{\partial W_r}{\partial A_{mn}} = \sum_{i=1}^M \sum_{j=1}^N \left\{ N_o \int_0^{L_i'} \frac{dX_m}{dx} \frac{dX_i}{dx} dx \int_0^b Y_n Y_j dy \right\} \tag{2.84}$$

where, upper limit of the integration, L_i' , is the length of imaginary resin ply in x direction of the tapered laminated plate, subscript 'r' stands for resin and b is the width of resin plies.

2.4.4 Buckling analysis of thin part

For thin part $(D_{ij})_c$ is calculated from the equation (2.67) by setting the taper angle to zero ($\varphi = 0$) and differentiating potential and strain energy equations with respect to A_{mn} :

$$\frac{\partial W_c}{\partial A_{mn}} = \sum_{i=1}^M \sum_{j=1}^N \left\{ N_o \int_0^{L_c} \frac{dX_m}{dx} \frac{dX_i}{dx} dx \int_0^b Y_n Y_j dy \right\} \tag{2.85}$$

$$\begin{aligned}
\frac{\partial U_c}{\partial A_{mn}} = & \sum_{i=1}^M \sum_{j=1}^N \left\{ \int_0^{L_c} (D_{11})_c \frac{d^2 X_m}{dx^2} \frac{d^2 X_i}{dx^2} dx \int_0^b Y_n Y_j dy \right. \\
& + \left[\int_0^{L_c} (D_{12})_c X_m \frac{d^2 X_i}{dx^2} dx \int_0^b \frac{d^2 Y_n}{dy^2} Y_j dy + \int_0^{L_c} (D_{12})_c \frac{d^2 X_m}{dx^2} X_i dx \int_0^b Y_n \frac{d^2 Y_j}{dy^2} dy \right] \\
& + \int_0^{L_c} (D_{22})_c X_m X_i dx \int_0^b \frac{d^2 Y_n}{dy^2} \frac{d^2 Y_j}{dy^2} dy + 4 \int_0^{L_c} (D_{66})_c \frac{dX_m}{dx} \frac{dX_i}{dx} dx \int_0^b \frac{dY_n}{dy} \frac{dY_j}{dy} dy \\
& + 2 \left[\int_0^{L_c} (D_{16})_c \frac{dX_m}{dx} \frac{d^2 X_i}{dx^2} dx \int_0^b \frac{dY_n}{dy} Y_j dy + \int_0^{L_c} (D_{16})_c \frac{d^2 X_m}{dx^2} \frac{dX_i}{dx} dx \int_0^b Y_n \frac{dY_j}{dy} dy \right] \\
& \left. + 2 \left[\int_0^{L_c} (D_{26})_c X_m \frac{dX_i}{dx} dx \int_0^b \frac{d^2 Y_n}{dy^2} \frac{dY_j}{dy} dy + \int_0^{L_c} (D_{26})_c \frac{dX_m}{dx} X_i dx \int_0^b \frac{dY_n}{dy} \frac{d^2 Y_j}{dy^2} dy \right] \right\} A_{mn}
\end{aligned} \tag{2.86}$$

where, L_c is the length of thin part of the laminated plate and subscript 'c' stands for thin part.

2.4.5 Final form of the equation for critical buckling load

The strain energy equations of all segments, that are thick, taper, resin and thin parts, are combined together by adding the equations (2.79), (2.81), (2.83) and (2.86):

$$\frac{\partial U_{(a+b+r+c)}}{\partial A_{mn}} = \frac{\partial U_a}{\partial A_{mn}} + \frac{\partial U_b}{\partial A_{mn}} + \frac{\partial U_r}{\partial A_{mn}} + \frac{\partial U_c}{\partial A_{mn}} \tag{2.87}$$

Likewise, final potential energy equation is obtained by adding the equations (2.78), (2.80), (2.84) and (2.85):

$$\frac{\partial W_{(a+b+r+c)}}{\partial A_{mn}} = \frac{\partial W_a}{\partial A_{mn}} + \frac{\partial W_b}{\partial A_{mn}} + \frac{\partial W_r}{\partial A_{mn}} + \frac{\partial W_c}{\partial A_{mn}} \tag{2.88}$$

According to equation (2.75):

$$\frac{\partial U_{(a+b+r+c)}}{\partial A_{mn}} = \frac{\partial W_{(a+b+r+c)}}{\partial A_{mn}} \tag{2.89}$$

Equation (2.89) can be written in the form:

$$|[K] - N_o[Z]| = 0 \quad (2.90)$$

where, $[K]$ and $[Z]$ are the stiffness matrix and geometric stiffness matrix respectively.

Equation (2.90) is solved using MATLAB[®] program as an eigenvalue problem for which the eigenvalues are the values of N_o of the buckling loads and the eigenvectors determine the buckling mode shapes. Smallest value of N_o is the critical buckling load, N_{cr} .

2.5 Analysis of taper models with different boundary conditions

Following taper models are analyzed for different boundary conditions.

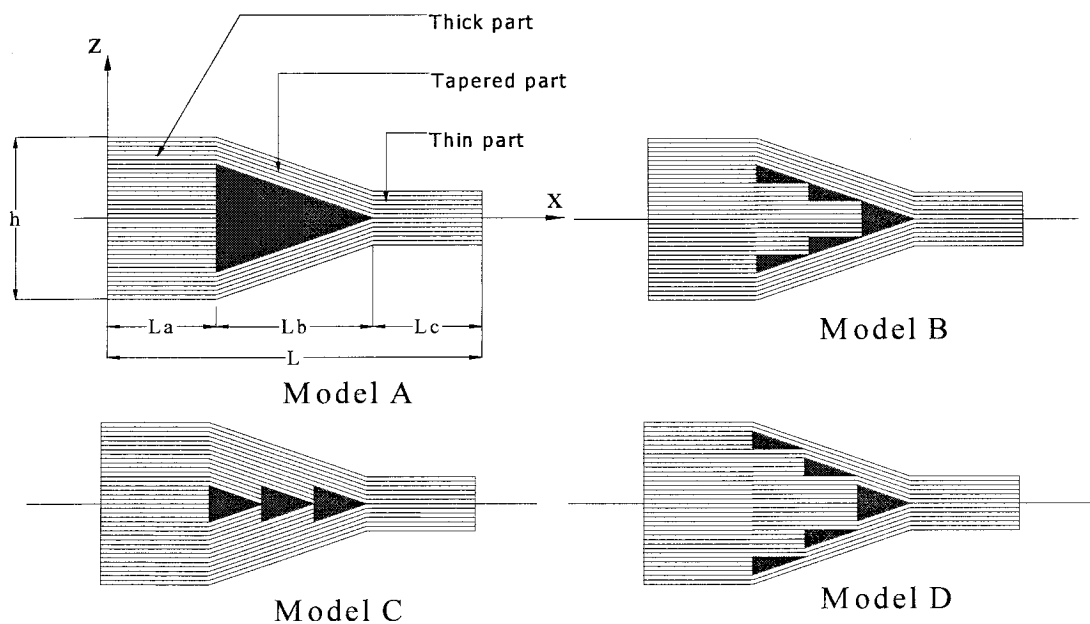


Figure 2.13 Taper models A, B, C and D for buckling analysis.

2.5.1 Simply supported laminated plate

In the case of a plate that is simply supported along its four edges (SSSS) the boundary conditions are:

- Along edges $x = 0$ and $x = L$:

$$w_o = 0, M_x = 0 \quad (2.91)$$

- Along edges $y = 0$ and $y = b$:

$$w_o = 0, M_y = 0 \quad (2.92)$$

These boundary conditions are satisfied by the following function [1,34]:

$$w_o(x, y) = \sum_{m=1}^M \sum_{n=1}^N A_{mn} X_m(x) Y_n(y) \quad (2.93)$$

where,

$$X_m(x) = \sin \frac{m\pi x}{L} \quad (2.94)$$

$$Y_n(y) = \sin \frac{n\pi y}{b} \quad (2.95)$$

Applying equation (2.93) in equation (2.89) we can get a eigenvalue problem like equation (2.90) and it can be solved using MATLAB[®] program to calculate the critical buckling load.

2.5.2 Laminated plate clamped at two adjacent ends and with other two ends free (CFCF)

For CFCF the approximate solution is [29]:

$$w_o(x, y) = \sum_{m=1}^M \sum_{n=1}^N A_{mn} X_m(x) Y_n(y) \quad (2.97)$$

where,

$$X_m(x) = \left(\cos \frac{\lambda_m x}{L} - \cosh \frac{\lambda_m x}{L} \right) - \gamma_m \left(\sin \frac{\lambda_m x}{L} - \sinh \frac{\lambda_m x}{L} \right) \quad (2.98)$$

$$Y_n(y) = \left(\cos \frac{\lambda_n y}{b} - \cosh \frac{\lambda_n y}{b} \right) - \gamma_n \left(\sin \frac{\lambda_n y}{b} - \sinh \frac{\lambda_n y}{b} \right) \quad (2.99)$$

Applying boundary condition along x direction:

$$\text{At } x = L, M_x|_{x=L} = 0 \text{ or } \left. \frac{d^2 w_o}{dx^2} \right|_{x=L} = 0 \quad (2.100)$$

$$\text{At } x = L, Q_x|_{x=L} = 0 \text{ or } \left. \frac{d^3 w_o}{dx^3} \right|_{x=L} = 0 \quad (2.101)$$

From equations (2.98), (2.99), (2.100) and (2.101):

$$\left. \frac{d^2 X_m}{dx^2} \right|_{x=L} = 0 \quad (2.102)$$

$$\left. \frac{d^3 X_m}{dx^3} \right|_{x=L} = 0 \quad (2.103)$$

where X_m satisfy the boundary conditions at $x = L$.

Solving equations (2.102) and (2.103) we get,

$$\cos(\lambda_m) \cosh(\lambda_m) = -1 \quad (2.104)$$

$$\gamma_m = \frac{\cos(\lambda_m) + \cosh(\lambda_m)}{\sin(\lambda_m) + \sinh(\lambda_m)} \quad (2.105)$$

Solving the boundary conditions in the direction of y we shall get the same type of results as that in x direction; in general we can write:

$$\cos(\lambda_i) \cosh(\lambda_i) = -1 \quad (2.106)$$

$$\gamma_i = \frac{\cos(\lambda_i) + \cosh(\lambda_i)}{\sin(\lambda_i) + \sinh(\lambda_i)} \quad (2.107)$$

where, $i = m, n$

The values of λ_i and γ_i are given in the Table 2.3.

m	1	2	3	4
λ_i	1.875	4.694	7.855	10.996
γ_i	0.734	1.018	0.999	1.000

Table 2.3 Co-efficients of the clamped-free beam functions.

Using the values given in Table 2.3 in equations (2.98) and (2.99) and the results in equation (2.89) we can calculate the critical buckling load.

2.5.3 Laminated plate clamped at four ends (CCCC)

For the case of a plate with opposite edges clamped the beam functions [29] are:

- For clamped edges $x = 0$ and $x = L$:

$$X_m(x) = \left(\cos \frac{\lambda_m x}{L} - \cosh \frac{\lambda_m x}{L} \right) - \gamma_m \left(\sin \frac{\lambda_m x}{L} - \sinh \frac{\lambda_m x}{L} \right) \quad (2.108)$$

- For clamped edges $y = 0$ and $y = b$:

$$Y_n(y) = \left(\cos \frac{\lambda_n y}{b} - \cosh \frac{\lambda_n y}{b} \right) - \gamma_n \left(\sin \frac{\lambda_n y}{b} - \sinh \frac{\lambda_n y}{b} \right) \quad (2.109)$$

In the case of a plate clamped along its four edges (CCCC), the boundary conditions are:

- Along edges $x = 0$ and $x = L$:

$$w_o = 0, \quad \frac{\partial w_o}{\partial x} = 0 \quad (2.110)$$

- Along edges $y = 0$ and $y = b$:

$$w_o = 0, \quad \frac{\partial w_o}{\partial y} = 0 \quad (2.111)$$

From equations (2.108), (2.109), (2.110) and (2.111):

$$X_m \Big|_{x=L} = 0, \quad \frac{dX_m}{dx} \Big|_{x=L} = 0 \quad (2.112)$$

$$Y_n \Big|_{y=b} = 0, \quad \frac{dY_n}{dy} \Big|_{y=b} = 0 \quad (2.113)$$

where X_m and Y_n satisfy the boundary conditions at $x = L$ and $y = b$.

Solving equations (2.108), (2.109) and (2.112) we get,

$$\cos(\lambda_i) \cosh(\lambda_i) = 1 \quad (2.114)$$

$$\gamma_i = \frac{\cos(\lambda_i) - \cosh(\lambda_i)}{\sin(\lambda_i) - \sinh(\lambda_i)} \quad (2.115)$$

where, $i = m, n$

The values of λ_i and γ_i are given in the Table 2.4.

m	1	2	3	4
λ_i	4.7300408	7.8532046	10.9956078	14.1371655
γ_i	0.9825022	1.000777	0.99996645	1.00000145

Table 2.4 Co-efficients of the clamped-clamped beam functions.

Using the values given in Table 2.4 in equations (2.108) and (2.109) and the results in equation (2.89) we can calculate the critical buckling load.

2.5.4 Laminated plate simply supported at two opposite ends and with other two ends free (SSFF)

- For simply supported edges $x = 0$ and $x = L$:

$$X_m(x) = \sin \frac{m\pi x}{L} \quad (2.116)$$

In the case of a plate with two opposite edges free, the beam function is [29]:

- For free edges $y = 0$ and $y = b$:

$$Y_n(y) = \left(\cos \frac{\lambda_n y}{b} + \cosh \frac{\lambda_n y}{b} \right) + \gamma_n \left(\sin \frac{\lambda_n y}{b} + \sinh \frac{\lambda_n y}{b} \right), n \geq 3 \quad (2.117)$$

Boundary conditions at $y = 0$ and $y = b$:

$$\left. \frac{d^2 Y_n}{dy^2} \right|_{y=b} = 0 \quad (2.118)$$

$$\left. \frac{d^3 Y_n}{dy^3} \right|_{y=b} = 0 \quad (2.119)$$

Solving equations (2.117), (2.118) and (2.119):

$$\cos(\lambda_i) \cosh(\lambda_i) = 1 \quad (2.120)$$

$$\gamma_i = \frac{\sin(\lambda_i) + \sinh(\lambda_i)}{\cos(\lambda_i) - \cosh(\lambda_i)} \quad (2.121)$$

where, $i = m, n$

The values of λ_i and γ_i are given in the Table 2.5.

m	1	2	3	4	5	6
λ_i	0	0	4.7300408	7.8532046	10.9956078	14.1371655
γ_i	0	0	-0.9825022	-1.000777	-1.000	-1.00000

Table 2.5 Values of co-efficients of the free-free beam function.

Using the values given in Table 2.5 in equation (2.117) and the results of X_m and Y_n in equation (2.89) we can calculate the critical buckling load.

2.6 Exact solutions for uniform laminated beam and plate

2.6.1 Uniform laminated beam

For simply supported edges $x = 0$ and $x = L$:

$$w_o(x) = \sin \frac{m\pi x}{L} \quad (2.122)$$

The critical buckling load of simply supported laminated beam [29]:

$$N_{cr} = \frac{m^2 \pi^2}{L^2} \frac{1}{D_{11}^*} \quad (2.123)$$

where,

$$D_{11}^* = \frac{1}{\Delta} (D_{22} D_{66} - D_{26}^2), \quad (2.124)$$

$$\Delta = D_{11} D_{22} D_{66} + 2D_{12} D_{16} D_{26} - D_{11} D_{26}^2 - D_{22} D_{16}^2 - D_{66} D_{12}^2 \quad (1.125)$$

and L is the length of the beam and D_{ij} is given in equation (2.67).

2.6.2 Uniform laminated plate

The critical buckling load of a plate under uniaxial compression [29]:

- Simply supported at four ends :

$$N_{cr} = \frac{\pi^2}{9L^2} [81D_{11} + 18(D_{12} + 2D_{66})R^2 + D_{22}R^4] \quad \text{for } m=3 \quad (2.126)$$

- Simply supported at two opposite ends and other two ends free:

$$N_{cr} = \frac{1}{L^2 m^2} [10D_{11} - 47(D_{12} + 2D_{66}) + 51D_{22}] \quad (2.127)$$

where R is the ratio of length to width (L/b) of a laminated plate.

2.7 Numerical examples

2.7.1 Examples of uniform laminate

Example 2.7.1

Variation of critical buckling load with E_L/E_T ratio for symmetric cross-ply uniform laminates, with $a/h = 10$, $b/a = 1$, $G_{LT} = 0.6E_T$, $G_{TT} = 0.5E_T$ and $\nu_{LT} = \nu_{TT} = 0.25$ and with the stacking sequences $(0^\circ/90^\circ/0^\circ)$ and $(0^\circ/90^\circ/0^\circ/90^\circ/0^\circ)$ were determined. The laminate is analyzed using beam and plate theories.

The uniform beam is simply supported at the two ends and the uniform plate has two types of boundary conditions as shown in Table 2.6. The results are given in Table 2.6 to compare the buckling loads with that of beam and plate theories.


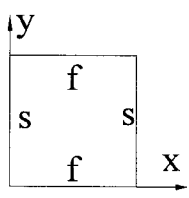
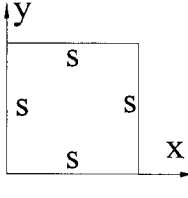
E_L/E_T	No Of Plies			
		Beam Theory (Exact Solution)	CLPT (Exact Solution)	CLPT (Exact Solution)
15	3	321.43	309.66	329.91
	5	447.86	432.41	462.16
20	3	428.26	417.34	436.69
	5	594.27	582.90	608.92

Table 2.6 Comparison of critical buckling Load ($\times 10^4 N$) for uniform laminates.

2.7.1.1 Discussion of results for uniform laminates

In case of beam analysis, boundary conditions of two opposite sides of a plate are considered and the boundary conditions of other two remaining sides are not taken into account. On the other hand, four sides are considered in plate analysis. From Table 2.6 we have observed that the critical buckling load of simply supported plates are larger than that of simply supported beams results. The critical buckling loads for the plates with simply supported condition at two opposite ends and with other two ends free are smaller than that of simply supported beams results.

2.7.2 Examples of tapered laminated beam and plate

Example 2.7.2

Tapered plate models that are shown in Figure 2.13 are considered with 36 and 12 plies at thick and thin sections respectively, which results in 24 drop-off plies. The configuration of the thick section is $(0/90)_9$, and that of the thin section is $(0/90)_3$. The mechanical properties of the composite material (NCT/301 graphite-epoxy) are: $E_1=113.9$ GPa, $E_2=7.9856$ GPa, $G_{12}=3.138$ GPa, $G_{23}=2.852$ GPa, $\nu_{12}=0.288$, $\nu_{21}=0.018$, $\rho=1480$ kg/m³. Resin properties: $E = 3.93$ GPa, $G = 1.034$ GPa, $\nu = 0.37$. The values of m and n in equation (2.89) are determined so as to obtain the converged solutions.

The geometric properties of the tapered laminates are: Thickness of each ply is 0.125 mm. The tapered part of laminated plates are square in shape and the lengths of plates and beams change with the change of taper angles that are given in Table 2.7.

The buckling problem is solved for different taper angles and for various boundary conditions and the results are given in Table 2.7 and Table 2.8.


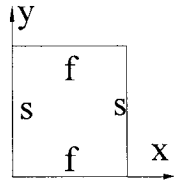
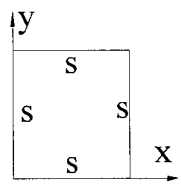
Angles in degrees	Length in meters	Beam Analysis by Finite Element Method [16]	Plate Analysis by Ritz Method	
				
0.75	0.1146	8.3810	7.7363	8.9161
2.0	0.04295	59.5466	54.938	63.322
3.0	0.0286	135.8107	123.45	142.30

Table 2.7 Comparison of critical buckling Load ($\times 10^4 N$) of taper model-C with the result of corresponding tapered beam.


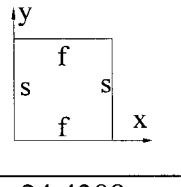
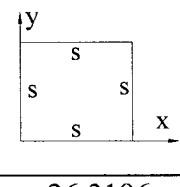
Angles in degrees	Beam Analysis by Finite Element Method [16]	Plate Analysis by Ritz Method	
			
0.75	25.5014	24.4398	26.3196
2.0	181.222	179.3484	186.972
3.0	407.3539	403.2120	420.36

Table 2.8 Comparison of critical buckling Load ($\times 10^4 N$) of taper model-D with the result of corresponding tapered beam.

2.7.2.1 Discussion of results for tapered laminates

In Table 2.8 critical buckling load of tapered laminated beam calculated using finite element method [16] is compared with that of tapered laminated plate calculated using Ritz method. The plate is analyzed considering two types of boundary conditions:

simply supported at four ends (SSSS) and simply support at two opposite ends and other two ends free (SSFF). Results for the beam are in between the results of the simply supported plate and the plate with SSFF boundary condition; we have observed same type of beam characteristic for exact solutions in Table 2.6. Simply supported plate is stronger than the plate that is simply supported at two ends and with other two ends free.

2.7.3 Example of tapered plate analyzed using Ritz method

Example 2.7.3

The tapered plates described in example 2.7.2 are considered for buckling analysis. The solutions have been obtained using Ritz method for simply supported, clamped-free and clamped-clamped boundary conditions. The results are given in Tables 2.9 - 2.12.

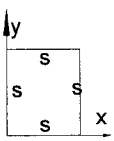
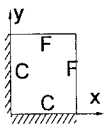
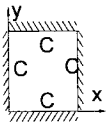
Taper length in meters	Taper angle in degrees			
		N_{cr}	N_{cr}	N_{cr}
0.8594	0.1	0.1471	0.0588	0.55393
0.1719	0.5	3.678	1.4698	13.846
0.1146	0.75	8.270	3.3063	31.142
0.08594	1.0	14.710	5.8805	55.387
0.0573	1.5	33.070	13.2210	124.48
0.04295	2.0	58.660	23.4610	221.41
0.03435	2.5	91.600	36.6400	345.77
0.0286	3.0	132.40	52.9970	498.39

Table 2.9 Critical buckling load ($\times 10^4 N$) of tapered part of model A

2.7.3.1 Discussion on model A

- Buckling load of clamped plate is larger than that of the simply supported plate.
- Clamped-Free plate is the worst case when two extreme boundary conditions, clamped and free, are considered.
- With the increase of taper angle, buckling loads increase for all types of boundary conditions.

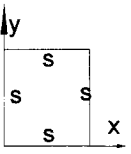
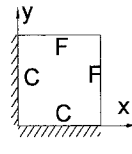
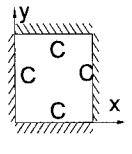
Taper length in meters	Taper angle in degrees			
		N_{cr}	N_{cr}	N_{cr}
0.8594	0.1	0.46305	0.130	0.6371
0.1719	0.5	11.5713	3.249	15.930
0.1146	0.75	26.0289	7.310	35.840
0.08594	1.0	46.305	13.000	63.706
0.0573	1.5	103.986	29.192	143.300
0.04295	2.0	184.869	51.890	254.280
0.03435 56	2.5	288.459	80.968	396.960
0.0286	3.0	415.557	116.590	569.780

Table 2.10 Critical buckling load ($\times 10^4 N$) of tapered part of model B

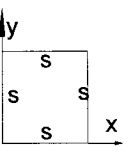
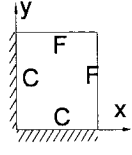
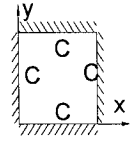
Taper length in meters	Taper angle in degrees			
		N_{cr}	N_{cr}	N_{cr}
0.8594	0.1	0.158617	0.0924	0.58107
0.1719	0.5	3.963667	2.3093	14.53095
0.1146	0.75	8.916111	5.1945	32.6928
0.08594	1.0	15.86167	9.242	58.1091
0.0573	1.5	35.62	20.750	130.7355
0.04295	2.0	63.32222	38.578	231.9555
0.0343556	2.5	98.8	57.556	362.1555
0.0286	3.0	142.3	82.914	519.729

Table 2.11 Critical buckling load ($\times 10^4 N$) of tapered part of model C

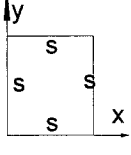
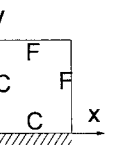
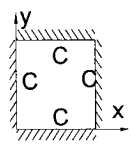
Taper length in meters	Taper angle in degrees			
		N_{cr}	N_{cr}	N_{cr}
0.8594	0.1	0.468192	0.0999	0.8375
0.1719	0.5	11.7	2.4977	20.943
0.1146	0.75	26.3196	5.6188	47.119
0.08594	1.0	46.8192	9.9946	83.759
0.0573	1.5	105.1632	22.451	188.390
0.04295	2.0	186.972	39.911	334.340
0.0343556	2.5	291.84	62.285	521.930
0.0286	3.0	420.36	89.701	749.360

Table 2.12 Critical buckling load ($\times 10^4 N$) of tapered part of model D

2.7.3.2 Discussion of models A, B, C and D

From the results given in Table 2.9 - Table 2.12, it can be concluded that the critical buckling loads increase by increasing the taper angle for all types of boundary conditions and taper models. Buckling load of clamped plate is larger than that of the simply supported plate and further, clamped-free plate is the worst case. The Figure 2.14 reveals that taper model D is the strongest and taper model A is the weakest one.

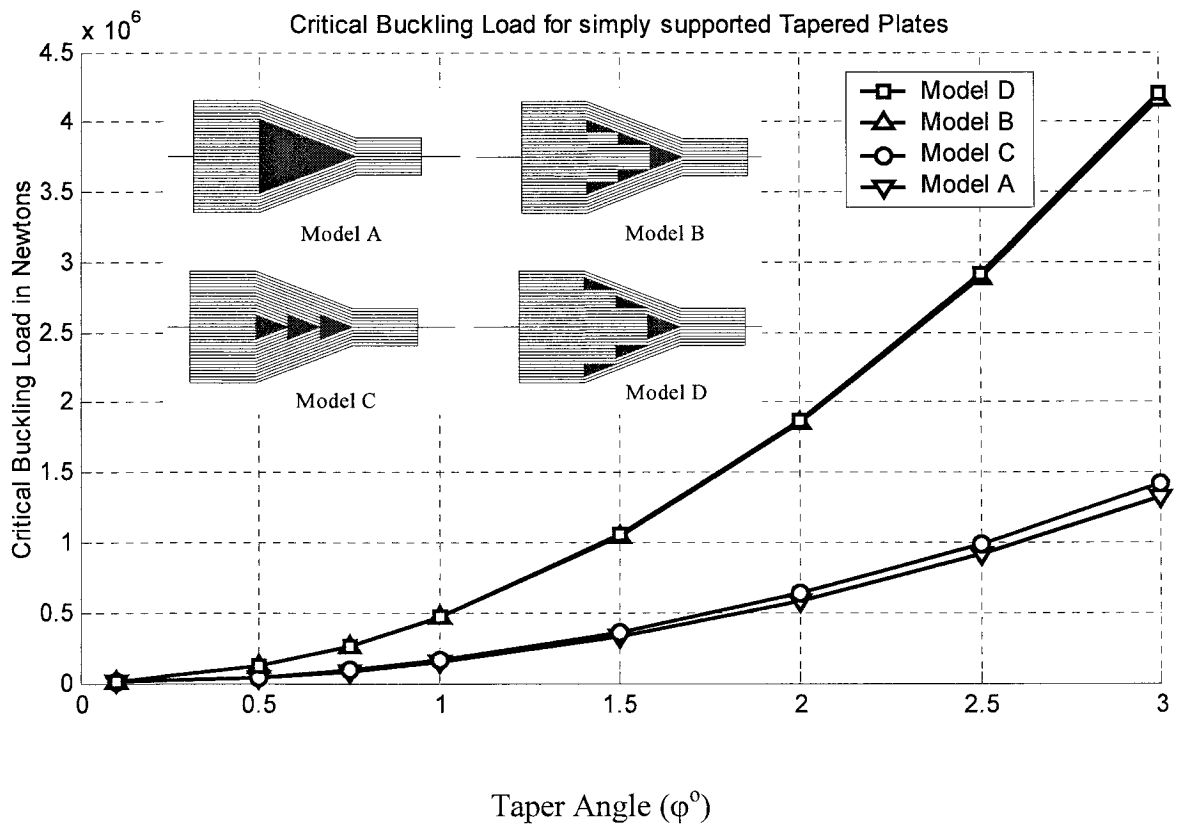


Figure 2.14 Comparison of critical buckling loads of tapered laminates of models A, B, C and D.

2.8 Discussions and conclusions

In this chapter, [A], [B] and [D] matrices are developed for tapered laminated plates. Transformed reduced stiffness, Q_{ij} , is analyzed by varying both the taper angle and ply orientation angle. The system equations of critical buckling loads are developed for four types of boundary conditions and taper models using Ritz method based on classical laminated plate theory. Buckling loads of tapered laminated plates are also compared with that of tapered laminated beam models that were analyzed using finite element method [4].

The fiber orientation angles have more influence on transformed reduced stiffness, Q_{ij} , than the taper angles.

Results of the tapered laminated beam are in between the results of the simply supported tapered plate and the tapered plate with simply supported boundary condition at two opposite ends and with other two ends free.

Tapered plate of model D is the strongest one; model B and model C take the second and third ranks respectively. Model A has the lowest stiffness. The critical buckling loads of models D and B are closer to each other. On the other hand, values of the critical buckling loads of models A and C are closer. The models A and C have more resin at the core and this is responsible for weak behavior compared to the models B and D.

Buckling load of clamped plate is larger than that of the simply supported plate. The clamped-free plate is the weakest one.

The critical buckling loads increase for increasing taper angles for all types of boundary conditions and taper models.

CHAPTER 3

Buckling Analysis Based On First-order Shear Deformation Theory (FSDT)

3.1 Introduction

Classical (Kirchhoff) plate theory has been widely used to model plate behavior, but is adequate only for thin laminated plates. Since the ratio of the in-plane elastic modulus to the transverse shear modulus is large for composite plates, Kirchhoff theory, which neglects transverse shear deformation, is usually inadequate for the analysis of thick or moderately thick plates. Many plate theories have been proposed to include the effect of shear deformation, of which the laminated plate version of the first-order shear deformation theory developed by Reissner (1945) and Mindlin (1951) is the simplest. This theory assumes a linear distribution of the in-plane normal and shear stresses over the thickness, which results in nonzero transverse shear stresses but does not reproduce the nonlinear transverse shear stress distribution through the plate's thickness.

In this chapter strain field of first-order model with transverse shear is considered. It should be possible to compute appropriate values of the transverse shear correction factors for specific lamination schemes [39]. In case of relatively thick plate, shear correction factor can be considered equal to $5/6$ [18]. Thus in the present study a shear correction factor of $5/6$ is used for transverse shear resultants.

3.2 Fundamental equations for buckling

3.2.1 Displacement field

The basic assumptions for the shear deformation theory remain the same as that of the classical laminate theory, with an exception concerning the neglect of the interlaminar shear strains γ_{xz} and γ_{yz} . Thus for the first-order shear deformation theory, the displacements are assumed to be of the forms [29]:

$$u(x,y,z,t) = u^o(x,y,t) + z\phi_x(x,y,t) \quad (3.1)$$

$$v(x,y,z,t) = v^o(x,y,t) + z\phi_y(x,y,t) \quad (3.2)$$

$$w(x,y,z,t) = w^o(x,y,t) \quad (3.3)$$

where,

(u_o, v_o, w_o) are the displacements of transverse normal on plane $z = 0$;

ϕ_x and ϕ_y are the rotations of the transverse normal on plane $z = 0$ about x and y axes, respectively.

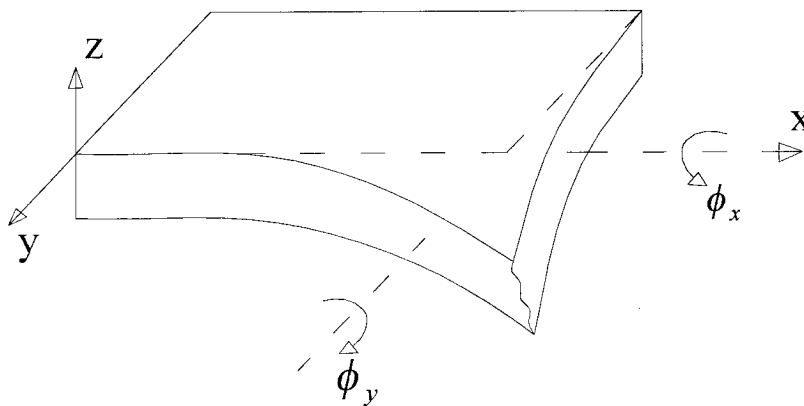


Figure 3.1 Explanation of rotations considered in FSDT

3.2.2 Strain field with transverse shear

Substituting displacement equations (3.1 - 3.3) into linear strain-displacement relations, the strain-displacement relations of the laminate are obtained as:

$$\varepsilon_{xx} = \frac{\partial u_o}{\partial x} + z \frac{\partial \phi_x}{\partial x} = \varepsilon_{xx}^o + z \kappa_{xx} \quad (3.4)$$

$$\varepsilon_{yy} = \frac{\partial v_o}{\partial y} + z \frac{\partial \phi_y}{\partial y} = \varepsilon_{yy}^o + z \kappa_{yy} \quad (3.5)$$

$$\varepsilon_{zz} \neq 0 \quad (3.6)$$

$$\gamma_{xy} = \left(\frac{\partial u_o}{\partial y} + \frac{\partial v_o}{\partial x} \right) + z \left(\frac{\partial \phi_x}{\partial y} + \frac{\partial \phi_y}{\partial x} \right) = \gamma_{xy}^o + z \kappa_{xy} \quad (3.7)$$

$$\gamma_{xz} = \gamma_{xz}^o = \frac{\partial w_o}{\partial x} + \phi_x \quad (3.8)$$

$$\gamma_{yz} = \gamma_{yz}^o = \frac{\partial w_o}{\partial y} + \phi_y \quad (3.9)$$

where, κ_{xx} , κ_{yy} and κ_{xy} are the curvatures.

3.2.3 Stress field

We can write the stress field for a ply as follows:

$$\begin{Bmatrix} \sigma_{xx} \\ \sigma_{yy} \\ \sigma_{zz} = 0 \\ \tau_{yz} \\ \tau_{xz} \\ \tau_{xy} \end{Bmatrix} = \begin{bmatrix} C_{11} & C_{12} & C_{13} & C_{14} & C_{15} & C_{16} \\ C_{12} & C_{22} & C_{23} & C_{24} & C_{25} & C_{26} \\ C_{13} & C_{23} & C_{33} & C_{34} & C_{35} & C_{36} \\ C_{14} & C_{24} & C_{34} & C_{44} & C_{45} & C_{46} \\ C_{15} & C_{25} & C_{35} & C_{45} & C_{55} & C_{56} \\ C_{16} & C_{26} & C_{36} & C_{46} & C_{56} & C_{66} \end{bmatrix} \begin{Bmatrix} \varepsilon_{xx} \\ \varepsilon_{yy} \\ \varepsilon_{zz} \neq 0 \\ \gamma_{yz} \\ \gamma_{xz} \\ \gamma_{xy} \end{Bmatrix} \quad (3.10)$$

where,

σ_{ij} and τ_{ij} are the normal stress and shear stress respectively ;

ε_{ij} and γ_{ij} are the normal strain and shear strain respectively in coordinate system

xyz ;

C_{ij} is the corresponding stiffness co-efficient given by the equation (2.39).

And also:

$$\varepsilon_{zz} = -(1/C_{33})(C_{13}\varepsilon_{xx} + C_{23}\varepsilon_{yy} + C_{34}\gamma_{yz} + C_{35}\gamma_{xz} + C_{36}\gamma_{xy}) \quad (3.11)$$

$$\begin{aligned} \sigma_{xx} = & (C_{11} - C_{13}^2/C_{33})\varepsilon_{xx} + (C_{12} - C_{13}C_{23}/C_{33})\varepsilon_{yy} + (C_{14} - C_{13}C_{34}/C_{33})\gamma_{yz} \\ & + (C_{15} - C_{13}C_{35}/C_{33})\gamma_{xz} + (C_{16} - C_{13}C_{36}/C_{33})\gamma_{xy} \end{aligned} \quad (3.12)$$

and equations for σ_{yy} , τ_{yz} , τ_{xz} and τ_{xy} are analogous to that for σ_{xx} .

Therefore, the reduced stiffness matrix is in the form of:

$$\begin{Bmatrix} \sigma_{xx} \\ \sigma_{yy} \\ \tau_{yz} \\ \tau_{xz} \\ \tau_{xy} \end{Bmatrix} = \begin{bmatrix} Q_{11} & Q_{12} & Q_{14} & Q_{15} & Q_{16} \\ Q_{12} & Q_{22} & Q_{24} & Q_{25} & Q_{26} \\ Q_{14} & Q_{24} & Q_{44} & Q_{45} & Q_{46} \\ Q_{15} & Q_{25} & Q_{45} & Q_{55} & Q_{56} \\ Q_{16} & Q_{26} & Q_{46} & Q_{56} & Q_{66} \end{bmatrix} \begin{Bmatrix} \varepsilon_{xx} \\ \varepsilon_{yy} \\ \gamma_{yz} \\ \gamma_{xz} \\ \gamma_{xy} \end{Bmatrix} \quad (3.13)$$

Rearranging equation (3.13), we get:

$$\begin{Bmatrix} \sigma_{xx} \\ \sigma_{yy} \\ \tau_{xy} \\ \tau_{yz} \\ \tau_{xz} \end{Bmatrix} = \begin{bmatrix} Q_{11} & Q_{12} & Q_{16} & Q_{14} & Q_{15} \\ Q_{12} & Q_{22} & Q_{26} & Q_{24} & Q_{25} \\ Q_{16} & Q_{26} & Q_{66} & Q_{46} & Q_{56} \\ Q_{14} & Q_{24} & Q_{46} & Q_{44} & Q_{45} \\ Q_{15} & Q_{25} & Q_{56} & Q_{45} & Q_{55} \end{bmatrix} \begin{Bmatrix} \varepsilon_{xx} \\ \varepsilon_{yy} \\ \gamma_{xy} \\ \gamma_{yz} \\ \gamma_{xz} \end{Bmatrix} \quad (3.14)$$

where,

$$(Q_{ij})_{ij} = C_{ij} - \frac{C_{i3}C_{j3}}{C_{33}} ; \quad (3.15)$$

C_{ij} is given by equation (2.39) ;

ε_{ij} and γ_{ij} are given by the equations (3.4 - 3.9);

$i, j = 1, 2, 3, 4, 5, 6$.

3.2.4 Constitutive equation

The constitutive equation with transverse shear of tapered laminate is written by associating the force resultants and the moments, in the form:

$$\begin{Bmatrix} N_{xx} \\ N_{yy} \\ N_{xy} \\ M_{xx} \\ M_{yy} \\ M_{xy} \\ Q_{yz} \\ Q_{xz} \end{Bmatrix} = \begin{bmatrix} A_{11} & A_{12} & A_{16} & B_{11} & B_{12} & B_{16} & A_{14} & A_{15} \\ A_{12} & A_{22} & A_{26} & B_{12} & B_{22} & B_{26} & A_{24} & A_{25} \\ A_{16} & A_{26} & A_{66} & B_{16} & B_{26} & B_{66} & A_{46} & A_{56} \\ B_{11} & B_{12} & B_{16} & D_{11} & D_{12} & D_{16} & B_{14} & B_{15} \\ B_{12} & B_{22} & B_{26} & D_{12} & D_{22} & D_{26} & B_{24} & B_{25} \\ B_{16} & B_{26} & B_{66} & D_{16} & D_{26} & D_{66} & B_{46} & B_{56} \\ \frac{5}{6} \left(A_{14} & A_{24} & A_{46} & B_{14} & B_{24} & B_{46} & A_{44} & A_{45} \right) \\ \frac{5}{6} \left(A_{15} & A_{25} & A_{56} & B_{15} & B_{25} & B_{56} & A_{45} & A_{55} \right) \end{bmatrix} \begin{Bmatrix} \varepsilon_{xx}^o \\ \varepsilon_{yy}^o \\ \gamma_{xy}^o \\ \kappa_{xx} \\ \kappa_{yy} \\ \kappa_{xy} \\ \gamma_{yz}^o \\ \gamma_{xz}^o \end{Bmatrix} \quad (3.16)$$

where, A_{ij} , B_{ij} and D_{ij} for tapered laminate based on FSDT are given in the following equations and 5/6 is the value of the shear correction factor.

$$(A_{ij})_{ij} = \sum_{k=1}^n (Q_{ij}^{ij})_k e_k \quad (3.17)$$

$$(B_{ij})_{ij} = \sum_{k=1}^n (Q_{ij}^{ij})_k e_k z_k \quad (3.18)$$

$$(D_{ij})_{ij} = \sum_{k=1}^n (Q_{ij}^{ij})_k (e_k z_k^2 + e_k^3 / 12) \quad (3.19)$$

with $i, j = 1, 2, 3, 4, 5, 6$.

e_k and z_k are calculated using the equations (2.59) and (2.62) respectively. $(Q_{ij})_{if}$ of ply is calculated from the equation (3.15). In case of resin, $(Q_{ij}^{rf})_k$ is also calculated using the same equation (3.15) but using the properties of resin.

3.3 Energy formulation

In the sub-section 2.2.5, we have derived the energy equation considering that $\sigma_{zz} = 0$, $\gamma_{xz} = 0$ and $\gamma_{yz} = 0$; but for the present case “transverse shears” are not equal to zero. So energy equation will be much more complex than before. For simplification, we have assumed some conditions that will be discussed in the following section.

3.3.1 Energy equations for tapered laminate and resin pocket

3.3.1.1 Strain energy

Strain energy can be written in the form of:

$$(U)_{if} = \frac{1}{2} \iiint \{ (\sigma_{xx} \varepsilon_{xx} + \sigma_{yy} \varepsilon_{yy} + \tau_{xy} \gamma_{xy}) + (\tau_{yz} \gamma_{yz} + \tau_{xz} \gamma_{xz}) \} dx dy dz \quad (3.20)$$

since $\sigma_{zz} = 0$; using the values of σ_{ij} from equation (3.14) in equation (3.20), we get the equation for the tapered laminate:

$$\begin{aligned}
(U)_{ff} = & \frac{1}{2} \iiint \left\{ [Q_{11} \quad Q_{12} \quad Q_{16}] \begin{bmatrix} \varepsilon_{xx}^2 \\ \varepsilon_{yy} \varepsilon_{xx} \\ \gamma_{xy} \varepsilon_{xx} \end{bmatrix} + [Q_{14} \quad Q_{15}] \begin{bmatrix} \gamma_{yz} \varepsilon_{xx} \\ \gamma_{xz} \varepsilon_{xx} \end{bmatrix} \right. \\
& + [Q_{12} \quad Q_{22} \quad Q_{26}] \begin{bmatrix} \varepsilon_{xx} \varepsilon_{yy} \\ \varepsilon_{yy}^2 \\ \gamma_{xy} \varepsilon_{yy} \end{bmatrix} + [Q_{24} \quad Q_{25}] \begin{bmatrix} \gamma_{yz} \varepsilon_{yy} \\ \gamma_{xz} \varepsilon_{yy} \end{bmatrix} \\
& + [Q_{16} \quad Q_{26} \quad Q_{66}] \begin{bmatrix} \varepsilon_{xx} \gamma_{xy} \\ \varepsilon_{yy} \gamma_{xy} \\ \gamma_{xy}^2 \end{bmatrix} + [Q_{46} \quad Q_{56}] \begin{bmatrix} \gamma_{yz} \gamma_{xy} \\ \gamma_{xz} \gamma_{xy} \end{bmatrix} \\
& + [Q_{14} \quad Q_{24} \quad Q_{46}] \begin{bmatrix} \varepsilon_{xx} \gamma_{yz} \\ \varepsilon_{yy} \gamma_{yz} \\ \gamma_{xy} \gamma_{yz} \end{bmatrix} + [Q_{44} \quad Q_{45}] \begin{bmatrix} \gamma_{yz} \gamma_{yz} \\ \gamma_{xz} \gamma_{yz} \end{bmatrix} \\
& \left. + [Q_{15} \quad Q_{25} \quad Q_{56}] \begin{bmatrix} \varepsilon_{xx} \gamma_{xz} \\ \varepsilon_{yy} \gamma_{xz} \\ \gamma_{xy} \gamma_{xz} \end{bmatrix} + [Q_{45} \quad Q_{55}] \begin{bmatrix} \gamma_{yz} \gamma_{xz} \\ \gamma_{xz} \gamma_{xz} \end{bmatrix} \right\} dx dy dz
\end{aligned} \tag{3.21}$$

The above relation can be written as a function of the displacements u_0 , v_0 and w_0 by substituting the strain-displacement equations (3.4 - 3.9) in equation (3.21).

3.3.1.1.a Tapered laminate

By integrating the equation (3.21) with respect to z across the thickness of the tapered laminate, we obtain the final form of strain energy that is shown at the next page:

$$\begin{aligned}
U_{II} = 1/2 \int_{y=0}^b \int_{x=0}^{L_b} & \left[A_{11} \left(\frac{\partial u_o}{\partial x} \right)^2 + 2A_{12} \left(\frac{\partial u_o}{\partial x} \cdot \frac{\partial v_o}{\partial y} \right) + 2A_{16} \left(\frac{\partial u_o}{\partial x} \cdot \frac{\partial u_o}{\partial y} + \frac{\partial u_o}{\partial x} \cdot \frac{\partial v_o}{\partial x} \right) \right. \\
& + 2A_{14} \left(\frac{\partial w_o}{\partial y} \cdot \frac{\partial u_o}{\partial x} + \varphi_y \frac{\partial u_o}{\partial x} \right) + 2A_{15} \left(\frac{\partial w_o}{\partial x} \cdot \frac{\partial u_o}{\partial x} + \varphi_x \frac{\partial u_o}{\partial x} \right) \\
& + A_{22} \left(\frac{\partial v_o}{\partial y} \right)^2 + 2A_{26} \left(\frac{\partial u_o}{\partial y} \cdot \frac{\partial v_o}{\partial y} + \frac{\partial v_o}{\partial x} \cdot \frac{\partial v_o}{\partial y} \right) + 2A_{24} \left(\frac{\partial w_o}{\partial y} \cdot \frac{\partial v_o}{\partial y} + \varphi_y \frac{\partial v_o}{\partial y} \right) \\
& + 2A_{25} \left(\frac{\partial w_o}{\partial x} \cdot \frac{\partial v_o}{\partial y} + \varphi_x \frac{\partial v_o}{\partial y} \right) + A_{66} \left(\frac{\partial u_o}{\partial y} + \frac{\partial v_o}{\partial x} \right)^2 + 2A_{46} \left(\frac{\partial w_o}{\partial y} + \varphi_y \right) \left(\frac{\partial u_o}{\partial y} + \frac{\partial v_o}{\partial x} \right) \\
& + 2A_{56} \left(\frac{\partial w_o}{\partial x} + \varphi_x \right) \left(\frac{\partial u_o}{\partial y} + \frac{\partial v_o}{\partial x} \right) + 2A_{45} \left(\frac{\partial w_o}{\partial y} + \varphi_y \right) \left(\frac{\partial w_o}{\partial x} + \varphi_x \right) + A_{55} \left(\frac{\partial w_o}{\partial x} + \varphi_x \right)^2 \\
& + A_{44} \left(\frac{\partial w_o}{\partial y} + \varphi_y \right)^2 + 2B_{11} \left(\frac{\partial u_o}{\partial x} \cdot \frac{\partial \varphi_x}{\partial x} \right) + 2B_{12} \left(\frac{\partial u_o}{\partial x} \cdot \frac{\partial \varphi_y}{\partial y} + \frac{\partial v_o}{\partial y} \cdot \frac{\partial \varphi_x}{\partial x} \right) \\
& + 2B_{16} \left(\frac{\partial u_o}{\partial x} \cdot \frac{\partial \varphi_x}{\partial y} + \frac{\partial u_o}{\partial x} \cdot \frac{\partial \varphi_y}{\partial x} \right) + 2B_{22} \left(\frac{\partial v_o}{\partial y} \cdot \frac{\partial \varphi_y}{\partial y} \right) + 2B_{36} \left(\frac{\partial \varphi_x}{\partial y} + \frac{\partial \varphi_y}{\partial x} \right) \left(\frac{\partial w_o}{\partial x} + \varphi_x \right) \\
& + 2B_{26} \left(\frac{\partial \varphi_x}{\partial y} \cdot \frac{\partial v_o}{\partial y} + \frac{\partial \varphi_y}{\partial x} \cdot \frac{\partial v_o}{\partial y} + \frac{\partial u_o}{\partial y} \cdot \frac{\partial \varphi_y}{\partial y} + \frac{\partial v_o}{\partial x} \cdot \frac{\partial \varphi_y}{\partial y} \right) \\
& + 2B_{66} \left(\frac{\partial u_o}{\partial y} + \frac{\partial v_o}{\partial x} \right) \left(\frac{\partial \varphi_x}{\partial y} + \frac{\partial \varphi_y}{\partial x} \right) + 2B_{14} \left(\frac{\partial w_o}{\partial y} \cdot \frac{\partial \varphi_x}{\partial x} + \varphi_y \cdot \frac{\partial \varphi_x}{\partial x} \right) \\
& + 2B_{15} \left(\frac{\partial w_o}{\partial x} \cdot \frac{\partial \varphi_x}{\partial x} + \varphi_x \cdot \frac{\partial \varphi_x}{\partial x} \right) + 2B_{24} \left(\frac{\partial w_o}{\partial y} \cdot \frac{\partial \varphi_y}{\partial x} + \varphi_y \cdot \frac{\partial \varphi_y}{\partial y} \right) \\
& + 2B_{25} \left(\frac{\partial w_o}{\partial x} \cdot \frac{\partial \varphi_y}{\partial y} + \varphi_x \cdot \frac{\partial \varphi_y}{\partial y} \right) + 2B_{46} \left(\frac{\partial \varphi_x}{\partial y} + \frac{\partial \varphi_y}{\partial x} \right) \left(\frac{\partial w_o}{\partial y} + \varphi_y \right) \\
& + D_{11} \left(\frac{\partial \varphi_x}{\partial x} \right)^2 + 2D_{12} \left(\frac{\partial \varphi_x}{\partial x} \cdot \frac{\partial \varphi_y}{\partial y} \right) + 2D_{16} \left(\frac{\partial \varphi_x}{\partial x} \cdot \frac{\partial \varphi_x}{\partial y} + \frac{\partial \varphi_y}{\partial x} \cdot \frac{\partial \varphi_x}{\partial x} \right) \\
& \left. + D_{22} \left(\frac{\partial \varphi_y}{\partial x} \right)^2 + 2D_{26} \left(\frac{\partial \varphi_x}{\partial y} \cdot \frac{\partial \varphi_y}{\partial y} + \frac{\partial \varphi_y}{\partial x} \cdot \frac{\partial \varphi_y}{\partial y} \right) + D_{66} \left(\frac{\partial \varphi_x}{\partial y} + \frac{\partial \varphi_y}{\partial x} \right)^2 \right] dx dy
\end{aligned} \tag{3.22}$$

where,

L_b and b are the length and width of the tapered part of the laminate as defined in Figure 2.13;

A_{ij} , B_{ij} and D_{ij} for tapered laminate are calculated from the equations (3.17), (3.18) and (3.19) respectively.

3.3.1.1.b Resin pocket

By integrating the equation (3.21) with respect to z across the thickness of the resin we obtain the final form of strain energy for resin pocket as:

$$\begin{aligned}
U_{rp} = & 1/2 \int_{y=0}^b \int_{x=0}^{L_r} \left[A_{11} \left(\frac{\partial u_o}{\partial x} \right)^2 + 2A_{12} \left(\frac{\partial u_o}{\partial x} \cdot \frac{\partial v_o}{\partial y} \right) + 2A_{16} \left(\frac{\partial u_o}{\partial x} \cdot \frac{\partial u_o}{\partial y} + \frac{\partial u_o}{\partial x} \cdot \frac{\partial v_o}{\partial x} \right) \right. \\
& + 2A_{14} \left(\frac{\partial w_o}{\partial y} \cdot \frac{\partial u_o}{\partial x} + \varphi_y \cdot \frac{\partial u_o}{\partial x} \right) + 2A_{15} \left(\frac{\partial w_o}{\partial x} \cdot \frac{\partial u_o}{\partial x} + \varphi_x \cdot \frac{\partial u_o}{\partial x} \right) \\
& + A_{22} \left(\frac{\partial v_o}{\partial y} \right)^2 + 2A_{26} \left(\frac{\partial u_o}{\partial y} \cdot \frac{\partial v_o}{\partial y} + \frac{\partial v_o}{\partial x} \cdot \frac{\partial v_o}{\partial y} \right) + 2A_{24} \left(\frac{\partial w_o}{\partial y} \cdot \frac{\partial v_o}{\partial y} + \varphi_y \cdot \frac{\partial v_o}{\partial y} \right) \\
& + 2A_{25} \left(\frac{\partial w_o}{\partial x} \cdot \frac{\partial v_o}{\partial y} + \varphi_x \cdot \frac{\partial v_o}{\partial y} \right) + A_{66} \left(\frac{\partial u_o}{\partial y} + \frac{\partial v_o}{\partial x} \right)^2 + 2A_{46} \left(\frac{\partial w_o}{\partial y} + \varphi_y \right) \left(\frac{\partial u_o}{\partial y} + \frac{\partial v_o}{\partial x} \right) \\
& + 2A_{56} \left(\frac{\partial w_o}{\partial x} + \varphi_x \right) \left(\frac{\partial u_o}{\partial y} + \frac{\partial v_o}{\partial x} \right) + 2A_{45} \left(\frac{\partial w_o}{\partial y} + \varphi_y \right) \left(\frac{\partial w_o}{\partial x} + \varphi_x \right) + A_{55} \left(\frac{\partial w_o}{\partial x} + \varphi_x \right)^2 \\
& + A_{44} \left(\frac{\partial w_o}{\partial y} + \varphi_y \right)^2 + 2B_{11} \left(\frac{\partial u_o}{\partial x} \cdot \frac{\partial \varphi_x}{\partial x} \right) + 2B_{12} \left(\frac{\partial u_o}{\partial x} \cdot \frac{\partial \varphi_y}{\partial y} + \frac{\partial v_o}{\partial y} \cdot \frac{\partial \varphi_x}{\partial x} \right) \\
& + 2B_{16} \left(\frac{\partial u_o}{\partial x} \cdot \frac{\partial \varphi_x}{\partial y} + \frac{\partial u_o}{\partial x} \cdot \frac{\partial \varphi_y}{\partial x} \right) + 2B_{22} \left(\frac{\partial v_o}{\partial y} \cdot \frac{\partial \varphi_y}{\partial y} \right) + 2B_{56} \left(\frac{\partial \varphi_x}{\partial y} + \frac{\partial \varphi_y}{\partial x} \right) \left(\frac{\partial w_o}{\partial x} + \varphi_x \right) \\
& + 2B_{26} \left(\frac{\partial \varphi_x}{\partial y} \cdot \frac{\partial v_o}{\partial y} + \frac{\partial \varphi_y}{\partial x} \cdot \frac{\partial v_o}{\partial y} + \frac{\partial u_o}{\partial y} \cdot \frac{\partial \varphi_y}{\partial y} + \frac{\partial v_o}{\partial x} \cdot \frac{\partial \varphi_y}{\partial y} \right) \\
& + 2B_{66} \left(\frac{\partial u_o}{\partial y} + \frac{\partial v_o}{\partial x} \right) \left(\frac{\partial \varphi_x}{\partial y} + \frac{\partial \varphi_y}{\partial x} \right) + 2B_{14} \left(\frac{\partial w_o}{\partial y} \cdot \frac{\partial \varphi_x}{\partial x} + \varphi_y \cdot \frac{\partial \varphi_x}{\partial x} \right) \\
& + 2B_{15} \left(\frac{\partial w_o}{\partial x} \cdot \frac{\partial \varphi_x}{\partial x} + \varphi_x \cdot \frac{\partial \varphi_x}{\partial x} \right) + 2B_{24} \left(\frac{\partial w_o}{\partial y} \cdot \frac{\partial \varphi_y}{\partial x} + \varphi_y \cdot \frac{\partial \varphi_y}{\partial y} \right) \\
& + 2B_{25} \left(\frac{\partial w_o}{\partial x} \cdot \frac{\partial \varphi_y}{\partial y} + \varphi_x \cdot \frac{\partial \varphi_y}{\partial y} \right) + 2B_{46} \left(\frac{\partial \varphi_x}{\partial y} + \frac{\partial \varphi_y}{\partial x} \right) \left(\frac{\partial w_o}{\partial y} + \varphi_y \right) \\
& + D_{11} \left(\frac{\partial \varphi_x}{\partial x} \right)^2 + 2D_{12} \left(\frac{\partial \varphi_x}{\partial x} \cdot \frac{\partial \varphi_y}{\partial y} \right) + 2D_{16} \left(\frac{\partial \varphi_x}{\partial x} \cdot \frac{\partial \varphi_x}{\partial y} + \frac{\partial \varphi_y}{\partial x} \cdot \frac{\partial \varphi_x}{\partial x} \right) \\
& \left. + D_{22} \left(\frac{\partial \varphi_y}{\partial x} \right)^2 + 2D_{26} \left(\frac{\partial \varphi_x}{\partial y} \cdot \frac{\partial \varphi_y}{\partial y} + \frac{\partial \varphi_y}{\partial x} \cdot \frac{\partial \varphi_y}{\partial y} \right) + D_{66} \left(\frac{\partial \varphi_x}{\partial y} + \frac{\partial \varphi_y}{\partial x} \right)^2 \right] dx dy
\end{aligned} \tag{3.23}$$

where,

L_r and b are the length and width of resin ply;

A_{ij} , B_{ij} and D_{ij} for resin pocket are calculated from the equations (3.17), (3.18) and (3.19) using the properties of resin.

3.3.1.2 Potential energy

The potential energy of external loads for tapered laminate and resin pocket are:

$$W_{ul} = -(1/2) \iint_A N_x \left(\frac{\partial w_o}{\partial x} \right)^2 dx dy \quad (3.24)$$

$$W_{rp} = -(1/2) \iint_{A_r} N_x \left(\frac{\partial w_o}{\partial x} \right)^2 dx dy \quad (3.25)$$

where, A and A_r are the areas of tapered laminate and resin pocket respectively.

3.3.2 General expressions for buckling analysis

The approximate solution is expressed in a double series as:

$$\begin{aligned} u_o(x, y) &= \sum_{m=1}^M \sum_{n=1}^N U_{mn} U_m(x) U_n(y) \\ v_o(x, y) &= \sum_{m=1}^M \sum_{n=1}^N V_{mn} V_m(x) V_n(y) \\ w_o(x, y) &= \sum_{m=1}^M \sum_{n=1}^N W_{mn} W_m(x) W_n(y) \\ \phi_x(x, y) &= \sum_{m=1}^M \sum_{n=1}^N X_{mn} X_m(x) X_n(y) \\ \phi_y(x, y) &= \sum_{m=1}^M \sum_{n=1}^N Y_{mn} Y_m(x) Y_n(y) \end{aligned} \quad (3.26)$$

The functions $U_m(x)$, $U_n(y)$, $V_m(x)$, $V_n(y)$, $W_m(x)$, $W_n(y)$, $X_m(x)$, $X_n(y)$, $Y_m(x)$ and $Y_n(x)$ are chosen so as to satisfy the boundary conditions and the co-efficients U_{mn} , V_{mn} , W_{mn} , X_{mn} and Y_{mn} are determined by the stationary conditions:

$$\frac{\partial U_{il}}{\partial U_{mn}} + \frac{\partial U_{rp}}{\partial U_{mn}} = 0 \quad (3.27)$$

$$\frac{\partial U_{il}}{\partial V_{mn}} + \frac{\partial U_{rp}}{\partial V_{mn}} = 0 \quad (3.28)$$

$$\frac{\partial U_{il}}{\partial X_{mn}} + \frac{\partial U_{rp}}{\partial X_{mn}} = 0 \quad (3.29)$$

$$\frac{\partial U_{il}}{\partial Y_{mn}} + \frac{\partial U_{rp}}{\partial Y_{mn}} = 0 \quad (3.30)$$

$$\frac{\partial U_{il}}{\partial W_{mn}} + \frac{\partial U_{rp}}{\partial W_{mn}} = \frac{\partial W_{il}}{\partial W_{mn}} + \frac{\partial W_{rp}}{\partial W_{mn}} \quad (3.31)$$

where,

U_{il} and U_{rp} are defined in equations (3.22) and (3.23) for tapered laminate and resin pocket respectively;

W_{il} and W_{rp} are defined in equations (3.24) and (3.25);

m and n represent the desired number of approximation terms.

In case of $m = n = 1$, No. of equations are: $5 \times 1 = 5$;

$m = n = 2$, No. of equations are: $5 \times (2 \times 2) = 20$;

$m = n = 3$, No. of equations are: $5 \times (3 \times 3) = 45$

and so on.

Solving equations (3.27) – (3.30) and using the results in the equation (3.31), final form of the equation can be written as:

$$\left| [K_{tf}] - \lambda [Z_{tf}] \right| = 0 \quad (3.32)$$

where K_{tf} and Z_{tf} are the stiffness and load matrices of tapered part of the laminate based on FSDT and λ is a buckling parameter (eigenvalue). Equation (3.32) represents an eigenvalue problem. For a non-trivial solution, the determinant of the co-efficient matrix is set equal to zero. The roots of the determinant are the eigenvalues. Substituting each eigenvalue back into the equation generating the eigenvalue determinant yields the corresponding eigenvector.

3.3.3 The system equations of tapered laminate for special cases

For simplicity we consider the following:

- $u = v = 0$ as these values are very small w.r.t. other displacement variables; this leads the values A_{ij} to be equal to zero except A_{44} , A_{45} and A_{55} .
- *Symmetric Cross Ply $[90/0]_s$ Laminate:* The values of B_{11} , B_{12} , B_{16} , B_{22} , B_{26} and B_{66} are equal to zero. On the other hand, the values of B_{14} , B_{24} , B_{15} , B_{25} , B_{46} and B_{56} are nonzero.

Now taking into account the equation (3.22) and the shear correction factor, we easily obtain the system of equations giving the co-efficients of W_{ij} , X_{ij} and Y_{ij} . Thus:

$$\begin{aligned}
\frac{\partial U_{it}}{\partial W_m} = & \sum_{i=1}^M \sum_{j=1}^N \left[\frac{5}{6} \left\{ \int_0^{L_b} A_{45} \frac{dW_m}{dx} W_i dx \int_0^b W_n \frac{dW_j}{dy} dy + \int_0^{L_b} A_{45} W_m \frac{dW_i}{dx} dx \int_0^b \frac{dW_n}{dy} W_j dy \right. \right. \\
& + \int_0^{L_b} A_{55} \frac{dW_m}{dx} \frac{dW_i}{dx} dx \int_0^b W_n W_j dy + \int_0^{L_b} A_{44} W_m W_i dx \int_0^b \frac{dW_n}{dy} \frac{dW_j}{dy} dy \left. \right\} W_{ij} \\
& + \left\{ \int_0^{L_b} \frac{5}{6} A_{45} W_m X_i dx \int_0^b \frac{dW_n}{dy} X_j dy + \int_0^{L_b} \frac{5}{6} A_{55} \frac{dW_m}{dx} X_i dx \int_0^b W_n X_j dy \right. \\
& + \int_0^{L_b} \frac{11}{12} B_{14} W_m \frac{dX_i}{dx} dx \int_0^b \frac{dW_n}{dy} X_j dy + \int_0^{L_b} \frac{11}{12} B_{15} \frac{dW_m}{dx} \frac{dX_i}{dx} dx \int_0^b W_n X_j dy \\
& + \int_0^{L_b} \frac{11}{12} B_{46} W_m X_i dx \int_0^b \frac{dW_n}{dy} \frac{dX_j}{dy} dy + \int_0^{L_b} \frac{11}{12} B_{56} \frac{dX_m}{dx} X_i dx \int_0^b W_n \frac{dX_j}{dy} dy \left. \right\} X_{ij} \\
& + \left\{ \int_0^{L_b} \frac{5}{6} A_{45} \frac{dW_m}{dx} Y_i dx \int_0^b W_n Y_j dy + \int_0^{L_b} \frac{5}{6} A_{44} W_m Y_i dx \int_0^b \frac{dW_n}{dy} Y_j dy \right. \\
& + \int_0^{L_b} \frac{11}{12} B_{24} W_m Y_i dx \int_0^b \frac{dW_n}{dy} \frac{dY_j}{dy} dy + \int_0^{L_b} \frac{11}{12} B_{25} \frac{dW_m}{dx} Y_i dx \int_0^b W_n \frac{dY_j}{dy} dy \\
& + \left. \int_0^{L_b} \frac{11}{12} B_{46} W_m \frac{dY_i}{dx} dx \int_0^b \frac{dW_n}{dy} Y_j dy + \int_0^{L_b} \frac{11}{12} B_{56} \frac{dW_m}{dx} \frac{dY_i}{dx} dx \int_0^b W_n Y_j dy \right\} Y_{ij} \left. \right]
\end{aligned}$$

(3.33)

$$\begin{aligned}
\frac{\partial U_{tl}}{\partial X_{mn}} = & \sum_{i=1}^M \sum_{j=1}^N \left[\int_0^{L_b} \frac{5}{6} A_{45} X_m W_i dx \int_0^b X_n \frac{dW_j}{dy} dy + \int_0^{L_b} \frac{5}{6} A_{55} X_m \frac{dW_i}{dx} dx \int_0^b X_n W_j dy \right. \\
& + \int_0^{L_b} \frac{11}{12} B_{14} \frac{dX_m}{dx} W_i dx \int_0^b X_n \frac{dW_j}{dy} dy + \int_0^{L_b} \frac{11}{12} B_{15} \frac{dX_m}{dx} \frac{dW_i}{dx} dx \int_0^b X_n W_j dy \\
& + \left. \int_0^{L_b} \frac{11}{12} B_{46} X_m W_i dx \int_0^b \frac{dX_n}{dy} \frac{dW_j}{dy} dy + \int_0^{L_b} \frac{11}{12} B_{56} X_m \frac{dW_i}{dx} dx \int_0^b \frac{dX_n}{dy} W_j dy \right\} W_{ij} \\
& + \left\{ \int_0^{L_b} \frac{5}{6} A_{55} X_m X_i dx \int_0^b X_n X_j dy + \int_0^{L_b} D_{11} \frac{dX_m}{dx} \frac{dX_i}{dx} dx \int_0^b X_n X_j dy \right. \\
& + \int_0^{L_b} D_{16} \frac{dX_m}{dx} X_i dx \int_0^b X_n \frac{dX_j}{dy} dy + \int_0^L D_{16} X_m \frac{dX_i}{dx} dx \int_0^b \frac{dX_n}{dy} X_j dy \\
& + \int_0^{L_b} D_{66} X_m X_i dx \int_0^b \frac{dX_n}{dy} \frac{dX_j}{dy} dy + \int_0^{L_b} \frac{11}{12} B_{15} X_m \frac{dX_i}{dx} dx \int_0^b X_n X_j dy \\
& + \int_0^{L_b} \frac{11}{12} B_{15} \frac{dX_m}{dx} X_i dx \int_0^b X_n X_j dy \\
& + \left. \int_0^{L_b} \frac{11}{12} B_{56} X_m X_i dx \int_0^b X_n \frac{dX_j}{dy} dy + \int_0^{L_b} \frac{11}{12} B_{56} X_m X_i dx \int_0^b \frac{dX_n}{dy} X_j dy \right\} X_{ij} \\
& + \left\{ \int_0^{L_b} \frac{5}{6} A_{45} X_m Y_i dx \int_0^b X_n Y_j dy + \int_0^{L_b} D_{12} \frac{dX_m}{dx} Y_i dx \int_0^b X_n \frac{dY_j}{dy} dy \right. \\
& + \int_0^{L_b} D_{16} \frac{dX_m}{dx} \frac{dY_i}{dx} dx \int_0^b X_n Y_j dy + \int_0^{L_b} D_{26} X_m Y_i dx \int_0^b \frac{dX_n}{dy} \frac{dY_j}{dy} dy \\
& + \int_0^{L_b} \frac{11}{12} B_{14} \frac{dX_m}{dx} Y_i dx \int_0^b X_n Y_j dy + \int_0^{L_b} \frac{11}{12} B_{25} X_m Y_i dx \int_0^b X_n \frac{dY_j}{dy} dy \\
& + \int_0^{L_b} \frac{11}{12} B_{46} X_m Y_i dx \int_0^b \frac{dX_n}{dy} Y_j dy \\
& + \left. \int_0^{L_b} \frac{11}{12} B_{56} X_m \frac{dY_i}{dx} dx \int_0^b X_n Y_j dy + \int_0^{L_b} D_{66} X_m \frac{dY_i}{dx} dx \int_0^b \frac{dX_n}{dy} Y_j dy \right\} Y_{ij} \Big]
\end{aligned} \tag{3.34}$$

$$\begin{aligned}
\frac{\partial U_{tl}}{\partial Y_{mn}} = & \sum_{i=1}^M \sum_{j=1}^N \left[\int_0^{L_b} \frac{5}{6} A_{45} Y_m \frac{dW_i}{dx} dx \int_0^b Y_n W_j dy + \int_0^{L_b} \frac{5}{6} A_{44} Y_m W_i dx \int_0^b Y_n \frac{dW_j}{dy} dy \right. \\
& + \int_0^{L_b} \frac{11}{12} B_{24} Y_m W_i dx \int_0^b \frac{dY_n}{dy} \frac{dW_j}{dy} dy + \int_0^{L_b} \frac{11}{12} B_{25} Y_m \frac{dW_i}{dx} dx \int_0^b \frac{dY_n}{dy} W_j dy \\
& + \left. \int_0^{L_b} \frac{11}{12} B_{46} \frac{dY_m}{dx} W_i dx \int_0^b Y_n \frac{dW_j}{dy} dy + \int_0^{L_b} \frac{11}{12} B_{56} \frac{dY_m}{dx} \frac{dW_i}{dx} dx \int_0^b Y_n W_j dy \right\} W_{ij} \\
& + \left\{ \int_0^{L_b} \frac{5}{6} A_{45} Y_m X_i dx \int_0^b Y_n X_j dy + \int_0^{L_b} D_{12} Y_m \frac{dX_i}{dx} dx \int_0^b \frac{dY_n}{dy} X_j dy \right. \\
& + \int_0^{L_b} D_{16} \frac{dY_m}{dx} \frac{dX_i}{dx} dx \int_0^b Y_n X_j dy + \int_0^{L_b} D_{26} Y_m X_i dx \int_0^b \frac{dY_n}{dy} \frac{dX_j}{dy} dy \\
& + \int_0^{L_b} D_{66} \frac{dY_m}{dx} X_i dx \int_0^b Y_n \frac{dX_j}{dy} dy + \int_0^{L_b} \frac{11}{12} B_{14} Y_m \frac{dX_i}{dx} dx \int_0^b Y_n X_j dy \\
& + \int_0^{L_b} \frac{11}{12} B_{25} Y_m X_i dx \int_0^b \frac{dY_n}{dy} X_j dy \\
& + \left. \int_0^{L_b} \frac{11}{12} B_{46} Y_m X_i dx \int_0^b Y_n \frac{dX_j}{dy} dy + \int_0^{L_b} \frac{11}{12} B_{56} \frac{dY_m}{dx} X_i dx \int_0^b Y_n X_j dy \right\} X_{ij} \\
& + \left\{ \int_0^{L_b} \frac{5}{6} A_{44} Y_m Y_i dx \int_0^b Y_n Y_j dy + \int_0^{L_b} D_{22} Y_m Y_i dx \int_0^b \frac{dY_n}{dy} \frac{dY_j}{dy} dy \right. \\
& + \int_0^{L_b} D_{26} \frac{dY_m}{dx} Y_i dx \int_0^b Y_n \frac{dY_j}{dy} dy + \int_0^{L_b} D_{26} Y_m \frac{dY_i}{dx} dx \int_0^b \frac{dY_n}{dy} Y_j dy \\
& + \int_0^{L_b} D_{66} \frac{dY_m}{dx} \frac{dY_i}{dx} dx \int_0^b Y_n Y_j dy + \int_0^{L_b} \frac{11}{12} B_{24} Y_m Y_i dx \int_0^b Y_n \frac{dY_j}{dy} dy \\
& + \int_0^{L_b} \frac{11}{12} B_{24} Y_m Y_i dx \int_0^b \frac{dY_n}{dy} Y_j dy \\
& + \left. \int_0^{L_b} \frac{11}{12} B_{46} \frac{dY_m}{dx} Y_i dx \int_0^b Y_n Y_j dy + \int_0^{L_b} \frac{11}{12} B_{46} Y_m \frac{dY_i}{dx} dx \int_0^b Y_n Y_j dy \right\} Y_{ij} \Big]
\end{aligned} \tag{3.35}$$

From equation (3.24) we get:

$$\frac{\partial W_{tl}}{\partial W_{mn}} = \sum_{i=1}^M \sum_{j=1}^N \left\{ N_o \int_0^{L_b} \frac{dW_m}{dx} \frac{dW_i}{dx} dx \int_0^b W_n W_j dy \right\} \quad (3.36)$$

where, L_b is the taper length of tapered plate and subscript 'tl' stands for tapered laminate.

3.3.4 The system equations of resin pocket for special cases

Taking into account the conditions mentioned in the Section 3.3.3, the system equations of resin pocket are calculated. Same equations (3.33 - 3.36) are also considered for resin, with an exception concerning length, A_{ij} , B_{ij} and D_{ij} . Resin ply length, L_r , is calculated from equation (2.64). A_{ij} , B_{ij} and D_{ij} for resin pocket are calculated from the equations (3.17), (3.18) and (3.19) respectively.

The system equations developed for tapered laminate and resin are applied into the equations (3.27 - 3.30). Solving the equations (3.27 - 3.30) and substituting the results into the equation (3.31), the final form is similar to the equation (3.32). The MATLAB[®] program is used to solve the equation (3.32) for buckling analysis.

3.3.5 Tapered laminated plate simply supported at four ends

In case of a plate simply supported along its four edges (SSSS) the boundary conditions are [19]:

- Along edges $x = 0$ and $x = L_b$:

$$w_o = 0, \quad M_x = 0 \quad (3.37)$$

- Along edges $y = 0$ and $y = b$:

$$w_o = 0, \quad M_y = 0 \quad (3.38)$$

The above-mentioned boundary conditions are satisfied by the following approximate solutions:

$$w_o(x, y) = \sum_{m=1}^M \sum_{n=1}^N W_{mn} \sin \frac{m\pi x}{L_b} \sin \frac{n\pi y}{b} \quad (3.39)$$

$$\phi_x(x, y) = \sum_{m=1}^M \sum_{n=1}^N X_{mn} \cos \frac{m\pi x}{L_b} \sin \frac{n\pi y}{b} \quad (3.40)$$

$$\phi_y(x, y) = \sum_{m=1}^M \sum_{n=1}^N Y_{mn} \sin \frac{m\pi x}{L_b} \cos \frac{n\pi y}{b} \quad (3.41)$$

Applying equations (3.39), (3.40) and (3.41) in the equations (3.27) - (3.30) and equating the co-efficient of W_{mn} to zero we can get a eigenvalue problem like equation (3.32) and that can be solved using MATLAB[®] program to calculate the critical buckling load.

3.3.6 Tapered laminated plate clamped at four ends (CCCC)

In case of a plate clamped along its four edges (CCCC), the boundary conditions are [35,36]:

- Along edges $x = 0$ and $x = L_b$:

$$w_o = 0, \quad \frac{\partial w_o}{\partial x} = 0 \quad (3.42)$$

- Along edges $y = 0$ and $y = b$:

$$w_o = 0, \quad \frac{\partial w_o}{\partial y} = 0 \quad (3.43)$$

The above-mentioned boundary conditions are satisfied by the following approximate solutions:

$$\phi_x(x, y) = \sum_{m=1}^M \sum_{n=1}^N X_{mn} \sin \frac{m\pi x}{L_b} \sin \frac{n\pi y}{b} \quad (3.44)$$

$$\phi_y(x, y) = \sum_{m=1}^M \sum_{n=1}^N Y_{mn} \sin \frac{m\pi x}{L_b} \sin \frac{n\pi y}{b} \quad (3.45)$$

$$w_o(x, y) = \sum_{m=1}^M \sum_{n=1}^N W_{mn} W_m(x) W_n(y) \quad (3.46)$$

where,

$$W_m(x) = \left(\cos \frac{\lambda_m x}{L_b} - \cosh \frac{\lambda_m x}{L_b} \right) - \gamma_m \left(\sin \frac{\lambda_m x}{L_b} - \sinh \frac{\lambda_m x}{L_b} \right) \quad (3.47)$$

$$W_n(y) = \left(\cos \frac{\lambda_n y}{b} - \cosh \frac{\lambda_n y}{b} \right) - \gamma_n \left(\sin \frac{\lambda_n y}{b} - \sinh \frac{\lambda_n y}{b} \right) \quad (3.48)$$

Applying the boundary conditions into approximate solutions, we get:

$$\cos(\lambda_i) \cosh(\lambda_i) = 1; \quad (3.49)$$

$$\text{and } \gamma_i = \frac{\cos(\lambda_i) - \cosh(\lambda_i)}{\sin(\lambda_i) - \sinh(\lambda_i)}; \quad \text{where } i = m, n. \quad (3.50)$$

The values of λ_i and γ_i are given in the Table 2.4 .

Using the values given in Table 2.4 in the above-mentioned approximate solutions and the results in equation (3.32) we can calculate the critical buckling load.

3.4 Example of tapered plate analyzed using Ritz method based on FSDT

Example 3.4.1

The tapered plates described in example 2.7.2 are considered for buckling analysis. The solutions have been obtained using Ritz method for simply supported and clamped-clamped boundary conditions. The results are listed in Tables 3.1 - 3.4.

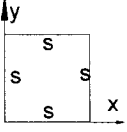
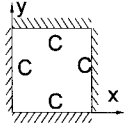
Taper length in meter	Taper angle in degrees	L_b/h				
			CLPT	FSDT	CLPT	FSDT
0.1719	0.5	38.2	3.678	3.600	13.846	13.4306
0.1146	0.75	25.47	8.270	8.030	31.142	29.8963
0.08594	1.0	19.098	14.710	13.9745	55.387	52.6176
0.0573	1.5	12.73	33.070	30.7551	124.48	117.0112
0.04295	2.0	9.54	58.660	53.3806	221.41	205.9113
0.03435	2.5	7.63	91.600	81.5240	345.77	318.1084
0.0286	3.0	6.36	132.40	115.188	498.39	453.5349

Table 3.1 Critical buckling load ($\times 10^4 N$) for different support conditions for tapered laminate model A

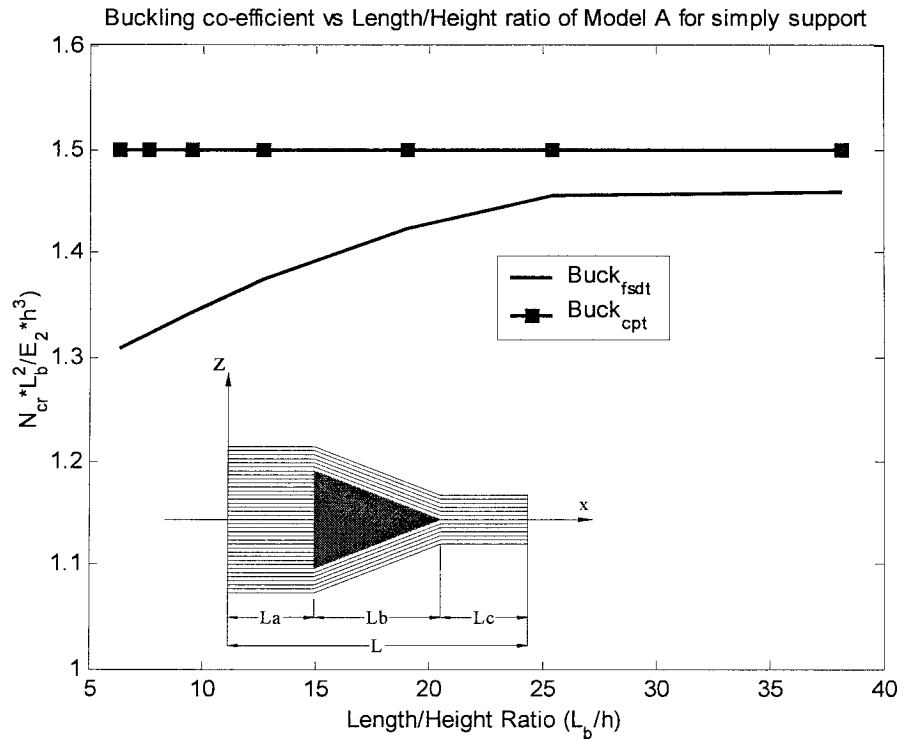


Figure 3.2 Effect of transverse shear on buckling co-efficient for simply supported tapered laminate model A

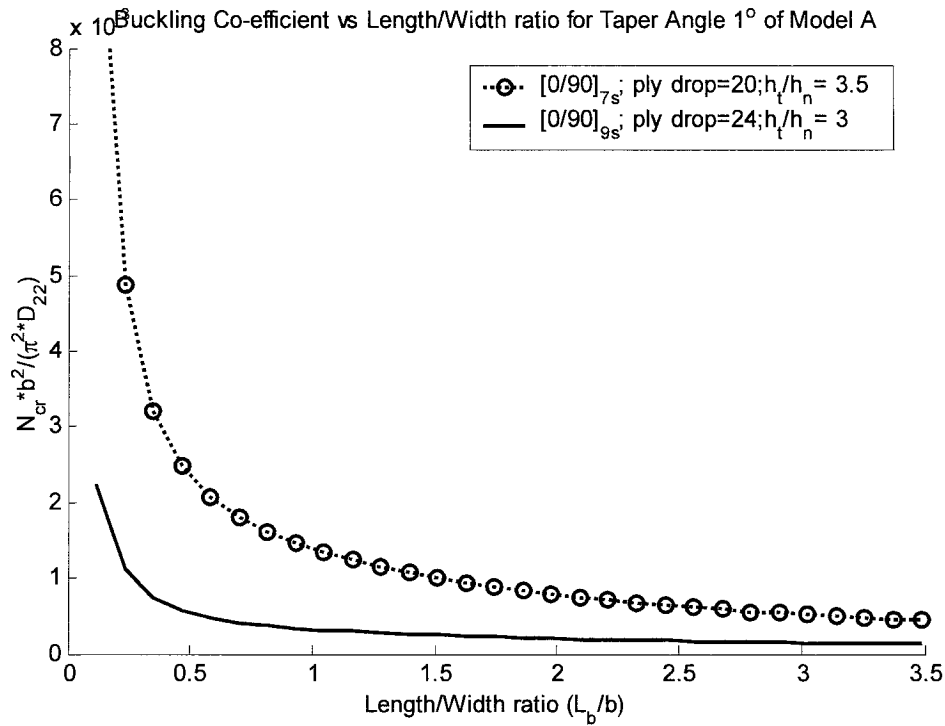


Figure 3.3 Variation of buckling co-efficient due to thickness variation for simply supported tapered laminate model A

3.4.2 Discussion on model A

The buckling co-efficient curves in Figure 3.2 reveal that the buckling co-efficient of thin plate based on first-order shear deformation theory (FSDT) is closer to that for CLPT. In case of thick plate, results vary from each other. As a whole, the results based on FSDT gives improved results compared to CLPT.

Figure 3.3 has good agreement with that of uniform laminate given in reference [38]. It is apparent from the curves that, for a given degree of taper, i.e. for a constant value of h_t/h_n , the buckling co-efficient rapidly reaches an asymptotic value, as the thickness ratio, that is the ratio of laminate thicknesses at thick and thin sections, increases. It is intuitively obvious that this should happen, since the buckle will be essentially confined to the vicinity of the thinner end.

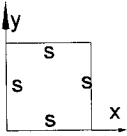
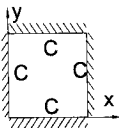
Taper length in meter	Taper angle in degrees	L_b/h				
			CLPT	FSDT	CLPT	FSDT
0.1719	0.5	38.2	11.5713	11.108	15.930	15.09
0.1146	0.75	25.47	26.0289	24.785	35.840	34.037
0.08594	1.0	19.098	46.305	43.5267	63.706	59.8836
0.0573	1.5	12.73	103.986	96.7069	143.300	133.269
0.04295	2.0	9.54	184.869	170.0795	254.280	233.9376
0.03435	2.5	7.63	288.459	262.4976	396.960	361.2336
0.0286	3.0	6.36	415.557	374.0013	569.780	512.802

Table 3.2 Critical buckling load ($\times 10^4 N$) for different support conditions for tapered laminate model B

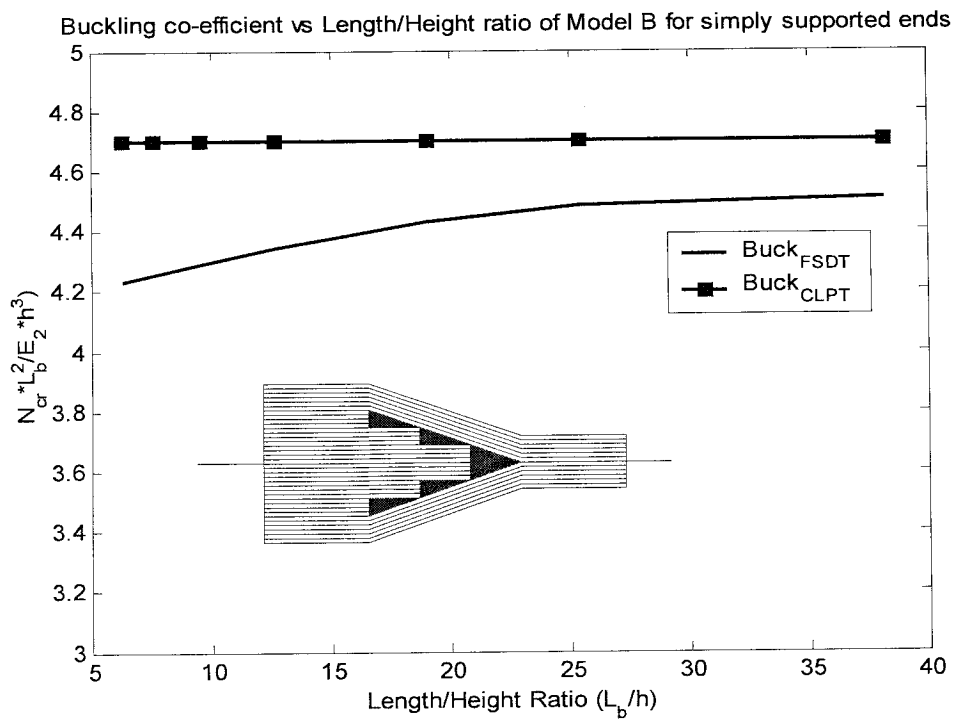


Figure 3.4 Effect of transverse shear on buckling co-efficient for simply supported tapered laminate model B

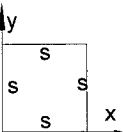
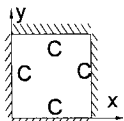
Taper length in meter	Taper angle in degrees	L_b/h				
			CLPT	FSDT	CLPT	FSDT
0.1719	0.5	38.2	3.963667	3.8447	14.53095	14.0950
0.1146	0.75	25.47	8.916111	8.580	32.6928	31.30851
0.08594	1.0	19.098	15.86167	15.0685	58.1091	55.2036
0.0573	1.5	12.73	35.62	33.4828	130.7355	122.8914
0.04295	2.0	9.54	63.3222	58.8896	231.9555	215.7186
0.03435	2.5	7.63	98.8	90.896	362.1555	333.18306
0.0286	3.0	6.36	142.3	129.493	519.729	472.9534

Table 3.3 Critical buckling load ($\times 10^4 N$) for different support conditions for tapered laminate model C

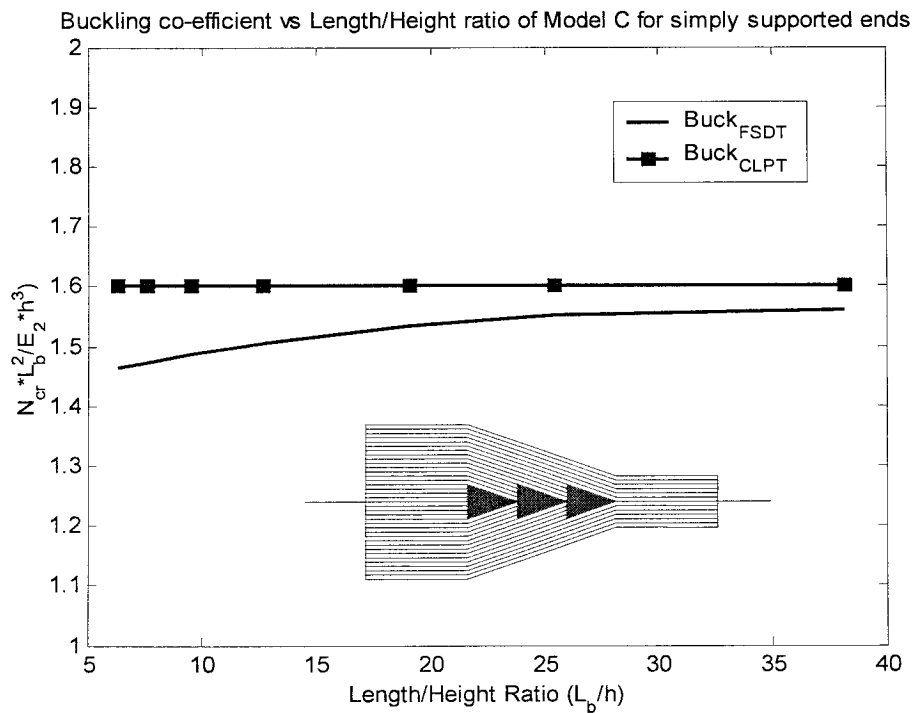


Figure 3.5 Effect of transverse shear on buckling co-efficient for simply supported tapered laminate model C

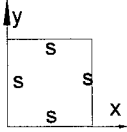
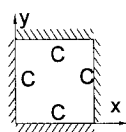
Taper length in meter	Taper angle in degrees	L_b/h				
			CLPT	FSDT	CLPT	FSDT
0.1719	0.5	38.2	11.7	11.349	20.943	19.4769
0.1146	0.75	25.47	26.3196	25.25145	47.119	43.3495
0.08594	1.0	19.098	46.8192	44.4782	83.759	76.2207
0.0573	1.5	12.73	105.1632	98.8534	188.390	169.551
0.04295	2.0	9.54	186.972	173.8839	334.340	297.5626
0.03435	2.5	7.63	291.84	268.4928	521.930	459.2984
0.0286	3.0	6.36	420.36	382.5276	749.360	651.9432

Table 3.4 Critical buckling load ($\times 10^4 N$) for different support conditions for tapered laminate model D

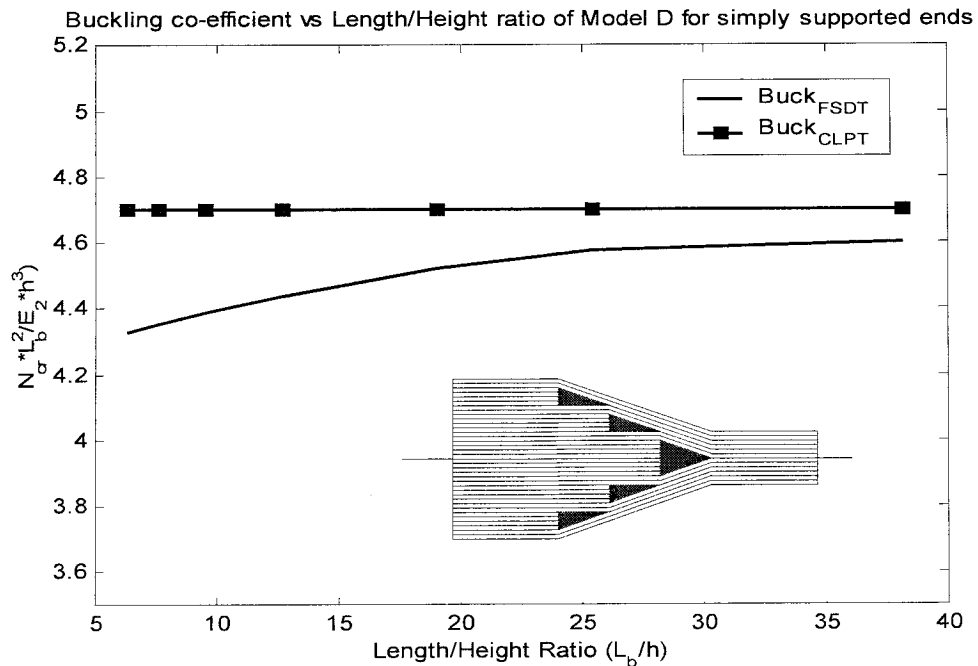


Figure 3.6 Effect of transverse shear on buckling co-efficient for simply supported tapered laminate model D

3.4.3 Discussion of models A, B, C and D

It can be seen from Tables 3.1 - 3.4 that shear deformation decreases critical buckling loads. The buckling curves in Figures 3.2 - 3.6 reveal that the buckling coefficient of thin plate based on First-order Shear Deformation Theory (FSDT) is closer to that for CLPT. In case of thick plate, results vary from each other. As a whole, FSDT gives improved results compared to CLPT.

We can conclude from Figure 3.7 that the tapered plate of model D is the strongest one; model B and model C take the second and third ranks respectively. Model A has the lowest stiffness. The buckling loads of models D and B are closer to each other; on the other hand, models A and C are closer.

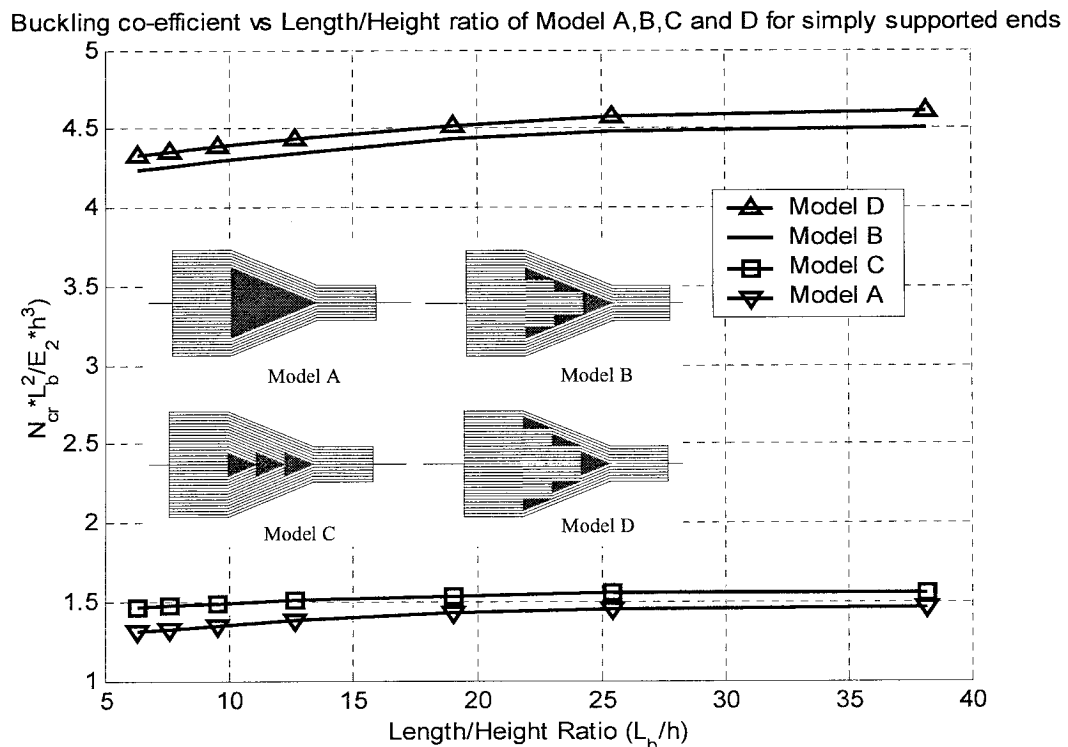


Figure 3.7 Effect of transverse shear on buckling co-efficient for simply supported tapered laminate models A, B, C and D

3.5 Discussions and conclusions

In this chapter, constitutive equation of tapered laminated plate based on shear deformation theory is developed. The system equations of critical buckling loads are developed for two types of boundary conditions and four types of taper models using Ritz method based on First-order Shear Deformation Theory (FSDT). The results based on FSDT are also compared with that of CLPT.

It can be seen from Tables 3.1 - 3.4 that shear deformation decreases critical buckling loads.

The buckling curves in Figures 3.1 - 3.5 reveal that FSDT gives improved results compared to CLPT.

It is apparent from the Figure 3.2 that the buckling co-efficient rapidly reaches an asymptotic value, as the thickness ratio, that is the ratio of laminate thicknesses at thick and thin sections, increases.

Chapter 4

Buckling Analysis Based on Third-order Shear Deformation Theory (TSDT)

4.1 Introduction

Although the Mindlin-type first-order shear deformation theory is quite accurate for the gross response, such as buckling of moderately thick laminates, the accuracy of solutions will be strongly dependent on predicting better estimates for the shear correction factors. It has been shown that the Mindlin-type first-order shear deformation theories are inadequate for the accurate prediction of the modal displacements and inter-laminar stresses of laminated composite plates (see, for example, [42]).

High-order shear deformation theories can overcome the limitations of the first-order theory by introducing additional Degrees Of Freedom (DOF). The third-order theory proposed by Reddy (1984) not only accounts for transverse shear effects but also produces a parabolic variation of the transverse shear stress through the thickness of the plate. Third-order shear deformation theory, which is one of the Equivalent Single Layer (ESL) theories, is based on the same assumptions as the classical (CLPT) and First-order Shear Deformation Theories (FSDT), except that the assumption on the straightness and normality of the transverse normal is relaxed [43]. Theories higher than third-order are

not used because the accuracy gained is so little that the effort required to solve the equations is not justified [40].

In the present work, the equations of critical buckling loads for tapered laminates subjected to uniaxial compression load have been derived using Ritz method based on third-order shear deformation plate theory in conjunction with the Von Karman strains. Unlike the first-order shear deformation theory, the higher-order theory does not require shear correction factors as $k_x = k_y = \pi / \sqrt{10} = 0.99345$ is close to unity [39]. Finally, the system equations of critical buckling loads for the tapered laminated plate are derived.

4.2 Fundamental equations for buckling

4.2.1 Displacement field

The following displacement field was introduced by Robins and Reddy [40,41] for Third-order Shear Deformation Theory (TSDT):

$$u(x, y, z, t) = u_o + z\phi_x - z^2 \left(\frac{1}{2} \frac{\partial \phi_z}{\partial x} \right) - z^3 \left[C_1 \left(\frac{\partial w_o}{\partial x} + \phi_x \right) + \frac{1}{3} \frac{\partial \phi_z}{\partial x} \right] \quad (4.1)$$

$$v(x, y, z, t) = v_o + z\phi_y - z^2 \left(\frac{1}{2} \frac{\partial \phi_z}{\partial y} \right) - z^3 \left[C_1 \left(\frac{\partial w_o}{\partial y} + \phi_y \right) + \frac{1}{3} \frac{\partial \phi_z}{\partial y} \right] \quad (4.2)$$

$$w(x, y, z, t) = w_o + z\phi_z + z^2 \phi_z \quad (4.3)$$

where,

$$C_1 = \frac{4}{3h^2} \quad (4.4)$$

$$u_o = u(x, y, 0, t) \quad (4.5)$$

$$v_o = v(x, y, 0, t) \quad (4.6)$$

$$w_o = w(x, y, 0, t) \quad (4.7)$$

h is the height of the laminate;

u_o, v_o and w_o are the displacements of transverse normal on plane $z = 0$;

$\phi_x(x, y, 0, t)$ and $\phi_y(x, y, 0, t)$ are the rotations of transverse normal on plane $z = 0$;

$\phi_z(x, y, 0, t)$ is the extension of transverse normal;

$\varphi_z(x, y, 0, t)$ is interpreted as a higher-order rotation of transverse normal.

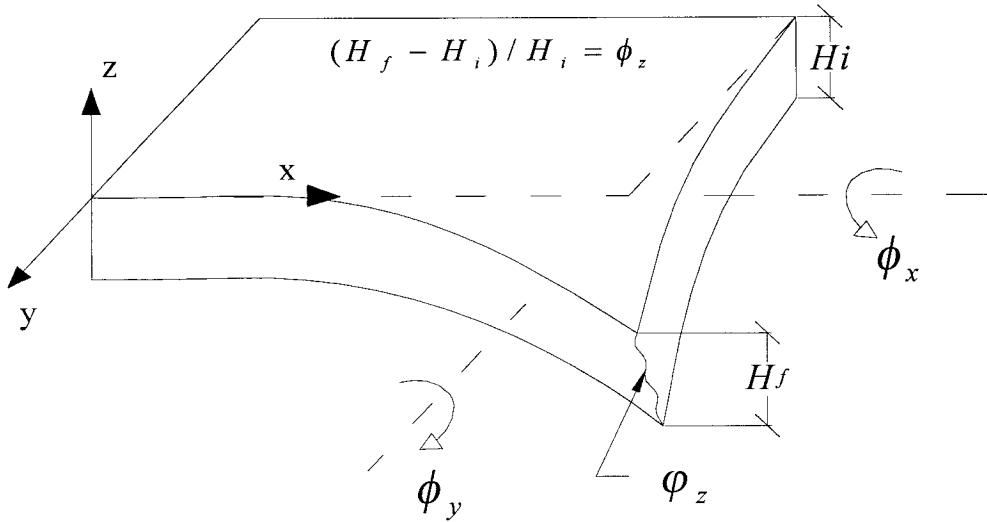


Figure 4.1 Explanation of displacement terms for TSDT

4.2.2 Strain field with transverse shear

The linear small strains according to displacement field equations (4.1 – 4.3) are [40, 41]:

$$\varepsilon_{xx} = \varepsilon_{xx}^0 + z\kappa_{xx}^0 + z^2\kappa_{xx}^1 + z^3\kappa_{xx}^2 \quad (4.8)$$

$$\varepsilon_{yy} = \varepsilon_{yy}^0 + z\kappa_{yy}^0 + z^2\kappa_{yy}^1 + z^3\kappa_{yy}^2 \quad (4.9)$$

$$\varepsilon_{zz} = 0 \quad (4.10)$$

$$\gamma_{yz} = \gamma_{yz}^0 + z^2\kappa_{yz}^1 \quad (4.11)$$

$$\gamma_{xz} = \gamma_{xz}^0 + z^2\kappa_{xz}^1 \quad (4.12)$$

$$\gamma_{xy} = \gamma_{xy}^0 + z\kappa_{xy}^0 + z^2\kappa_{xy}^1 + z^3\kappa_{xy}^2 \quad (4.13)$$

where,

$$\varepsilon_{xx}^0 = \frac{\partial u_o}{\partial x} \quad (4.14)$$

$$\kappa_{xx}^0 = \frac{\partial \phi_x}{\partial x} \quad (4.15)$$

$$\kappa_{xx}^1 = -\frac{1}{2} \frac{\partial^2 \phi_z}{\partial x^2} \quad (4.16)$$

$$\kappa_{xx}^2 = -\left[C_1 \left(\frac{\partial^2 w_o}{\partial x^2} + \frac{\partial \phi_x}{\partial x} \right) + \frac{1}{3} \frac{\partial^2 \phi_z}{\partial x^2} \right] \quad (4.17)$$

$$\varepsilon_{yy}^0 = \frac{\partial v_o}{\partial y} \quad (4.18)$$

$$\kappa_{yy}^0 = \frac{\partial \phi_y}{\partial y} \quad (4.19)$$

$$\kappa_{yy}^1 = -\frac{1}{2} \frac{\partial^2 \phi_z}{\partial y^2} \quad (4.20)$$

$$\kappa_{yy}^2 = -\left[C_1 \left(\frac{\partial^2 w_o}{\partial y^2} + \frac{\partial \phi_y}{\partial y} \right) + \frac{1}{3} \frac{\partial^2 \phi_z}{\partial y^2} \right] \quad (4.21)$$

$$\gamma_{yz}^0 = \frac{\partial w_o}{\partial y} + \phi_y \quad (4.22)$$

$$\kappa_{yz}^1 = -3C_1 \left(\frac{\partial w_o}{\partial y} + \phi_y \right) \quad (4.23)$$

$$\gamma_{xz}^0 = \frac{\partial w_o}{\partial x} + \phi_x \quad (4.24)$$

$$\kappa_{xz}^1 = -3C_1 \left(\frac{\partial w_o}{\partial x} + \phi_x \right) \quad (4.25)$$

$$\gamma_{xy}^0 = \frac{\partial u_o}{\partial y} + \frac{\partial v_o}{\partial x} \quad (4.26)$$

$$\kappa_{xy}^0 = \frac{\partial \phi_x}{\partial y} + \frac{\partial \phi_y}{\partial x} \quad (4.27)$$

$$\kappa_{xy}^1 = -\frac{\partial^2 \phi_z}{\partial x \partial y} \quad (4.28)$$

$$\kappa_{xy}^2 = -\left[C_1 \left(2 \frac{\partial^2 w_o}{\partial x \partial y} + \frac{\partial \phi_x}{\partial y} + \frac{\partial \phi_y}{\partial x} \right) + \frac{2}{3} \frac{\partial^2 \phi_z}{\partial x \partial y} \right] \quad (4.29)$$

where, κ_{ij} is the curvature.

4.2.3 Stress field

The stress field given in equation (2.44) can be rewritten as follows:

$$\begin{Bmatrix} \sigma_{xx} \\ \sigma_{yy} \\ \sigma_{zz} = 0 \\ \tau_{yz} \\ \tau_{xz} \\ \tau_{xy} \end{Bmatrix} = \begin{bmatrix} C_{11} & C_{12} & C_{13} & C_{14} & C_{15} & C_{16} \\ C_{12} & C_{22} & C_{23} & C_{24} & C_{25} & C_{26} \\ C_{13} & C_{23} & C_{33} & C_{34} & C_{35} & C_{36} \\ C_{14} & C_{24} & C_{34} & C_{44} & C_{45} & C_{46} \\ C_{15} & C_{25} & C_{35} & C_{45} & C_{55} & C_{56} \\ C_{16} & C_{26} & C_{36} & C_{46} & C_{56} & C_{66} \end{bmatrix} \begin{Bmatrix} \varepsilon_{xx} \\ \varepsilon_{yy} \\ \varepsilon_{zz} \\ \gamma_{yz} \\ \gamma_{xz} \\ \gamma_{xy} \end{Bmatrix} \quad (4.30)$$

where,

σ_{ij} and τ_{ij} are the normal stress and shear stress respectively ;

ε_{ij} and γ_{ij} are the normal strain and shear strain respectively in the coordinate

system xyz and these values are given in the Section-4.2.2 ;

C_{ij} is the corresponding stiffness co-efficient given in the equation (2.39).

$$\varepsilon_{zz} = -(1/C_{33})(C_{13}\varepsilon_{xx} + C_{23}\varepsilon_{yy} + C_{34}\gamma_{yz} + C_{35}\gamma_{xz} + C_{36}\gamma_{xy}) \quad (4.31)$$

$$\begin{aligned} \sigma_{xx} = & (C_{11} - C_{13}^2/C_{33})\varepsilon_{xx} + (C_{12} - C_{13}C_{23}/C_{33})\varepsilon_{yy} + (C_{14} - C_{13}C_{34}/C_{33})\gamma_{yz} \\ & + (C_{15} - C_{13}C_{35}/C_{33})\gamma_{xz} + (C_{16} - C_{13}C_{36}/C_{33})\gamma_{xy} \end{aligned} \quad (4.32)$$

and the equations for σ_{yy} , τ_{yz} , τ_{xz} and τ_{xy} are analogous to that for σ_{xx} .

Therefore, the reduced stiffness matrix is in the form of:

$$\begin{Bmatrix} \sigma_{xx} \\ \sigma_{yy} \\ \tau_{yz} \\ \tau_{xz} \\ \tau_{xy} \end{Bmatrix} = \begin{bmatrix} Q_{11} & Q_{12} & Q_{14} & Q_{15} & Q_{16} \\ Q_{12} & Q_{22} & Q_{24} & Q_{25} & Q_{26} \\ Q_{14} & Q_{24} & Q_{44} & Q_{45} & Q_{46} \\ Q_{15} & Q_{25} & Q_{45} & Q_{55} & Q_{56} \\ Q_{16} & Q_{26} & Q_{46} & Q_{56} & Q_{66} \end{bmatrix} \begin{Bmatrix} \varepsilon_{xx} \\ \varepsilon_{yy} \\ \gamma_{yz} \\ \gamma_{xz} \\ \gamma_{xy} \end{Bmatrix} \quad (4.33)$$

Rearranging (4.33) we get:

$$\begin{Bmatrix} \sigma_{xx} \\ \sigma_{yy} \\ \tau_{xy} \\ \tau_{yz} \\ \tau_{xz} \end{Bmatrix} = \begin{bmatrix} Q_{11} & Q_{12} & Q_{16} & Q_{14} & Q_{15} \\ Q_{12} & Q_{22} & Q_{26} & Q_{24} & Q_{25} \\ Q_{16} & Q_{26} & Q_{66} & Q_{46} & Q_{56} \\ Q_{14} & Q_{24} & Q_{46} & Q_{44} & Q_{45} \\ Q_{15} & Q_{25} & Q_{56} & Q_{45} & Q_{55} \end{bmatrix} \begin{Bmatrix} \varepsilon_{xx} \\ \varepsilon_{yy} \\ \gamma_{xy} \\ \gamma_{yz} \\ \gamma_{xz} \end{Bmatrix} \quad (4.34)$$

where,

$$Q_{ij} = C_{ij} - \frac{C_{i3}C_{j3}}{C_{33}} ; \quad (4.35)$$

C_{ij} is given in equation (2.39) ;

ε_{ij} and γ_{ij} are given in equations (4.8 - 4.13);

$i,j = 1, 2, 3, 4, 5, 6.$

‘Stress field’ of First-order Shear Deformation Theory (FSDT) and TSDT are of the same format but the values of ‘strain field’ are different.

4.2.4 Constitutive equation

The constitutive equation with transverse shear is written by associating the force resultants and the moments; the same equation can be used for both tapered laminate and resin pocket. The equation is given in the next page:

$$\begin{Bmatrix}
\left. \begin{matrix} N_{xx} \\ N_{yy} \\ N_{xy} \\ N_{yz} \\ N_{xz} \end{matrix} \right\} \\
\left. \begin{matrix} M_{xx} \\ M_{yy} \\ M_{xy} \\ M_{yz} \\ M_{xz} \end{matrix} \right\} \\
\left. \begin{matrix} P_{xx} \\ P_{yy} \\ P_{xy} \\ P_{yz} \\ P_{xz} \end{matrix} \right\} \\
\left. \begin{matrix} S_{xx} \\ S_{yy} \\ S_{xy} \\ S_{yz} \\ S_{xz} \end{matrix} \right\}
\end{Bmatrix} = \begin{bmatrix}
\left[\begin{matrix} A' \\ B' \\ D' \\ E' \end{matrix} \right] & \left[\begin{matrix} B' \\ D' \\ E' \\ F' \end{matrix} \right] & \left[\begin{matrix} D' \\ E' \\ F' \\ H' \end{matrix} \right] & \left[\begin{matrix} E' \\ F' \\ H' \\ J' \end{matrix} \right]
\end{bmatrix} \begin{Bmatrix}
\left. \begin{matrix} \varepsilon_{xx}^0 \\ \varepsilon_{yy}^0 \\ \gamma_{xy}^0 \\ \gamma_{yz}^0 \\ \gamma_{xz}^0 \end{matrix} \right\} \\
\left. \begin{matrix} \kappa_{xx}^0 \\ \kappa_{yy}^0 \\ \kappa_{xy}^0 \\ \kappa_{yz}^0 \\ \kappa_{xz}^0 \end{matrix} \right\} \\
\left. \begin{matrix} \kappa_{xx}^1 \\ \kappa_{yy}^1 \\ \kappa_{xy}^1 \\ \kappa_{yz}^1 \\ \kappa_{xz}^1 \end{matrix} \right\} \\
\left. \begin{matrix} \kappa_{xx}^2 \\ \kappa_{yy}^2 \\ \kappa_{xy}^2 \\ \kappa_{yz}^2 \\ \kappa_{xz}^2 \end{matrix} \right\}
\end{Bmatrix} \quad (4.36)$$

In the equation (4.36), the elements of stiffness matrix can for example be defined

as:

$$[A'] = \begin{bmatrix}
A_{11} & A_{12} & A_{16} & A_{14} & A_{15} \\
& A_{22} & A_{26} & A_{24} & A_{25} \\
& & A_{66} & A_{64} & A_{65} \\
& & & A_{44} & A_{45} \\
sym & & & & A_{55}
\end{bmatrix} \quad (4.37)$$

Elements of matrices $[A']$, $[B']$, $[D']$, $[E']$, $[F']$, $[H']$ and $[J']$ are defined as follows:

$$(A'_{ij}, B'_{ij}, D'_{ij}, E'_{ij}, F'_{ij}, H'_{ij}, J'_{ij}) = \int_{-\frac{h}{2}}^{\frac{h}{2}} Q_{ij}(1, z, z^2, z^3, z^4, z^5, z^6) dz \quad (4.38)$$

Laminate stress resultants are defined as follow:

$$(N_{ij}, M_{ij}, P_{ij}, S_{ij}) = \sum_{n=1}^N \int_{z_n}^{z_{n-1}} \sigma_i(1, z, z^2, z^3) dz \quad (4.39)$$

where,

N_{ij} is the in plane resultant force;

M_{ij} is the resultant moments (bending and twisting);

P_{ij} and S_{ij} are the higher-order terms;

Q_{ij} and σ_i are given by equation (4.35) and equation (4.34) respectively, ($ij = 1,2,4,5,6$).

4.3 Energy formulation

In the case of FSDT, unknown displacement terms were 5 (u_o, v_o, w_o, ϕ_x & ϕ_y) in number but for TSDT unknown displacement terms are 7 ($u_o, v_o, w_o, \phi_x, \phi_y, \phi_z$ & φ_z) in number. The procedure of strain energy calculation of TSDT is the same as FSDT.

4.3.1 Energy equations for tapered laminate and resin pocket

4.3.1.1 Strain energy

Strain energy can be written in the form of:

$$U = \frac{1}{2} \iiint \{ (\sigma_{xx} \varepsilon_{xx} + \sigma_{yy} \varepsilon_{yy} + \tau_{xy} \gamma_{xy}) + (\tau_{yz} \gamma_{yz} + \tau_{xz} \gamma_{xz}) \} dx dy dz \quad (4.40)$$

where, $\sigma_{zz} = 0$; using the values of σ_{ij} from equation (4.34) in equation (4.40), we get the equation for the tapered laminate:

$$\begin{aligned}
U = \frac{1}{2} \iiint & \left\{ [Q_{11} \quad Q_{12} \quad Q_{16}] \begin{bmatrix} \epsilon_{xx}^2 \\ \epsilon_{yy} \epsilon_{xx} \\ \gamma_{xy} \epsilon_{xx} \end{bmatrix} + [Q_{14} \quad Q_{15}] \begin{bmatrix} \gamma_{yz} \epsilon_{xx} \\ \gamma_{xz} \epsilon_{xx} \end{bmatrix} \right. \\
& + [Q_{12} \quad Q_{22} \quad Q_{26}] \begin{bmatrix} \epsilon_{xx} \epsilon_{yy} \\ \epsilon_{yy}^2 \\ \gamma_{xy} \epsilon_{yy} \end{bmatrix} + [Q_{24} \quad Q_{25}] \begin{bmatrix} \gamma_{yz} \epsilon_{yy} \\ \gamma_{xz} \epsilon_{yy} \end{bmatrix} \\
& + [Q_{16} \quad Q_{26} \quad Q_{66}] \begin{bmatrix} \epsilon_{xx} \gamma_{xy} \\ \epsilon_{yy} \gamma_{xy} \\ \gamma_{xy}^2 \end{bmatrix} + [Q_{46} \quad Q_{56}] \begin{bmatrix} \gamma_{yz} \gamma_{xy} \\ \gamma_{xz} \gamma_{xy} \end{bmatrix} \\
& + [Q_{14} \quad Q_{24} \quad Q_{46}] \begin{bmatrix} \epsilon_{xx} \gamma_{yz} \\ \epsilon_{yy} \gamma_{yz} \\ \gamma_{xy} \gamma_{yz} \end{bmatrix} + [Q_{44} \quad Q_{45}] \begin{bmatrix} \gamma_{yz} \gamma_{yz} \\ \gamma_{xz} \gamma_{yz} \end{bmatrix} \\
& \left. + [Q_{15} \quad Q_{25} \quad Q_{56}] \begin{bmatrix} \epsilon_{xx} \gamma_{xz} \\ \epsilon_{yy} \gamma_{xz} \\ \gamma_{xy} \gamma_{xz} \end{bmatrix} + [Q_{45} \quad Q_{55}] \begin{bmatrix} \gamma_{yz} \gamma_{xz} \\ \gamma_{xz} \gamma_{xz} \end{bmatrix} \right\} dx dy dz
\end{aligned} \tag{4.41}$$

The above relation can be written as a function of the displacements $u_o, v_o, w_o, \phi_x, \phi_y, \phi_z$ & φ_z by substituting the strain-displacement relations (4.8) - (4.13) into (4.41). Next, by integrating with respect to z across the thickness of the tapered laminate or resin pocket we obtain the final form of strain energy as follows:

$$\begin{aligned}
U = & \frac{1}{2} \int_{y=0}^b \int_{x=0}^L \left[A_{11} \frac{\partial^2 u}{\partial x^2} + A_{22} \frac{\partial^2 v}{\partial y^2} + A_{44} \left(\frac{\partial^2 w}{\partial y^2} + 2 \frac{\partial w}{\partial y} \phi_y + \phi_y^2 \right) + A_{55} \left(2 \frac{\partial w}{\partial x} \phi_x + \phi_x^2 + \frac{\partial^2 w}{\partial x^2} \right) \right. \\
& + A_{66} \left(\frac{\partial^2 v}{\partial x^2} + \frac{\partial u^2}{\partial y^2} + 2 \frac{\partial u}{\partial y} \frac{\partial v}{\partial x} \right) + 2A_{12} \frac{\partial v}{\partial y} \frac{\partial u}{\partial x} + 2A_{14} \left(\frac{\partial w}{\partial y} \frac{\partial u}{\partial x} + \phi_y \frac{\partial u}{\partial x} \right) + 2A_{15} \left(\frac{\partial w \partial u}{\partial x^2} + \phi_x \frac{\partial u}{\partial x} \right) \\
& + 2A_{16} \left(\frac{\partial^2 u}{\partial y \partial x} + \frac{\partial v \partial u}{\partial x^2} \right) + 2A_{24} \left(\frac{\partial w \partial v}{\partial y^2} + \phi_y \frac{\partial v}{\partial y} \right) + 2A_{26} \left(\frac{\partial u \partial v}{\partial y^2} + \frac{\partial^2 v}{\partial x \partial y} \right) + 2A_{25} \left(\phi_x \frac{\partial v}{\partial y} + \frac{\partial w}{\partial x} \frac{\partial v}{\partial y} \right) \\
& + 2A_{45} \left(\frac{\partial^2 w}{\partial x \partial y} + \frac{\partial w}{\partial x} \phi_y + \phi_x \phi_y + \phi_x \frac{\partial w}{\partial y} \right) + 2A_{46} \left(\frac{\partial w \partial u}{\partial y^2} + \phi_y \frac{\partial v}{\partial x} + \phi_y \frac{\partial u}{\partial y} + \frac{\partial w}{\partial y} \frac{\partial v}{\partial x} \right) \\
& + 2A_{56} \left(\frac{\partial w}{\partial x} \frac{\partial u}{\partial y} + \phi_x \frac{\partial u}{\partial y} + \phi_x \frac{\partial v}{\partial x} + \frac{\partial w \partial v}{\partial x^2} \right) \\
& + 2 \left\{ B_{11} \frac{\partial u}{\partial x} \frac{\partial \phi_x}{\partial x} + B_{22} \frac{\partial v}{\partial y} \frac{\partial \phi_y}{\partial y} + B_{66} \left(\frac{\partial v}{\partial x} \frac{\partial \phi_y}{\partial x} + \frac{\partial u}{\partial y} \frac{\partial \phi_x}{\partial x} + \frac{\partial v}{\partial x} \frac{\partial \phi_x}{\partial y} + \frac{\partial u}{\partial y} \frac{\partial \phi_x}{\partial y} \right) \right. \\
& + B_{12} \left(\frac{\partial \phi_y}{\partial y} \frac{\partial u}{\partial x} + \frac{\partial v}{\partial y} \frac{\partial \phi_x}{\partial x} \right) + B_{14} \left(\frac{\partial w}{\partial y} \frac{\partial \phi_x}{\partial x} + \phi_y \frac{\partial \phi_x}{\partial x} \right) + B_{15} \left(\frac{\partial w}{\partial x} \frac{\partial \phi_x}{\partial x} + \phi_x \frac{\partial \phi_x}{\partial x} \right) \\
& + B_{16} \left(\frac{\partial v}{\partial x} \frac{\partial \phi_x}{\partial x} + 2 \frac{\partial u}{\partial y} \frac{\partial \phi_x}{\partial x} + \frac{\partial \phi_y}{\partial x} \frac{\partial u}{\partial x} \right) + B_{24} \left(\frac{\partial w}{\partial y} \frac{\partial \phi_y}{\partial y} + \phi_y \frac{\partial \phi_y}{\partial y} \right) + B_{25} \left(\frac{\partial w}{\partial x} \frac{\partial \phi_y}{\partial y} + \phi_x \frac{\partial \phi_y}{\partial y} \right) \\
& + B_{26} \left(2 \frac{\partial \phi_y}{\partial x} \frac{\partial v}{\partial y} + \frac{\partial u}{\partial y} \frac{\partial \phi_y}{\partial y} + \frac{\partial \phi_x}{\partial y} \frac{\partial v}{\partial y} \right) + B_{46} \left(\phi_y \frac{\partial \phi_y}{\partial x} + \phi_y \frac{\partial \phi_x}{\partial y} + \frac{\partial w}{\partial y} \frac{\partial \phi_y}{\partial x} + \frac{\partial w}{\partial y} \frac{\partial \phi_x}{\partial y} \right) \\
& \left. + B_{56} \left(\frac{\partial w}{\partial x} \frac{\partial \phi_y}{\partial x} + \frac{\partial w}{\partial x} \frac{\partial \phi_x}{\partial y} + \phi_x \frac{\partial \phi_x}{\partial y} + \phi_x \frac{\partial \phi_y}{\partial x} \right) \right\} \\
& + D_{11} \left(\frac{\partial \phi_x^2}{\partial x^2} - \frac{\partial u}{\partial x} \frac{\partial^2 \phi_z}{\partial x^2} \right) + D_{22} \left(\frac{\partial \phi_y^2}{\partial y^2} - \frac{\partial v}{\partial y} \frac{\partial^2 \phi_z}{\partial y^2} \right) - 6D_{44} C_1 \left(\frac{\partial^2 w}{\partial y^2} + 2 \frac{\partial w}{\partial y} \phi_y + \phi_y^2 \right) \\
& - 6D_{55} C_1 \left(\frac{\partial^2 w}{\partial x^2} + 2 \frac{\partial w}{\partial x} \phi_x + \phi_x^2 \right) + D_{66} \left(\frac{\partial \phi_y^2}{\partial x^2} + 2 \frac{\partial \phi_x}{\partial y} \frac{\partial \phi_y}{\partial x} + \frac{\partial \phi_x^2}{\partial y^2} - 2 \frac{\partial v}{\partial x} \frac{\partial^2 \phi_z}{\partial x \partial y} - 2 \frac{\partial u}{\partial x} \frac{\partial^2 \phi_z}{\partial x \partial y} \right) \\
& - 12D_{45} C_1 \left(\phi_x \frac{\partial w}{\partial y} + \frac{\partial w}{\partial x} \phi_y + \frac{\partial^2 w}{\partial x \partial y} + \phi_x \phi_y \right) - D_{12} \left(\frac{\partial v}{\partial y} \frac{\partial^2 \phi_z}{\partial x^2} - 2 \frac{\partial \phi_y}{\partial y} \frac{\partial \phi_x}{\partial x} + \frac{\partial^2 \phi_z}{\partial y^2} \frac{\partial u}{\partial x} \right) \\
& - D_{14} \left(6C_1 \frac{\partial w}{\partial y} \frac{\partial u}{\partial x} + 6C_1 \phi_y \frac{\partial u}{\partial x} + \frac{\partial w}{\partial y} \frac{\partial^2 \phi_z}{\partial x^2} + \phi_y \frac{\partial^2 \phi_z}{\partial x^2} \right) \\
& - D_{15} \left(6C_1 \frac{\partial w}{\partial x} \frac{\partial u}{\partial x} + 6C_1 \phi_x \frac{\partial u}{\partial x} + \phi_x \frac{\partial^2 \phi_z}{\partial x^2} + \frac{\partial w}{\partial x} \frac{\partial^2 \phi_z}{\partial x^2} \right)
\end{aligned}$$

$$\begin{aligned}
& + D_{16} \left(2 \frac{\partial \phi_y}{\partial x} \frac{\partial \phi_x}{\partial x} - \frac{\partial v}{\partial x} \frac{\partial^2 \phi_z}{\partial x^2} - \frac{\partial u}{\partial y} \frac{\partial^2 \phi_z}{\partial x^2} + 2 \frac{\partial \phi_x}{\partial x} \frac{\partial \phi_x}{\partial y} - 2 \frac{\partial^2 \phi_z}{\partial x \partial y} \frac{\partial u}{\partial x} \right) \\
& - D_{24} \left(6C_1 \frac{\partial w}{\partial y} \frac{\partial v}{\partial y} + 6\phi_y C_1 \frac{\partial v}{\partial y} + \frac{\partial w}{\partial y} \frac{\partial^2 \phi_z}{\partial y^2} + \phi_y \frac{\partial^2 \phi_z}{\partial y^2} \right) \\
& - D_{25} \left(6C_1 \frac{\partial w}{\partial x} \frac{\partial v}{\partial y} + 6C_1 \phi_x \frac{\partial v}{\partial y} + \phi_x \frac{\partial^2 \phi_z}{\partial y^2} + \frac{\partial w}{\partial x} \frac{\partial^2 \phi_z}{\partial y^2} \right) \\
& + D_{26} \left(2 \frac{\partial \phi_y}{\partial x} \frac{\partial \phi_y}{\partial y} - \frac{\partial v}{\partial x} \frac{\partial^2 \phi_z}{\partial y^2} + 2 \frac{\partial \phi_x}{\partial y} \frac{\partial \phi_y}{\partial y} - 2 \frac{\partial^2 \phi_z}{\partial x \partial y} \frac{\partial v}{\partial y} - \frac{\partial u}{\partial y} \frac{\partial^2 \phi_z}{\partial y^2} \right) \\
& - D_{46} \left(2\phi_y \frac{\partial^2 \phi_z}{\partial x \partial y} + 2 \frac{\partial w}{\partial y} \frac{\partial^2 \phi_z}{\partial x \partial y} + 6C_1 \frac{\partial w}{\partial y} \frac{\partial v}{\partial x} + 6C_1 \frac{\partial w}{\partial y} \frac{\partial u}{\partial y} + 6C_1 \phi_y \frac{\partial u}{\partial y} + 6C_1 \phi_y \frac{\partial v}{\partial x} \right) \\
& - D_{56} \left(2\phi_x \frac{\partial^2 \phi_z}{\partial x \partial y} + 2 \frac{\partial w}{\partial x} \frac{\partial^2 \phi_z}{\partial x \partial y} + 6C_1 \frac{\partial w}{\partial x} \frac{\partial u}{\partial y} + 6C_1 \frac{\partial w}{\partial x} \frac{\partial v}{\partial x} + 6C_1 \phi_x \frac{\partial v}{\partial x} + 6C_1 \phi_x \frac{\partial u}{\partial y} \right) \\
& - E_{12} \left(2C_1 \frac{\partial v}{\partial y} \frac{\partial^2 w}{\partial x^2} + 2/3 \frac{\partial^2 \phi_z}{\partial y^2} \frac{\partial u}{\partial x} + 2C_1 \frac{\partial \phi_y}{\partial y} \frac{\partial u}{\partial x} + 2C_1 \frac{\partial v}{\partial y} \frac{\partial \phi_x}{\partial x} + \frac{\partial \phi_y}{\partial y} \frac{\partial^2 \phi_z}{\partial x^2} + \frac{\partial^2 \phi_z}{\partial y^2} \frac{\partial \phi_x}{\partial x} \right. \\
& + 2/3 \frac{\partial v}{\partial y} \frac{\partial^2 \phi_z}{\partial x^2} + 2C_1 \frac{\partial^2 w}{\partial y^2} \frac{\partial u}{\partial x} \left. \right) - E_{14} \left(2C_1 \phi_y \frac{\partial^2 w}{\partial x^2} + 2/3 \phi_y \frac{\partial^2 \phi_z}{\partial x^2} + 8C_1 \phi_y \frac{\partial \phi_x}{\partial x} + 2C_1 \frac{\partial w}{\partial y} \frac{\partial^2 w}{\partial x^2} \right. \\
& + 2/3 \frac{\partial w}{\partial y} \frac{\partial^2 \phi_z}{\partial x^2} + 8C_1 \frac{\partial w}{\partial y} \frac{\partial \phi_x}{\partial x} \left. \right) - E_{15} \left(2/3 \frac{\partial w}{\partial x} \frac{\partial^2 \phi_z}{\partial x^2} + 2C_1 \frac{\partial w}{\partial x} \frac{\partial^2 w}{\partial x^2} + 8C_1 \frac{\partial w}{\partial x} \frac{\partial \phi_x}{\partial x} + 2/3 \phi_x \frac{\partial^2 \phi_z}{\partial x^2} \right. \\
& + 2C_1 \phi_x \frac{\partial^2 w}{\partial x^2} + 8C_1 \phi_x \frac{\partial \phi_x}{\partial x} \left. \right) - E_{16} \left(2/3 \frac{\partial u}{\partial y} \frac{\partial^2 \phi_z}{\partial x^2} + 2 \frac{\partial^2 \phi_z}{\partial x \partial y} \frac{\partial \phi_x}{\partial x} + 2C_1 \frac{\partial v}{\partial x} \frac{\partial^2 w}{\partial x^2} + 2/3 \frac{\partial v}{\partial x} \frac{\partial^2 \phi_z}{\partial x^2} \right. \\
& + \frac{\partial \phi_y}{\partial x} \frac{\partial^2 \phi_z}{\partial x^2} + 2C_1 \frac{\partial u}{\partial y} \frac{\partial^2 w}{\partial x^2} + \frac{\partial \phi_x}{\partial y} \frac{\partial^2 \phi_z}{\partial x^2} + 4C_1 \frac{\partial^2 w}{\partial x \partial y} \frac{\partial u}{\partial x} + 2C_1 \frac{\partial \phi_y}{\partial x} \frac{\partial u}{\partial x} + 4C_1 \frac{\partial u}{\partial y} \frac{\partial \phi_x}{\partial x} \left. \right) \\
& + 4/3 \frac{\partial^2 \phi_z}{\partial x \partial y} \frac{\partial u}{\partial x} + 2C_1 \frac{\partial v}{\partial x} \frac{\partial \phi_x}{\partial x} \left. \right) - E_{24} \left(2/3 \phi_y \frac{\partial^2 \phi_z}{\partial y^2} + 2C_1 \phi_y \frac{\partial^2 w}{\partial y^2} + 2C_1 \frac{\partial w}{\partial y} \frac{\partial^2 w}{\partial y^2} + 2/3 \frac{\partial w}{\partial y} \frac{\partial^2 \phi_z}{\partial y^2} \right. \\
& + 8C_1 \phi_y \frac{\partial \phi_y}{\partial y} + 8C_1 \frac{\partial w}{\partial y} \frac{\partial \phi_y}{\partial y} \left. \right) - E_{25} \left(2C_1 \phi_x \frac{\partial^2 w}{\partial y^2} + 8C_1 \phi_x \frac{\partial \phi_y}{\partial y} + 2/3 \phi_x \frac{\partial^2 \phi_z}{\partial y^2} + 2C_1 \frac{\partial w}{\partial x} \frac{\partial^2 w}{\partial y^2} \right. \\
& + 8C_1 \frac{\partial w}{\partial x} \frac{\partial \phi_y}{\partial y} + 2/3 \frac{\partial w}{\partial x} \frac{\partial^2 \phi_z}{\partial y^2} \left. \right) - E_{26} \left(2C_1 \frac{\partial u}{\partial y} \frac{\partial \phi_y}{\partial y} + 4C_1 \frac{\partial^2 w}{\partial x \partial y} \frac{\partial v}{\partial y} + 2 \frac{\partial^2 \phi_z}{\partial x \partial y} \frac{\partial \phi_y}{\partial y} + 2C_1 \frac{\partial v}{\partial x} \frac{\partial^2 w}{\partial y^2} \right. \\
& + 2/3 \frac{\partial u}{\partial y} \frac{\partial^2 \phi_z}{\partial y^2} + 4C_1 \frac{\partial \phi_y}{\partial x} \frac{\partial v}{\partial y} + \frac{\partial \phi_x}{\partial y} \frac{\partial^2 \phi_z}{\partial y^2} + \frac{\partial \phi_y}{\partial x} \frac{\partial^2 \phi_z}{\partial y^2} + 4/3 \frac{\partial^2 \phi_z}{\partial x \partial y} \frac{\partial v}{\partial y} + 2/3 \frac{\partial v}{\partial x} \frac{\partial^2 \phi_z}{\partial y^2} + 2C_1 \frac{\partial u}{\partial y} \frac{\partial^2 w}{\partial y^2} \left. \right) \\
& + 2C_1 \frac{\partial \phi_x}{\partial y} \frac{\partial v}{\partial y} \left. \right) - E_{11} \left(2C_1 \frac{\partial u}{\partial x} \frac{\partial \phi_x}{\partial x} + 2/3 \frac{\partial u}{\partial x} \frac{\partial^2 \phi_z}{\partial x^2} + 2C_1 \frac{\partial u}{\partial x} \frac{\partial^2 w}{\partial x^2} + \frac{\partial \phi_x}{\partial x} \frac{\partial^2 \phi_z}{\partial x^2} \right) - E_{22} \left(\frac{\partial \phi_y}{\partial y} \frac{\partial^2 \phi_z}{\partial y^2} \right. \\
& + 2/3 \frac{\partial v}{\partial y} \frac{\partial^2 \phi_z}{\partial y^2} + 2C_1 \frac{\partial v}{\partial y} \frac{\partial \phi_y}{\partial y} + 2C_1 \frac{\partial v}{\partial y} \frac{\partial^2 w}{\partial y^2} \left. \right) - E_{66} \left(2C_1 \frac{\partial u}{\partial y} \frac{\partial \phi_y}{\partial x} + 4/3 \frac{\partial u}{\partial y} \frac{\partial^2 \phi_z}{\partial x \partial y} + 2C_1 \frac{\partial u}{\partial y} \frac{\partial \phi_x}{\partial y} \right.
\end{aligned}$$

$$\begin{aligned}
& + 4C_1 \frac{\partial u}{\partial y} \frac{\partial^2 w}{\partial x \partial y} + 2 \frac{\partial \phi_x}{\partial y} \frac{\partial^2 \phi_z}{\partial x \partial y} + 4C_1 \frac{\partial v}{\partial x} \frac{\partial^2 w}{\partial x \partial y} + 2C_1 \frac{\partial v}{\partial x} \frac{\partial \phi_x}{\partial y} + 4/3 \frac{\partial v}{\partial x} \frac{\partial^2 \phi_z}{\partial x \partial y} + 2C_1 \frac{\partial v}{\partial x} \frac{\partial \phi_y}{\partial x} \\
& + 2 \frac{\partial \phi_y}{\partial x} \frac{\partial^2 \phi_z}{\partial x \partial y} \Big) - E_{46} \left(4/3 \phi_y \frac{\partial^2 \phi_z}{\partial x \partial y} + 8C_1 \frac{\partial w}{\partial y} \frac{\partial \phi_x}{\partial y} + 4C_1 \frac{\partial w}{\partial y} \frac{\partial^2 w}{\partial x \partial y} + 8\phi_y C_1 \frac{\partial \phi_y}{\partial x} + 8 \frac{\partial w}{\partial y} C_1 \frac{\partial \phi_y}{\partial x} \right. \\
& + 4/3 \frac{\partial w}{\partial y} \frac{\partial^2 \phi_z}{\partial x \partial y} + 4\phi_y C_1 \frac{\partial^2 w}{\partial x \partial y} + 8\phi_y C_1 \frac{\partial \phi_x}{\partial y} \Big) - E_{56} \left(4/3 \frac{\partial w}{\partial x} \frac{\partial^2 \phi_z}{\partial x \partial y} + 8C_1 \frac{\partial w}{\partial x} \frac{\partial \phi_x}{\partial y} + 8C_1 \phi_x \frac{\partial \phi_x}{\partial y} \right. \\
& + 8C_1 \phi_x \frac{\partial \phi_y}{\partial x} + 8C_1 \frac{\partial w}{\partial x} \frac{\partial \phi_y}{\partial x} + 4C_1 \frac{\partial w}{\partial x} \frac{\partial^2 w}{\partial x \partial y} + 4C_1 \phi_x \frac{\partial^2 w}{\partial x \partial y} + 4/3 \phi_x \frac{\partial^2 \phi_z}{\partial x \partial y} \Big) \\
& + F_{11} \left(1/4 \frac{\partial^2 \phi_z^2}{(\partial x^2)^2} - 2/3 \frac{\partial \phi_x}{\partial x} \frac{\partial^2 \phi_z}{\partial x^2} - 2C_1 \frac{\partial \phi_x^2}{\partial x^2} - 2C_1 \frac{\partial \phi_x}{\partial x} \frac{\partial^2 w}{\partial x^2} \right) + F_{22} \left(1/4 \frac{\partial^2 \phi_z^2}{(\partial y^2)^2} \right. \\
& - 2C_1 \frac{\partial \phi_y^2}{\partial y^2} - 2C_1 \frac{\partial \phi_y}{\partial y} \frac{\partial^2 w}{\partial y^2} - 2/3 \frac{\partial \phi_y}{\partial y} \frac{\partial^2 \phi_z}{\partial y^2} \Big) + F_{44} \left(9C_1^2 \frac{\partial w^2}{\partial y^2} + 9C_1^2 \phi_y^2 + 18C_1^2 \frac{\partial w}{\partial y} \phi_y \right) \\
& + 9F_{55} C_1^2 \left(\frac{\partial w^2}{\partial x^2} + \phi_x^2 + 2 \frac{\partial w}{\partial x} \phi_x \right) + F_{66} \left(\frac{\partial^2 \phi_z^2}{(\partial x \partial y)^2} - 4/3 \frac{\partial \phi_y}{\partial x} \frac{\partial^2 \phi_z}{\partial x \partial y} - 4/3 \frac{\partial \phi_x}{\partial y} \frac{\partial^2 \phi_z}{\partial x \partial y} - 2C_1 \frac{\partial \phi_x^2}{\partial y^2} \right. \\
& - 2C_1 \frac{\partial \phi_y^2}{\partial x^2} - 4C_1 \frac{\partial \phi_y}{\partial x} \frac{\partial^2 w}{\partial x \partial y} - 4C_1 \frac{\partial \phi_x}{\partial y} \frac{\partial^2 w}{\partial x \partial y} - 4C_1 \frac{\partial \phi_x}{\partial y} \frac{\partial \phi_y}{\partial x} \Big) + F_{12} \left(1/2 \frac{\partial^2 \phi_z}{\partial x^2} \frac{\partial^2 \phi_z}{\partial y^2} \right. \\
& - 2/3 \frac{\partial^2 \phi_z}{\partial y^2} \frac{\partial \phi_x}{\partial x} - 2/3 \frac{\partial \phi_y}{\partial y} \frac{\partial^2 \phi_z}{\partial x^2} - 4C_1 \frac{\partial \phi_y}{\partial y} \frac{\partial \phi_x}{\partial x} - 2C_1 \frac{\partial \phi_y}{\partial y} \frac{\partial^2 w}{\partial x^2} - 2C_1 \frac{\partial^2 w}{\partial y^2} \frac{\partial \phi_x}{\partial x} \Big) \\
& + 3F_{14} C_1 \left(\phi_y \frac{\partial^2 \phi_z}{\partial x^2} + \frac{\partial w}{\partial y} \frac{\partial^2 \phi_z}{\partial x^2} \right) + 3F_{15} C_1 \left(\frac{\partial w}{\partial x} \frac{\partial^2 \phi_z}{\partial x^2} + \phi_x \frac{\partial^2 \phi_z}{\partial x^2} \right) + F_{16} \left(\frac{\partial^2 \phi_z}{\partial x \partial y} \frac{\partial^2 \phi_z}{\partial x^2} - 4C_1 \frac{\partial \phi_y}{\partial x} \frac{\partial \phi_x}{\partial x} \right. \\
& - 2C_1 \frac{\partial \phi_x}{\partial y} \frac{\partial^2 w}{\partial x^2} - 4C_1 \frac{\partial \phi_x}{\partial x} \frac{\partial \phi_x}{\partial y} - 4/3 \frac{\partial^2 \phi_z}{\partial x \partial y} \frac{\partial \phi_x}{\partial x} - 2/3 \frac{\partial \phi_y}{\partial x} \frac{\partial^2 \phi_z}{\partial x^2} - 2/3 \frac{\partial \phi_x}{\partial y} \frac{\partial^2 \phi_z}{\partial x^2} - 4C_1 \frac{\partial^2 w}{\partial x \partial y} \frac{\partial \phi_x}{\partial x} \\
& - 2C_1 \frac{\partial \phi_y}{\partial x} \frac{\partial^2 w}{\partial x^2} \Big) + 3F_{24} C_1 \left(\phi_y \frac{\partial^2 \phi_z}{\partial y^2} + \frac{\partial w}{\partial y} \frac{\partial^2 \phi_z}{\partial y^2} \right) + 3F_{25} C_1 \left(\frac{\partial w}{\partial x} \frac{\partial^2 \phi_z}{\partial y^2} + \phi_x \frac{\partial^2 \phi_z}{\partial y^2} \right) \\
& + F_{26} \left(\frac{\partial^2 \phi_z}{\partial x \partial y} \frac{\partial^2 \phi_z}{\partial y^2} - 2C_1 \frac{\partial \phi_y}{\partial x} \frac{\partial^2 w}{\partial y^2} - 2/3 \frac{\partial \phi_x}{\partial y} \frac{\partial^2 \phi_z}{\partial y^2} - 4C_1 \frac{\partial^2 w}{\partial x \partial y} \frac{\partial \phi_y}{\partial y} - 4C_1 \frac{\partial \phi_y}{\partial x} \frac{\partial \phi_y}{\partial y} - 4C_1 \frac{\partial \phi_x}{\partial y} \frac{\partial \phi_y}{\partial y} \right. \\
& - 4/3 \frac{\partial^2 \phi_z}{\partial x \partial y} \frac{\partial \phi_y}{\partial y} - 2/3 \frac{\partial \phi_y}{\partial x} \frac{\partial^2 \phi_z}{\partial y^2} - 2C_1 \frac{\partial \phi_x}{\partial y} \frac{\partial^2 w}{\partial y^2} \Big) + 18F_{45} C_1^2 \left(\frac{\partial w}{\partial x} \phi_y + \phi_x \phi_y + \phi_x \frac{\partial w}{\partial y} + \frac{\partial w}{\partial x} \frac{\partial w}{\partial y} \right) \\
& + 6F_{46} C_1 \left(\frac{\partial^2 \phi_z}{\partial x \partial y} \phi_y + \frac{\partial w}{\partial y} \frac{\partial^2 \phi_z}{\partial x \partial y} \right) + 6F_{56} C_1 \left(\frac{\partial^2 \phi_z}{\partial x \partial y} \phi_x + \frac{\partial w}{\partial x} \frac{\partial^2 \phi_z}{\partial x \partial y} \right)
\end{aligned}$$

$$\begin{aligned}
& +3F_{14}C_1\left(\phi_y\frac{\partial^2\phi_z}{\partial x^2}+\frac{\partial w}{\partial y}\frac{\partial^2\phi_z}{\partial x^2}\right)+3F_{15}C_1\left(\frac{\partial w}{\partial x}\frac{\partial^2\phi_z}{\partial x^2}+\phi_x\frac{\partial^2\phi_z}{\partial x^2}\right)+F_{16}\left(\frac{\partial^2\phi_z}{\partial x\partial y}\frac{\partial^2\phi_z}{\partial x^2}-4C_1\frac{\partial\phi_y}{\partial x}\frac{\partial\phi_x}{\partial x}\right. \\
& -2C_1\frac{\partial\phi_x}{\partial y}\frac{\partial^2 w}{\partial x^2}-4C_1\frac{\partial\phi_x}{\partial x}\frac{\partial\phi_x}{\partial y}-4/3\frac{\partial^2\varphi_z}{\partial x\partial y}\frac{\partial\phi_x}{\partial x}-2/3\frac{\partial\phi_y}{\partial x}\frac{\partial^2\varphi_z}{\partial x^2}-2/3\frac{\partial\phi_x}{\partial y}\frac{\partial^2\varphi_z}{\partial x^2}-4C_1\frac{\partial^2 w}{\partial x\partial y}\frac{\partial\phi_x}{\partial x} \\
& \left.-2C_1\frac{\partial\phi_y}{\partial x}\frac{\partial^2 w}{\partial x^2}\right)+3F_{24}C_1\left(\phi_y\frac{\partial^2\phi_z}{\partial y^2}+\frac{\partial w}{\partial y}\frac{\partial^2\phi_z}{\partial y^2}\right)+3F_{25}C_1\left(\frac{\partial w}{\partial x}\frac{\partial^2\phi_z}{\partial y^2}+\phi_x\frac{\partial^2\phi_z}{\partial y^2}\right) \\
& +H_{11}\left(C_1\frac{\partial^2\phi_z}{\partial x^2}\frac{\partial\phi_x}{\partial x}+1/3\frac{\partial^2\phi_z}{\partial x^2}\frac{\partial^2\varphi_z}{\partial x^2}+C_1\frac{\partial^2\phi_z}{\partial x^2}\frac{\partial^2 w}{\partial x^2}\right)+H_{22}\left(C_1\frac{\partial^2\phi_z}{\partial y^2}\frac{\partial^2 w}{\partial y^2}+C_1\frac{\partial^2\phi_z}{\partial y^2}\frac{\partial\phi_y}{\partial y}\right. \\
& \left.+1/3\frac{\partial^2\phi_z}{\partial y^2}\frac{\partial^2\varphi_z}{\partial y^2}\right)+2H_{66}\left(C_1\frac{\partial^2\phi_z}{\partial x\partial y}\frac{\partial\phi_y}{\partial x}+2C_1\frac{\partial^2\phi_z}{\partial x\partial y}\frac{\partial^2 w}{\partial x\partial y}+C_1\frac{\partial^2\phi_z}{\partial x\partial y}\frac{\partial\phi_x}{\partial y}+2/3\frac{\partial^2\phi_z}{\partial x\partial y}\frac{\partial^2\varphi_z}{\partial x\partial y}\right) \\
& +H_{12}\left(2C_1\frac{\partial^2\phi_z}{\partial y^2}\frac{\partial^2 w}{\partial x^2}+2/3\frac{\partial^2\varphi_z}{\partial y^2}\frac{\partial^2\phi_z}{\partial x^2}+C_1\frac{\partial\phi_y}{\partial y}\frac{\partial^2\phi_z}{\partial x^2}+C_1\frac{\partial^2\phi_z}{\partial y^2}\frac{\partial\phi_x}{\partial x}\right)+2H_{14}C_1\left(\frac{\partial^2\varphi_z}{\partial x^2}\phi_y\right. \\
& \left.+3C_1\phi_y\frac{\partial\phi_x}{\partial x}+3C_1\frac{\partial w}{\partial y}\frac{\partial\phi_x}{\partial x}+3C_1\phi_y\frac{\partial^2 w}{\partial x^2}+\frac{\partial w}{\partial y}\frac{\partial^2\varphi_z}{\partial x^2}+3C_1\frac{\partial w}{\partial y}\frac{\partial^2 w}{\partial x^2}\right)+2H_{15}C_1\left(\frac{\partial w}{\partial x}\frac{\partial^2\varphi_z}{\partial x^2}\right. \\
& \left.+\phi_x\frac{\partial^2\varphi_z}{\partial x^2}+3C_1\frac{\partial w}{\partial x}\frac{\partial\phi_x}{\partial x}+3C_1\phi_x\frac{\partial^2 w}{\partial x^2}+3C_1\frac{\partial w}{\partial x}\frac{\partial^2 w}{\partial x^2}+3C_1\phi_x\frac{\partial\phi_x}{\partial x}\right) \\
& +H_{16}\left(C_1\frac{\partial\phi_x}{\partial y}\frac{\partial^2\phi_z}{\partial x^2}+C_1\frac{\partial\phi_y}{\partial x}\frac{\partial^2\phi_z}{\partial x^2}+4/3\frac{\partial^2\phi_z}{\partial x\partial y}\frac{\partial^2\varphi_z}{\partial x^2}+4C_1\frac{\partial^2 w}{\partial x\partial y}\frac{\partial^2\phi_z}{\partial x^2}+2C_1\frac{\partial^2\phi_z}{\partial x\partial y}\frac{\partial\phi_x}{\partial x}\right) \\
& +2H_{24}C_1\left(\phi_y\frac{\partial^2\varphi_z}{\partial y^2}+\frac{\partial w}{\partial y}\frac{\partial^2\phi_z}{\partial y^2}+3C_1\phi_y\frac{\partial^2 w}{\partial y^2}+3C_1\frac{\partial w}{\partial y}\frac{\partial\phi_y}{\partial y}+3C_1\frac{\partial w}{\partial y}\frac{\partial^2 w}{\partial y^2}+3C_1\phi_y\frac{\partial\phi_y}{\partial y}\right) \\
& +2H_{25}C_1\left(3C_1\phi_x\frac{\partial^2 w}{\partial y^2}+3C_1\frac{\partial w}{\partial x}\frac{\partial^2 w}{\partial y^2}+3C_1\phi_x\frac{\partial\phi_y}{\partial y}+\frac{\partial w}{\partial x}\frac{\partial^2\varphi_z}{\partial y^2}+3C_1\frac{\partial w}{\partial x}\frac{\partial\phi_y}{\partial y}+\phi_x\frac{\partial^2\varphi_z}{\partial y^2}\right) \\
& +H_{26}\left(4C_1\frac{\partial^2\phi_z}{\partial x\partial y}\frac{\partial^2 w}{\partial y^2}+2C_1\frac{\partial^2\phi_z}{\partial x\partial y}\frac{\partial\phi_y}{\partial y}+4/3\frac{\partial^2\phi_z}{\partial x\partial y}\frac{\partial^2\varphi_z}{\partial y^2}+C_1\frac{\partial\phi_y}{\partial x}\frac{\partial^2\phi_z}{\partial y^2}+C_1\frac{\partial\phi_x}{\partial y}\frac{\partial^2\phi_z}{\partial y^2}\right) \\
& +H_{46}C_1\left(12C_1\phi_y\frac{\partial^2 w}{\partial x\partial y}+4\phi_y\frac{\partial^2\varphi_z}{\partial x\partial y}+6C_1\phi_y\frac{\partial\phi_y}{\partial x}+6C_1\frac{\partial w}{\partial y}\frac{\partial\phi_x}{\partial y}+12C_1\frac{\partial w}{\partial y}\frac{\partial^2 w}{\partial x\partial y}+4\frac{\partial w}{\partial y}\frac{\partial^2\varphi_z}{\partial x\partial y}\right. \\
& \left.+6C_1\frac{\partial w}{\partial y}\frac{\partial\phi_y}{\partial x}+6C_1\phi_y\frac{\partial\phi_x}{\partial y}\right)+H_{56}C_1\left(6C_1\phi_x\frac{\partial\phi_x}{\partial y}+6C_1\frac{\partial w}{\partial x}\frac{\partial\phi_y}{\partial x}+6C_1\frac{\partial w}{\partial x}\frac{\partial\phi_x}{\partial y}+4\phi_x\frac{\partial^2\varphi_z}{\partial x\partial y}\right. \\
& \left.+12C_1\phi_x\frac{\partial^2 w}{\partial x\partial y}+12C_1\frac{\partial w}{\partial x}\frac{\partial^2 w}{\partial x\partial y}+6C_1\phi_x\frac{\partial\phi_y}{\partial x}+4\frac{\partial w}{\partial x}\frac{\partial^2\varphi_z}{\partial x\partial y}\right)
\end{aligned}$$

$$\begin{aligned}
& + J_{11} \left(1/9 \frac{\partial^2 \varphi_z^2}{(\partial x^2)^2} + 2/3 C_1 \frac{\partial^2 w}{\partial x^2} \frac{\partial^2 \varphi_z}{\partial x^2} + C_1^2 \left(\frac{\partial \phi_x}{\partial x} \right)^2 + C_1^2 \frac{(\partial^2 w)^2}{(\partial x^2)^2} + 2/3 \frac{\partial \phi_x}{\partial x} C_1 \frac{\partial^2 \varphi_z}{\partial x^2} + 2C_1^2 \frac{\partial^2 w}{\partial x^2} \frac{\partial \phi_x}{\partial x} \right) \\
& + J_{22} \left(2/3 C_1 \frac{\partial \phi_y}{\partial y} \frac{\partial^2 \varphi_z}{\partial y^2} + 1/9 \frac{(\partial^2 \varphi_z)^2}{(\partial y^2)^2} + 2/3 C_1 \frac{\partial^2 w}{\partial y^2} \frac{\partial^2 \varphi_z}{\partial y^2} + C_1^2 \frac{\partial^2 \phi_y}{\partial y^2} + C_1^2 \frac{(\partial^2 w)^2}{(\partial y^2)^2} + 2C_1^2 \frac{\partial^2 w}{\partial y^2} \frac{\partial \phi_y}{\partial y} \right) \\
& + J_{66} \left(4C_1^2 \frac{(\partial^2 w)^2}{(\partial x \partial y)^2} + 4/9 \frac{(\partial^2 \varphi_z)^2}{(\partial x \partial y)^2} + 2C_1^2 \frac{\partial \phi_x}{\partial y} \frac{\partial \phi_y}{\partial x} + 4/3 C_1 \frac{\partial \phi_x}{\partial y} \frac{\partial^2 \varphi_z}{\partial x \partial y} + C_1^2 \left(\frac{\partial \phi_y}{\partial x} \right)^2 + C_1^2 \left(\frac{\partial \phi_x}{\partial y} \right)^2 \right) \\
& + 8/3 C_1 \frac{\partial^2 w}{\partial x \partial y} \frac{\partial^2 \varphi_z}{\partial x \partial y} + 4C_1^2 \frac{\partial^2 w}{\partial x \partial y} \frac{\partial \phi_x}{\partial y} + 4/3 C_1 \frac{\partial \phi_y}{\partial x} \frac{\partial^2 \varphi_z}{\partial x \partial y} + 4C_1^2 \frac{\partial^2 w}{\partial x \partial y} \frac{\partial \phi_y}{\partial x} \left. \right) + J_{12} \left(2C_1^2 \frac{\partial \phi_y}{\partial y} \frac{\partial \phi_x}{\partial x} \right. \\
& + 2/3 C_1 \frac{\partial^2 \varphi_z}{\partial y^2} \frac{\partial \phi_x}{\partial x} + 2C_1^2 \frac{\partial^2 w}{\partial x^2} \frac{\partial^2 w}{\partial y^2} + 2C_1^2 \frac{\partial^2 w}{\partial y^2} \frac{\partial \phi_x}{\partial x} + 2C_1^2 \frac{\partial \phi_y}{\partial y} \frac{\partial^2 w}{\partial x^2} + 2/3 C_1 \frac{\partial \phi_y}{\partial y} \frac{\partial^2 \varphi_z}{\partial x^2} \\
& + 2/9 \frac{\partial^2 \varphi_z}{\partial x^2} \frac{\partial^2 \varphi_z}{\partial y^2} + 4/3 C_1 \frac{\partial^2 \varphi_z}{\partial y^2} \frac{\partial^2 w}{\partial x^2} \left. \right) + J_{16} \left(2C_1^2 \frac{\partial \phi_y}{\partial x} \frac{\partial^2 w}{\partial x^2} + 2C_1^2 \frac{\partial \phi_y}{\partial x} \frac{\partial \phi_x}{\partial x} + 2C_1^2 \frac{\partial \phi_x}{\partial x} \frac{\partial \phi_x}{\partial y} \right. \\
& + 2C_1^2 \frac{\partial \phi_x}{\partial y} \frac{\partial^2 w}{\partial x^2} + 4/3 C_1 \frac{\partial^2 \varphi_z}{\partial x \partial y} \frac{\partial \phi_x}{\partial x} + 4/9 \frac{\partial^2 \varphi_z}{\partial x \partial y} \frac{\partial^2 \varphi_z}{\partial x^2} + 8/3 C_1 \frac{\partial^2 \varphi_z}{\partial x \partial y} \frac{\partial^2 w}{\partial x^2} + 2/3 C_1 \frac{\partial \phi_y}{\partial x} \frac{\partial^2 \varphi_z}{\partial x^2} \\
& + 4C_1^2 \frac{\partial^2 w}{\partial x \partial y} \frac{\partial \phi_x}{\partial x} + 4C_1^2 \frac{\partial^2 w}{\partial x \partial y} \frac{\partial^2 w}{\partial x^2} + 2/3 C_1 \frac{\partial \phi_x}{\partial y} \frac{\partial^2 \varphi_z}{\partial x^2} \left. \right) + J_{26} \left(4/3 C_1 \frac{\partial^2 \varphi_z}{\partial x \partial y} \frac{\partial \phi_y}{\partial y} + 4C_1^2 \frac{\partial^2 w}{\partial x \partial y} \frac{\partial^2 w}{\partial y^2} \right. \\
& + 8/3 C_1 \frac{\partial^2 \varphi_z}{\partial x \partial y} \frac{\partial^2 w}{\partial y^2} + 2/3 C_1 \frac{\partial \phi_x}{\partial y} \frac{\partial^2 \varphi_z}{\partial y^2} + 2C_1^2 \frac{\partial \phi_y}{\partial x} \frac{\partial^2 w}{\partial y^2} + 2C_1^2 \frac{\partial \phi_x}{\partial y} \frac{\partial \phi_y}{\partial y} + 2/3 C_1 \frac{\partial \phi_y}{\partial x} \frac{\partial^2 \varphi_z}{\partial y^2} \\
& \left. \left. + 4C_1^2 \frac{\partial^2 w}{\partial x \partial y} \frac{\partial \phi_y}{\partial y} + 2C_1^2 \frac{\partial \phi_y}{\partial x} \frac{\partial \phi_y}{\partial y} + 2C_1^2 \frac{\partial \phi_x}{\partial y} \frac{\partial^2 w}{\partial y^2} + 4/9 \frac{\partial^2 \varphi_z}{\partial x \partial y} \frac{\partial^2 \varphi_z}{\partial y^2} \right) \right]
\end{aligned}
\tag{4.42}$$

where,

L is the length of tapered laminate (L_b) or resin ply (L_r) and b is the width of the laminate;

$[A']$, $[B']$, $[D']$, $[E']$, $[F']$, $[H']$ and $[J']$ for tapered laminate are calculated from the equation (4.38).

4.3.1.2 Potential energy

The potential energy of external loads for tapered laminate and resin pocket are:

$$W_t' = -(1/2) \iint_{A_t} N_x \left(\frac{\partial w_o}{\partial x} \right)^2 dx dy \quad (4.43)$$

$$W_r' = -(1/2) \iint_{A_r} N_x \left(\frac{\partial w_o}{\partial x} \right)^2 dx dy \quad (4.44)$$

where, A and A_r are the areas of tapered laminate and resin pocket respectively.

4.3.2 General expressions

The approximate solution is expressed as a double series:

$$u_o(x, y) = \sum_{m=1}^M \sum_{n=1}^N U_{mn} U_m(x) U_n(y) \quad (4.45)$$

$$v_o(x, y) = \sum_{m=1}^M \sum_{n=1}^N V_{mn} V_m(x) V_n(y) \quad (4.46)$$

$$w_o(x, y) = \sum_{m=1}^M \sum_{n=1}^N W_{mn} W_m(x) W_n(y) \quad (4.47)$$

$$\phi_x(x, y) = \sum_{m=1}^M \sum_{n=1}^N X_{mn} X_m(x) X_n(y) \quad (4.48)$$

$$\phi_y(x, y) = \sum_{m=1}^M \sum_{n=1}^N Y_{mn} Y_m(x) Y_n(y) \quad (4.49)$$

$$\phi_z(x, y) = \sum_{m=1}^M \sum_{n=1}^N Z_{mn} Z_m(x) Z_n(y) \quad (4.50)$$

$$\phi_z(x, y) = \sum_{m=1}^M \sum_{n=1}^N S_{mn} S_m(x) S_n(y) \quad (4.51)$$

The functions U_m(x), U_n(y), V_m(x), V_n(y), W_m(x), W_n(y), X_m(x), X_n(y), Y_m(x), Y_n(x), Z_m(x), Z_n(x) S_m(x) and S_n(x) are chosen so as to satisfy the boundary conditions and the co-efficients U_{mn}, V_{mn}, W_{mn}, X_{mn}, Y_{mn}, Z_{mn} and S_{mn} are determined using the stationary conditions:

$$\frac{\partial U'_t}{\partial U_{mn}} + \frac{\partial U'_r}{\partial U_{mn}} = 0 \quad (4.52)$$

$$\frac{\partial U'_t}{\partial V_{mn}} + \frac{\partial U'_r}{\partial V_{mn}} = 0 \quad (4.53)$$

$$\frac{\partial U'_t}{\partial X_{mn}} + \frac{\partial U'_r}{\partial X_{mn}} = 0 \quad (4.54)$$

$$\frac{\partial U'_t}{\partial Y_{mn}} + \frac{\partial U'_r}{\partial Y_{mn}} = 0 \quad (4.55)$$

$$\frac{\partial U'_t}{\partial Z_{mn}} + \frac{\partial U'_r}{\partial Z_{mn}} = 0 \quad (4.56)$$

$$\frac{\partial U'_t}{\partial S_{mn}} + \frac{\partial U'_r}{\partial S_{mn}} = 0 \quad (4.57)$$

$$\frac{\partial U'_t}{\partial W_{mn}} + \frac{\partial U'_r}{\partial W_{mn}} = \frac{\partial W'_t}{\partial W_{mn}} + \frac{\partial W'_r}{\partial W_{mn}} \quad (4.58)$$

where,

U'_t and U'_r are defined in equation (4.42) for tapered laminate and resin pocket respectively using respective geometric properties;

W'_t and W'_r are defined in equations (4.43) and (4.44);

m and n represent the desired number of approximate terms taken in the series appearing in equations (4.45 – 4.51).

In case of $m = n = 1$, no. of equations are: $7 \times 1 = 7$;

$m = n = 2$, no. of equations are: $7 \times (2 \times 2) = 28$;

$m = n = 3$, no. of equations are: $7 \times (3 \times 3) = 63$

and so on.

Solving equations (4.52 - 4.57) and substituting the results into the equation (4.58), final form of the equation can be written as:

$$[K^u] - N_o^u [Z^u] = 0 \quad (4.59)$$

where, $[K^u]$ and $[Z^u]$ are the stiffness matrix and geometric stiffness matrix respectively.

Equation (4.59) is solved using MATLAB[®] program as an eigenvalue and eigenvector problem for which the eigenvalues are the values of N_o^u of the buckling loads and the eigenvectors determine the buckling mode shapes. Smallest value of N_o^u is the critical buckling load, N_{cr}^u .

4.3.3 The system equations

Now taking into account the energy equation (4.42) we easily obtain the system of equations for both the tapered laminate and resin pocket in terms of the co-efficients of W_{ij} , X_{ij} , Y_{ij} , Z_{ij} and S_{ij} . Thus:

$$\frac{\partial U}{\partial W_{mn}} = \sum_{i=1}^M \sum_{j=1}^N [W_1 W_{ij} + X_1 X_{ij} + Y_1 Y_{ij} + Z_1 Z_{ij} + S_1 S_{ij}] \quad (4.60)$$

$$\frac{\partial U}{\partial X_{mn}} = \sum_{i=1}^M \sum_{j=1}^N [W_2 W_{ij} + X_2 X_{ij} + Y_2 Y_{ij} + Z_2 Z_{ij} + S_2 S_{ij}] \quad (4.61)$$

$$\frac{\partial U}{\partial Y_{mn}} = \sum_{i=1}^M \sum_{j=1}^N [W_3 W_{ij} + X_3 X_{ij} + Y_3 Y_{ij} + Z_3 Z_{ij} + S_3 S_{ij}] \quad (4.62)$$

$$\frac{\partial U}{\partial Z_{mn}} = \sum_{i=1}^M \sum_{j=1}^N [W_4 W_{ij} + X_4 X_{ij} + Y_4 Y_{ij} + Z_4 Z_{ij} + S_4 S_{ij}] \quad (4.63)$$

$$\frac{\partial U}{\partial S_{mn}} = \sum_{i=1}^M \sum_{j=1}^N [W_5 W_{ij} + X_5 X_{ij} + Y_5 Y_{ij} + Z_5 Z_{ij} + S_5 S_{ij}] \quad (4.64)$$

$$\frac{\partial W}{\partial W_{mn}} = \sum_{i=1}^M \sum_{j=1}^N \left\{ N_o \int_0^L \frac{dW_m}{dx} \frac{dW_i}{dx} dx \int_0^b W_n W_j dy \right\} \quad (4.65)$$

where,

U and W are the strain energy and potential energy, and those are calculated for both tapered laminate and resin pocket using respective geometric properties;

W_i, X_i, Y_i, Z_i and S_i are given in Appendix A;

U_i and V_i are neglected in calculation as these values are very small with respect to other displacements

and $i = 1,2,3,4,5$.

The system equations developed for tapered laminate and resin pocket are applied into the equations (4.52 - 4.57). Solving the equations (4.52 - 4.57) and using the results into the equation (4.58), the final form is like the equation (4.59). The MATLAB[®] program is used to solve the equation (4.59) for buckling analysis.

4.3.4 Tapered laminated plate simply supported at four ends

In case of a plate simply supported along its four edges (SSSS) the boundary conditions are:

- Along edges $x = 0$ and $x = L_b$:

$$w_o = 0, M_x = 0 \quad (4.66)$$

- Along edges $y = 0$ and $y = b$:

$$w_o = 0, M_y = 0 \quad (4.67)$$

The above-mentioned boundary conditions are satisfied by the following approximate solutions [39]:

$$w_o(x, y) = \sum_{m=1}^M \sum_{n=1}^N W_{mn} \sin \frac{m\pi x}{L_b} \sin \frac{n\pi y}{b} \quad (4.68)$$

$$\phi_x(x, y) = \sum_{m=1}^M \sum_{n=1}^N X_{mn} \cos \frac{m\pi x}{L_b} \sin \frac{n\pi y}{b} \quad (4.69)$$

$$\phi_y(x, y) = \sum_{m=1}^M \sum_{n=1}^N Y_{mn} \sin \frac{m\pi x}{L_b} \cos \frac{n\pi y}{b} \quad (4.70)$$

$$\phi_z(x, y) = \sum_{m=1}^M \sum_{n=1}^N Y_{mn} \sin \frac{m\pi x}{L_b} \sin \frac{n\pi y}{b} \quad (4.71)$$

$$\varphi_z(x, y) = \sum_{m=1}^M \sum_{n=1}^N Y_{mn} \sin \frac{m\pi x}{L_b} \sin \frac{n\pi y}{b} \quad (4.72)$$

Applying equations (4.68 - 4.72) in the equations (4.52 - 4.57) and equating the co-efficient of W_{mn} to zero we can get a eigenvalue problem like equation (4.59) and that can be solved using MATLAB[®] program to calculate the critical buckling load.

4.3.5 Numerical results and discussion

Example 4.3.5.1

The tapered plates described in example 2.7.2 are considered for buckling analysis. The solutions have been obtained using Ritz method for simply supported boundary conditions. The results are given in Tables 4.1 - 4.4.

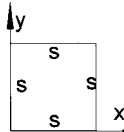
Taper length in meters	Taper angle in degrees	L_b/h			
			CLPT	FSDT	TSDT
0.1719	0.5	38.2	3.678	3.600	3.520
0.1146	0.75	25.47	8.270	8.030	7.883
0.08594	1.0	19.098	14.710	13.9745	13.4745
0.0573	1.5	12.73	33.070	30.7551	29.7551
0.04295	2.0	9.54	58.660	53.3806	51.8806
0.03435	2.5	7.63	91.600	81.5240	79.524
0.0286	3.0	6.36	132.40	115.188	112.688

Table 4.1 Comparison of critical buckling loads ($\times 10^4 N$) for simply supported tapered laminate model A

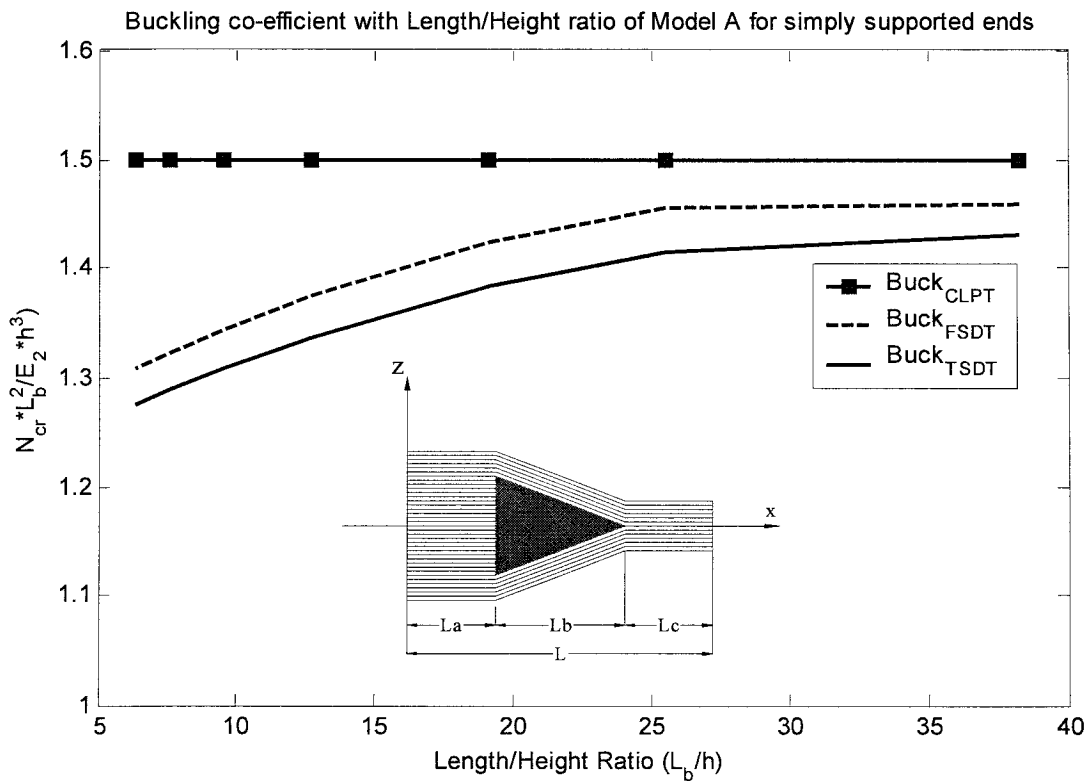


Figure 4.2 Effect of transverse shear on buckling co-efficient for simply supported tapered laminate model A

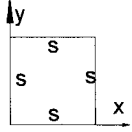
Taper length in meters	Taper angle in degrees	L_b/h			
			CLPT	FSDT	TSDT
0.1719	0.5	38.200	11.5713	11.108	10.980
0.1146	0.75	25.470	26.0289	24.785	24.420
0.08594	1.0	19.098	46.305	43.5267	43.0267
0.0573	1.5	12.730	103.986	96.7069	95.2069
0.04295	2.0	9.540	184.869	170.0795	167.5795
0.03435	2.5	7.630	288.459	262.4976	258.9976
0.0286	3.0	6.360	415.557	374.0013	369.5013

Table 4.2 Comparison of critical buckling loads ($\times 10^4 N$) for simply supported tapered laminate model B

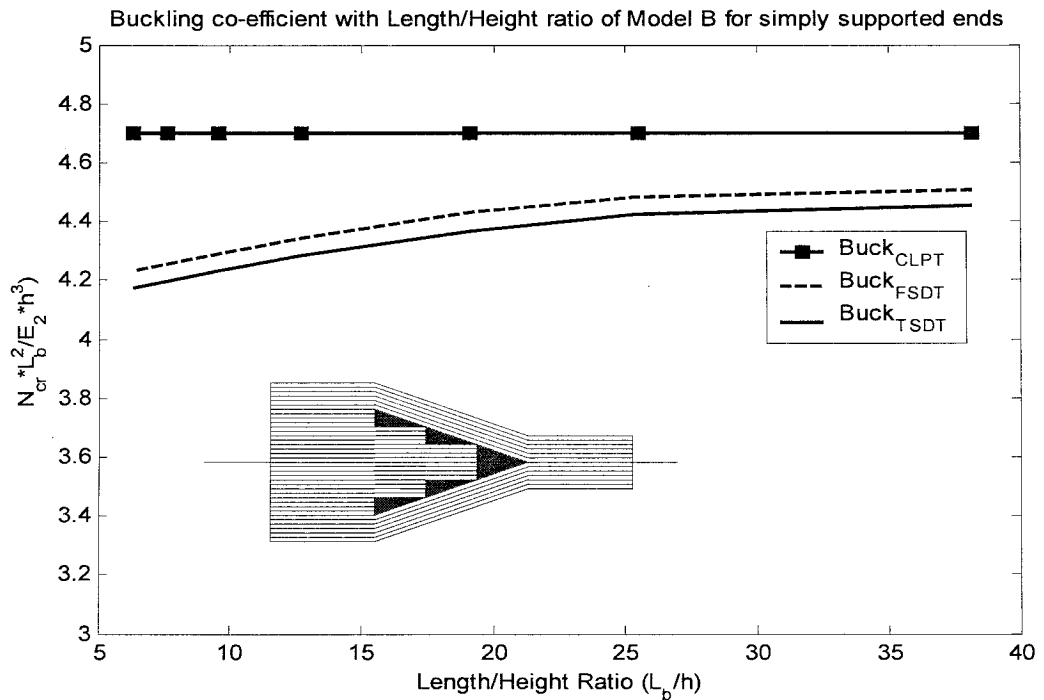


Figure 4.3 Effect of transverse shear on buckling co-efficient for simply supported tapered laminate model B

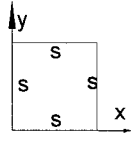
Taper length in meters	Taper angle in degrees	L_b/h			
			CLPT	FSDT	TSDT
0.1719	0.5	38.2	3.963667	3.8447	3.7055
0.1146	0.75	25.47	8.916111	8.580	8.395
0.08594	1.0	19.098	15.86167	15.0685	14.558
0.0573	1.5	12.73	35.62	33.4828	31.980
0.04295	2.0	9.54	63.3222	58.8896	56.3898
0.03435	2.5	7.63	98.8	90.896	87.3960
0.0286	3.0	6.36	142.3	129.493	124.993

Table 4.3 Comparison of critical buckling loads ($\times 10^4 N$) for simply supported tapered laminate model C

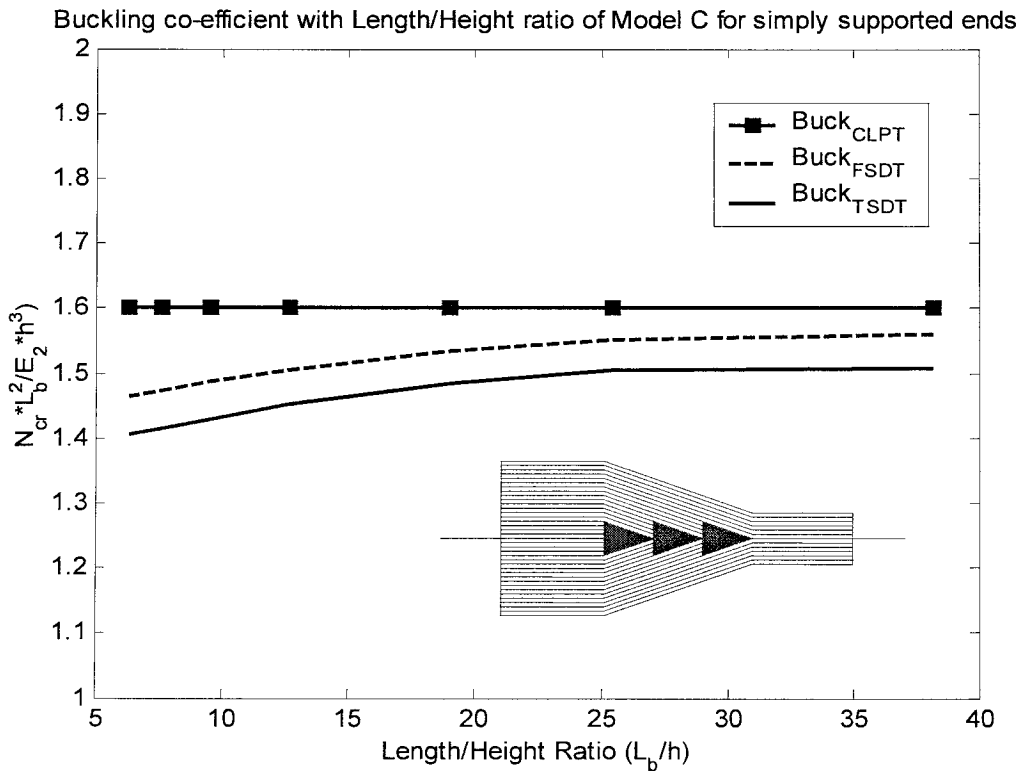


Figure 4.4 Effect of transverse shear on buckling co-efficient for simply supported tapered laminate model C

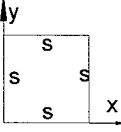
Taper length in meters	Taper angle in degrees	L_b/h			
			CLPT	FSDT	TSDT
0.1719	0.5	38.2	11.7	11.349	11.020
0.1146	0.75	25.47	26.3196	25.25145	25.1212
0.08594	1.0	19.098	46.8192	44.4782	42.9782
0.0573	1.5	12.73	105.1632	98.8534	96.3534
0.04295	2.0	9.54	186.972	173.8839	170.3839
0.03435	2.5	7.63	291.84	268.4928	263.9928
0.0286	3.0	6.36	420.36	382.5276	377.0276

Table 4.4 Comparison of critical buckling loads ($\times 10^4 N$) for simply supported tapered laminate model D

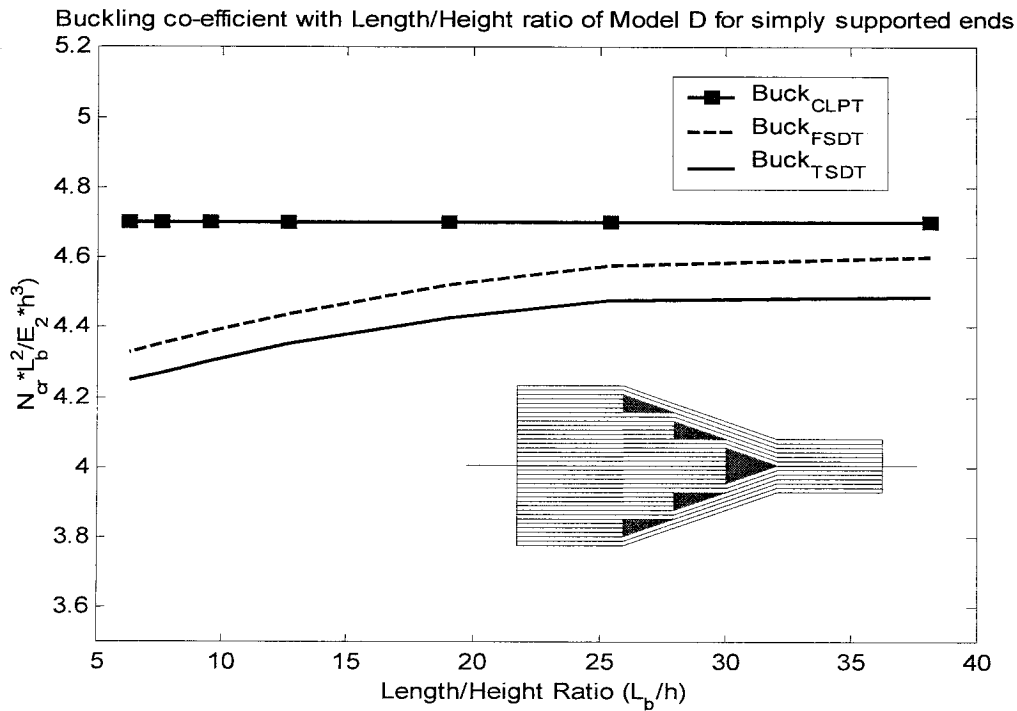


Figure 4.5 Effect of transverse shear on buckling co-efficient for simply supported tapered laminate model D

4.3.5.2 Discussion of models A, B, C and D

From Figures 4.2 - 4.5 we observe that CLPT, FSDT and TSDT predict the same behavior after the ratio of height to width becomes equal to 25. Results of CLPT form a straight line as u_o, v_o and w_o are not playing any role on thickness change. Buckling coefficient based on FSDT departs away from that of CLPT after a certain thickness of the tapered laminate as ϕ_x and ϕ_y are having important role on thickness change. In addition, the results of TSDT are parallel to that of FSDT as the values of ϕ_z and φ_z do not change significantly with the change of plate thickness.

We can conclude from Figure 4.6 that the tapered plate of model D is the strongest one; model B and model C take the second and third ranks respectively. Model A has the lowest stiffness. The buckling loads of models D and B are closer to each other; on the other hand, models A and C are closer.

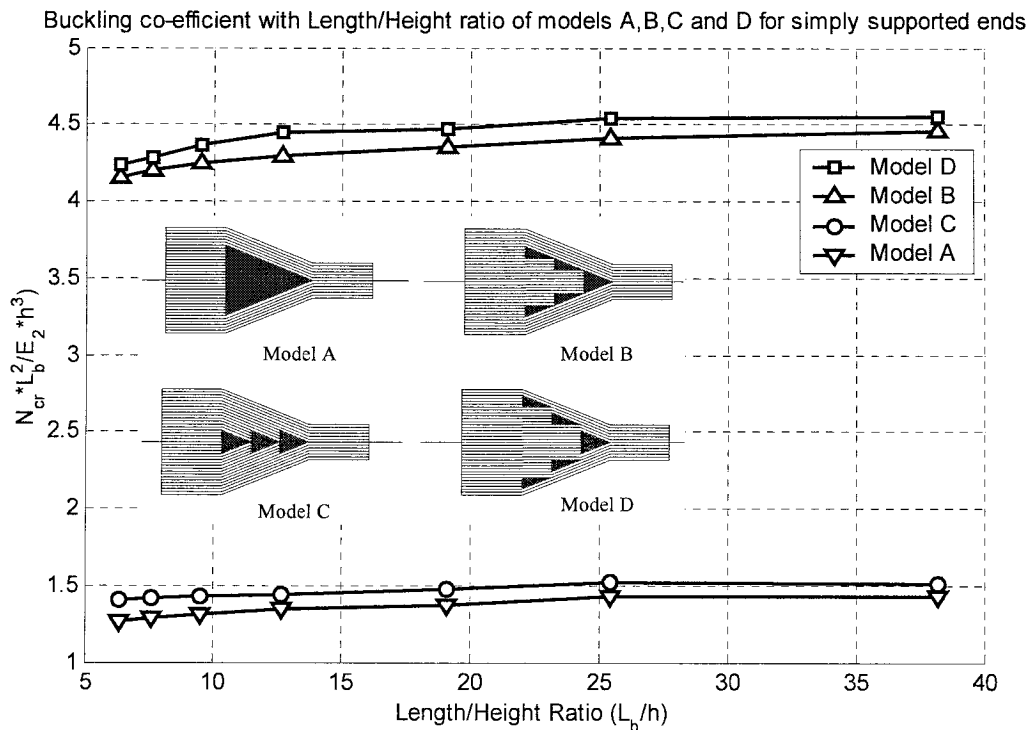


Figure 4.6 Effect of transverse shear on buckling co-efficient for simply supported tapered laminate models A, B, C and D

4.4 Discussions and conclusions

In this chapter, constitutive equation of tapered laminated plate based on third-order shear deformation theory is developed. The system equations of critical buckling loads are developed for simply supported boundary condition and for four types of taper models using Ritz method based on Third-order Shear Deformation Theory (TSDT). The results based on TSDT are also compared with that of CLPT and FSDT.

It can be seen from Tables 4.1 - 4.4 that results of FSDT depart away from CLPT after a certain thickness of the tapered laminate. In addition, the results of TSDT are parallel to that of FSDT.

It can be concluded from Figure 4.6 that the tapered plate of model D is the strongest one and hence results in the largest critical buckling load value; model B and model C take the second and third ranks respectively. Model A has the lowest stiffness and hence results in the smallest critical buckling load value.

Chapter 5

Parametric Study on Tapered Composite Plates Models

5.1 Introduction

In the previous chapters 2, 3, and 4 different types of tapered laminate models, shown in Figure 2.13, were analyzed based on Classical Laminated Plate Theory (CLPT), First-order Shear Deformation Theory (FSDT) and Third-order Shear Deformation Theory (TSDT) respectively. In this chapter, we will conduct a study of those tapered models with different configurations (Table 5.6) considering the entire length (thick + taper + thin) of tapered laminate models.

In chapter two, the tapered laminate models were analyzed based on Classical Laminated Plate Theory (CLPT) and the results were compared with that of tapered laminated beam models that were analyzed using finite element method [16]. In chapter three, the tapered laminate models were analyzed based on First-order Shear Deformation Theory (FSDT) and the results were compared with that of CLPT. In chapter four, the tapered laminate models were analyzed based on Third-order Shear Deformation Theory (TSDT) and the results were compared with that of CLPT and FSDT.

In this chapter uniform laminates (taper angle = 0) are analyzed using Ritz method and the results are compared with that given in published works. Further, the new models AA, BB, CC and DD (Figure 5.1) with very small taper angles and few dropped plies that are almost uniform are analyzed and the results are compared with that of equivalent uniform laminates. Finally, different tapered laminated plates with various configurations are considered for study.

5.2 Comparison of critical buckling co-efficients

Example 5.2.1

The uniform plates described in example 2.7.1 are considered for buckling analysis. The solutions have been obtained using Ritz method for simply supported boundary conditions. The values of critical buckling co-efficient are given in Table 5.1.

No of layers	Sources	Theory Applied	E_L/E_T				
			3	10	20	30	40
3	Ref [44]	Local Higher Order Plate theory	5.3112	9.7961	15.0757	19.3761	22.9643
	Ref [45]	Refined Plate Theory	5.3933	9.9406	15.298	19.674	23.34
	Ref [46]	Simple Higher Order Plate Theory	5.439	9.926	15.022	19.052	22.312
	Ref [22]	Global Higher Order Plate Theory	5.3208	9.7172	14.729	18.6834	21.8977
	Ref [47]	3D Elasticity Solution	5.3044	9.7621	15.0191	19.304	22.8807
	Ref [23]	Higher Order Plate Theory	5.3254	9.827	15-1394	19.481	23.117
	Present	Third Order SDT, Ritz Method	4.7727	8.8898	13.8849	18.0781	21.6653
	Ref [44]	First Order SDP theory	5.3991	9.9652	15.351	19.756	23.453
	Present	First Order SDT, Ritz Method	5.3961	9.8711	14.9847	19.0266	22.3151
	Ref [44]	Classical Plate theory	5.7538	11.4918	19.7124	27.9357	36.1597
	Present	Classical Plate Theory	5.7538	11.4918	19.7128	27.9357	36.1597
	5	Ref [44]	Local Higher Order Plate theory	5.3323	9.9851	15.6934	20.5176
Ref [45]		Refined Plate Theory	5.4096	10.15	16.008	20.999	25.308
Ref [46]		Simple Higher Order Plate Theory	5.452	10.157	15.862	20.644	24.727
Ref [22]		Global Higher Order Plate Theory	5.3348	9.9414	15.5142	20.1656	24.1158
Ref [47]		3D Elasticity Solution	5.3255	9.9603	15.6527	20.4663	24.5929
Ref [23]		Higher Order Plate Theory
Present		Third Order SDT, Ritz Method	5.3258	9.9046	15.4581	20.1438	24.1823
Ref [44]		First Order SDP theory	5.4093	10.136	15.956	20.908	25.185
Present		First Order SDT, Ritz Method	5.4068	10.0762	15.7362	20.4847	24.5468
Ref [44]		Classical Plate theory	5.7538	11.4918	19.7124	27.9357	36.1597
Present		Classical Plate Theory	5.7538	11.4918	19.7124	27.9357	36.1597
9		Ref [44]	Local Higher Order Plate theory	5.34	10.0572	15.9403	20.9926
	Ref [45]	Refined Plate Theory	5.4313	10.197	16.172	21.315	25.79
	Ref [46]	Simple Higher Order Plate Theory	5.457	10.249	16.192	21.272	25.671
	Ref [22]	Global Higher Order Plate Theory	5.3432	10.0529	15.9085	20.925	25.2741
	Ref [47]	3D Elasticity Solution	5.3352	10.0417	15.9153	20.9614	25.3436
	Ref [23]	Higher Order Plate Theory	5.3446	10.0694	15.965	21.0332	25.439
	Present	Third Order SDT, Ritz Method	5.3299	9.9741	15.7089	20.6218	24.8967
	Ref [44]	First Order SDP theory	5.4126	10.189	16.146	21.265	25.715
	Present	First Order SDT, Ritz Method	5.4116	10.1682	16.0682	21.1171	25.4946
	Ref [44]	Classical Plate theory	5.7538	11.4918	19.7124	27.9357	36.1597
	Present	Classical Plate Theory	5.7538	11.4918	19.7124	27.9357	36.1597

Table 5.1 Comparison of buckling co-efficient with previously published results.

5.3 Comparison of buckling load of tapered plate with that of equivalent uniform plate

Example 5.3.1

Tapered plate models that are shown in Figure 5.1 are considered with 18 and 12 plies at thick and thin sections respectively, which results in 6 drop-off plies. The configuration of the thick section is $[(0/90)_4/0]_s$ and that of the thin section is $[0/90]_{3s}$. The configuration of equivalent uniform laminates are $[(0/90)_3/0/0/(90/0)_3]$ for models BB and DD; on the other hand $[(0/90)/0]_{3s}$ for models AA and CC. Thickness of each ply is 0.125 mm. The lengths of both the equivalent uniform and tapered plate correspond to the taper angle. The values of m and n in the equations (2.89), (3.31) and (4.58) are determined so as to obtain the converged solutions.

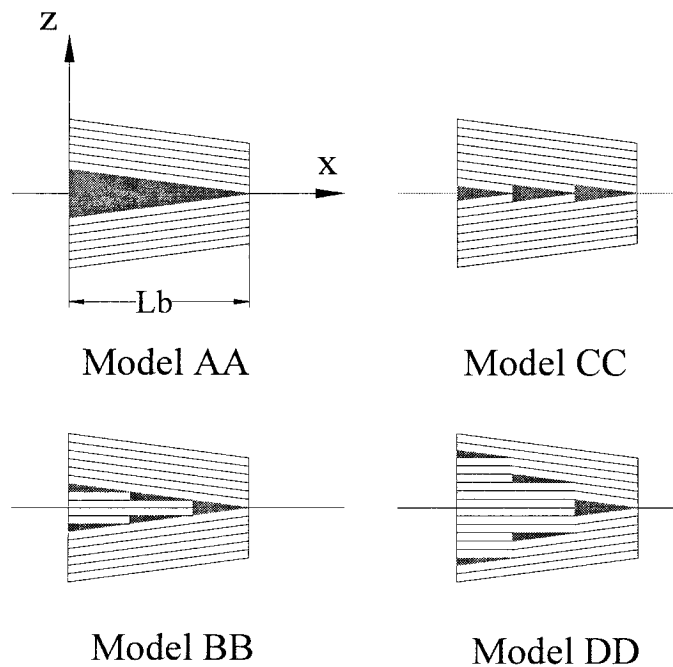


Figure 5.1 Tapered laminate models AA, BB, CC and DD for buckling analysis.

The mechanical properties of the composite material (NCT/301 graphite-epoxy) are: $E_1=113.9$ GPa, $E_2=7.9856$ GPa, $G_{12}=3.138$ GPa, $G_{23}=2.543$ GPa, $\nu_{12}=0.288$, $\nu_{23}=0.576$, $\rho=1480$ kg/m³. Resin properties: $E = 3.93$ GPa, $G = 1.034$ GPa, $\nu = 0.37$.

The results obtained for example 5.3.1 are tabulated in the Tables 5.2 –5.5.

Angles in degrees	CLPT		FSDT		TSDT	
	Tapered	Uniform	Tapered	Uniform	Tapered	Uniform
0.05	0.19274	0.21013	0.17129	0.21007	0.16850	0.2070
0.10	0.77052	0.84015	0.6378	0.83912	0.62962	0.82699
0.50	19.271	21.013	17.4845	20.389	16.0788	20.074

Table 5.2 Comparison of critical buckling load ($\times 10^4 N$) for tapered laminate model AA with that of equivalent uniform plate for simply supported boundary conditions.

Angles in degrees	CLPT		FSDT		TSDT	
	Tapered	Uniform	Tapered	Uniform	Tapered	Uniform
0.05	0.46036	0.41042	0.44557	0.4102	0.40572	0.40659
0.10	1.8456	1.6409	1.8115	1.6380	1.620	1.6146
0.50	46.036	41.042	44.066	39.285	42.482	38.659

Table 5.3 Comparison of critical buckling load ($\times 10^4 N$) for tapered laminate model BB with that of equivalent uniform plate for simply supported boundary conditions.

Angles in degrees	CLPT		FSDT		TSDT	
	Tapered	Uniform	Tapered	Uniform	Tapered	Uniform
0.05	0.2056	0.21013	0.2000	0.21007	0.1914	0.2066
0.10	0.8221	0.84015	0.7389	0.83912	0.6830	0.82743
0.50	20.5628	21.013	18.9057	20.389	17.5500	20.074

Table 5.4 Comparison of critical buckling load ($\times 10^4 N$) for tapered laminate model CC with that of equivalent uniform plate for simply supported boundary conditions.

Angles in degrees	CLPT		FSDT		TSDT	
	Tapered	Uniform	Tapered	Uniform	Tapered	Uniform
0.05	0.49399	0.41042	0.4762	0.4102	0.4547	0.40659
0.10	1.9752	1.6409	1.8414	1.6380	1.80169	1.6140
0.50	49.399	41.042	47.142	39.285	45.4714	38.555

Table 5.5 Comparison of critical buckling load ($\times 10^4 N$) for tapered laminate model DD with that of equivalent uniform plate for simply supported boundary conditions.

5.4 Critical buckling loads calculated using different plate theories

Example 5.4.1

For parametric study NCT/301 graphite-epoxy is chosen.

Mechanical properties of

(a) Unidirectional Graphite-epoxy:-

$$\text{Longitudinal Modulus (E}_1\text{)} = 113.9 \text{ GPa}$$

$$\text{Transverse Modulus (E}_2\text{)} = 7.9856 \text{ GPa}$$

$$E_2 = E_3 = 7.9856 \text{ GPa}$$

$$\text{In Plane shear Modulus (G}_{12}\text{)} = 3.138 \text{ GPa}$$

$$\text{Out of Plane shear Modulus (G}_{23}\text{)} = 2.543 \text{ GPa}$$

$$\text{Major Poisson's ratio (}\nu_{12}\text{)} = 0.288$$

$$\text{Minor Poisson's ratio (}\nu_{21}\text{)} = 0.018$$

(b) Resin:-

$$\text{Elastic Modulus (E)} = 3.93 \text{ GPa}$$

$$\text{Shear Modulus (G)} = 1.034 \text{ GPa}$$

$$\text{Poisson's ratio (}\nu\text{)} = 0.37$$

The total length ($L = L_a + L_b + L_c$) of all Models A, B, C and D is 298.60mm and $L_a = L_b = (L - L_b)/2$. The models are shown in figure 2.13. In the analysis, taper angle is considered 0.75 degree. The thickness of each ply is 0.125 mm. The values of m and n in the equations (2.89), (3.31) and (4.58) are determined so as to obtain the converged solutions. The laminate configurations are shown in Table 5.6 and the results are given in the Table 5.7.

Laminates	Configurations	
	Thick Section	Thin Section
LC(1)	$[0/90]_{9s}$	$[0/90]_{3s}$
LC(2)	$[\pm 45]_{9s}$	$[\pm 45]_{3s}$
LC(3)	$[0_2/\pm 45_8]_s$	$[0_2/\pm 45_2]_s$

Table 5.6 List of different tapered laminate configurations.

Models	Critical Buckling load, $\times 10^4$ N		
	CLPT	FSDT	TSDT
A	1.4285	1.2500	1.1500
B	3.9824	3.7833	3.5941
C	1.4971	1.4222	1.3511
D	4.1920	3.9924	3.8023

Table 5.7 Influence of different theories on critical buckling load ($\times 10^4$ N) for the laminate configuration LC(1) with simply supported ends.

5.5 Effect of laminate configuration

Example 5.5.1

The tapered models described in example 5.4.1 are considered for buckling analysis. The solutions have been obtained using Ritz method for simply supported boundary conditions. The results are given in Table 5.8.

Laminates	Theories	Critical Buckling load, $\times 10^4$ N			
	Applied	Model A	Model B	Model C	Model D
LC(1)	CLPT	1.4285	3.9824	1.4971	4.1920
	FSDT	1.2500	3.7833	1.4222	3.9924
	TSDT	1.1500	3.5941	1.3511	3.8023
LC(2)	CLPT	1.2169	3.430	1.2777	3.6500
	FSDT	1.1560	3.350	1.2139	3.4400
	TSDT	1.0982	3.092	1.15316	3.2699
LC(3)	CLPT	1.5825	4.4301	1.6616	4.6530
	FSDT	1.5033	4.2200	1.5785	4.4320
	TSDT	1.4282	3.9990	1.4996	4.2202

Table 5.8 Effect of laminate configuration on critical buckling load ($\times 10^4$ N) for simply supported ends.

5.6 Discussion and conclusion

In this chapter a parametric study on critical buckling loads of uniform laminates has been carried out. Then moderately tapered plate models AA, BB, CC and DD (Figure 5.1) have been analyzed. Finally, taper models A, B, C and D (Figure 2.13) have been analyzed. The problems have been solved for different laminate configurations (Table 5.6) using various taper angles based on three different theories, CLPT, FSDT and TSDT.

We can conclude the following:

- ✓ Tapered plate of model D has the highest values of critical buckling loads compared to other taper models.
- ✓ Consequently tapered plate models B, C and A take the second, third and fourth positions respectively.
- ✓ Increasing the taper angle results in the increase in the critical buckling load value.
- ✓ Laminate configuration LC(3) is the strongest with respect to the configurations LC(1) and LC(2).
- ✓ Laminate configuration LC(2) is the weakest and the configuration LC(1) is the moderate one.
- ✓ For all tapered laminate models the critical buckling load value calculated using TSDT is the lowest.

Chapter 6

Conclusions and Future Work

In the present thesis buckling of tapered composite plate is analyzed using Ritz method based on Classical Laminated Plate Theory (CLPT), First-order Shear Deformation Theory (FSDT) and Third-order Shear Deformation Theory (TSDT). The effect on the laminate stiffness of the composite plate caused by the taper angle has been quantified. Different configurations of tapered plates have been investigated.

The taper angle of composite plate changes not only the geometric properties but also the stiffness of the oblique plies. Consequently, the mechanical behavior of tapered composite plate differs from that of uniform plate. The effect on the ply stiffness can be ignored if the taper angle is very small. With the increase in the taper angle, this influence is not negligible.

Considering the effect of taper angle, stiffness matrices have been derived. Applying these stiffness matrices, energy equations have been developed for CLPT, FSDT and TSDT respectively. Finally, system equations of critical buckling loads of tapered composite plates have been derived.

The programming, involving symbolic and numerical computations, is done using MATLAB[®] software. At the end of each formulation, appropriate problems have been solved and the results are vindicated physically and graphically and compared with that of published works.

The parametric study is carried out for the tapered composite plates to see the effects of various changes in the laminate parameters on buckling. These changes include the change in the boundary conditions, change in the laminate configuration and change in the taper angle. The imperative and prime conclusions are:

- ✓ CLPT is applicable for thin plate but for thick plate we need to apply higher-order theory.
- ✓ Tapered plate of model D has the highest critical buckling load compared to other taper models as it has more inner continuous plies than others and its core is almost made up of plies. Model B is closer to model D as its core has same characteristic as model D.
- ✓ Consequently tapered plate models 'C and A' are weaker than models 'D and B' due to resin pockets at core.
- ✓ Laminate configurations LC(3), LC(1) and LC(2) are the strongest, moderate and weakest laminates respectively. The variation of geometric properties of the laminates are explained in the following table:

	Fiber direction of continuous plies			Remarks
	90^0	$\pm 45^0$	0^0	
Stiffness	Weakest	Moderate	Strongest	
No. of Plies of LC(1)	6	0	6	Moderate Configuration
No. of Plies of LC(2)	0	6+6	0	Weakest Configuration
No. of Plies of LC(3)	0	4+4	4	Strongest Configuration

Table 6.1 Physical explanation for variation of geometric properties of laminates.

Laminate LC(3) is the strongest as it is constructed by two types of plies: moderate plies (4+4) and strongest plies (4). Laminate LC(2) is the weakest one as it is constructed by moderate plies (6+6) only. On the other hand, laminate LC(1) is the moderate one as two extreme types of plies namely, the weakest plies (6) and strongest plies (6), are used to construct it.

The study on buckling of the tapered laminates can be continued in the long run based on the following recommendations:

1. Higher-order finite element analysis of tapered laminate can be developed based on the Ritz solution presented in this thesis.
2. Ritz method presented in this thesis can be extended to stochastic buckling analysis.
3. Present work can be extended for the analysis of the free and forced vibration response of different types of laminated plates.
4. The effect of damping can be considered in the free and forced vibrations of tapered composite plates.

References

- [1] Reddy, J. N., *Mechanics of Laminated Composite Plates – Theory and Analysis*, 1997, CRC Press, U.S.A.
- [2] Whitney, J. M., “The Effect of Boundary Conditions on the Response of Laminated Composite”, *Journal of Composite Materials*, Vol. 4, 1970, pp. 360-378.
- [3] Ashton, J. E., “Anisotropic Plate Analysis – Boundary Conditions”, *Journal of Composite Materials*, Vol. 3, 1969, pp. 230-235.
- [4] Baharlou, B. and Leissa, A. W., “Vibration and Buckling of Generally Laminated Composite Plates with Arbitrary Edge Conditions”, *International Journal of Mechanical Sciences*, Vol. 29, 1987, pp. 545-555.
- [5] Venini, P. and Mariani, C., “Free Vibration of Uncertain Composite Plates via Stochastic Rayleigh Ritz Approach”, *Computers and Structures*, Vol. 64 No.1-4, 1997, pp. 407-423.
- [6] Chao, M. and Kim, H. S., “Interlaminar Stress Analysis of Composite Laminates with Internal Ply-drop”, *AIAA Journal* - 1340, 2000, pp. 1-7.
- [7] Cheung, Y. K. and Zhou, D., “The Free Vibrations of Tapered Rectangular Plates Using a New Set of Beam Functions with the Rayleigh Ritz Method”, *Journal of Sound and Vibration*, Vol. 223(5), 1990, pp. 703-722.
- [8] Curry, J. M. and Johnson, E. R. and Starnes, J. H., “Effect of Dropped Plies on The Strength of Graphite-Epoxy Laminates”, *AIAA Journal*, Vol. 30 No. 2, Feb. 1992, pp. 449-456.

- [9] Mukharjee, A. and Varughese, B., "Design Guidelines for Ply Drop-Off in Laminated Composite Structures", *Composites: Part B*, Vol. 32, 2001, pp. 153-164.
- [10] Varughese, B. and Mukharjee, A., "A Ply Drop-Off Element for Analysis of Tapered Laminated Composites", *Composite Structures*, Vol. 39, No. 1-2, 1997, pp. 123-144,.
- [11] Thomas, D. M. and Webber, J. P. H., "A Design Study into the Delamination Behaviour of Tapered Composites", *Composite Structures*, Vol. 27, 1994, pp. 379-388.
- [12] Mukherjee, A. and Varughese, B., "Development of Specialized Finite Element for The Analysis of Composite Structures with Ply Drop-off", *Composite Structures*, Vol. 46, 1999, pp. 1-16.
- [13] Wang, X. and Lu, G., "Local Buckling of Composite Laminar Plates with Various Delaminated Shapes", *Thin-Walled Structures*, Vol. 41, 2003, pp. 493-506.
- [14] Gaudenzi, P., "On delamination buckling of composite laminated under composite loading", *Composite Structures*, Vol. 1-2, 1997, pp. 21-30,.
- [15] Fish, J. C. and Lee, S. W., "Delamination of Tapered Composite Structures", *Engineering Fracture Mechanics*, Vol. 34. No. 1, 1989, pp. 43-54.
- [16] Zabihollah, A., "Vibration and Buckling Analysis of Tapered Composite Beams Using Conventional and Advanced Finite Element Formulations", M.A.Sc. Thesis, 2003, Concordia University.

- [17] DiNardo, M. T. and Lagace, P. A., "Buckling and Post Buckling of Laminated Composite Plates With Ply Drop-offs", *AIAA Journal*, Vol. 27, No10, 1989, pp. 1392-1398.
- [18] Whitney, J. M., "Stress Analysis of Thick Laminated Composite Sandwich Plates". *Journal of Composite Materials*, Vol. 6, 1972, pp. 426-430.
- [19] Kabir, H. R. H., "On the Frequency Response of Moderately Thick Simply Supported Rectangular Plates With Arbitrarily Lamination", *International Journal of Solids And Structures*, Vol. 36; 1999, pp. 2285-2301.
- [20] Jensen, D.W. and Lagace, P.A., "Influence of Mechanical Coupling on the Buckling and Post-Buckling of Anisotropic Plates", *AIAA Journal*, Vol. 26(10), 1988, pp. 1269-77.
- [21] Wu, C. P. and Chen, W. Y., "Vibration and Stability of Laminated Plates Based on a Local High Order Plate Theory", *Journal of Sound and Vibration*, Vol. 177(4), 1994, pp. 503-520.
- [22] Matsunaga, H., "Vibration and Stability of Cross-ply Laminated Composite Plates According to a Global Higher-order Plate Theory", *Composite Structures*, Vol. 48, 2000, pp. 231-244.
- [23] Wang, W. J., Tseng, Y. R. and Lin, K. J., "Stability of Laminated Plates Using Finite Strip Method Based on a Higher-order Plate Theory", *Composite Structures*, Vol. 34, 1996, pp. 65-16.
- [24] Kulkarni, S. A. and Bajoria, K. M., "Finite Element Modeling of Smart Plates/Shells Using Higher Order Shear Deformation Theory", *Composite Structures*, Vol. 62, 2003, pp. 41-50.

- [25] Chattopadhyay, A. and Radu, A.G., “Dynamic Instability of Composite Laminates Using a Higher-order Theory”. *Composite Structures*, Vol. 77, 2000, pp. 453-460.
- [26] Matsunaga, H., “Assessment of a Global Higher-Order Deformation Theory for Laminated Composite and Sandwich Plates”, *Composite Structures*, Vol. 56, 2002, pp. 279-291.
- [27] Matsunaga, H., “Vibration and Buckling of Multilayered Composite Beams According to Higher Order Deformation Theories”, *Journal of Sound and Vibration*, Vol. 246(1), 2001, pp. 47-62.
- [28] Rao, S. R. and Ganesan, N., “Dynamic Response of Tapered Composite Beams Using Higher Order Shear Deformation Theory”, *Journal of Sound and Vibration*, Vol. 187(5), 1995, pp. 737-756.
- [29] Berthelot, J. M., *Composite Materials -Mechanical Behavior And Structural Analysis*, 1999, Springer Verlag, New York.
- [30] Boresi, A. P. and Chong, K. P., *Elasticity in Engineering Mechanics*, Second Edition, John Wiley & Sons, Inc.
- [31] Ganesan, R., *Stress Analysis in Engineering Mechanics*, Class Notes, Mechanical Dept., Concordia University.
- [32] Hyer, M. W., *Stress Analysis of Fiber-Reinforced Composite Materials*, McGraw-Hill book Company, Inc. (1998).
- [33] Whitney, J. M. and Ashton, J. E., “Structural Analysis of Laminated Anisotropic Plates”, 1987, Lancaster, Pa, U.S.A., Technomic Publishing Company.

- [34] Timushenko, S. P. and Gere, J.M., *Theory Of Elastic Stability*, Second Edition, McGraw-Hill book Company, Inc. (1961).
- [35] Shi, J. W., Nakatani, A. and Kitagawa, H., “Vibration Analysis of Fully Clamped Arbitrarily Laminated Plate”, *Composite Structures*, Vol. 63, 2004, pp. 115-122.
- [36] Bert, C. W. and Mayberry, B. L., “Free Vibration Of Unsymmetrically Laminated Anisotropic Plates with Clamped Edges”, *Journal of Composite Materials*, Vol. 1, 1968, pp. 210-230.
- [37] Whitney, J. M., “The Effect of Transverse Shear Deformation on the Bending of Laminated Plates”, *Journal of Composite Materials*, Vol. 2, 1969, pp. 110-115.
- [38] Wittrick, W. H. and Ellen, C. H., “Buckling of Tapered Rectangular Plates in Compression”, *The Aeronautical Quaterly*, 1962, pp. 308-327.
- [39] Tessler, A., Saether, E. and Tsui, T., “Vibration of Thick Laminated Composite Plates”, *Journal of Sound and Vibration*, Vol. 179(3), 1995, pp. 475-498.
- [40] Reddy, J. N. and Robbins, D. H., “Theories and Computational Models for Composite Laminates”, *Applied Mechanics Review*, Vol. 47, No. 6, Part 1, June 1994, pp. 147-169.
- [41] Agaah, M. R., Mahinfalah, M. and Jahar, G. N., “Linear Static Analysis and Finite Element Modeling for Laminated Composite Plates Using Third Order Deformation Theory”, *Composite Structures*, Vol. 62, 2003, pp. 27-39.
- [42] Burton, W. S., “Stress and Free Vibration Analyses of Multilayered Composite Plates”, *Composite Structure*, Vol. 11, 1989, pp. 183–204.

- [43] Bose, P. and Reddy, J N., “Analysis of Composite Plates Using Various Plate Theories. Part 1: Formulation and Analytical Solutions”, *Structural Engineering Mechanics*, Vol. 6(6), 1998, pp. 583- 612.
- [44] Wu, C. P. and Chen, W. Y., “Vibration and Stability of Laminated Plates Based on a Local High Order Plate Theory”, *Journal of Sound and Vibration*, Vol. 177(4), 1994, pp. 503-520.
- [45] Putcha, N. S. and Reddy, J. N., “Stability and Natural Vibration Analysis of Laminated Plates by Using a Mixed Element Based on Refined Plate Theory”, *Journal of Sound and Vibration*, Vol. 14, 1986, pp. 185-300.
- [46] Khdeir, A. A. and Libriscu, L., “Analysis of Symmetric Cross-ply Laminated Elastic Plates Using a Higher-order Theory, Part-II: Buckling and Free Vibration”, *Composite Structures*, Vol. 9, 1988, pp. 259-277.
- [47] Noor, A. K., “Stability of Multilayered Composite Plates”, *Journal Of Science and Technology*, Vol. 8, 1975, pp. 81-89.

Appendix A

System Equations Based on Third-order Shear Deformation Theory

For simply support case:

[See the equations (4.60 – 4.64)]

$$W_m = \sin(m \cdot \pi \cdot x / L); \quad W_n = \sin(m \cdot \pi \cdot y / b);$$

$$X_m = \cos(m \cdot \pi \cdot x / L); \quad X_n = \sin(m \cdot \pi \cdot y / b);$$

$$Y_m = \sin(m \cdot \pi \cdot x / L); \quad Y_n = \cos(m \cdot \pi \cdot y / b);$$

$$Z_m = \sin(m \cdot \pi \cdot x / L); \quad Z_n = \sin(m \cdot \pi \cdot y / b);$$

$$S_m = \sin(m \cdot \pi \cdot x / L); \quad S_n = \sin(m \cdot \pi \cdot y / b);$$

$$W_i = \sin(n \cdot \pi \cdot x / L); \quad W_j = \sin(n \cdot \pi \cdot y / b);$$

$$X_i = \cos(n \cdot \pi \cdot x / L); \quad X_j = \sin(n \cdot \pi \cdot y / b);$$

$$Y_i = \sin(n \cdot \pi \cdot x / L); \quad Y_j = \cos(n \cdot \pi \cdot y / b);$$

$$Z_i = \sin(n \cdot \pi \cdot x / L); \quad Z_j = \sin(n \cdot \pi \cdot y / b);$$

$$S_{ii} = \sin(n \cdot \pi \cdot x / L); \quad S_j = \sin(n \cdot \pi \cdot y / b);$$

Differentiating w.r.t. W_{mn} :

$$\begin{aligned} W_1 = & -\text{int}((6 \cdot D_{55} \cdot C_1 \cdot dW_m/dx \cdot dW_i/dx), x, 0, L) \cdot \text{int}((W_n \cdot W_j), y, 0, b) + \\ & \text{int}((3 \cdot H_{14} \cdot C_1^2 \cdot W_m \cdot d^2W_i/dx^2), x, 0, L) \cdot \text{int}((W_j \cdot dW_n/dy), y, 0, b) - \\ & \text{int}((2 \cdot E_{46} \cdot C_1 \cdot dW_m/dx \cdot W_i), x, 0, L) \cdot \text{int}((dW_n/dy \cdot dW_j/dy), y, 0, b) + \\ & \text{int}((3 \cdot H_{24} \cdot C_1^2 \cdot W_m \cdot W_i), x, 0, L) \cdot \text{int}((d^2W_j/dy^2 \cdot dW_n/dy), y, 0, b) + \\ & \text{int}((9 \cdot F_{45} \cdot C_1^2 \cdot W_m \cdot dW_i/dx), x, 0, L) \cdot \text{int}((W_j \cdot dW_n/dy), y, 0, b) + \end{aligned}$$

$$\begin{aligned}
& \text{int}((6*H56*C1^2*dWm/dx*dWi/dx),x,0,L) * \text{int}((dWj/dy*Wn),y,0,b) - \\
& \text{int}((6*D45*C1*dWm/dx*Wi),x,0,L) * \text{int}((Wn*dWj/dy),y,0,b) + \\
& \text{int}((6*H46*C1^2*dWm/dx*Wi),x,0,L) * \text{int}((dWn/dy*dWj/dy),y,0,b) + \\
& \text{int}((3*H15*C1^2*dWm/dx*d2Wi/dx2),x,0,L) * \text{int}((Wj*Wn),y,0,b) + \\
& \text{int}((3*H24*C1^2*Wm*Wi),x,0,L) * \text{int}((dWj/dy*d2Wn/dy2),y,0,b) - \\
& \text{int}((2*E56*C1*dWm/dx*dWi/dx),x,0,L) * \text{int}((dWn/dy*Wj),y,0,b) - \\
& \text{int}((2*E56*C1*dWm/dx*dWi/dx),x,0,L) * \text{int}((dWj/dy*Wn),y,0,b) + \\
& \text{int}((3*H15*C1^2*d2Wm/dx2*dWi/dx),x,0,L) * \text{int}((Wj*Wn),y,0,b) + \\
& \text{int}((9*F44*C1^2*Wm*Wi),x,0,L) * \text{int}((dWn/dy*dWj/dy),y,0,b) + \\
& \text{int}((J12*C1^2*d2Wm/dx2*Wi),x,0,L) * \text{int}((Wn*d2Wj/dy2),y,0,b) + \\
& \text{int}((J12*C1^2*Wm*d2Wi/dx2),x,0,L) * \text{int}((Wj*d2Wn/dy2),y,0,b) + \\
& \text{int}((3*H25*C1^2*dWm/dx*Wi),x,0,L) * \text{int}((Wn*d2Wj/dy2),y,0,b) + \\
& \text{int}((9*F45*C1^2*dWm/dx*Wi),x,0,L) * \text{int}((Wn*dWj/dy),y,0,b) - \\
& \text{int}((E24*C1*Wm*Wi),x,0,L) * \text{int}((d2Wj/dy2*dWn/dy),y,0,b) - \\
& \text{int}((E25*C1*dWm/dx*Wi),x,0,L) * \text{int}((Wn*d2Wj/dy2),y,0,b) + \\
& \text{int}((9*F55*C1^2*dWm/dx*dWi/dx),x,0,L) * \text{int}((Wn*Wj),y,0,b) - \\
& \text{int}((6*D45*C1*Wm*dWi/dx),x,0,L) * \text{int}((Wj*dWn/dy),y,0,b) + \\
& \text{int}((6*H56*C1^2*dWm/dx*dWi/dx),x,0,L) * \text{int}((dWn/dy*Wj),y,0,b) + \\
& \text{int}((3*H14*C1^2*d2Wm/dx2*Wi),x,0,L) * \text{int}((Wn*dWj/dy),y,0,b) + \\
& \text{int}((4*J66*C1^2*dWm/dx*dWi/dx),x,0,L) * \text{int}((dWn/dy*dWj/dy),y,0,b) - \\
& \text{int}((2*E46*C1*Wm*dWi/dx),x,0,L) * \text{int}((dWj/dy*dWn/dy),y,0,b) + \\
& \text{int}((6*H46*C1^2*Wm*dWi/dx),x,0,L) * \text{int}((dWj/dy*dWn/dy),y,0,b) - \\
& \text{int}((E24*C1*Wm*Wi),x,0,L) * \text{int}((dWj/dy*d2Wn/dy2),y,0,b) -
\end{aligned}$$

$$\begin{aligned}
& \text{int}((E14*C1*Wm*d2Wi/dx2),x,0,L) * \text{int}((Wj*dWn/dy),y,0,b) - \\
& \text{int}((E15*C1*dWm/dx*d2Wi/dx2),x,0,L) * \text{int}((Wj*Wn),y,0,b) + \\
& \text{int}((2*J26*C1^2*dWm/dx*Wi),x,0,L) * \text{int}((dWn/dy*d2Wj/dy2),y,0,b) + \\
& \text{int}((A45*dWm/dx*Wi),x,0,L) * \text{int}((Wn*dWj/dy),y,0,b) + \\
& \text{int}((A55*dWm/dx*dWi/dx),x,0,L) * \text{int}((Wn*Wj),y,0,b) + \\
& \text{int}((2*J26*C1^2*Wm*dWi/dx),x,0,L) * \text{int}((dWj/dy*d2Wn/dy2),y,0,b) + \\
& \text{int}((J22*C1^2*Wm*Wi),x,0,L) * \text{int}((d2Wj/dy2*d2Wn/dy2),y,0,b) + \\
& \text{int}((J11*C1^2*d2Wm/dx2*d2Wi/dx2),x,0,L) * \text{int}((Wj*Wn),y,0,b) - \\
& \text{int}((E25*C1*Wm*dWi/dx),x,0,L) * \text{int}((Wj*d2Wn/dy2),y,0,b) - \\
& \text{int}((E15*C1*d2Wm/dx2*dWi/dx),x,0,L) * \text{int}((Wn*Wj),y,0,b) + \\
& \text{int}((A45*Wm*dWi/dx),x,0,L) * \text{int}((Wj*dWn/dy),y,0,b) - \\
& \text{int}((E14*C1*d2Wm/dx2*Wi),x,0,L) * \text{int}((Wn*dWj/dy),y,0,b) + \\
& \text{int}((2*J16*C1^2*d2Wm/dx2*dWi/dx),x,0,L) * \text{int}((dWj/dy*Wn),y,0,b) + \\
& \text{int}((2*J16*C1^2*dWm/dx*d2Wi/dx2),x,0,L) * \text{int}((dWn/dy*Wj),y,0,b) + \\
& \text{int}((A44*Wm*Wi),x,0,L) * \text{int}((dWj/dy*dWn/dy),y,0,b) - \\
& \text{int}((6*D44*C1*Wm*Wi),x,0,L) * \text{int}((dWj/dy*dWn/dy),y,0,b) + \\
& \text{int}((3*H25*C1^2*Wm*dWi/dx),x,0,L) * \text{int}((Wj*d2Wn/dy2),y,0,b);
\end{aligned}$$

X1 = -

$$\begin{aligned}
& \text{int}((E15*C1*d2Wm/dx2*Xi),x,0,L)*\text{int}((Wn*Xj),y,0,b)+\text{int}((B14*Wm*dXi/dx),x,0,L)*i \\
& \text{nt}((Xj*dWn/dy),y,0,b)+\text{int}((3*H15*C1^2*d2Wm/dx2*Xi),x,0,L)*\text{int}((Xj*Wn),y,0,b)- \\
& \text{int}((4*E46*C1*Wm*Xi),x,0,L)*\text{int}((dXj/dy*dWn/dy),y,0,b)+\text{int}((J16*C1^2*d2Wm/dx2 \\
& *Xi),x,0,L)*\text{int}((Wn*dXj/dy),y,0,b)+\text{int}((2*J66*C1^2*dWm/dx*Xi),x,0,L)*\text{int}((dWn/dy
\end{aligned}$$

$$\begin{aligned}
& *dX_j/dy),y,0,b)- \\
& \text{int}((4*E56*C1*dW_m/dx*X_i),x,0,L)*\text{int}((W_n*dX_j/dy),y,0,b)+\text{int}((2*J16*C1^2*dW_m/dx \\
& *dX_i/dx),x,0,L)*\text{int}((X_j*dW_n/dy),y,0,b)+\text{int}((3*H46*C1^2*W_m*X_i),x,0,L)*\text{int}((dX_j/dy \\
& *dW_n/dy),y,0,b)+\text{int}((9*F45*C1^2*W_m*X_i),x,0,L)*\text{int}((X_j*dW_n/dy),y,0,b)+\text{int}((3*H14 \\
& *C1^2*W_m*dX_i/dx),x,0,L)*\text{int}((X_j*dW_n/dy),y,0,b)- \\
& \text{int}((2*F66*C1*dW_m/dx*X_i),x,0,L)*\text{int}((dW_n/dy*dX_j/dy),y,0,b)+\text{int}((J12*C1^2*W_m*d \\
& X_i/dx),x,0,L)*\text{int}((X_j*d^2W_n/dy^2),y,0,b)- \\
& \text{int}((2*E56*C1*dW_m/dx*X_i),x,0,L)*\text{int}((dW_n/dy*X_j),y,0,b)- \\
& \text{int}((4*E14*C1*W_m*dX_i/dx),x,0,L)*\text{int}((X_j*dW_n/dy),y,0,b)+\text{int}((6*H56*C1^2*dW_m/d \\
& x*X_i),x,0,L)*\text{int}((dW_n/dy*X_j),y,0,b)- \\
& \text{int}((6*D55*C1*dW_m/dx*X_i),x,0,L)*\text{int}((W_n*X_j),y,0,b)+\text{int}((9*F55*C1^2*dW_m/dx*X_i \\
&),x,0,L)*\text{int}((X_j*W_n),y,0,b)+\text{int}((3*H25*C1^2*W_m*X_i),x,0,L)*\text{int}((X_j*d^2W_n/dy^2),y,0, \\
& b)-\text{int}((2*F16*C1*dW_m/dx*dX_i/dx),x,0,L)*\text{int}((X_j*dW_n/dy),y,0,b)- \\
& \text{int}((4*E15*C1*dW_m/dx*dX_i/dx),x,0,L)*\text{int}((X_j*W_n),y,0,b)+\text{int}((3*H56*C1^2*dW_m/d \\
& x*X_i),x,0,L)*\text{int}((W_n*dX_j/dy),y,0,b)- \\
& \text{int}((6*D45*C1*W_m*X_i),x,0,L)*\text{int}((X_j*dW_n/dy),y,0,b)+\text{int}((J11*C1^2*d^2W_m/dx^2*dX \\
& i/dx),x,0,L)*\text{int}((X_j*W_n),y,0,b)+\text{int}((3*H15*C1^2*dW_m/dx*dX_i/dx),x,0,L)*\text{int}((X_j*W_n \\
&),y,0,b)+\text{int}((B15*dW_m/dx*dX_i/dx),x,0,L)*\text{int}((X_j*W_n),y,0,b)+\text{int}((A55*dW_m/dx*X_i),x \\
& ,0,L)*\text{int}((W_n*X_j),y,0,b)-\text{int}((F16*C1*d^2W_m/dx^2*X_i),x,0,L)*\text{int}((W_n*dX_j/dy),y,0,b)- \\
& \text{int}((F12*C1*W_m*dX_i/dx),x,0,L)*\text{int}((X_j*d^2W_n/dy^2),y,0,b)+\text{int}((J26*C1^2*W_m*X_i),x, \\
& 0,L)*\text{int}((dX_j/dy*d^2W_n/dy^2),y,0,b)- \\
& \text{int}((F11*C1*d^2W_m/dx^2*dX_i/dx),x,0,L)*\text{int}((X_j*W_n),y,0,b)+\text{int}((A45*W_m*X_i),x,0,L)*i \\
& \text{nt}((X_j*dW_n/dy),y,0,b)+\text{int}((B56*dW_m/dx*X_i),x,0,L)*\text{int}((dX_j/dy*W_n),y,0,b)-
\end{aligned}$$

$$\begin{aligned}
& \int((F26*C1*Wm*Xi),x,0,L)*\int((dXj/dy*d2Wn/dy2),y,0,b)+\int((B46*Wm*Xi),x,0,L)*i \\
& \int((dXj/dy*dWn/dy),y,0,b)-\int((E25*C1*Wm*Xi),x,0,L)*\int((Xj*d2Wn/dy2),y,0,b); \\
\mathbf{Y1= -} \\
& \int((6*D45*C1*dWm/dx*Yi),x,0,L)*\int((Wn*Yj),y,0,b)+\int((J26*C1^2*Wm*dYi/dx),x, \\
& 0,L)*\int((Yj*d2Wn/dy2),y,0,b)- \\
& \int((2*F66*C1*dWm/dx*dYi/dx),x,0,L)*\int((dWn/dy*Yj),y,0,b)- \\
& \int((6*D44*C1*Wm*Yi),x,0,L)*\int((Yj*dWn/dy),y,0,b)+\int((3*H14*C1^2*d2Wm/dx2* \\
& Yi),x,0,L)*\int((Wn*Yj),y,0,b)+\int((3*H56*C1^2*dWm/dx*dYi/dx),x,0,L)*\int((Wn*Yj), \\
& y,0,b)+\int((3*H24*C1^2*Wm*Yi),x,0,L)*\int((dYj/dy*dWn/dy),y,0,b)- \\
& \int((4*E24*C1*Wm*Yi),x,0,L)*\int((dYj/dy*dWn/dy),y,0,b)+\int((B24*Wm*Yi),x,0,L)*i \\
& \int((dYj/dy*dWn/dy),y,0,b)- \\
& \int((F12*C1*d2Wm/dx2*Yi),x,0,L)*\int((Wn*dYj/dy),y,0,b)+\int((J12*C1^2*d2Wm/dx2 \\
& *Yi),x,0,L)*\int((Wn*dYj/dy),y,0,b)- \\
& \int((F26*C1*Wm*dYi/dx),x,0,L)*\int((Yj*d2Wn/dy2),y,0,b)+\int((A44*Wm*Yi),x,0,L)*i \\
& \int((Yj*dWn/dy),y,0,b)+\int((A45*dWm/dx*Yi),x,0,L)*\int((Yj*Wn),y,0,b)+\int((J22*C1^ \\
& 2*Wm*Yi),x,0,L)*\int((dYj/dy*d2Wn/dy2),y,0,b)- \\
& \int((4*E25*C1*dWm/dx*Yi),x,0,L)*\int((dYj/dy*Wn),y,0,b)- \\
& \int((E14*C1*d2Wm/dx2*Yi),x,0,L)*\int((Yj*Wn),y,0,b)+\int((9*F45*C1^2*dWm/dx*Yi) \\
& ,x,0,L)*\int((Yj*Wn),y,0,b)+\int((6*H46*C1^2*dWm/dx*Yi),x,0,L)*\int((Yj*dWn/dy),y,0, \\
& b)+\int((B56*dWm/dx*dYi/dx),x,0,L)*\int((Yj*Wn),y,0,b)- \\
& \int((E24*C1*Wm*Yi),x,0,L)*\int((Yj*d2Wn/dy2),y,0,b)+\int((3*H24*C1^2*Wm*Yi),x,0 \\
& ,L)*\int((Yj*d2Wn/dy2),y,0,b)- \\
& \int((F22*C1*Wm*Yi),x,0,L)*\int((dYj/dy*d2Wn/dy2),y,0,b)+\int((B46*Wm*dYi/dx),x,0,
\end{aligned}$$

$$\begin{aligned}
&L) \int \int (Y_j \cdot dW_n/dy), y, 0, b) + \int \int ((2 \cdot J_{26} \cdot C_1^2 \cdot dW_m/dx \cdot Y_i), x, 0, L) \int \int ((dW_n/dy \cdot dY_j/dy), \\
&y, 0, b) + \int \int ((9 \cdot F_{44} \cdot C_1^2 \cdot W_m \cdot Y_i), x, 0, L) \int \int (Y_j \cdot dW_n/dy), y, 0, b) + \int \int ((2 \cdot J_{66} \cdot C_1^2 \cdot dW \\
&m/dx \cdot dY_i/dx), x, 0, L) \int \int ((dW_n/dy \cdot Y_j), y, 0, b) + \int \int ((J_{16} \cdot C_1^2 \cdot d^2W_m/dx^2 \cdot dY_i/dx), x, 0, L) \\
&\int \int ((Y_j \cdot W_n), y, 0, b) - \int \int ((F_{16} \cdot C_1 \cdot d^2W_m/dx^2 \cdot dY_i/dx), x, 0, L) \int \int ((W_n \cdot Y_j), y, 0, b) - \\
&\int \int ((2 \cdot E_{46} \cdot C_1 \cdot dW_m/dx \cdot Y_i), x, 0, L) \int \int (Y_j \cdot dW_n/dy), y, 0, b) - \\
&\int \int ((4 \cdot E_{56} \cdot C_1 \cdot dW_m/dx \cdot dY_i/dx), x, 0, L) \int \int (Y_j \cdot W_n), y, 0, b) - \\
&\int \int ((4 \cdot E_{46} \cdot C_1 \cdot W_m \cdot dY_i/dx), x, 0, L) \int \int (Y_j \cdot dW_n/dy), y, 0, b) + \int \int ((3 \cdot H_{46} \cdot C_1^2 \cdot W_m \cdot dY \\
&i/dx), x, 0, L) \int \int (Y_j \cdot dW_n/dy), y, 0, b) + \int \int ((3 \cdot H_{25} \cdot C_1^2 \cdot dW_m/dx \cdot Y_i), x, 0, L) \int \int ((W_n \cdot dY \\
&j/dy), y, 0, b) + \int \int ((B_{25} \cdot dW_m/dx \cdot Y_i), x, 0, L) \int \int ((W_n \cdot dY_j/dy), y, 0, b) - \\
&\int \int ((2 \cdot F_{26} \cdot C_1 \cdot dW_m/dx \cdot Y_i), x, 0, L) \int \int ((dW_n/dy \cdot dY_j/dy), y, 0, b);
\end{aligned}$$

$$\begin{aligned}
\mathbf{Z1} = & - \int \int ((1/2 \cdot D_{14} \cdot W_m \cdot d^2Z_i/dx^2), x, 0, L) \int \int ((Z_j \cdot dW_n/dy), y, 0, b) - \\
& \int \int ((D_{56} \cdot dW_m/dx \cdot dZ_i/dx), x, 0, L) \int \int ((dZ_j/dy \cdot W_n), y, 0, b) - \\
& \int \int ((D_{46} \cdot W_m \cdot dZ_i/dx), x, 0, L) \int \int ((dZ_j/dy \cdot dW_n/dy), y, 0, b) + \int \int ((1/2 \cdot H_{22} \cdot C_1 \cdot W_m \cdot Z_i), x, \\
& 0, L) \int \int ((d^2Z_j/dy^2 \cdot d^2W_n/dy^2), y, 0, b) + \int \int ((H_{12} \cdot C_1 \cdot d^2W_m/dx^2 \cdot Z_i), x, 0, L) \int \int ((W_n \cdot d^2 \\
& Z_j/dy^2), y, 0, b) + \int \int ((3 \cdot F_{46} \cdot C_1 \cdot W_m \cdot dZ_i/dx), x, 0, L) \int \int ((dZ_j/dy \cdot dW_n/dy), y, 0, b) + \int \int ((3/2 \\
& \cdot F_{25} \cdot C_1 \cdot dW_m/dx \cdot Z_i), x, 0, L) \int \int ((W_n \cdot d^2Z_j/dy^2), y, 0, b) + \int \int ((1/2 \cdot H_{11} \cdot C_1 \cdot d^2W_m/dx^2 \cdot \\
& d^2Z_i/dx^2), x, 0, L) \int \int ((Z_j \cdot W_n), y, 0, b) + \int \int ((3/2 \cdot F_{24} \cdot C_1 \cdot W_m \cdot Z_i), x, 0, L) \int \int ((d^2Z_j/dy^2 \cdot d \\
& W_n/dy), y, 0, b) + \int \int ((3 \cdot F_{56} \cdot C_1 \cdot dW_m/dx \cdot dZ_i/dx), x, 0, L) \int \int ((dZ_j/dy \cdot W_n), y, 0, b) + \int \int ((3/2 \\
& \cdot F_{15} \cdot C_1 \cdot dW_m/dx \cdot d^2Z_i/dx^2), x, 0, L) \int \int ((Z_j \cdot W_n), y, 0, b) - \\
& \int \int ((1/2 \cdot D_{24} \cdot W_m \cdot Z_i), x, 0, L) \int \int ((d^2Z_j/dy^2 \cdot dW_n/dy), y, 0, b) - \\
& \int \int ((1/2 \cdot D_{15} \cdot dW_m/dx \cdot d^2Z_i/dx^2), x, 0, L) \int \int ((Z_j \cdot W_n), y, 0, b) + \int \int ((3/2 \cdot F_{14} \cdot C_1 \cdot W_m \cdot d^2 \\
& Z_i/dx^2), x, 0, L) \int \int ((Z_j \cdot dW_n/dy), y, 0, b) + \int \int ((2 \cdot H_{16} \cdot C_1 \cdot dW_m/dx \cdot d^2Z_i/dx^2), x, 0, L) \int \int ((
\end{aligned}$$

$Z_j * dW_n/dy, y, 0, b) -$

$\int((1/2 * D25 * dW_m/dx * Z_i), x, 0, L) * \int((d2Z_j/dy^2 * W_n), y, 0, b) + \int((2 * H66 * C1 * dW_m/dx * dZ_i/dx), x, 0, L) * \int((dW_n/dy * dZ_j/dy), y, 0, b) + \int((2 * H26 * C1 * W_m * dZ_i/dx), x, 0, L) * \int((dZ_j/dy * d2W_n/dy^2), y, 0, b);$

S1 =

$\int((2 * H46 * C1 * W_m * dS_i/dx), x, 0, L) * \int((dS_j/dy * dW_n/dy), y, 0, b) + \int((H14 * C1 * W_m * d2S_i/dx^2), x, 0, L) * \int((S_j * dW_n/dy), y, 0, b) + \int((H24 * C1 * W_m * S_{ii}), x, 0, L) * \int((d2S_j/dy^2 * dW_n/dy), y, 0, b) + \int((2/3 * J12 * C1 * d2W_m/dx^2 * S_{ii}), x, 0, L) * \int((W_n * d2S_j/dy^2), y, 0, b) + \int((H25 * C1 * dW_m/dx * S_{ii}), x, 0, L) * \int((W_n * d2S_j/dy^2), y, 0, b) -$

$\int((2/3 * E46 * W_m * dS_i/dx), x, 0, L) * \int((dS_j/dy * dW_n/dy), y, 0, b) + \int((1/3 * J22 * C1 * W_m * S_{ii}), x, 0, L) * \int((d2S_j/dy^2 * d2W_n/dy^2), y, 0, b) -$

$\int((1/3 * E25 * dW_m/dx * S_{ii}), x, 0, L) * \int((d2S_j/dy^2 * W_n), y, 0, b) + \int((1/3 * J11 * C1 * d2W_m/dx^2 * d2S_i/dx^2), x, 0, L) * \int((S_j * W_n), y, 0, b) -$

$\int((1/3 * E14 * W_m * d2S_i/dx^2), x, 0, L) * \int((S_j * dW_n/dy), y, 0, b) -$

$\int((1/3 * E15 * dW_m/dx * d2S_i/dx^2), x, 0, L) * \int((S_j * W_n), y, 0, b) -$

$\int((1/3 * E24 * W_m * S_{ii}), x, 0, L) * \int((d2S_j/dy^2 * dW_n/dy), y, 0, b) -$

$\int((2/3 * E56 * dW_m/dx * dS_i/dx), x, 0, L) * \int((dS_j/dy * W_n), y, 0, b) + \int((2 * H56 * C1 * dW_m/dx * dS_i/dx), x, 0, L) * \int((dS_j/dy * W_n), y, 0, b) + \int((4/3 * J16 * C1 * d2W_m/dx^2 * dS_i/dx), x, 0, L) * \int((dS_j/dy * W_n), y, 0, b) + \int((4/3 * J26 * C1 * W_m * dS_i/dx), x, 0, L) * \int((dS_j/dy * d2W_n/dy^2), y, 0, b) + \int((4/3 * J66 * C1 * dW_m/dx * dS_i/dy), x, 0, L) * \int((dS_j/dx * dW_n/dy), y, 0, b) + \int((H15 * C1 * dW_m/dx * d2S_i/dx^2), x, 0, L) * \int((S_j * W_n), y, 0, b);$

Differentiating w.r.t. Xmn:

W2 = -

$$\begin{aligned} & \text{int}((4 * E46 * C1 * Xm * Wi), x, 0, L) * \text{int}((dWj/dy * dXn/dy), y, 0, b) + \text{int}((J11 * C1^2 * dXm/dx * d2 \\ & Wi/dx2), x, 0, L) * \text{int}((Wj * Xn), y, 0, b) + \text{int}((9 * F55 * C1^2 * Xm * dWi/dx), x, 0, L) * \text{int}((Wj * Xn), \\ & y, 0, b) - \\ & \text{int}((2 * F16 * C1 * dXm/dx * dWi/dx), x, 0, L) * \text{int}((dWj/dy * Xn), y, 0, b) + \text{int}((9 * F45 * C1^2 * Xm \\ & * Wi), x, 0, L) * \text{int}((dWj/dy * Xn), y, 0, b) + \text{int}((3 * H25 * C1^2 * Xm * Wi), x, 0, L) * \text{int}((Xn * d2Wj/d \\ & y2), y, 0, b) + \text{int}((2 * J66 * C1^2 * Xm * dWi/dx), x, 0, L) * \text{int}((dWj/dy * dXn/dy), y, 0, b) + \text{int}((3 * H5 \\ & 6 * C1^2 * Xm * dWi/dx), x, 0, L) * \text{int}((Wj * dXn/dy), y, 0, b) - \\ & \text{int}((4 * E56 * C1 * Xm * dWi/dx), x, 0, L) * \text{int}((Wj * dXn/dy), y, 0, b) - \\ & \text{int}((F16 * C1 * Xm * d2Wi/dx2), x, 0, L) * \text{int}((Wj * dXn/dy), y, 0, b) - \\ & \text{int}((F11 * C1 * dXm/dx * d2Wi/dx2), x, 0, L) * \text{int}((Wj * Xn \\ &), y, 0, b) + \text{int}((A55 * Xm * dWi/dx), x, 0, L) * \text{int}((Wj * Xn), y, 0, b) - \\ & \text{int}((4 * E14 * C1 * dXm/dx * Wi), x, 0, L) * \text{int}((Xn * dWj/dy), y, 0, b) + \text{int}((3 * H46 * C1^2 * Xm * Wi \\ &), x, 0, L) * \text{int}((dWj/dy * dXn/dy), y, 0, b) - \\ & \text{int}((2 * F66 * C1 * Xm * dWi/dx), x, 0, L) * \text{int}((dWj/dy * dXn/dy), y, 0, b) - \\ & \text{int}((4 * E15 * C1 * dXm/dx * dWi/dx), x, 0, L) * \text{int}((Wj * Xn), y, 0, b) + \text{int}((3 * H15 * C1^2 * dXm/dx \\ & * dWi/dx), x, 0, L) * \text{int}((Wj * Xn), y, 0, b) + \text{int}((J12 * C1^2 * dXm/dx * Wi), x, 0, L) * \text{int}((Xn * d2Wj/ \\ & dy2), y, 0, b) + \text{int}((2 * J16 * C1^2 * dXm/dx * dWi/dx), x, 0, L) * \text{int}((dWj/dy * Xn), y, 0, b) + \text{int}((6 * H \\ & 56 * C1^2 * Xm * dWi/dx), x, 0, L) * \text{int}((dWj/dy * Xn), y, 0, b) - \\ & \text{int}((F12 * C1 * dXm/dx * Wi), x, 0, L) * \text{int}((d2Wj/dy2 * Xn), y, 0, b) + \text{int}((3 * H15 * C1^2 * Xm * d2 \\ & Wi/dx2), x, 0, L) * \text{int}((Wj * Xn), y, 0, b) + \text{int}((3 * H14 * C1^2 * dXm/dx * Wi), x, 0, L) * \text{int}((dWj/dy * \\ & Xn), y, 0, b) + \text{int}((B56 * Xm * dWi/dx), x, 0, L) * \text{int}((Wj * dXn/dy), y, 0, b) + \text{int}((J16 * C1^2 * Xm * d \end{aligned}$$

$$\begin{aligned}
& 2W_i/dx^2)_{,x,0,L} * \int((W_j * dX_n/dy)_{,y,0,b}) + \int((B46 * X_m * W_i)_{,x,0,L}) * \int((dW_j/dy * dX_n/dy)_{,y,0,b}) \\
& + \int((B15 * dX_m/dx * dW_i/dx)_{,x,0,L}) * \int((W_j * X_n)_{,y,0,b}) - \\
& \int((6 * D55 * C1 * X_m * dW_i/dx)_{,x,0,L}) * \int((W_j * X_n)_{,y,0,b}) - \\
& \int((6 * D45 * C1 * X_m * W_i)_{,x,0,L}) * \int((X_n * dW_j/dy)_{,y,0,b}) + \int((B14 * dX_m/dx * W_i)_{,x,0,L}) * \int((dW_j/dy * X_n)_{,y,0,b}) \\
& - \int((2 * E56 * C1 * X_m * dW_i/dx)_{,x,0,L}) * \int((dW_j/dy * X_n)_{,y,0,b}) - \\
& \int((E25 * C1 * X_m * W_i)_{,x,0,L}) * \int((d^2W_j/dy^2 * X_n)_{,y,0,b}) + \int((J26 * C1^2 * X_m * W_i)_{,x,0,L}) \\
& * \int((d^2W_j/dy^2 * dX_n/dy)_{,y,0,b}) + \int((A45 * X_m * W_i)_{,x,0,L}) * \int((dW_j/dy * X_n)_{,y,0,b}) - \\
& \int((F26 * C1 * X_m * W_i)_{,x,0,L}) * \int((d^2W_j/dy^2 * dX_n/dy)_{,y,0,b}) - \\
& \int((E15 * C1 * X_m * d^2W_i/dx^2)_{,x,0,L}) * \int((W_j * X_n)_{,y,0,b});
\end{aligned}$$

$$\begin{aligned}
\mathbf{X2} = & - \int((2 * F11 * C1 * dX_m/dx * dX_i/dx)_{,x,0,L}) * \int((X_j * X_n)_{,y,0,b}) - \\
& \int((2 * F16 * C1 * X_m * dX_i/dx)_{,x,0,L}) * \int((X_j * dX_n/dy)_{,y,0,b}) + \int((3 * H56 * C1^2 * X_m * X_i)_{,x,0,L}) \\
& * \int((dX_j/dy * X_n)_{,y,0,b}) - \\
& \int((2 * F16 * C1 * dX_m/dx * X_i)_{,x,0,L}) * \int((dX_j/dy * X_n)_{,y,0,b}) - \\
& \int((6 * D55 * C1 * X_m * X_i)_{,x,0,L}) * \int((X_j * X_n)_{,y,0,b}) + \int((J66 * C1^2 * X_m * X_i)_{,x,0,L}) * \int((dX_j/dy * dX_n/dy)_{,y,0,b}) \\
& + \int((3 * H56 * C1^2 * X_m * X_i)_{,x,0,L}) * \int((X_j * dX_n/dy)_{,y,0,b}) - \\
& \int((2 * F66 * C1 * X_m * X_i)_{,x,0,L}) * \int((dX_j/dy * dX_n/dy)_{,y,0,b}) - \\
& \int((4 * E15 * C1 * X_m * dX_i/dx)_{,x,0,L}) * \int((X_j * X_n)_{,y,0,b}) - \\
& \int((4 * E56 * C1 * X_m * X_i)_{,x,0,L}) * \int((dX_j/dy * X_n)_{,y,0,b}) - \\
& \int((4 * E15 * C1 * dX_m/dx * X_i)_{,x,0,L}) * \int((X_j * X_n)_{,y,0,b}) + \int((J16 * C1^2 * dX_m/dx * X_i)_{,x,0,L}) \\
& * \int((dX_j/dy * X_n)_{,y,0,b}) + \int((B15 * X_m * dX_i/dx)_{,x,0,L}) * \int((X_j * X_n)_{,y,0,b}) + \int((A55 * X_m * X_i)_{,x,0,L}) \\
& * \int((X_j * X_n)_{,y,0,b}) - \\
& \int((4 * E56 * C1 * X_m * X_i)_{,x,0,L}) * \int((X_j * dX_n/dy)_{,y,0,b}) + \int((J16 * C1^2 * X_m * dX_i/dx)_{,x,0,L})
\end{aligned}$$

$L) \cdot \text{int}((X_j \cdot dX_n/dy), y, 0, b) + \text{int}((D66 \cdot X_m \cdot X_i), x, 0, L) \cdot \text{int}((dX_j/dy \cdot dX_n/dy), y, 0, b) + \text{int}((B56 \cdot X_m \cdot X_i), x, 0, L) \cdot \text{int}((X_j \cdot dX_n/dy), y, 0, b) + \text{int}((9 \cdot F55 \cdot C1^2 \cdot X_m \cdot X_i), x, 0, L) \cdot \text{int}((X_j \cdot X_n), y, 0, b) + \text{int}((D16 \cdot dX_m/dx \cdot X_i), x, 0, L) \cdot \text{int}((dX_j/dy \cdot X_n), y, 0, b) + \text{int}((D11 \cdot dX_m/dx \cdot dX_i/dx), x, 0, L) \cdot \text{int}((X_j \cdot X_n), y, 0, b) + \text{int}((B56 \cdot X_m \cdot X_i), x, 0, L) \cdot \text{int}((dX_j/dy \cdot X_n), y, 0, b) + \text{int}((J11 \cdot C1^2 \cdot dX_m/dx \cdot dX_i/dx), x, 0, L) \cdot \text{int}((X_j \cdot X_n), y, 0, b) + \text{int}((B15 \cdot dX_m/dx \cdot X_i), x, 0, L) \cdot \text{int}((X_j \cdot X_n), y, 0, b) + \text{int}((3 \cdot H15 \cdot C1^2 \cdot dX_m/dx \cdot X_i), x, 0, L) \cdot \text{int}((X_j \cdot X_n), y, 0, b) + \text{int}((3 \cdot H15 \cdot C1^2 \cdot X_m \cdot dX_i/dx), x, 0, L) \cdot \text{int}((X_j \cdot X_n), y, 0, b) + \text{int}((D16 \cdot X_m \cdot dX_i/dx), x, 0, L) \cdot \text{int}((X_j \cdot dX_n/dy), y, 0, b);$

$Y2 = \text{int}((9 \cdot F45 \cdot C1^2 \cdot X_m \cdot Y_i), x, 0, L) \cdot \text{int}((Y_j \cdot X_n), y, 0, b) - \text{int}((6 \cdot D45 \cdot C1 \cdot X_m \cdot Y_i), x, 0, L) \cdot \text{int}((Y_j \cdot X_n), y, 0, b) + \text{int}((A45 \cdot X_m \cdot Y_i), x, 0, L) \cdot \text{int}((Y_j \cdot X_n), y, 0, b) + \text{int}((D12 \cdot dX_m/dx \cdot Y_i), x, 0, L) \cdot \text{int}((dY_j/dy \cdot X_n), y, 0, b) + \text{int}((J26 \cdot C1^2 \cdot X_m \cdot Y_i), x, 0, L) \cdot \text{int}((dY_j/dy \cdot dX_n/dy), y, 0, b) + \text{int}((B14 \cdot dX_m/dx \cdot Y_i), x, 0, L) \cdot \text{int}((Y_j \cdot X_n), y, 0, b) + \text{int}((J12 \cdot C1^2 \cdot dX_m/dx \cdot Y_i), x, 0, L) \cdot \text{int}((dY_j/dy \cdot X_n), y, 0, b) + \text{int}((D66 \cdot X_m \cdot dY_i/dx), x, 0, L) \cdot \text{int}((Y_j \cdot dX_n/dy), y, 0, b) + \text{int}((D26 \cdot X_m \cdot Y_i), x, 0, L) \cdot \text{int}((dY_j/dy \cdot dX_n/dy), y, 0, b) - \text{int}((2 \cdot F12 \cdot C1 \cdot dX_m/dx \cdot Y_i), x, 0, L) \cdot \text{int}((dY_j/dy \cdot X_n), y, 0, b) - \text{int}((2 \cdot F66 \cdot C1 \cdot X_m \cdot dY_i/dx), x, 0, L) \cdot \text{int}((Y_j \cdot dX_n/dy), y, 0, b) + \text{int}((3 \cdot H14 \cdot C1^2 \cdot dX_m/dx \cdot Y_i), x, 0, L) \cdot \text{int}((Y_j \cdot X_n), y, 0, b) - \text{int}((4 \cdot E25 \cdot C1 \cdot X_m \cdot Y_i), x, 0, L) \cdot \text{int}((dY_j/dy \cdot X_n), y, 0, b) + \text{int}((3 \cdot H56 \cdot C1^2 \cdot X_m \cdot dY_i/dx), x, 0, L) \cdot \text{int}((Y_j \cdot X_n), y, 0, b) + \text{int}((J16 \cdot C1^2 \cdot dX_m/dx \cdot dY_i/dx), x, 0, L) \cdot \text{int}((Y_j \cdot X_n), y, 0, b) - \text{int}((4 \cdot E56 \cdot C1 \cdot X_m \cdot dY_i/dx), x, 0, L) \cdot \text{int}((Y_j \cdot X_n), y, 0, b) + \text{int}((3 \cdot H25 \cdot C1^2 \cdot X_m \cdot Y_i), x, 0, L) \cdot \text{int}((dY_j/dy \cdot X_n), y, 0, b) + \text{int}((J66 \cdot C1^2 \cdot X_m \cdot dY_i/dx), x, 0, L) \cdot \text{int}((Y_j \cdot dX_n/dy), y, 0, b) + \text{int}((B56 \cdot X_m \cdot dY_i/dx), x, 0, L) \cdot \text{int}((Y_j \cdot X_n), y, 0, b) -$

$$\begin{aligned}
& \text{int}((4 * E14 * C1 * dXm/dx * Yi), x, 0, L) * \text{int}((Yj * Xn), y, 0, b) - \\
& \text{int}((2 * F26 * C1 * Xm * Yi), x, 0, L) * \text{int}((dYj/dy * dXn/dy), y, 0, b) - \\
& \text{int}((2 * F16 * C1 * dXm/dx * dYi/dx), x, 0, L) * \text{int}((Yj * Xn), y, 0, b) + \text{int}((B46 * Xm * Yi), x, 0, L) * \text{int} \\
& ((Yj * dXn/dy), y, 0, b) - \\
& \text{int}((4 * E46 * C1 * Xm * Yi), x, 0, L) * \text{int}((Yj * dXn/dy), y, 0, b) + \text{int}((D16 * dXm/dx * dYi/dx), x, 0, L \\
&) * \text{int}((Yj * Xn), y, 0, b) + \text{int}((B25 * Xm * Yi), x, 0, L) * \text{int}((dYj/dy * Xn), y, 0, b) + \text{int}((3 * H46 * C1^2 \\
& * Xm * Yi), x, 0, L) * \text{int}((Yj * dXn/dy), y, 0, b);
\end{aligned}$$

$$\begin{aligned}
\mathbf{Z2} = & \text{int}((3/2 * F15 * C1 * Xm * d2Zi/dx2), x, 0, L) * \text{int}((Zj * Xn), y, 0, b) - \\
& \text{int}((E16 * dXm/dx * dZi/dx), x, 0, L) * \text{int}((dZj/dy * Xn), y, 0, b) + \text{int}((1/2 * H16 * C1 * Xm * d2Zi/dx \\
& 2), x, 0, L) * \text{int}((Zj * dXn/dy), y, 0, b) + \text{int}((1/2 * H26 * C1 * Xm * Zi), x, 0, L) * \text{int}((d2Zj/dy2 * dXn/d \\
& y), y, 0, b) - \\
& \text{int}((E66 * Xm * dZi/dx), x, 0, L) * \text{int}((dZj/dy * dXn/dy), y, 0, b) + \text{int}((H66 * C1 * Xm * dZi/dx), x, 0, \\
& L) * \text{int}((dZj/dy * dXn/dy), y, 0, b) - \text{int}((D56 * Xm * dZi/dx), x, 0, L) * \text{int}((dZj/dy * Xn), y, 0, b) - \\
& \text{int}((1/2 * D15 * Xm * d2Zi/dx2), x, 0, L) * \text{int}((Zj * Xn), y, 0, b) - \\
& \text{int}((1/2 * E11 * dXm/dx * d2Zi/dx2), x, 0, L) * \text{int}((Zj * Xn), y, 0, b) + \text{int}((1/2 * H12 * C1 * dXm/dx * \\
& Zi), x, 0, L) * \text{int}((d2Zj/dy2 * Xn), y, 0, b) - \\
& \text{int}((1/2 * D25 * Xm * Zi), x, 0, L) * \text{int}((d2Zj/dy2 * Xn), y, 0, b) + \text{int}((1/2 * H11 * C1 * dXm/dx * d2Zi \\
& /dx2), x, 0, L) * \text{int}((Zj * Xn), y, 0, b) - \\
& \text{int}((1/2 * E16 * Xm * d2Zi/dx2), x, 0, L) * \text{int}((Zj * dXn/dy), y, 0, b) + \text{int}((H16 * C1 * dXm/dx * dZi/d \\
& x), x, 0, L) * \text{int}((dZj/dy * Xn), y, 0, b) - \\
& \text{int}((1/2 * E12 * dXm/dx * Zi), x, 0, L) * \text{int}((d2Zj/dy2 * Xn), y, 0, b) + \text{int}((3/2 * F25 * C1 * Xm * Zi), x, \\
& 0, L) * \text{int}((d2Zj/dy2 * Xn), y, 0, b) -
\end{aligned}$$

$$\int((1/2 * E26 * X_m * Z_i), x, 0, L) * \int((d^2 Z_j / dy^2 * dX_n / dy), y, 0, b) + \int((3 * F56 * C1 * X_m * dZ_i / dx), x, 0, L) * \int((dZ_j / dy * X_n), y, 0, b);$$

$$\begin{aligned} S2 = & -\int((1/3 * F11 * dX_m / dx * d^2 S_i / dx^2), x, 0, L) * \int((S_j * X_n), y, 0, b) - \\ & \int((2/3 * F66 * X_m * dS_i / dx), x, 0, L) * \int((dS_j / dy * dX_n / dy), y, 0, b) - \\ & \int((1/3 * F26 * X_m * S_{ii}), x, 0, L) * \int((d^2 S_j / dy^2 * dX_n / dy), y, 0, b) + \int((H25 * C1 * X_m * S_{ii}), x, 0, L) \\ & * \int((d^2 S_j / dy^2 * X_n), y, 0, b) - \int((1/3 * F16 * X_m * d^2 S_i / dx^2), x, 0, L) * \int((S_j * dX_n / dy), y, 0, b) - \\ & \int((2/3 * E56 * X_m * dS_i / dx), x, 0, L) * \int((dS_j / dy * X_n), y, 0, b) - \\ & \int((1/3 * E25 * X_m * S_{ii}), x, 0, L) * \int((d^2 S_j / dy^2 * X_n), y, 0, b) - \\ & \int((1/3 * E15 * X_m * d^2 S_i / dx^2), x, 0, L) * \int((S_j * X_n), y, 0, b) + \int((H15 * C1 * X_m * d^2 S_i / dx^2), x, 0, L) \\ & * \int((S_j * X_n), y, 0, b) + \int((1/3 * J16 * C1 * X_m * d^2 S_i / dx^2), x, 0, L) * \int((S_j * dX_n / dy), y, 0, b) + \int \\ & ((1/3 * J11 * C1 * dX_m / dx * d^2 S_i / dx^2), x, 0, L) * \int((S_j * X_n), y, 0, b) + \int((2 * H56 * C1 * X_m * dS_i / dx), x, 0, L) \\ & * \int((dS_j / dy * X_n), y, 0, b) + \int((1/3 * J12 * C1 * dX_m / dx * S_{ii}), x, 0, L) * \int((d^2 S_j / dy^2 * X_n), y, 0, b) \\ & + \int((2/3 * J16 * C1 * dX_m / dx * dS_i / dx), x, 0, L) * \int((dS_j / dy * X_n), y, 0, b) + \int((1/3 * J26 * C1 * X_m * S_{ii}), x, 0, L) \\ & * \int((d^2 S_j / dy^2 * dX_n / dy), y, 0, b) + \int((2/3 * J66 * C1 * X_m * dS_i / dx), x, 0, L) * \int((dS_j / dy * dX_n / dy), y, 0, b) \\ & - \int((1/3 * F12 * dX_m / dx * S_{ii}), x, 0, L) * \int((d^2 S_j / dy^2 * X_n), y, 0, b) - \\ & \int((2/3 * F16 * dX_m / dx * dS_i / dx), x, 0, L) * \int((dS_j / dy * X_n), y, 0, b); \end{aligned}$$

Differentiating w.r.t. Ymn:

$$\begin{aligned} W3 = & -\int((E24 * C1 * Y_m * W_i), x, 0, L) * \int((d^2 W_j / dy^2 * Y_n), y, 0, b) - \\ & \int((F16 * C1 * dY_m / dx * d^2 W_i / dx^2), x, 0, L) * \int((W_j * Y_n), y, 0, b) + \int((A44 * Y_m * W_i), x, 0, L) * \int \\ & ((dW_j / dy * Y_n), y, 0, b) - \end{aligned}$$

$$\begin{aligned}
& \int((F12*C1*Ym*d2Wi/dx2),x,0,L)*\int((Wj*dYn/dy),y,0,b)+\int((B46*dYm/dx*Wi),x,0, \\
& L)*\int((dWj/dy*Yn),y,0,b)+\int((J12*C1^2*Ym*d2Wi/dx2),x,0,L)*\int((Wj*dYn/dy),y,0, \\
& b)+\int((B25*Ym*dWi/dx),x,0,L)*\int((Wj*dYn/dy),y,0,b)+\int((J22*C1^2*Ym*Wi),x,0,L \\
&)*\int((d2Wj/dy2*dYn/dy),y,0,b)+\int((J16*C1^2*dYm/dx*d2Wi/dx2),x,0,L)*\int((Wj*Yn \\
&),y,0,b)+\int((B56*dYm/dx*dWi/dx),x,0,L)*\int((Wj*Yn),y,0,b)- \\
& \int((F26*C1*dYm/dx*Wi),x,0,L)*\int((d2Wj/dy2*Yn),y,0,b)+\int((B24*Ym*Wi),x,0,L)*i \\
& \int((dWj/dy*dYn/dy),y,0,b)+\int((9*F44*C1^2*Ym*Wi),x,0,L)*\int((Yn*dWj/dy),y,0,b)- \\
& \int((6*D45*C1*Ym*dWi/dx),x,0,L)*\int((Wj*Yn),y,0,b)+\int((3*H14*C1^2*Ym*d2Wi/d \\
& x2),x,0,L)*\int((Wj*Yn),y,0,b)+\int((J26*C1^2*dYm/dx*Wi),x,0,L)*\int((d2Wj/dy2*Yn),y \\
& ,0,b)+\int((6*H46*C1^2*Ym*dWi/dx),x,0,L)*\int((dWj/dy*Yn),y,0,b)- \\
& \int((4*E25*C1*Ym*dWi/dx),x,0,L)*\int((Wj*dYn/dy),y,0,b)- \\
& \int((E14*C1*Ym*d2Wi/dx2),x,0,L)*\int((Wj*Yn),y,0,b)- \\
& \int((4*E24*C1*Ym*Wi),x,0,L)*\int((dWj/dy*dYn/dy),y,0,b)- \\
& \int((6*D44*C1*Ym*Wi),x,0,L)*\int((dWj/dy*Yn),y,0,b)+\int((3*H46*C1^2*dYm/dx*Wi \\
&),x,0,L)*\int((dWj/dy*Yn),y,0,b)+\int((2*J26*C1^2*Ym*dWi/dx),x,0,L)*\int((dWj/dy*dY \\
& n/dy),y,0,b)- \\
& \int((4*E46*C1*dYm/dx*Wi),x,0,L)*\int((dWj/dy*Yn),y,0,b)+\int((3*H25*C1^2*Ym*dW \\
& i/dx),x,0,L)*\int((Wj*dYn/dy),y,0,b)+\int((2*J66*C1^2*dYm/dx*dWi/dx),x,0,L)*\int((dW \\
& j/dy*Yn),y,0,b)- \\
& \int((2*F66*C1*dYm/dx*dWi/dx),x,0,L)*\int((dWj/dy*Yn),y,0,b)+\int((3*H24*C1^2*Ym \\
& *Wi),x,0,L)*\int((dWj/dy*dYn/dy),y,0,b)+\int((3*H24*C1^2*Ym*Wi),x,0,L)*\int((d2Wj/d \\
& y2*Yn),y,0,b)-\int((2*F26*C1*Ym*dWi/dx),x,0,L)*\int((dWj/dy*dYn/dy),y,0,b)- \\
& \int((4*E56*C1*dYm/dx*dWi/dx),x,0,L)*\int((Wj*Yn),y,0,b)+\int((3*H56*C1^2*dYm/dx
\end{aligned}$$

$$\begin{aligned}
& *dWi/dx),x,0,L)*int((Wj*Yn),y,0,b)+int((9*F45*C1^2*Ym*dWi/dx),x,0,L)*int((Wj*Yn \\
&),y,0,b)+int((A45*Ym*dWi/dx),x,0,L)*int((Wj*Yn),y,0,b)- \\
& int((F22*C1*Ym*Wi),x,0,L)*int((d2Wj/dy2*dYn/dy),y,0,b)- \\
& int((2*E46*C1*Ym*dWi/dx),x,0,L)*int((dWj/dy*Yn),y,0,b);
\end{aligned}$$

$$\begin{aligned}
\mathbf{X3} = & int((3*H25*C1^2*Ym*Xi),x,0,L)*int((Xj*dYn/dy),y,0,b)- \\
& int((4*E56*C1*dYm/dx*Xi),x,0,L)*int((Xj*Yn),y,0,b)+int((9*F45*C1^2*Ym*Xi),x,0,L \\
&)*int((Xj*Yn),y,0,b)+int((B56*dYm/dx*Xi),x,0,L)*int((Xj*Yn),y,0,b)- \\
& int((4*E46*C1*Ym*Xi),x,0,L)*int((dXj/dy*Yn),y,0,b)+int((B46*Ym*Xi),x,0,L)*int((d \\
& Xj/dy*Yn),y,0,b)- \\
& int((2*F16*C1*dYm/dx*dXi/dx),x,0,L)*int((Xj*Yn),y,0,b)+int((B14*Ym*dXi/dx),x,0,L \\
&)*int((Xj*Yn),y,0,b)+int((A45*Ym*Xi),x,0,L)*int((Xj*Yn),y,0,b)+int((B25*Ym*Xi),x,0 \\
& ,L)*int((Xj*dYn/dy),y,0,b)+int((3*H14*C1^2*Ym*dXi/dx),x,0,L)*int((Xj*Yn),y,0,b)+in \\
& t((3*H46*C1^2*Ym*Xi),x,0,L)*int((dXj/dy*Yn),y,0,b)+int((D26*Ym*Xi),x,0,L)*int((d \\
& Xj/dy*dYn/dy),y,0,b)- \\
& int((4*E25*C1*Ym*Xi),x,0,L)*int((Xj*dYn/dy),y,0,b)+int((J26*C1^2*Ym*Xi),x,0,L)*i \\
& nt((dXj/dy*dYn/dy),y,0,b)+int((J66*C1^2*dYm/dx*Xi),x,0,L)*int((dXj/dy*Yn),y,0,b)+i \\
& nt((J12*C1^2*Ym*dXi/dx),x,0,L)*int((Xj*dYn/dy),y,0,b)+int((D12*Ym*dXi/dx),x,0,L) \\
& *int((Xj*dYn/dy),y,0,b)+int((D16*dYm/dx*dXi/dx),x,0,L)*int((Xj*Yn),y,0,b)- \\
& int((2*F12*C1*Ym*dXi/dx),x,0,L)*int((Xj*dYn/dy),y,0,b)- \\
& int((4*E14*C1*Ym*dXi/dx),x,0,L)*int((Xj*Yn),y,0,b)- \\
& int((6*D45*C1*Ym*Xi),x,0,L)*int((Xj*Yn),y,0,b)+int((D66*dYm/dx*Xi),x,0,L)*int((d \\
& Xj/dy*Yn),y,0,b)+int((3*H56*C1^2*dYm/dx*Xi),x,0,L)*int((Xj*Yn),y,0,b)-
\end{aligned}$$

$$\begin{aligned} & \text{int}((2 * F66 * C1 * dYm/dx * Xi), x, 0, L) * \text{int}((dXj/dy * Yn), y, 0, b) - \\ & \text{int}((2 * F26 * C1 * Ym * Xi), x, 0, L) * \text{int}((dXj/dy * dYn/dy), y, 0, b) + \text{int}((J16 * C1^2 * dYm/dx * dXi \\ & /dx), x, 0, L) * \text{int}((Xj * Yn), y, 0, b); \end{aligned}$$

$$\begin{aligned} Y3 = & \text{int}((A44 * Ym * Yi), x, 0, L) * \text{int}((Yj * Yn), y, 0, b) - \\ & \text{int}((2 * F26 * C1 * dYm/dx * Yi), x, 0, L) * \text{int}((dYj/dy * Yn), y, 0, b) - \\ & \text{int}((4 * E46 * C1 * Ym * dYi/dx), x, 0, L) * \text{int}((Yj * Yn), y, 0, b) + \text{int}((3 * H24 * C1^2 * Ym * Yi), x, 0, \\ & L) * \text{int}((dYj/dy * Yn), y, 0, b) - \\ & \text{int}((2 * F26 * C1 * Ym * dYi/dx), x, 0, L) * \text{int}((Yj * dYn/dy), y, 0, b) + \text{int}((3 * H24 * C1^2 * Ym * Yi), \\ & x, 0, L) * \text{int}((Yj * dYn/dy), y, 0, b) + \text{int}((3 * H46 * C1^2 * Ym * dYi/dx), x, 0, L) * \text{int}((Yj * Yn), y, 0, b) \\ & - \text{int}((4 * E24 * C1 * Ym * Yi), x, 0, L) * \text{int}((dYj/dy * Yn), y, 0, b) - \\ & \text{int}((4 * E46 * C1 * dYm/dx * Yi), x, 0, L) * \text{int}((Yj * Yn), y, 0, b) - \\ & \text{int}((4 * E24 * C1 * Ym * Yi), x, 0, L) * \text{int}((Yj * dYn/dy), y, 0, b) - \\ & \text{int}((2 * F22 * C1 * Ym * Yi), x, 0, L) * \text{int}((dYj/dy * dYn/dy), y, 0, b) + \text{int}((J26 * C1^2 * dYm/dx * Yi) \\ & , x, 0, L) * \text{int}((dYj/dy * Yn), y, 0, b) + \text{int}((3 * H46 * C1^2 * dYm/dx * Yi), x, 0, L) * \text{int}((Yj * Yn), y, 0, b) \\ &) + \text{int}((J26 * C1^2 * Ym * dYi/dx), x, 0, L) * \text{int}((Yj * dYn/dy), y, 0, b) + \text{int}((D66 * dYm/dx * dYi/dx) \\ & , x, 0, L) * \text{int}((Yj * Yn), y, 0, b) + \text{int}((B46 * Ym * dYi/dx), x, 0, L) * \text{int}((Yj * Yn), y, 0, b) + \text{int}((J66 * C \\ & 1^2 * dYm/dx * dYi/dx), x, 0, L) * \text{int}((Yj * Yn), y, 0, b) + \text{int}((J22 * C1^2 * Ym * Yi), x, 0, L) * \text{int}((dYj \\ & /dy * dYn/dy), y, 0, b) + \text{int}((B24 * Ym * Yi), x, 0, L) * \text{int}((dYj/dy * Yn), y, 0, b) + \text{int}((B46 * dYm/dx \\ & * Yi), x, 0, L) * \text{int}((Yj * Yn), y, 0, b) + \text{int}((B24 * Ym * Yi), x, 0, L) * \text{int}((Yj * dYn/dy), y, 0, b) + \text{int}((D \\ & 26 * Ym * dYi/dx), x, 0, L) * \text{int}((Yj * dYn/dy), y, 0, b) + \text{int}((D22 * Ym * Yi), x, 0, L) * \text{int}((dYj/dy * d \\ & Yn/dy), y, 0, b) + \text{int}((D26 * dYm/dx * Yi), x, 0, L) * \text{int}((dYj/dy * Yn), y, 0, b) + \text{int}((9 * F44 * C1^2 * \\ & Ym * Yi), x, 0, L) * \text{int}((Yj * Yn), y, 0, b) - \end{aligned}$$

$$\text{int}((2 * F66 * C1 * dYm/dx * dYi/dx), x, 0, L) * \text{int}((Yj * Yn), y, 0, b) -$$

$$\text{int}((6 * D44 * C1 * Ym * Yi), x, 0, L) * \text{int}((Yj * Yn), y, 0, b);$$

Z3 = -

$$\text{int}((1/2 * D14 * Ym * d2Zi/dx2), x, 0, L) * \text{int}((Zj * Yn), y, 0, b) + \text{int}((1/2 * H22 * C1 * Ym * Zi), x, 0, L) * \text{int}((d2Zj/dy2 * dYn/dy), y, 0, b) -$$

$$\text{int}((E26 * Ym * dZi/dx), x, 0, L) * \text{int}((dZj/dy * dYn/dy), y, 0, b) -$$

$$\text{int}((D46 * Ym * dZi/dx), x, 0, L) * \text{int}((dZj/dy * Yn), y, 0, b) + \text{int}((H66 * C1 * dYm/dx * dZi/dx), x, 0, L) * \text{int}((dZj/dy * Yn), y, 0, b) -$$

$$\text{int}((E66 * dYm/dx * dZi/dx), x, 0, L) * \text{int}((dZj/dy * Yn), y, 0, b) + \text{int}((H26 * C1 * Ym * dZi/dx), x, 0, L) * \text{int}((dZj/dy * dYn/dy), y, 0, b) + \text{int}((3 * F46 * C1 * Ym * dZi/dx), x, 0, L) * \text{int}((dZj/dy * Yn), y, 0, b) - \text{int}((1/2 * E16 * dYm/dx * d2Zi/dx2), x, 0, L) * \text{int}((Zj * Yn), y, 0, b) -$$

$$\text{int}((1/2 * E26 * dYm/dx * Zi), x, 0, L) * \text{int}((d2Zj/dy2 * Yn), y, 0, b) -$$

$$\text{int}((1/2 * E22 * Ym * Zi), x, 0, L) * \text{int}((d2Zj/dy2 * dYn/dy), y, 0, b) + \text{int}((1/2 * H26 * C1 * dYm/dx * Zi), x, 0, L) * \text{int}((d2Zj/dy2 * Yn), y, 0, b) + \text{int}((1/2 * H12 * C1 * Ym * d2Zi/dx2), x, 0, L) * \text{int}((Zj * dYn/dy), y, 0, b) - \text{int}((1/2 * D24 * Ym * Zi), x, 0, L) * \text{int}((d2Zj/dy2 * Yn), y, 0, b) -$$

$$\text{int}((1/2 * E12 * Ym * d2Zi/dx2), x, 0, L) * \text{int}((Zj * dYn/dy), y, 0, b) + \text{int}((3/2 * F24 * C1 * Ym * Zi), x, 0, L) * \text{int}((d2Zj/dy2 * Yn), y, 0, b) + \text{int}((1/2 * H16 * C1 * dYm/dx * d2Zi/dx2), x, 0, L) * \text{int}((Zj * Yn), y, 0, b) + \text{int}((3/2 * F14 * C1 * Ym * d2Zi/dx2), x, 0, L) * \text{int}((Zj * Yn), y, 0, b);$$

S3 = -

$$\text{int}((1/3 * F22 * Ym * Sii), x, 0, L) * \text{int}((d2Sj/dy2 * dYn/dy), y, 0, b) + \text{int}((1/3 * J12 * C1 * Ym * d2Si/dx2), x, 0, L) * \text{int}((Sj * dYn/dy), y, 0, b) + \text{int}((2/3 * J26 * C1 * Ym * dSi/dx), x, 0, L) * \text{int}((dSj/dy * dYn/dy), y, 0, b);$$

n/dy),y,0,b)-

int((1/3*F12*Ym*d2Si/dx2),x,0,L)*int((Sj*dYn/dy),y,0,b)+int((1/3*J16*C1*dYm/dx*d2Si/dx2),x,0,L)*int((Sj*Yn),y,0,b)-

int((1/3*E14*Ym*d2Si/dx2),x,0,L)*int((Sj*Yn),y,0,b)+int((1/3*J26*C1*dYm/dx*Sii),x,0,L)*int((d2Sj/dy2*Yn),y,0,b)+int((1/3*J22*C1*Ym*Sii),x,0,L)*int((d2Sj/dy2*dYn/dy),y,0,b)+int((H24*C1*Ym*Sii),x,0,L)*int((d2Sj/dy2*Yn),y,0,b)+int((2/3*J66*C1*dYm/dx*dSi/dx),x,0,L)*int((dSj/dy*Yn),y,0,b)+int((H14*C1*Ym*d2Si/dx2),x,0,L)*int((Sj*Yn),y,0,b)-int((1/3*F26*dYm/dx*Sii),x,0,L)*int((d2Sj/dy2*Yn),y,0,b)-

int((2/3*E46*Ym*dSi/dx),x,0,L)*int((dSj/dy*Yn),y,0,b)-

int((2/3*F66*dYm/dx*dSi/dx),x,0,L)*int((dSj/dy*Yn),y,0,b)-

int((2/3*F26*Ym*dSi/dx),x,0,L)*int((dSj/dy*dYn/dy),y,0,b)-

int((1/3*F16*dYm/dx*d2Si/dx2),x,0,L)*int((Sj*Yn),y,0,b)-

int((1/3*E24*Ym*Sii),x,0,L)*int((d2Sj/dy2*Yn),y,0,b)+int((2*H46*C1*Ym*dSi/dx),x,0,L)*int((dSj/dy*Yn),y,0,b);

Differentiating w.r.t. Zmn:

W4 = -

int((1/2*D15*d2Zm/dx2*dWi/dx),x,0,L)*int((Wj*Zn),y,0,b)+int((2*H26*C1*dZm/dx*Wi),x,0,L)*int((d2Wj/dy2*dZn/dy),y,0,b)-

int((D46*dZm/dx*Wi),x,0,L)*int((dWj/dy*dZn/dy),y,0,b)+int((3*F56*C1*dZm/dx*dWi/dx),x,0,L)*int((Wj*dZn/dy),y,0,b)+int((2*H66*C1*dZm/dx*dWi/dx),x,0,L)*int((dWj/dy*dZn/dy),y,0,b)+int((3*F46*C1*dZm/dx*Wi),x,0,L)*int((dWj/dy*dZn/dy),y,0,b)-

int((D56*dZm/dx*dWi/dx),x,0,L)*int((Wj*dZn/dy),y,0,b)+int((3/2*F24*C1*Zm*Wi),x,

$$\begin{aligned}
&0,L)*\int((dWj/dy*d2Zn/dy2),y,0,b)+\int((3/2*F25*C1*Zm*dWi/dx),x,0,L)*\int((Wj*d2Zn/dy2),y,0,b)+\int((3/2*F14*C1*d2Zm/dx2*Wi),x,0,L)*\int((Zn*dWj/dy),y,0,b)+\int((H12*C1*Zm*d2Wi/dx2),x,0,L)*\int((Wj*d2Zn/dy2),y,0,b)+\int((3/2*F15*C1*d2Zm/dx2*dWi/dx),x,0,L)*\int((Wj*Zn),y,0,b)+\int((2*H16*C1*d2Zm/dx2*dWi/dx),x,0,L)*\int((dWj/dy*Zn),y,0,b)+\int((1/2*H22*C1*Zm*Wi),x,0,L)*\int((d2Wj/dy2*d2Zn/dy2),y,0,b)- \\
&\int((1/2*D25*Zm*dWi/dx),x,0,L)*\int((Wj*d2Zn/dy2),y,0,b)+\int((1/2*H11*C1*d2Zm/dx2*d2Wi/dx2),x,0,L)*\int((Wj*Zn),y,0,b)- \\
&\int((1/2*D24*Zm*Wi),x,0,L)*\int((dWj/dy*d2Zn/dy2),y,0,b)- \\
&\int((1/2*D14*d2Zm/dx2*Wi),x,0,L)*\int((dWj/dy*Zn),y,0,b);
\end{aligned}$$

X4 =

$$\begin{aligned}
&\int((1/2*H11*C1*d2Zm/dx2*dXi/dx),x,0,L)*\int((Xj*Zn),y,0,b)+\int((H16*C1*dZm/dx*dXi/dx),x,0,L)*\int((Xj*dZn/dy),y,0,b)- \\
&\int((1/2*D25*Zm*Xi),x,0,L)*\int((Xj*d2Zn/dy2),y,0,b)+\int((H66*C1*dZm/dx*Xi),x,0,L)*\int((dZn/dy*dXj/dy),y,0,b)+\int((1/2*H26*C1*Zm*Xi),x,0,L)*\int((dXj/dy*d2Zn/dy2),y,0,b)-\int((1/2*E16*d2Zm/dx2*Xi),x,0,L)*\int((Zn*dXj/dy),y,0,b)- \\
&\int((E16*dZm/dx*dXi/dx),x,0,L)*\int((Xj*dZn/dy),y,0,b)- \\
&\int((D56*dZm/dx*Xi),x,0,L)*\int((dZn/dy*Xj),y,0,b)- \\
&\int((1/2*E26*Zm*Xi),x,0,L)*\int((dXj/dy*d2Zn/dy2),y,0,b)+\int((3/2*F15*C1*d2Zm/dx2*Xi),x,0,L)*\int((Xj*Zn),y,0,b)+\int((1/2*H12*C1*Zm*dXi/dx),x,0,L)*\int((Xj*d2Zn/dy2),y,0,b)+\int((1/2*H16*C1*d2Zm/dx2*Xi),x,0,L)*\int((dXj/dy*Zn),y,0,b)- \\
&\int((1/2*E11*d2Zm/dx2*dXi/dx),x,0,L)*\int((Xj*Zn),y,0,b)- \\
&\int((1/2*D15*d2Zm/dx2*Xi),x,0,L)*\int((Xj*Zn),y,0,b)-
\end{aligned}$$

$$\begin{aligned} & \int((1/2 * E12 * Zm * dXi/dx), x, 0, L) * \int((Xj * d2Zn/dy2), y, 0, b) + \int((3 * F56 * C1 * dZm/dx * Xi) \\ & , x, 0, L) * \int((dZn/dy * Xj), y, 0, b) - \\ & \int((E66 * dZm/dx * Xi), x, 0, L) * \int((dZn/dy * dXj/dy), y, 0, b) + \int((3/2 * F25 * C1 * Zm * Xi), x, 0, \\ & L) * \int((Xj * d2Zn/dy2), y, 0, b); \end{aligned}$$

$$\begin{aligned} Y4 = & \int((1/2 * H22 * C1 * Zm * Yi), x, 0, L) * \int((dYj/dy * d2Zn/dy2), y, 0, b) - \\ & \int((E66 * dZm/dx * dYi/dx), x, 0, L) * \int((Yj * dZn/dy), y, 0, b) + \int((H66 * C1 * dZm/dx * dYi/dx) \\ & , x, 0, L) * \int((Yj * dZn/dy), y, 0, b) - \int((E26 * dZm/dx * Yi), x, 0, L) * \int((dZn/dy * dYj/dy), y, 0, b) - \\ & \int((D46 * dZm/dx * Yi), x, 0, L) * \int((Yj * dZn/dy), y, 0, b) - \\ & \int((1/2 * E26 * Zm * dYi/dx), x, 0, L) * \int((Yj * d2Zn/dy2), y, 0, b) + \int((1/2 * H16 * C1 * d2Zm/dx2 \\ & * dYi/dx), x, 0, L) * \int((Yj * Zn), y, 0, b) + \int((3/2 * F14 * C1 * d2Zm/dx2 * Yi), x, 0, L) * \int((Yj * Zn), \\ & y, 0, b) + \int((1/2 * H12 * C1 * d2Zm/dx2 * Yi), x, 0, L) * \int((dYj/dy * Zn), y, 0, b) - \\ & \int((1/2 * E16 * d2Zm/dx2 * dYi/dx), x, 0, L) * \int((Yj * Zn), y, 0, b) - \\ & \int((1/2 * D24 * Zm * Yi), x, 0, L) * \int((Yj * d2Zn/dy2), y, 0, b) + \int((3 * F46 * C1 * dZm/dx * Yi), x, 0, \\ & L) * \int((Yj * dZn/dy), y, 0, b) - \\ & \int((1/2 * E12 * d2Zm/dx2 * Yi), x, 0, L) * \int((dYj/dy * Zn), y, 0, b) + \int((H26 * C1 * dZm/dx * Yi), x \\ & , 0, L) * \int((dYj/dy * dZn/dy), y, 0, b) - \\ & \int((1/2 * D14 * d2Zm/dx2 * Yi), x, 0, L) * \int((Yj * Zn), y, 0, b) - \\ & \int((1/2 * E22 * Zm * Yi), x, 0, L) * \int((dYj/dy * d2Zn/dy2), y, 0, b) + \int((1/2 * H26 * C1 * Zm * dYi/d \\ & x), x, 0, L) * \int((Yj * d2Zn/dy2), y, 0, b) + \int((3/2 * F24 * C1 * Zm * Yi), x, 0, L) * \int((Yj * d2Zn/dy2), \\ & y, 0, b); \end{aligned}$$

Z4 =

$$\begin{aligned} & \int((1/4 * F12 * d2Zm/dx2 * Zi),x,0,L) * \int((d2Zj/dy2 * Zn),y,0,b) + \int((1/2 * F26 * dZm/dx * Zi), \\ & x,0,L) * \int((d2Zj/dy2 * dZn/dy),y,0,b) + \int((1/2 * F26 * Zm * dZi/dx),x,0,L) * \int((dZj/dy * d2Zn \\ & /dy2),y,0,b) + \int((F66 * dZm/dx * dZi/dx),x,0,L) * \int((dZj/dy * dZn/dy),y,0,b) + \int((1/2 * F16 * \\ & d2Zm/dx2 * dZi/dx),x,0,L) * \int((dZj/dy * Zn),y,0,b) + \int((1/4 * F22 * Zm * Zi),x,0,L) * \int((d2Zj \\ & /dy2 * d2Zn/dy2),y,0,b) + \int((1/2 * F16 * dZm/dx * d2Zi/dx2),x,0,L) * \int((Zj * dZn/dy),y,0,b) + \\ & \int((1/4 * F12 * Zm * d2Zi/dx2),x,0,L) * \int((Zj * d2Zn/dy2),y,0,b) + \int((1/4 * F11 * d2Zm/dx2 * d \\ & 2Zi/dx2),x,0,L) * \int((Zj * Zn),y,0,b); \end{aligned}$$

S4 =

$$\begin{aligned} & \int((1/6 * H11 * d2Zm/dx2 * d2Si/dx2),x,0,L) * \int((Sj * Zn),y,0,b) + \int((2/3 * H26 * dZm/dx * Sii \\ &),x,0,L) * \int((d2Sj/dy2 * dZn/dy),y,0,b) + \int((1/6 * H22 * Zm * Sii),x,0,L) * \int((d2Sj/dy2 * d2Zn \\ & /dy2),y,0,b) + \int((2/3 * H16 * dZm/dx * d2Si/dx2),x,0,L) * \int((Sj * dZn/dy),y,0,b) + \int((1/3 * H1 \\ & 2 * d2Zm/dx2 * Sii),x,0,L) * \int((d2Sj/dy2 * Zn),y,0,b) + \int((2/3 * H66 * dZm/dx * dSi/dx),x,0,L) \\ & * \int((dSj/dy * dZn/dy),y,0,b); \end{aligned}$$

Differentiating w.r.t. Smn:

W5= -

$$\begin{aligned} & \int((1/3 * E14 * d2Sm/dx2 * Wi),x,0,L) * \int((dWj/dy * Sn),y,0,b) + \int((4/3 * J16 * C1 * dSm/dx * d \\ & 2Wi/dx2),x,0,L) * \int((Wj * dSn/dy),y,0,b) + \int((1/3 * J22 * C1 * Sm * Wi),x,0,L) * \int((d2Wj/dy \\ & 2 * d2Sn/dy2),y,0,b) - \\ & \int((2/3 * E56 * dSm/dx * dWi/dx),x,0,L) * \int((Wj * dSn/dy),y,0,b) + \int((4/3 * J66 * C1 * dSm/dx \\ & * dWi/dx),x,0,L) * \int((dWj/dy * dSn/dy),y,0,b) + \int((2 * H46 * C1 * dSm/dx * Wi),x,0,L) * \int((d \end{aligned}$$

$$\begin{aligned}
& W_j/dy * dS_n/dy, y, 0, b) - \text{int}((1/3 * E_{25} * S_m * dW_i/dx), x, 0, L) * \text{int}((W_j * d^2S_n/dy^2), y, 0, b) - \\
& \text{int}((1/3 * E_{15} * d^2S_m/dx^2 * dW_i/dx), x, 0, L) * \text{int}((W_j * S_n), y, 0, b) - \\
& \text{int}((2/3 * E_{46} * dS_m/dx * W_i), x, 0, L) * \text{int}((dW_j/dy * dS_n/dy), y, 0, b) + \text{int}((2/3 * J_{12} * C_1 * S_m * d^2 \\
& W_i/dx^2), x, 0, L) * \text{int}((W_j * d^2S_n/dy^2), y, 0, b) + \text{int}((2 * H_{56} * C_1 * dS_m/dx * dW_i/dx), x, 0, L) * \text{int}((\\
& W_j * dS_n/dy), y, 0, b) - \\
& \text{int}((1/3 * E_{24} * S_m * W_i), x, 0, L) * \text{int}((dW_j/dy * d^2S_n/dy^2), y, 0, b) + \text{int}((4/3 * J_{26} * C_1 * dS_m/dx * \\
& W_i), x, 0, L) * \text{int}((d^2W_j/dy^2 * dS_n/dy), y, 0, b) + \text{int}((H_{25} * C_1 * S_m * dW_i/dx), x, 0, L) * \text{int}((W_j * d^2 \\
& S_n/dy^2), y, 0, b) + \text{int}((1/3 * J_{11} * C_1 * d^2S_m/dx^2 * d^2W_i/dx^2), x, 0, L) * \text{int}((W_j * S_n), y, 0, b) + \text{int}((H \\
& 14 * C_1 * d^2S_m/dx^2 * W_i), x, 0, L) * \text{int}((dW_j/dy * S_n), y, 0, b) + \text{int}((H_{15} * C_1 * d^2S_m/dx^2 * dW_i/dx) \\
& , x, 0, L) * \text{int}((W_j * S_n), y, 0, b) + \text{int}((H_{24} * C_1 * S_m * W_i), x, 0, L) * \text{int}((dW_j/dy * d^2S_n/dy^2), y, 0, b);
\end{aligned}$$

$$\begin{aligned}
\mathbf{X5} = & -\text{int}((1/3 * E_{25} * S_m * X_i), x, 0, L) * \text{int}((X_j * d^2S_n/dy^2), y, 0, b) - \\
& \text{int}((1/3 * E_{15} * d^2S_m/dx^2 * X_i), x, 0, L) * \text{int}((X_j * S_n), y, 0, b) + \text{int}((1/3 * J_{26} * C_1 * S_m * X_i), x, 0, L) * \\
& \text{int}((dX_j/dy * d^2S_n/dy^2), y, 0, b) - \\
& \text{int}((2/3 * F_{16} * dS_m/dx * dX_i/dx), x, 0, L) * \text{int}((X_j * dS_n/dy), y, 0, b) + \text{int}((H_{25} * C_1 * S_m * X_i), x, 0, \\
& L) * \text{int}((X_j * d^2S_n/dy^2), y, 0, b) + \text{int}((1/3 * J_{12} * C_1 * S_m * dX_i/dx), x, 0, L) * \text{int}((X_j * d^2S_n/dy^2), y, \\
& 0, b) + \text{int}((1/3 * J_{16} * C_1 * d^2S_m/dx^2 * X_i), x, 0, L) * \text{int}((dX_j/dy * S_n), y, 0, b) - \\
& \text{int}((1/3 * F_{26} * S_m * X_i), x, 0, L) * \text{int}((dX_j/dy * d^2S_n/dy^2), y, 0, b) + \text{int}((2/3 * J_{16} * C_1 * dS_m/dx * d \\
& X_i/dx), x, 0, L) * \text{int}((X_j * dS_n/dy), y, 0, b) + \text{int}((2/3 * J_{66} * C_1 * dS_m/dx * X_i), x, 0, L) * \text{int}((dS_n/dy * \\
& dX_j/dy), y, 0, b) - \\
& \text{int}((1/3 * F_{16} * d^2S_m/dx^2 * X_i), x, 0, L) * \text{int}((dX_j/dy * S_n), y, 0, b) + \text{int}((1/3 * J_{11} * C_1 * d^2S_m/dx^2 * \\
& dX_i/dx), x, 0, L) * \text{int}((X_j * S_n), y, 0, b) + \text{int}((2 * H_{56} * C_1 * dS_m/dx * X_i), x, 0, L) * \text{int}((X_j * dS_n/dy), y \\
& , 0, b) - \text{int}((1/3 * F_{11} * d^2S_m/dx^2 * dX_i/dx), x, 0, L) * \text{int}((X_j * S_n), y, 0, b) -
\end{aligned}$$

$$\begin{aligned} & \int((1/3 * F12 * Sm * dXi/dx),x,0,L) * \int((Xj * d2Sn/dy2),y,0,b) - \\ & \int((2/3 * E56 * dSm/dx * Xi),x,0,L) * \int((Xj * dSn/dy),y,0,b) + \int((H15 * C1 * d2Sm/dx2 * Xi),x, \\ & 0,L) * \int((Xj * Sn),y,0,b) - \int((2/3 * F66 * dSm/dx * Xi),x,0,L) * \int((dXj/dy * dSn/dy),y,0,b); \end{aligned}$$

$$\begin{aligned} \mathbf{Y5} = & - \int((1/3 * E14 * d2Sm/dx2 * Yi),x,0,L) * \int((Yj * Sn),y,0,b) - \\ & \int((1/3 * E24 * Sm * Yi),x,0,L) * \int((Yj * d2Sn/dy2),y,0,b) - \\ & \int((1/3 * F16 * d2Sm/dx2 * dYi/dx),x,0,L) * \int((Yj * Sn),y,0,b) - \\ & \int((1/3 * F22 * Sm * Yi),x,0,L) * \int((dYj/dy * d2Sn/dy2),y,0,b) - \\ & \int((1/3 * F26 * Sm * dYi/dx),x,0,L) * \int((Yj * d2Sn/dy2),y,0,b) + \int((H24 * C1 * Sm * Yi),x,0,L) \\ & * \int((Yj * d2Sn/dy2),y,0,b) + \int((H14 * C1 * d2Sm/dx2 * Yi),x,0,L) * \int((Yj * Sn),y,0,b) + \int((1 \\ & /3 * J22 * C1 * Sm * Yi),x,0,L) * \int((dYj/dy * d2Sn/dy2),y,0,b) - \\ & \int((2/3 * F26 * dSm/dx * Yi),x,0,L) * \int((dYj/dy * dSn/dy),y,0,b) - \\ & \int((2/3 * E46 * dSm/dx * Yi),x,0,L) * \int((Yj * dSn/dy),y,0,b) - \\ & \int((2/3 * F66 * dSm/dx * dYi/dx),x,0,L) * \int((Yj * dSn/dy),y,0,b) + \int((2/3 * J26 * C1 * dSm/dx * \\ & Yi),x,0,L) * \int((dYj/dy * dSn/dy),y,0,b) + \int((2 * H46 * C1 * dSm/dx * Yi),x,0,L) * \int((Yj * dSn/ \\ & dy),y,0,b) + \int((2/3 * J66 * C1 * dSm/dx * dYi/dx),x,0,L) * \int((Yj * dSn/dy),y,0,b) + \int((1/3 * J26 \\ & * C1 * Sm * dYi/dx),x,0,L) * \int((Yj * d2Sn/dy2),y,0,b) - \\ & \int((1/3 * F12 * d2Sm/dx2 * Yi),x,0,L) * \int((dYj/dy * Sn),y,0,b) + \int((1/3 * J16 * C1 * d2Sm/dx2 * \\ & dYi/dx),x,0,L) * \int((Yj * Sn),y,0,b) + \int((1/3 * J12 * C1 * d2Sm/dx2 * Yi),x,0,L) * \int((dYj/dy * S \\ & n),y,0,b); \end{aligned}$$

Z5=

$$\begin{aligned} & \int((1/6 * H22 * Sm * Zi),x,0,L) * \int((d2Zj/dy2 * d2Sn/dy2),y,0,b) + \int((2/3 * H26 * Sm * dZi/dx), \\ & x,0,L) * \int((dZj/dy * d2Sn/dy2),y,0,b) + \int((1/6 * H11 * d2Sm/dx2 * d2Zi/dx2),x,0,L) * \int((Zj * \end{aligned}$$

$\text{Sn}),y,0,b)+\text{int}((2/3*H66*dSm/dx*dZi/dx),x,0,L)*\text{int}((dZj/dy*dSn/dy),y,0,b)+\text{int}((2/3*H1$
 $6*d2Sm/dx2*dZi/dx),x,0,L)*\text{int}((dZj/dy*Sn),y,0,b)+\text{int}((1/3*H12*Sm*d2Zi/dx2),x,0,L)*$
 $\text{int}((Zj*d2Sn/dy2),y,0,b);$

S5 =int((

$2/9*J16*dSm/dx*d2Si/dx2),x,0,L)*\text{int}((Sj*dSn/dy),y,0,b)+\text{int}((1/9*J11*d2Sm/dx2*d2Si/$
 $dx2),x,0,L)*\text{int}((Sj*Sn),y,0,b)+\text{int}((1/9*J12*d2Sm/dx2*Sii),x,0,L)*\text{int}((d2Sj/dy2*Sn),y,0$
 $,b)+\text{int}((2/9*J16*d2Sm/dx2*dSi/dx),x,0,L)*\text{int}((dSj/dy*Sn),y,0,b)+\text{int}((2/9*J26*dSm/dx$
 $*Sii),x,0,L)*\text{int}((d2Sj/dy2*dSn/dy),y,0,b)+\text{int}((1/9*J22*Sm*Sii),x,0,L)*\text{int}((d2Sj/dy2*d2$
 $Sn/dy2),y,0,b)+\text{int}((1/9*J12*Sm*d2Si/dx2),x,0,L)*\text{int}((Sj*d2Sn/dy2),y,0,b)+\text{int}((2/9*J26$
 $*Sm*dSi/dx),x,0,L)*\text{int}((dSj/dy*d2Sn/dy2),y,0,b)+\text{int}((4/9*J66*dSm/dx*dSi/dx),x,0,L)*$
 $\text{int}((dSj/dy*dSn/dy),y,0,b);$

Appendix B

CF_ABD

```

% Sub program to calculate [A], [B] and [D] matrices
% This is a generalized program for all models A, B, C and D

function[D,Q,top,bottom]=CF_ABD(E1,E2,G12,G23,v12,v23,a1,b1,N,LT,th)
no=1;
cth=0;
for y1=1:N
    cth=cth+th;          % Cumulative thickness
    top(1,no)=cth;      % Calculates the top of each layer
    bottom(1,no)=cth-th; %Calculates bottom of each layer

% Compliance matrix for theta (theta= fiber angle, plane stress case)
L1=cos(a1(1,no)*pi/180); M1=sin(a1(1,no)*pi/180);

T_sigma_theta=[L1^2, M1^2, 0, 0, 0, -2*L1*M1 ;
               M1^2, L1^2, 0, 0, 0, 2*L1*M1 ;
               0 , 0 , 1, 0, 0, 0 ;
               0 , 0 , 0, L1, M1, 0 ;
               0 , 0 , 0, -M1, L1, 0 ;
               L1*M1, -M1*L1, 0, 0, 0, L1^2-M1^2];

L2=cos(b1(1,no)*pi/180); M2=sin(b1(1,no)*pi/180);

% Transformation matrix of strain (fi=tapered angle, plane stress case)
T_sigma_fi=[L2^2, 0, M2^2, 0, 2*L2*M2, 0 ;
            0 , 1, 0, 0, 0, 0 ;
            M2^2, 0, L2^2, 0, -2*L2*M2, 0 ;
            0 , 0, 0, L2, 0, -M2;
            -L2*M2, 0, M2*L2, 0, L2^2-M2^2, 0 ;
            0, 0, 0, M2, 0, L2 ];

```

```

syms v13 v32 v31 v21 E3 G13;
delta=(1-v12*v21-v23*v32-v31*v13-2*v21*v32*v13)/(E1*E2*E3);
C11=(1-(v23*v32))/(E2*E3*delta); C12=(v12+(v32*v13))/(E1*E3*delta);
C13=(v13+(v12*v23))/(E1*E2*delta); C22=(1-(v13*v31))/(E1*E3*delta);
C23=(v23+(v21*v13))/(E1*E2*delta); C33=(1-(v12*v21))/(E1*E2*delta);
C44=G23; C55=G13; C66=G12;
%for transversly isotropic material
v13=v12; v32=v23;
v31=v13*E3/E1; v21=v12*E2/E1;
E3=E2;
G13=G12;
% C_double_bar is the stiffness matrix in fiber direction
C_double_bar=subs([C11 C12 C13 0 0 0;
                  C12 C22 C23 0 0 0;
                  C13 C23 C33 0 0 0;
                  0 0 0 C44 0 0;
                  0 0 0 0 C55 0;
                  0 0 0 0 0 C66]);

if b1(1,no)==1000 % Here 1000 is used for drop of ply
    Q(1,no) = {zeros(3,3)};
else
    C_xyz =
(T_sigma_fi)*(T_sigma_theta)*C_double_bar*transpose(T_sigma_theta)*transpose(T_sigma_fi);

%for plane stress case
Q11=C_xyz(1,1)-(C_xyz(1,3).^2/C_xyz(3,3));
Q12=C_xyz(1,2)-(C_xyz(1,3)*C_xyz(2,3)/C_xyz(3,3));
Q16=C_xyz(1,6)-(C_xyz(1,3)*C_xyz(3,6)/C_xyz(3,3));
Q22=C_xyz(2,2)-(C_xyz(2,3).^2/C_xyz(3,3));
Q26=C_xyz(2,6)-(C_xyz(2,3)*C_xyz(3,6)/C_xyz(3,3));
Q66=C_xyz(6,6)-(C_xyz(3,6).^2/C_xyz(3,3));

```

```

Q(1,no)={subs([Q11 Q12 Q16; Q12 Q22 Q26; Q16 Q26 Q66])};
    end
    no=no+1;
end

A=0;
B=0;
D=0;
syms x;

for p=1:N
    if b1(1,p)==1000 % Here 1000 is used for drop of ply
        z_k= 0;
        e_k= 0;
    else
        z_k= (1/2) * ((top(1,p)-LT/2)+(bottom(1,p)-LT/2)) + tan(b1(1,p)*pi/180)*x;
        e_k= ((top(1,p)-LT/2)-(bottom(1,p)-LT/2));
    end

    D1 = (e_k * z_k.^2 + e_k.^3/12) * Q{1,p};
    D = D+D1;
end

D;
% END of function CF_ABD

```

CF_energy

% Sub program to calculate stiffness matrix and load matrix of laminate plies

```
function[AA1,BB1,CC1,DD1,GG1,EE1,FF1]=
```

```
CF_energy(MM,NN,x,y,L,w,D11,D12,D22,D33,D13,D23)
```

% The values of following terms are given in Table 2.3

```
lamda_m= [1.875,4.694,7.855,10.996];
```

```
gama_m= [0.734,1.018,0.999,1.000];
```

```
lamda_n= [1.875,4.694,7.855,10.996];
```

```
gama_n= [0.734,1.018,0.999,1.000];
```

```
for m=1:MM
```

```
for n=1:NN
```

```
    % Beam function in x direction
```

```
    X(1,m)=cos(lamda_m(1,m)*x/L)-cosh(lamda_m(1,m)*x/L) -
```

```
    gama_m(1,m)*(sin(lamda_m(1,m)*x/L)-sinh(lamda_m(1,m)*x/L)); % beam function in x  
direction
```

```
    X=subs(X);
```

```
    % Beam function in y direction
```

```
    Y(1,n)=cos(lamda_n(1,n)*y/w)-cosh(lamda_n(1,n)*y/w) -
```

```
    gama_n(1,n)*(sin(lamda_n(1,n)*y/w)-sinh(lamda_n(1,n)*y/w)); % beam function in y direction
```

```
    Y=subs(Y);
```

```
end
```

```
end
```

```
for p=1:MM
```

```
for q=1:NN
```

```
    I1= D11 * diff(X(1,p),'x',2)* diff(X(1,q),'x',2);
```

```
    I2=Y(1,p)*Y(1,q);
```

```
    AA1(p,q)= int(I1,x,0,L)*int(I2,y,0,w);
```

```

I3=D12* X(1,p)* diff(X(1,q),'x',2);
I4=Y(1,q)*diff(Y(1,p),'y',2);
I5=D12* X(1,q)* diff(X(1,p),'x',2);
I6=Y(1,p)* diff (Y(1,q),'y',2);
BB1(p,q)= int(I3,x,0,L)*int(I4,y,0,w) + int(I5,x,0,L)*int(I6,y,0,w);

I7=D22* X(1,p)* X(1,q);
I8=diff(Y(1,p),'y',2)* diff(Y(1,q),'y',2) ;
CC1(p,q)= int(I7,x,0,L)*int(I8,y,0,w);

I9=D33* diff(X(1,p),'x',1)* diff(X(1,q),'x',1);
I10=diff(Y(1,p),'y',1)* diff(Y(1,q),'y',1);
DD1(p,q)= 4*int(I9,x,0,L)*int(I10,y,0,w);

I11=diff(X(1,p),'x',1)* diff(X(1,q),'x',1);
I12=Y(1,p)*Y(1,q);
GG1(p,q)= int(I11,x,0,L)*int(I12,y,0,w);

I13=D13* diff(X(1,q),'x',2)* diff(X(1,p),'x',1);
I14=Y(1,q)* diff(Y(1,p),'y',1);
I15=D13* diff(X(1,p),'x',2)* diff(X(1,q),'x',1);
I16=Y(1,p)* diff(Y(1,q),'y',1);
EE1(p,q)= 2*int(I13,x,0,L)*int(I14,y,0,w) + 2*int(I15,x,0,L)*int(I16,y,0,w);

I17=D23* X(1,p)* diff(X(1,q),'x',1);
I18=diff(Y(1,q),'y',1)* diff(Y(1,p),'y',2) ;
I19=D23* X(1,q)* diff(X(1,p),'x',1);
I20=diff(Y(1,p),'y',1)* diff(Y(1,q),'y',2);
FF1(p,q)= 2*int(I17,x,0,L)*int(I18,y,0,w) +2*int(I19,x,0,L)*int(I20,y,0,w);
end
ply=['No of terms of Rayleigh Approximation: ', num2str(p)]; disp(ply);
end

% END OF SUB PROGRAM CF_energy

```

CF_energy_resin

% Sub program to calculate stiffness matrix and load matrix of resin pocket

function[A333,B333,C333,D333,G333]=

CF_energy_resin(Q_resin,NDP,th,LT,MM,NN,x,y,b1,w,top,bottom,NDR)

r=NDR*NDP/2; % Half of total No. of imaginary resin plies

for p=1:NDR*NDP/2

L1(1,p)=cot(-b1(1,p)*pi/180)*((th/NDR)*p-th/(2*NDR)); % Upeer triangle of resin--bottom
to top

L2(1,p)=cot(-b1(1,p)*pi/180)*((th/NDR)*r-th/(2*NDR)); % Lower triangle of resin--bottom
to top

r=r-1;

end

Lii = [L2,L1]; % Length of imaginary resin pocket from bottom to top

size = size(Lii); % 2nd value is the total No. in column,

% in case of odd drop of ply it is required

syms Li;

% The values of following terms are given in Table 2.3

lamda_m= [1.875,4.694,7.855,10.996];

gama_m= [0.734,1.018,0.999,1.000];

lamda_n= [1.875,4.694,7.855,10.996];

gama_n= [0.734,1.018,0.999,1.000];

for m=1:MM

for n=1:NN

% Beam function in x direction

X(1,m)=cos(lamda_m(1,m)*x/Li)-cosh(lamda_m(1,m)*x/Li) -

gama_m(1,m)*(sin(lamda_m(1,m)*x/Li)-sinh(lamda_m(1,m)*x/Li));

X=subs(X);


```

% Beam function in y direction
Y(1,n)=cos(lamda_n(1,n)*y/w)-cosh(lamda_n(1,n)*y/w) -
gama_n(1,n)*(sin(lamda_n(1,n)*y/w)-sinh(lamda_n(1,n)*y/w));
Y=subs(Y);
end
end

A333=0; B333=0; C333=0; D333=0; G333=0;
for p=1:size(1,2) % size(1,2)=No. of immaginery resin plies
    Li=Lii(1,p);
    X=subs(X); % subs is used to insert the value of Li

% Q-resin, top, bottom is calculated from 'CF_ABD sub program'

z_k= (1/2) * ((top(1,p)-LT/2)+(bottom(1,p)-LT/2))+tan(b1(1,p)*pi/180)*x +;
e_k= ((top(1,p)-LT/2)-(bottom(1,p)-LT/2));
D_resin = (e_k * z_k.^2 + e_k.^3/12) * Q_resin{1,p};
D11=D_resin(1,1); D12=D_resin(1,2);
D22=D_resin(2,2); D33=D_resin(3,3);

for u=1:MM
    for v=1:NN
        I1= D11 * diff(X(1,u),'x',2)* diff(X(1,v),'x',2);
        I2=Y(1,u)*Y(1,v);
        A3(u,v)= int(I1,x,0,Li)*int(I2,y,0,w);

        I3=D12* X(1,u)* diff(X(1,v),'x',2);
        I4=Y(1,v)*diff(Y(1,u),'y',2);
        I5=D12* X(1,v)* diff(X(1,u),'x',2);
        I6=Y(1,u)* diff (Y(1,v),'y',2);
        B3(u,v)= int(I3,x,0,Li)*int(I4,y,0,w) + int(I5,x,0,Li)*int(I6,y,0,w);

        I7=D22* X(1,u)* X(1,v);
        I8=diff(Y(1,u),'y',2)* diff(Y(1,v),'y',2) ;

```

```

C3(u,v)= int(I7,x,0,Li)*int(I8,y,0,w);

I9=D33* diff(X(1,u),'x',1)* diff(X(1,v),'x',1);
I10=diff(Y(1,u),'y',1)* diff(Y(1,v),'y',1);
D3(u,v)= 4*int(I9,x,0,Li)*int(I10,y,0,w);

I11=diff(X(1,u),'x',1)* diff(X(1,v),'x',1);
I12=Y(1,u)*Y(1,v);
G3(u,v)= int(I11,x,0,Li)*int(I12,y,0,w);
end
end
A333=A333+A3;
B333=B333+B3;
C333=C333+C3;
D333=D333+D3;
G333=G333+G3;
ply=['Analysing resin ply No: ', num2str(p)]; disp(ply);
end
A333;
B333;
C333;
D333;
G333;

% END OF SUB PROGRAM CF_energy_resin

```

Main Program

```
% Main Program for Buckling Analysis of Tapered Plate model A
% for clamp-free boundary conditions based on CLPT
clear all;
close all;
clc;
%*****
% Geometric Properties
E1 = 113.9e9; E2 = 7.9856e9;
G12 = 3.138e9; G23 = 2.543e9;
v12 = 0.288; v23 = .576;
%*****

th=input('Enter the thickness of lamina = ');
MM=6; % Rayleigh Approximation terms
NN=6; %Rayleigh Approximation terms

ZONE_B=['ANALYSING TAPERED LAMINATE, ZONE-B'];disp(ZONE_B);

%*****
Nb = 36; % Number of plies at thick section
LTb = .0045; % Thickness of thick-part
% Ply orientation angles
ab = [0 90 0 90 0 90 0 90 0 90 0 90 0 90 0 90 0 90 0 90 0 90 0 90 0];
bb = [-2.5 -2.5 -2.5 -2.5 -2.5 -2.5 1000 1000 1000 1000 1000 1000 1000 ...
      1000 1000 1000 1000 1000 1000 1000 1000 1000 1000 1000 1000 1000
      1000 2.5 2.5 2.5 2.5 2.5 2.5]; % tapered angles, 1000 is for drop of ply
Lb = .0344; % Length of tapered part for taper angle of 2.5 degree
b=.0344; % Width of tapered laminate model A
%*****
```

```
[D_tapered]=CF_ABD(E1,E2,G12,G23,v12,v23,ab,bb,Nb,L Tb,th); % Recall CF_ABD function
D_tapered;
```

```
syms x y ;
```

```
D11t=vpa(D_tapered(1,1),4); D12t=vpa(D_tapered(1,2),4); D22t=vpa(D_tapered(2,2),4);
D33t=vpa(D_tapered(3,3),4); D13t=vpa(D_tapered(1,3),4); D23t=vpa(D_tapered(2,3),4);
```

```
% Recall of CF_energy function
```

```
[A22,B22,C22,D22,G22,E22,F22]=
```

```
CF_energy(MM,NN,x,y,Lb,b,D11t,D12t,D22t,D33t,D13t,D23t);
```

```
K_b = subs(A22+B22+C22+D22+E22+F22); % Stiffness matrix of taper section for ply
```

```
N_b = subs(G22); % Applied force at taper section for ply
```

```
ZONE_B=['ANALYSING RESIN, ZONE-B'];disp(ZONE_B);
```

```
%*****
```

```
NDP=24; %No of drop of plies
```

```
NDR=1; %No of deviation of each ply
```

```
% Resin Properties
```

```
E1 = 3.93e9; E2 = 3.93e9;
```

```
G12 = 1.034e9; G23 = 1.034e9;
```

```
v12 = 0.37; v23 = .37;
```

```
bbr = [-2.5 -2.5 -2.5 -2.5 -2.5 -2.5 -2.5 -2.5 -2.5 -2.5 -2.5 -2.5 ...
```

```
2.5 2.5 2.5 2.5 2.5 2.5 2.5 2.5 2.5 2.5 2.5 2.5]; % tapered angles
```

```
%*****
```

```
Nr = NDR*NDP; % No. of immaginery resin plies
```

```
abr = zeros(1,Nr); % Immeginery resin plies angles
```

```
LTr = NDP*th; % Thickness of resin pocket at thick part
```

```
th_resin=th/NDR; % Thickness of immaginery resin ply
```

```

% Recall CF_ABD function
[Dr,Q_resin,top,bottom]=CF_ABD(E1,E2,G12,G23,v12,v23,abr,bbr,Nr,LTr,th_resin);
Q_resin;
top;
bottom;
syms x y ;

% Recall of CF_energy_resin function
[A33,B33,C33,D33,G33]=
    F_energy_resin(Q_resin,NDP,th,LTr,MM,NN,x,y,bbr,b,top,bottom,NDR);

K_br = subs(A33+B33+C33+D33); % Stiffness matrix of taper section for resin plies
N_br = subs(G33);           % Applied force at taper section for resin plies

Buckling=['ANALYSING BUCKLING LOAD'];disp(Buckling);

K = subs(K_b + K_br);
N_F = subs( N_b + N_br);
N_buckling=eig(K,N_F) % eigenvalue of tapered laminate model A

%END OF Main PROGRAM

```